DOCTOR OF PHILOSOPHY

Investigation of regulation and downstream signaling pathway of Parkinson's disease associated kinase, PINK1

Kondapalli, Chandana

Award date:
2013

DOCTOR OF PHILOSOPHY

Investigation of regulation and downstream signaling pathway of Parkinson's disease associated kinase, PINK1

Chandana Kondapalli

2013

University of Dundee

Investigation of regulation and downstream signaling pathway of Parkinson's disease associated kinase, PINK1

Chandana Kondapalli

A thesis submitted for the degree of

Doctor of Philosophy

University of Dundee

August 2013

"The most beautiful experience we can have is the mysterious. It is the fundamental emotion that stands at the cradle of true art and true science."

- Albert Einstein (from his essay "The World as I see it")

I. Acknowledgements

My scientific journey would not have been possible without the support extended by many, to whom I would like to express my heartfelt gratitude. Firstly, I thank my supervisors Prof. Dario Alessi and Dr. Miratul Muqit for giving me a wonderful opportunity to cross borders and create a niche for my scientific career. I greatly admire Dario for his knowledge and straight-forwardness and I am ever grateful for his mentorship. I thank Miratul for being a supportive supervisor and his commitment towards science is truly inspiring. A special thanks to my thesis committee members, Dr. Anton Gartner and Prof. John Rouse, for their stimulating scientific discussions. I would also like to thank my collaborators: Dr. Francois Michel Boisvert from Prof. Angus Lamond's group and Dr. Matthias Trost and Dr. Brian Dill from MRC PPU.

MRC PPU has always fascinated me for its fantastic organization of multiple facilities. This thesis would not be possible if not for the millions of clones made by Maria Deak (former member of DSTT)–thank you very much, Maria! I would like to thank the DSTT cloning team – Mark Peggie, Rachel Toth and Thomas Macartney for their expertise in cloning virtually anything we ask for. I would like to thank James Hastie and Hilary McLaughan's team from DSTT for the wonderful antibodies that have been used in this thesis. Thanks to DSTT Protein production team and a special thanks to Axel Knebel and his team for outstanding protein purifications. I would like to thank the tissue culture staff - Kirsten and Janis, for their perfection in managing our everyday need in tissue culture. Special thanks to all support staff: Allison Bridges, Alison Hart, Gail Gilmour and Judith Hare for their great management skills in running the unit.

I would like to thank all past and present members of Dario's lab for useful scientific discussions and a great lab environment: my bay mates Ning and Esther, Ning – for endless scientific and philosophical conversations and SUSHI; Esther for her inspiring and pleasing personality; Helen for sharing my PINK1 woo-hoos and woes! Paul and Ayaz for words of wisdom; Agne for the wonderful friend I've found in you; Sourav – for being my cricket companion and for all the yummy food; Eeva for educating me about alternate career options

for scientists, Ana for being a lovely colleague and friend outside of lab; Kristina for her antics and fun moments and Noor for his calm and positive attitude. I would also like to thank all current members of Dario's group for various scientific and non-scientific discussions.

Although Dundee was not convincing enough to cheer me up, I am very grateful for some wonderful friends whom I will cherish for life. Thanks to Manju for helping me get comfortable with Dundee. I thank my dearest friends Bhavya and Priyanka for being my pillars of support. I also would like to thank Shraddha, Laura, Joe, Ritu and Gavuthami for great company.

This thesis is dedicated to my dear parents who have made several sacrifices to provide me with the best education possible. I thank my Ma and Daddy for having faith in me and for always being there in times of need. I would also like to thank my little brother, Babloo for sharing my trials and triumphs. A special thanks to my in-laws for being supportive of my career.

'Thank you' would be an understatement for my better half, Bob, who although has spent four long years away from me, has never failed to motivate me in achieving my dream. Thanks a lot for your realistic outlook of life, words of encouragement and most of all for your affection.

II. Declarations

I hereby declare that the following thesis is based on the results of investigations conducted by myself, and that this thesis is of my own composition. Work other than my own is clearly indicated in the text by reference to the researchers or their publications. This thesis has not in whole or in part been previously presented for a higher degree.

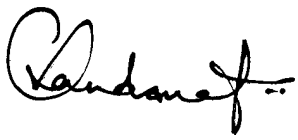

Chandana Kondapalli

We certify that Chandana Kondapalli has spent the equivalent of at least nine terms in research work in the School of Life Sciences, University of Dundee and that she has fulfilled the conditions of the Ordinance General No. 14 of the University of Dundee and is qualified to submit the accompanying thesis in application for the degree of Doctor of Philosophy.

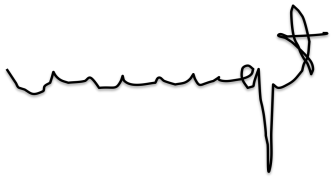

Prof. Dario R. Alessi, FRS, FRSE Dr. Miratul M. K. Muqit M.B. (Ch.B), Ph.D.

III. List of publications

The work presented in this thesis has resulted in the following publication:

Kondapalli C, Kazlauskaite A, Zhang N, Woodroof HI, Campbell DG, Gourlay R, Burchell L, Walden H, Macartney TJ, Deak M, Knebel A, Alessi DR, Muqit MM (2012) PINK1 is activated by mitochondrial membrane potential depolarization and stimulates Parkin E3 ligase activity by phosphorylating Serine 65. ***Open biology*** 2: 120080

IV. Abbreviations

Abl	Abelson murine leukemia viral oncogene homolog
$Al(OH)_3$	Aluminium hydroxide
ANT	Adenine nucleotide transporter
AR EOPD	Autosomal recessive early-onset Parkinson's disease
ATP	Adenosine tri-phosphate
cAMP	Cyclic Adenosine mono-phosphate
CaMK	Calcium/calmodulin dependent kinase
CCCP	m-chlorophenylhydrazone
CK1	Casein Kinase 1
DRP1	Dynamin related protein 1
DTT	Dithiothreitol
ER	Endoplasmic reticulum
GAP	GTPase Activating Protein
GDI	GDP-dissociation inhibitors
GEF	Guanine nucleotide Exchange Factor
HEK293	Human embryonic kidney 293 cell line
HILIC	Hydrophilic Interaction Liquid Chromatography
IMAC	Immobilized Metal Affinity Chromatography
IMM	Inner mitochondrial membrane
KO	Knockout
LC-MS	Liquid chromatography Mass spectrometry
L-DOPA	L-3,4 dihydroxyphenylalanine
LRRK2	Leucine-rich repeat kinase 2
LTP	Long term potentiation

MBP	Maltose binding protein
MEF	Mouse embryonic fibroblast
MFN1	Mitofusin 1
MFN2	Mitofusin 2
MOAC	Metal Oxide Affinity Chromatography
MPP	Mitochondrial processing peptidase
MPT	Membrane permeability transition
MPTP	1-methyl-4-phenyl-1,2,3,6– tetrahydropyridine
mtDNA	Mitochondrial DNA
MTS	Mitochondrial target sequence
Nb_2O_5	Niobium oxide
NTA	Nitrolotriacetate
PAGE	Polyacrylamide gel electrophoresis
PARL	Presenilin-associated rhomboid like protease
PD	Parkinson's disease
PINK1	PTEN-induced kinase 1
PKA	Protein Kinase A
PKG	Protein Kinase G
PKC	Protein kinase C
PTEN	Phosphatase and tensin homolog
RBR	RING in-between RING
REP	Repressor element of Parkin
SAX	Strong anion exchange
SCA11	Spinocerebellar ataxia 11
SILAC	Stable isotope labeling with amino acids in culture

siRNA	Small interfering RNA
shRNA	Short hairpin RNA
SNCA	α-Synuclein
SPE	Solid phase extraction
Tc	*Tribolium castaneum*
TiO_2	Titanium di-oxide
TK	Tyrosine kinase
TKL	Tyrosine kinase-like
TOM/TIM23	Translocase of Outer Membrane/ Translocase of Inner Membrane 23
TRAP1	Tumor necrosis factor type I receptor-associated protein
UBL	Ubiquitin-like domain
VDAC	Voltage dependent anion channel
ZrO_2	Zirconium di-oxide
ΔΨm	Mitochondrial membrane potential
ΔpH	Transmembrane pH gradient

V. Amino acid code

Amino acid or residue	Three letter symbol	One letter symbol
Alanine	Ala	A
Arginine	Arg	R
Asparagine	Asn	N
Aspartate	Asp	D
Cysteine	Cys	C
Glutamate	Glu	E
Glutamine	Gln	Q
Glycine	Gly	G
Histidine	His	H
Isoleucine	Ile	I
Leucine	Leu	L
Lysine	Lys	K
Methionine	Met	M
Phenylalanine	Phe	F
Proline	Pro	P
Serine	Ser	S
Threonine	Thr	T
Tryptophan	Trp	W
Tyrosine	Tyr	Y
Valine	Val	V
any amino acid	Xaa	X

VI. Summary

Parkinson's disease (PD) is the most common neurodegenerative movement disorder affecting about 1% of population above the age of 65. It is believed that common forms of the disease are caused by a combination of both genetic and environmental factors. Over the last 15 years, mutations in a growing number of genes have been identified in rare families with inherited PD; however, the function of many of these genes remains unknown. My PhD project involves the study of one such gene known as PTEN-induced kinase 1 (PINK1); in which missense mutations lead to autosomal recessive PD. PINK1 is unique amongst all known protein kinases since it is primarily localized to the mitochondria. When I started my project, little was known about the catalytic properties of PINK1 since the human enzyme was inactive *in vitro.* In particular it was unknown how PINK1 kinase activity was regulated or what was the identity of its downstream substrate(s). Following the discovery of catalytically active insect orthologues of PINK1 in the laboratory, I deployed these to investigate whether PINK1 could phosphorylate all known PD-linked proteins as well as proteins reported to interact with PINK1. I found that Parkin, a RING-IBR-RING E3 ubiquitin ligase, was the only protein robustly phosphorylated by insect PINK1 at residue Serine 65 (Ser65). This phosphorylation event led to marked activation of its E3 ligase activity. I also uncovered the mode of regulation of mammalian PINK1 and discovered that human PINK1 is specifically activated by mitochondrial membrane potential depolarization, enabling it to phosphorylate Parkin at Ser65 *in vivo*. Once activated, PINK1 also undergoes autophosphorylation at several sites including Threonine 257 (Thr257) and this event is accompanied by an electrophoretic mobility band-shift. Monitoring for

Parkin Ser65 or PINK1 Thr257 phosphorylation could represent the first biomarkers for monitoring PINK1-Parkin signaling *in vivo*.

The second part of my thesis describes the identification of PINK1 interacting proteins by a SILAC based interaction screen in mitochondrial fractions. I describe validation of these interactors by demonstrating that they can all form endogenous complex with PINK1 and investigate their role as potential PINK1 regulators using shRNA knockdown strategy.

In the final part, I describe the identification of novel substrates of PINK1 by a SILAC based phosphoproteomic screen, including the discovery of several Rab GTPase proteins namely, Rab8a, Rab8b and Rab13, which are all phosphorylated at Serine 111. I have presented validation of these substrates *in vivo* and propose strategies for future work to understand the physiological role of this phosphorylation event.

Overall, the work in this thesis outlines a signaling pathway for the PINK1 kinase in which PINK1 can phosphorylate Parkin and Rab proteins upon mitochondrial depolarisation. My work also indicates that monitoring the phosphorylation of Parkin at Ser65, PINK1 at Thr257 and/or Rabs at Ser111 represent the first biomarkers for examining the PINK1 signaling pathway *in vivo*.

VII. Table of contents

VIII. List of figures

IX. List of tables

Chapter 1

Introduction

1. General Introduction

1.1. Signal Transduction

Every living organism features an intelligently designed circuit for relay of information. A unicellular organism uses this circuit to communicate with its surrounding environment. At a multicellular level, this machinery is indispensible for communicating within the microenvironment of a cell as well as with cues from neighbouring cells in order to function as a whole organism. Signal transduction is a collective term used to describe a multistep relay of information initiated by binding of an extracellular signaling molecule called a ligand (e.g. growth factors, hormones, light) to surface receptor proteins embedded in the plasma membrane of a cell (Fig. 1.1). A ligand induced conformational change in the receptor triggers a cascade of intracellular events such as gene activation, metabolic changes or further activation of secondary messengers resulting in an amplification of the initial signal, thereby controlling a variety of cellular processes.

For effective signal amplification, the cell chooses to employ certain key intracellular players such as enzymes and small molecules called secondary messengers (e.g. cAMP, Ca^{2+}). Although they may vary in their physical properties both are extremely dynamic in amplifying a signal by either catalyzing a repertoire of enzymatic reactions or by diffusing in large quantities to trigger a chemical relay to downstream effectors, respectively (Fig.1.1). A

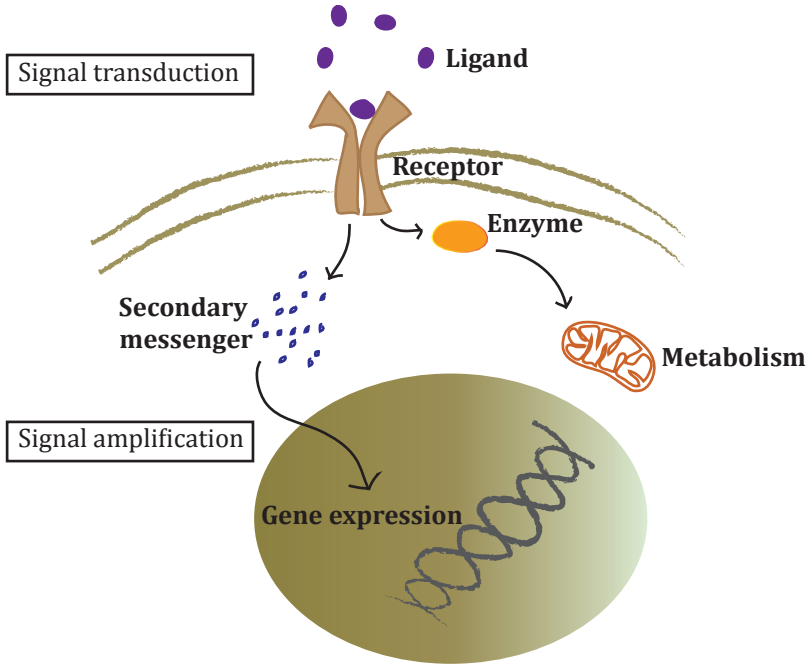

Figure 1.1 Signal transduction circuit within a cell

Illustration of a typical signal transduction pathway activated in response to an extracellular ligand binding to a membrane receptor. This triggers a cascade of intracellular signaling molecules that bring about changes in metabolism and/or gene expression.

classic example of a signal cascade is the photo-activation of Rhodopsin in rod cells of the human eye required for vision in dark light. The transmembrane protein comprises of a protein moiety, Opsin (receptor) reversibly linked to a c-o-factor, Retinal – a Vitamin A derivative. Light (ligand) induced conformational changes in Opsin leads to activation of an associated G-protein, which eventually signals to Phosphodiesterase (enzyme) leading to a decrease in cGMP levels (secondary messenger), hyperpolarization of the cell and subsequent change in neurotransmitter release.

1.2. Protein phosphorylation

Signaling mechanisms within a cell require proteins to function in a concerted manner. However, at various stages of signal transduction, protein function can be regulated by either co-translational or post-translational modifications mediated by enzymes. The majority of intracellular signaling involves a large and diverse family of enzymes known as protein kinases. These enzymes catalyze transfer of γ-phosphate from the energy source, Adenosine Tri-phosphate (ATP), to generate phosphate monoesters with protein alcohol groups (Ser/Thr) and/or protein phenolic groups (Tyr).

The first evidence for protein kinase activity dates back to 1954 when Eugene P. Kennedy described a liver enzyme that catalyzed casein phosphorylation (Burnett & Kennedy, 1954). Not long after, Fischer and Krebs as well as Sutherland and Wosilait presented evidence of protein phosphorylation in glycogen metabolism (Fischer & Krebs, 1955) (Sutherland & Wosilait, 1955). They discovered that the inactive 'b' form of glycogen phosphorylase could be converted to its active 'a' form by an enzyme termed phosphorylase kinase with the help of Mg^{2+}ATP (Krebs & Fischer, 1956). Almost a decade later, it was discovered that phosphorylase kinase was regulated by an upstream kinase Protein Kinase A (PKA), thus establishing the first evidence of a signaling cascade mechanism (Walsh et al, 1968). Although protein phosphorylation was initially regarded as a specialized mechanism to regulate glycogen metabolism, much research over the ensuing decades have established phosphorylation as an important event regulating many essential cellular processes (Cohen, 2002a; Cohen, 2002b).

A phosphorylation reaction is considered to be energetically favourable as it is reversible by another group of enzymes called phosphatases and hence releases the initial molecule of phosphate being consumed (Fig. 1.2). A phosphate group carries two negative charges and hence its addition to a polar group in a substrate may lead to a major conformational change. This change in conformation could alter activity of the substrate if it is an enzyme; modulate binding of interacting protein partners; affect stability or alter localisation (Fig.1.2a and c). In some cases, two phosphorylated sites in close proximity within a protein can recruit adaptor proteins called 14-3-3, which help in shuttling proteins between cellular compartments (Fig.1.2d) (Yaffe et al, 1997).

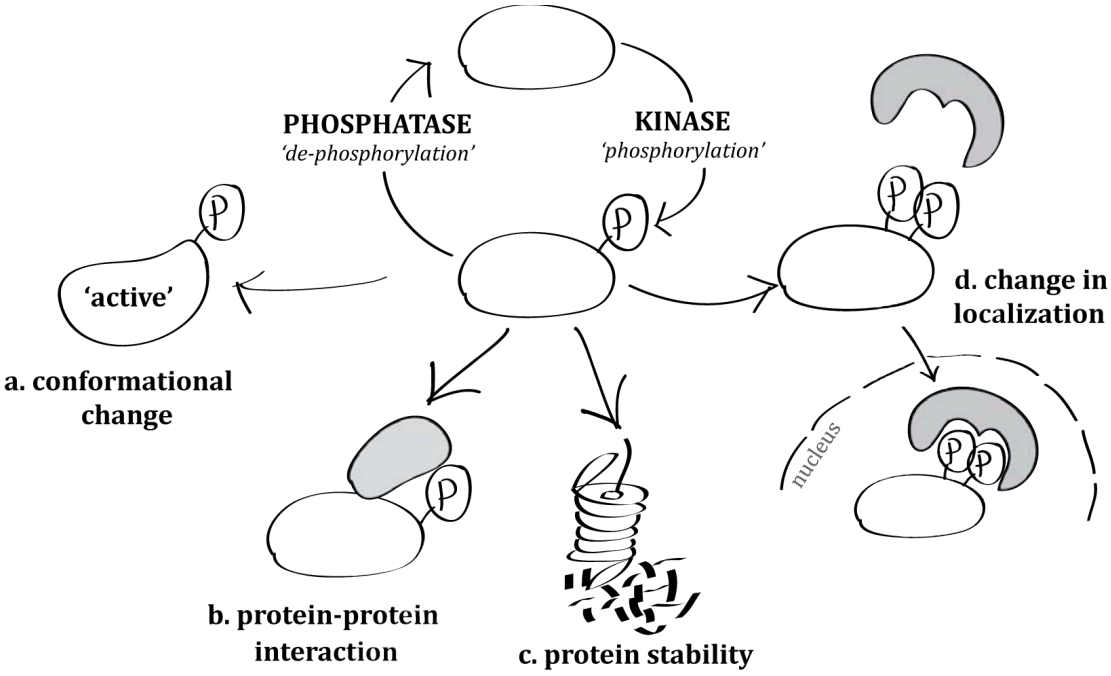

Figure 1.2 Protein phosphorylation

Illustration depicts reversible mechanism of protein phosphorylation that can **a)** activate a protein by conformational change, **b)** lead to association with a binding partner, **c)** can affect stability of a protein or **d)** aid binding of scaffold proteins to shuttle them between cellular compartments.

1.2.1. The Human Kinome

Approximately 1.7% of the human genome encodes for protein kinases, collectively termed the 'human kinome'. This translates to 518 different kinases classified into sub-groups based on sequence similarity and function (Fig 1.3) (Manning et al, 2002). With the discovery of the first crystal structure of a kinase PKA (Knighton et al, 1991) and several subsequent discoveries (De Bondt et al, 1993; Zhang et al, 1995) early on, it was exciting to see that most kinases fold into a common catalytic core structure. Many have evolved with additional domain fusions for functional diversity.

Kinases have been broadly classified into seven groups: AGC (containing PKA, PKG and PKC families), CaMK (calcium/calmodulin-dependent protein kinases), CK1 (Casein kinase 1), CMGC (containing the CDK, MAPK, GSK3, CLK families), STE (containing the homologues of yeast Sterile 7, Sterile 11, Sterile 20 kinases), TK (Tyrosine kinases), and TKL (Tyrosine kinase–like) (Manning et al, 2002). A subset of 32 kinases is considered to belong to the 'atypical' kinase family, which do not share sequence similarity with a typical kinase domain and yet retain catalytic activity e.g. ATM kinase implicated in DNA damage response. In some cases, atypical kinases retain structural similarity to a canonical kinase domain (e.g. RIO kinases). Another subset of kinases are known as 'pseudokinases', which retain a kinase fold but have lost essential motifs required for catalytic activity (Manning et al, 2002). Despite lack of catalytic activity, pseudokinases have emerged in recent years to play a key role as a scaffold to escort proteins or allosterically regulate a functional kinase e.g. the pseudokinase STRAD has been shown to regulate the activity of the

tumour suppressor kinase, LKB1 (Zeqiraj et al, 2009).

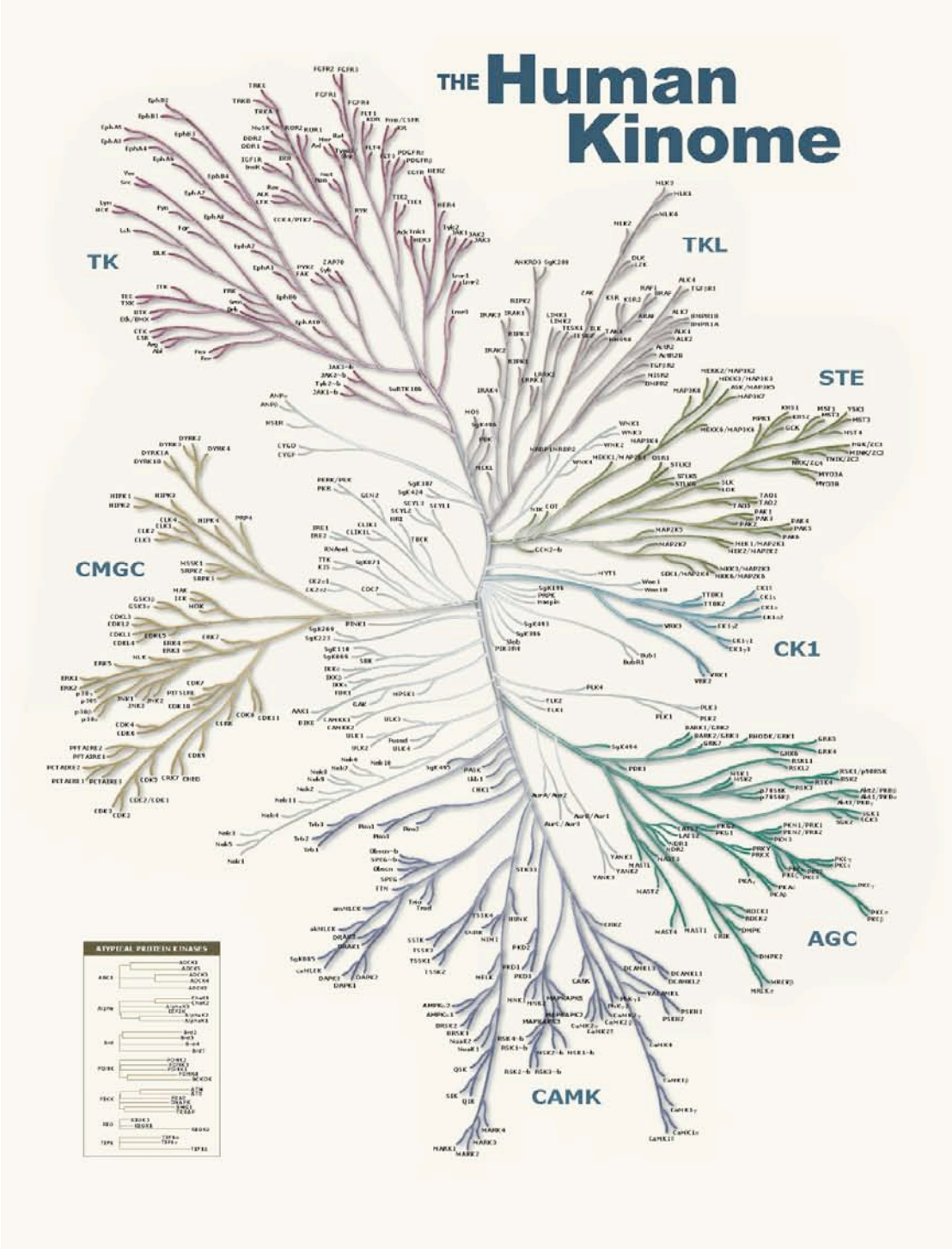

Figure 1.3 The Human Kinome

Phylogenetic tree of all known human protein kinases based on sequence similarity of the kinase domain (Manning et al, 2002).

1.2.2. Structural features of a kinase domain

A kinase domain usually spans around 250-300 amino acids with highly conserved sub-structural motifs. These conserved motifs are vital in understanding the mechanism of phosphoryl transfer mediated by a kinase. A kinase fold typically consists of 12 sub-domains arranged as a bi-lobed structure (Fig. 1.4A); the smaller N-terminal lobe (N-lobe) consists of up to 5 sub-domains primarily made up of β-sheets and the rest of them are organized into a larger C-terminal-lobe (C-lobe) comprising 6 α-helices (Hanks & Hunter, 1995). The two lobes are interconnected by a hinge region, which provides them with flexibility for adopting active and inactive conformations.

Sub-domain I contains a flexible glycine rich loop with GXGXXG motif (strands β1 and β2) that orients nucleotide phosphates by main-chain amide interactions. A lysine in sub-domain II and glutamic acid in sub-domain III (strand β3 and helix αC respectively) form an ion-pair interaction. An aspartic acid (HRDLKXXN) of sub-domain V in the catalytic loop (strand β7) serves as a base for phosphotransfer and an invariant Asp in the DFG motif of sub-domain VII (strand β8-β9) co-ordinates the divalent cation, Mg^{2+}, and the β and γ phosphates of ATP for phosphoryl transfer (Fig.1.4A) (Hanks & Hunter, 1995). Researchers have exploited the invariant nature of either Lys in sub-domain II or Asp in DFG motif by site-directed mutagenesis of either residue to create a kinase-inactive mutant for loss-of-function studies. Sub-domain VIII contains the substrate binding APE motif and the region between DFG and APE motif is called the “T loop” or “activation loop” containing a crucial Thr/Ser residue.

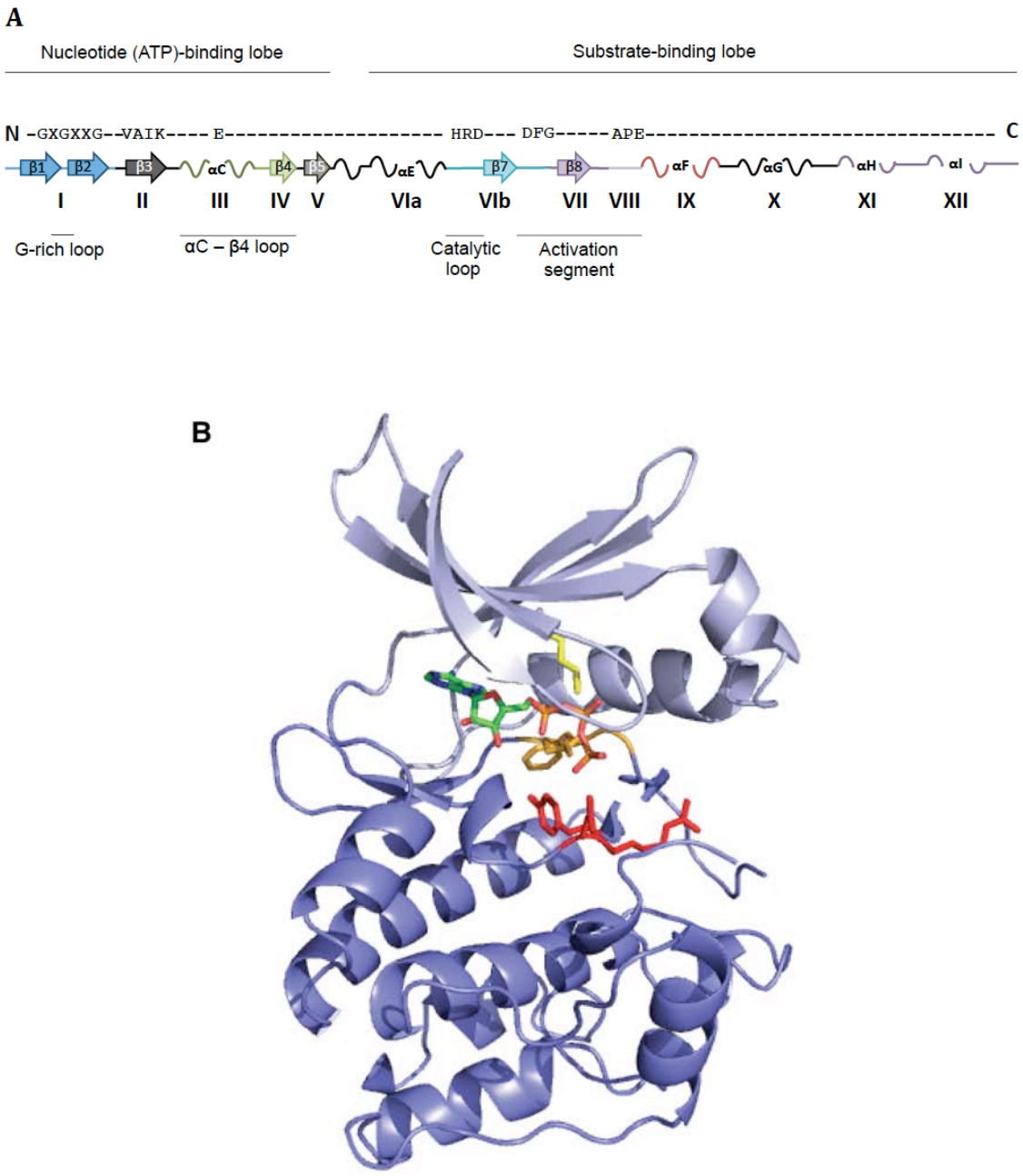

Figure 1.4 Structural features of a kinase

(A) Illustration highlighting the sub-domains and conserved motifs in the N-lobe and C-lobe of a kinase. α represents helices and β represents sheets.

(B) Crystal structure of mouse Protein Kinase A (PKA). N-lobe is represented in lilac and C-lobe in darker shade of lilac. Side chains highlighted in yellow represents the conserved Lysine in sub-domain II of N-lobe, in orange represents DFG motif and in red represents HRD motif. These are crucial for kinase activation by mediating ATP binding and metal co-ordination.

For most kinases, this Thr/Ser residue either undergoes cis-phosphorylation (auto-phosphorylation) or phosphorylation by an upstream kinase thereby stabilizing the activation loop for correct orientation of catalytic residues for phosphate transfer to a substrate (Hanks & Hunter, 1995). For example, maximal activation of PKA-Cα subunit occurs upon phosphorylation of Thr197 in the activation loop (Steinberg et al, 1993). Another interesting example is trans-autophosphorylation (phosphorylation by the adjacent kinase within a dimer or a higher order multimer) of CamKII Thr286 residue by the neighbouring active kinase within a multimeric CaMKII holoenzyme (Miller et al, 1988).

1.2.3. Protein kinases associated with human disease

Protein kinases participate in various cellular processes and hence it is not unexpected that they undergo a high selective pressure to resist genetic variations. Nevertheless, variations do occur leading to severe consequences such as inactivation of a kinase or an abnormal increase in kinase activity, which are causative of several debilitating inherited diseases and sporadic cancers. Table 1.1 lists protein kinases found to be mutated in inherited human diseases (Lahiry et al, 2010). Of relevance to this thesis, several kinases have been implicated in neurodegenerative diseases. Mutations in the LRRK2 or PINK1 kinases are causative of a devastating neurodegenerative disorder called Parkinson's disease; whilst mutations in TTBK2 or PKCγ lead to spinocerebellar ataxia 11 or 14 (SCA11 or 14) respectively. Mutations in the ATM kinase lead to a rare neurodegenerative disease called Ataxia telangiectasia (Table 1.1).

Elucidation of the signaling pathways associated with these disease-associated kinases is well underway and already delivered new knowledge on the key mechanisms underlying several diseases. This has led to the identification of novel drug targets. The proof-of-concept example was targeting of Abelson tyrosine kinase (Abl) in chronic myeloid leukemia that led to the discovery of Imatinib (commercially known as Gleevec), the first clinically approved kinase inhibitor used for targeted cancer therapy (Capdeville et al, 2002). To date the FDA has approved 23 small molecule kinase inhibitors used for cancer therapy, the latest one being Dabrafenib (developed by GlaxoSmithKline), a selective inhibitor of BRAF kinase used for treatment of metastatic melanoma, approved in May 2013 (Hauschild et al, 2012).

Kinase	Protein Name	Disease
ABL	Abelson murine leukemia viral oncogene homolog 1	Chronic myeloid leukemia
ALK1	Activin receptor-like kinase 1	Hereditary haemorrhagic telangiectasia type 2
AMRH2	Anti-Muellerian hormone type II receptor	Persistent Muellerian duct syndrome
AMPK	AMP-activated protein kinase	Wolff-Parkinson-White syndrome
ATM	Ataxia telangiectasia mutated	Ataxia telangiectasia
ATR	Ataxia telangiectasia and Rad-3 related protein	Seckel syndrome type 1
BMPR1A	Bone morphogenetic protein receptor 1A	Juvenile polyposis syndrome primary pulmonary hypertension
BMPR2	Bone morphogenetic protein receptor 2	Primary pulmonary hypertension
B-Raf	Ser/Thr protein kinase B-Raf	Cardiofaciocutaneous syndrome (CFC), melanoma, sporadic cancers
BTK	Bruton Tyrosine Kinase	X-linked agammaglobulinemia
CASK	Calcium/calmodulin-dependent Ser protein kinase	X-linked mental retardation
CDK4	Cell division protein kinase 4	Melanoma, sporadic cancers
CDKDL5	Cyclin-dependent kinase-like 5	X-linked infantile spasm syndrome
CHK2	Ser/Thr protein kinase Chk2	Li-Fraumeni syndrome, sporadic cancers
CK1δ	Casein kinase 1δ	Familial advanced sleep phase syndrome
DMPK	Myotonin protein kinase	Myotonic dystrophy
EGFR	Epidermal growth factor receptor	Non-small cell lung cancers
EIF2AK3	Eukaryotic initiation factor 2α kinase 3	Wolcott-Rallison syndrome
ERBB2	Receptor tyrosine kinase erbB2 (HER2)	Hereditary familial diffuse gastric cancer, glioma
FGFR1	Fibroblast growth factor receptor 1	Kallmann syndrome, Pfeiffer syndrome
FGFR2	Fibroblast growth factor receptor 2	Apert syndrome, Antley-Bixler syndrome, Beare-Stevenson cutis gyrate syndrome, Crouzon syndrome. Familial scaphocephaly syndrome, Jackson-Weiss syndrome, Pfeiffer syndrome
FGFR3	Fibroblast growth factor receptor 3	Achondroplasia, Crouzon syndrome, Muenke syndrome, Thanatophoric dwar□ism
FLT3	Fms-like tyrosine kinase 3	Acute myeloid leukemia
FLT4	Vascular endothelial growth factor receptor	Milroy disease, Juvenile hemangioma
GRK1	G protein-coupled receptor kinase 1	Oguchi disease
GRK4	G protein-coupled receptor kinase 4	Hypertension
GUCY2D	Guanylate cyclase 2D	Leber congenital amaurosis type 1, Cone-rod dystrophy
INSR	Insulin receptor	Insulin resistance, leprechaunism
IRAK4	Interleukin-1 receptor associated kinase 4	Hyporesponsiveness to bacterial infection
JAK2	Janus kinase 2	Polycythaemia
JAK3	Janus kinase 3	Severe combined immunode□iciency
KIT	Tyrosine protein kinase KIT	Gastrointestinal stromal tumours
LCK	Lymphocyte cell-speci□ic protein-tyrosine kinase	Leukaemia
LIMK1	LIM domain kinase 1	Williams-Beuren syndrome
LRRK2	Leucine-rich repeat kinase 2	Hereditary Parkinson's disease
LTK	Leucocyte tyrosine kinase receptor	Systemic lupus erythematosus
MAP2K3	Mitogen-activated protein kinase kinase 3	Colon cancer
MAST3	Microtubule-associated Ser/Thr kinase 3	In□lammatory bowel disease
MASTL	Microtubule associated Ser/Thr kinase-like	Thrombocytopaenia
MERTK	Tyrosine protein kinase MER	Retinitis pigmentosa
MET	Tyrosine protein kinase MET	Hereditary papillary renal carcinoma
MYLK2	Myosin light chain kinase 2	Cardiomyopathy
NTRK1	Neurotrophic tyrosine kinase receptor type 1	Congenital insensitivity to pain, thyroid papillary carcinoma
PAK3	p21-activated protein kinase 3	X-linked mental retardation
PDGFRβ	Platelet-derived growth factor receptor-β	Chronic myelogenous leukemia
PHKγ2	Phosphorylase kinase subunit γ	Autosomal liver glycogenosis
PI3K	Phosphatidylinositol 3-kinase	Sporadic cancers
PINK1	PTEN-induced kinase 1	Hereditary early-onset Parkinson's disease
PKCγ	Protein kinase Cγ	Spinocerebellar ataxia type 14
PRKX/Y	Protein kinase X/ Protein kinase Y	XX male syndrome and Swyer's syndrome (XY females)
RET	Tyrosine protein kinase RET	Hirschsprung disease, sporadic cancers
ROR2	Tyrosine protein kinase transmembrane receptor ROR2	Robinow disease
RSK2	Ribosomal protein S6 kinase 2	Co□in-Lowry syndrome
STK11	Ser/Thr protein kinase 11 (LKB1)	Peutz-Jeghers syndrome, sporadic cancers
TEK	Tyrosine protein kinase receptor TEK	Venous malformations
TTBK2	Tau-tubulin kinase 2	Spinocerebellar ataxia type 11
TGFBR2	Transforming growth factor β receptor II	Various cancers
WNK1/4	Ser/Thr protein kinase WNK1 and WNK4	Pseudohypoaldosteronism type II
ZAP70	Tyr protein kinase ZAP 70	Severe combined immunode□iciency

Table 1.1 Kinases mutated in human disease.

Kinase highlighted in red is central to the work in this thesis.

1.3. Introduction to Parkinson's disease

Parkinson's disease (PD) is the most common neurodegenerative movement disorder affecting about 1% of the population above the age of 65 (Van Laar & Berman, 2009). In 1817, James Parkinson, a British physician, documented the first medical description of the disease that was to bear his name in a monograph "An essay on the Shaking Palsy" where he described patients suffering from 'paralysis agitans'. He described the clinical features in succinct English as follows (Parkinson, 1817):

"Involuntary tremulous motion, with lessened muscular power, in parts not in action and even when supported; with a propensity to bend the trunk forward, and to pass from a walking to a running pace: the senses and intellects being uninjured."

Almost half a century later, Jean-Martin Charcot, who was instrumental in refining the clinical spectrum of the disease, renamed it as Parkinson's disease in honour of James Parkinson. The major clinical symptoms of this movement disorder include resting tremor, bradykinesia (slowness in execution of movement) and rigidity. Pathologically, PD is characterized by the relatively selective loss of pigmented dopaminergic neurons in the substantia nigra, with loss of dopamine in the striatum (Ehringer & Hornykiewicz, 1960). Surviving neurons typically contain proteinaceous cytoplasmic inclusions called 'Lewy bodies', first observed in 1912 by Frederick Lewy in post mortem PD brain (Lewy, 1912).

The onset of symptoms in PD is believe to appear after ~50-60% loss of dopaminergic neurons in the substantia nigra pars compacta (Riederer & Wuketich, 1976). Currently, L-DOPA (L-3,4 dihydroxyphenylalanine) is the most widely used drug for symptomatic relief. In dopaminergic neurons, the biosynthesis of dopamine involves an initial enzymatic reaction catalyzed by tyrosine hydroxylase that converts the amino acid L-tyrosine to L-DOPA. The enzyme DOPA decarboxylase then converts L-DOPA into the neurotransmitter, dopamine. While dopamine itself is restricted to the brain, L-DOPA can freely cross the blood brain barrier and serves in replenishing dopamine levels lost in PD as a consequence of neuronal death. Besides the central nervous system, L-DOPA is converted to dopamine also in the peripheral nervous system often leading to side effects when administered on its own. Most treatment strategies aim at combining L-DOPA with a peripheral L-DOPA decarboxylase inhibitor (carbidopa) depending on the stage of disease and predominating symptoms (Nyholm, 2006). Interestingly, a natural source of L-DOPA found in a tropical legume, *Mucuna pruriens*, has been described as early as 1500 BC in ancient Indian Ayurvedic medicine to treat neurological disorders bearing similarity with Parkinson's disease (Manyam, 1990). Although L-DOPA provides symptomatic relief, it has no effect on the underlying disease progression, and a cure for PD remains elusive.

1.3.1 Genetics of Parkinson's disease

Although the aetiology of PD is yet to be deduced, the prevailing hypothesis is that the common form of the disease is due to a combination of genetic and environmental factors. Despite the fact that most PD cases are sporadic,

genetic analysis of familial forms has opened a window to explore cellular mechanisms underlying PD pathogenesis. Only around 5-10% of cases are known to have familial forms of the disease (Corti et al, 2011). Genes that have been associated with PD are termed as PARK to denote their link to PD and are numbered in chronological order of their identification. Table 1.2 lists 18 PD-associated chromosomal loci or genes identified to date. These comprise confirmed loci, unconfirmed loci for which linkage analysis could not be replicated, unidentified genes with a confirmed linkage and potential risk factors (Klein & Westenberger, 2012). Among the genes identified, 5 genes have been confirmed in heritable monogenic forms of PD; mutations in α-Synuclein (SNCA) and Leucine-rich repeat kinase 2 (LRRK2) linked to autosomal-dominant forms of PD and mutations in Parkin, PTEN-induced kinase 1 (PINK1), and DJ1 linked to autosomal recessive forms.

1.3.2 Autosomal Dominant Parkinson's disease

α-Synuclein (SNCA) was the first PD gene identified in a large Italian-American family with autosomal dominant Parkinsonism (Polymeropoulos et al, 1997). SNCA forms a major component of Lewy body aggregates found in post-mortem brain of sporadic and inherited PD (Spillantini et al, 1997). Mutations in SNCA, although quite rare, are causative of autosomal dominant early–onset Parkinson's disease (age of onset <50 years). So far, five missense mutations (A30P, E46K, G51D, A53T and H50Q) as well as gene duplications and triplications have been reported (Appel-Cresswell et al, 2013; Kiely et al, 2013; Klein & Schlossmacher, 2006). The physiological function of SNCA is still

unknown, although recently it has been reported to play a role in hippocampal neurogenesis (Winner et al, 2012). SNCA is known to be natively unfolded but has a propensity to form toxic oligomers or protofibrils (Conway et al, 2000). Several missense mutations have been shown to accelerate the formation of these and ultimately lead to formation of β-sheets (Bertoncini et al, 2005; Wise-Scira et al, 2013). The occurrence of gene duplications or triplications leads to an early onset of clinical symptoms with a more severe phenotype and faster progression indicating a

Symbol	Gene locus	Disorder	Inheritance	Gene	Status
PARK1	4q21-22	EOPD	AD	SNCA	Confirmed
PARK2	6q25.2-q27	EOPD	AR	Parkin	Confirmed
PARK3	2p13	Classical PD	AD	Unknown	Unconfirmed
PARK4	4q21-q23	EOPD	AD	SNCA	Erroneous locus (Identical to PARK1)
PARK5	4p13	Classical PD	AD	UCHL1	Unconfirmed
PARK6	1p35-36	EOPD	AR	PINK1	Confirmed
PARK7	1p36	EOPD	AR	DJ1	Confirmed
PARK8	12q12	Classical PD	AD	LRRK2	Confirmed
PARK9	1p36	atypical PD with dementia	AR	ATP13A2	Confirmed
PARK10	1p32	Classical PD	Risk factor	Unknown	Confirmed
PARK11	2q36-27	Late-onset PD	AD	Unknown	Unconfirmed
PARK12	Xq21-25	Classical PD	Risk factor	Unknown	Confirmed
PARK13	2p12	Classical PD	AD/Risk factor	HTRA2	Unconfirmed
PARK14	22q13.1	EO dystonia-parkinsonism	AR	PLA2G6	Confirmed
PARK15	22q12-q13	EO parkinsonian-pyramidal syndrome	AR	FBXO7	Confirmed
PARK16	1q32	Classical PD	Risk factor	Unknown	Confirmed
PARK17	16q11.2	Classical PD	AD	VPS35	Confirmed
PARK18	3q27.1	Classical PD	AD	E1F4G1	Unconfirmed

EOPD - Early-onset Parkinson's disease, AD- Autosomal dominant, AR - Autosomal recessive

Table 1.2 PD-associated gene loci (Klein & Westenberger, 2012).

correlation with gene dosage (Fuchs et al, 2007). Another gene which numerically is a much more common cause of autosomal dominant PD, encodes a large multi-domain protein, Leucine Rich Repeat Kinase 2 (LRRK2). The N-terminal region of LRRK2 bears leucine-rich repeats and and both a GTPase and kinase domain. Around 5 definite pathogenic mutations have been identified most of which cluster around the GTPase or kinase domain. By far, the most frequent and best-studied pathogenic mutation is G2019S, which is known to significantly increase the kinase activity (Jaleel et al, 2007; MacLeod et al, 2006). Consequently, LRRK2 is a major drug target with several pharmaceutical companies developing selective inhibitors as a potential treatment for PD.

1.3.3 Autosomal Recessive Parkinson's disease

Mutations in the E3 ubiquitin ligase, Parkin, lead to early onset autosomal recessive early-onset Parkinson's disease (AR EOPD) (Kitada et al, 1998). The typical age of onset is 30-40 years, although certain homozygous missense mutations in Parkin lead to Juvenile Parkinson's disease (age of onset <21years). Parkin is the second largest gene in the human genome after dystrophin, consisting of 12 exons and together with intronic regions spans up to 1.3MB. Parkin is an enzyme that is 465 aa in length, comprising a regulatory Ubl domain (residues 1-76); a RING0 domain (residues 145-215); a RING1 domain (residues 236-293) that binds to an E2; an IBR domain (residues 327-380); and a RING2 domain that mediates the enzyme's catalytic activity (413-450).

Recent groundbreaking insights have revealed that Parkin and other members of the RING-IBR-RING (RBR) family of E3 ligases exhibit HECT-like properties (Lazarou et al, 2013; Wenzel et al, 2011). Specifically, Parkin contains a highly conserved catalytic cysteine (Cys^{431}) within its RING2 domain, which acts as a ubiquitin acceptor that forms an intermediate thioester bond prior to ubiquitylation of its substrate (Wenzel et al, 2011). The physiological relevance of this catalytic cysteine is underscored by the presence of human disease-causing mutations at this residue (Cys431Phe), which have been shown to abolish Parkin catalytic activity (Trempe et al, 2013). Missense mutations can occur in any domain throughout the protein and rearrangements such as deletions or duplications of exons also occur (Klein & Westenberger, 2012).

The second most common gene mutated in AR EOPD is the PINK1 gene that encodes a Ser/Thr protein kinase that localizes in mitochondria, which will be discussed in great detail in 1.4. In fact human patients with mutations in either PINK1 or the aforementioned Parkin display similar clinical symptoms (Abeliovich & Flint Beal, 2006). In contrast to Parkin, most of the variations in PINK1 are found to be missense mutations distributed throughout the length of the protein. The majority of missense mutations lead to loss-of-function of the kinase activity signifying the importance of PINK1's enzymatic function in PD pathogenesis. A major aim of this thesis has been to identify and understand the downstream signaling pathway of PINK1.

A third gene associated with AR EOPD is the DJ1 gene, with a fairly low frequency of occurrence of 1-2% (Pankratz et al, 2006). DJ1 protein is believed to function as an oxidative chaperone and so far around 10 mutations are reported to be inherited in a homozygous or compound heterozygous fashion. Mutations in DJ1 lead to instability and proteasomal degradation of the protein (Anderson & Daggett, 2008).

1.3.4 Genes with potential link to PD and risk factors

Apart from the six confirmed monogenic forms of PD, several other genes (ATP13A2, FBXO7, UCHL1, HTRA2) listed in Table 1.2 are found to be causative of PD either by linkage analysis or by candidate gene approach. However, some of these genes (HTRA2, UCHL1) are still unconfirmed, while others cause a more complex phenotype (ATP13A2, FBX07). Nevertheless a better understanding of the physiological function of these genes causing complex PD may still shed light on the mechanisms of more conventional types of PD due the likely existence of overlapping pathways.

1.4 PINK1

1.4.1 *Initial discovery*

A Japanese group published the first report on PINK1, in a study of the tumor suppressor gene PTEN (Phosphatase and Tensin Homolog). Their study found PINK1 to be transcriptionally upregulated in ovarian cancer cell lines over-

expressing exogenous PTEN (Unoki & Nakamura, 2001). However the first genetic link between PINK1 and Parkinson's disease was established in 2004, when disease-segregating mutations in PINK1 (G309D missense and W437X nonsense) were identified in two families with AR EOPD (Valente et al, 2004; Valente et al, 2001). As discussed earlier in 1.3.1.2, several missense and nonsense PINK1 mutations have been linked to early onset PD with an average age of onset ranging between 20-40 years (Farrer, 2006). The PINK1 gene comprises 8 exons that span 1.8kb and encodes a protein of 581 amino acids. At the messenger RNA level, a ubiquitous expression pattern is seen with higher levels of expression in heart, skeletal muscle, testis and brain (Taymans et al, 2006). PINK1 mRNA levels in the brain are predominantly neuronal in substantia nigra, hippocampus and cerebellar Purkinje cells (Blackinton et al, 2007).

1.4.2 *Domain architecture of PINK1*

PINK1 is unique amongst all protein kinases as it contains an N-terminal mitochondrial target sequence (MTS) (1-34 residues). Earlier work confirmed that PINK1 localizes to mitochondria and that this required an intact MTS (Muqit et al, 2006; Valente et al, 2004). The catalytic domain of PINK1 (150-513 residues) consists of a Ser/Thr kinase domain with conserved sub-structural motifs yet PINK1 is not closely related to any other protein kinase (refer to Human Kinome – Fig. 1.3). The kinase domain is quite unusual in that it contains three unique insertions interspersed between the β-sheets that constitute the N-lobe of a protein kinase (Woodroof et al, 2011). Further it

contains a C-terminal hydrophobic region of unknown function (513-581 residues).

Several pathogenic mutations comprising missense mutations or nonsense mutations have been identified across the length of the protein (Fig. 1.5) (Corti et al, 2011; Deas et al, 2009).

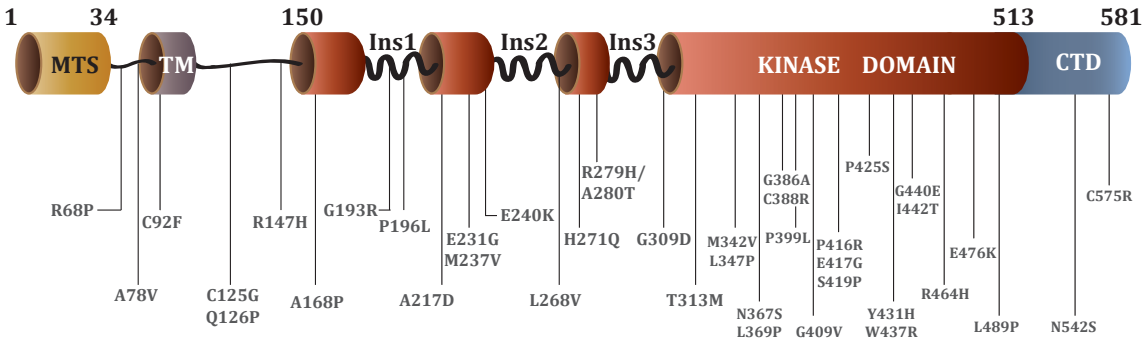

Figure 1.5 Domain architecture of PINK1 with PD-linked pathogenic mutations

MTS – Mitochondrial Target Sequence, TM – Transmembrane domain, Ins1 – Insertion 1, Ins2 – Insertion 2, Ins3 – Insertion 3, CTD – C-terminal domain

1.4.3 *Mitochondrial localization and processing of PINK1*

Whilst the mitochondrial localization of PINK1 has been established (Muqit et al, 2006; Silvestri et al, 2005), the exact location of PINK1 in the mitochondria has been unclear. Perhaps the most convincing data has come from the Przedborski lab in which they determined by limited proteolysis analysis of

mitochondria that PINK1 localizes to the outer mitochondrial membrane with its kinase domain facing the cytoplasm (Zhou et al, 2008).

PINK1 (through its MTS) is imported via the canonical mitochondrial TOM/TIM23 (Translocase of Outer Membrane/ Translocase of Inner Membrane 23) complex (Fig.1.6A) at the outer and inner membrane in a membrane potential dependent manner leading to cleavage of its MTS by Mitochondrial Processing Peptidase (MPP) located within the mitochondrial matrix (Greene et al, 2012) (Fig.1.6B). This cleaved import intermediate then undergoes sequential proteolytic cleavage by the transmembrane protease, PARL (Presenilin-associated rhomboid like protease), giving rise to a PINK1 fragment whose starting amino acid is residue Phe104 (Fig. 1.6D)(Meissner et al, 2011; Whitworth et al, 2008). This de-stabilizing amino acid then targets processed PINK1 for degradation by the N-end Rule pathway and ultimately removed by the 26S proteasome in the cytoplasm (Yamano K, 2013) (Fig.1.6C). This is consistent with the observation that treatment of PINK1-expressing cells with proteasomal inhibitor (MG132) leads to an accumulation of cleaved PINK1 (Muqit et al, 2006). However, PINK1 has been shown to still undergo cleavage albeit with a distinct cleavage pattern even in the absence of PARL indicating that PARL may not be the only protease involved PINK1 processing under basal conditions (Greene et al, 2012). Under conditions where the mitochondrial membrane potential is dissipated, PINK1 import and subsequent cleavage by its protease/s is inhibited (Jin et al, 2010), leading to a dramatic stabilization of PINK1 (Matsuda et al, 2010; Meissner et al, 2011; Narendra et al, 2010).

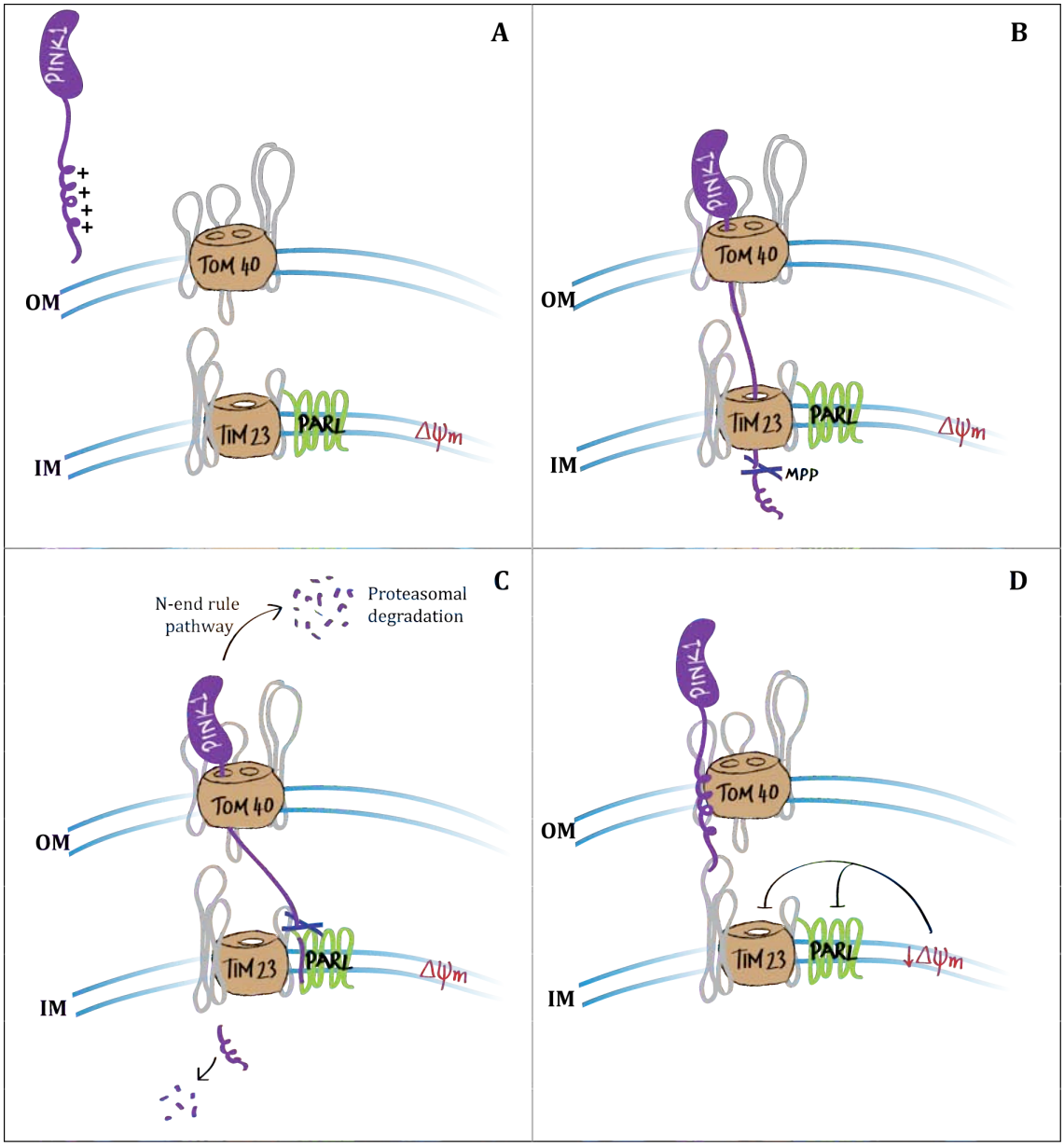

Figure 1.6 Mitochondrial import and processing of PINK1

Illustration depicts the complex mechanism of mitochondrial import and processing of PINK, which begins with **A)** PINK1 being imported from cytoplasm to mitochondria, **B)** Translocation of PINK1 through TOM/TIM23 import machinery and cleavage of presequence in the mitochondrial matrix by Mitochondrial Processing Peptidase (MPP), **C)** Cleaved import intermediate undergoes a second step of proteolytic cleavage by PARL and cleaved product is degraded by 26S proteasome and **D)** Upon dissipation of mitochondrial membrane potential, import and cleavage of PINK1 is inhibited and it stabilizes in the outer mitochondrial membrane. OM – Outer mitochondrial Membrane, IM - Inner mitochondrial Membrane, ΔΨ – mitochondrial membrane potential.

1.5 Signal Transduction by PINK1

1.5.3 *Kinase activity of PINK1*

Initial over-expression studies suggested that the kinase activity of PINK1 might have a neuroprotective role since disease mutants of PINK1 rendered cells vulnerable to apoptosis in the face of cellular stress (Petit et al, 2005; Valente et al, 2004). However, the catalytic properties of PINK1 remained unknown since in our hands and those of many other groups recombinant human PINK1 did not exhibit significant kinase activity. This prevented the establishment of a robust kinase assay of PINK1 and additionally has limited the ability to use traditional biochemical approaches to identify PINK1 substrates. However, a recent discovery from our lab has established that insect orthologues of PINK1, including *Tribolium castaneum* PINK1 (TcPINK1), are catalytically active when expressed in *Escherichia coli* (Woodroof et al, 2011). This has enabled the development of a PINK1 kinase assay which has revealed fundamental insights into the intrinsic catalytic properties of PINK1 and demonstrated that most disease-associated mutations of PINK1 abrogate its kinase activity (Woodroof et al, 2011). The discovery of TcPINK1 has also provided an opportunity to investigate the direct substrates of PINK1.

1.5.4 *Role of PINK1 in mitochondria*

The first link between Parkinson's disease and mitochondria was established in the early 1980s when a neurotoxin MPTP (1-methyl-4-phenyl-1,2,3,6–tetrahydropyridine), an accidental byproduct of illicitly synthesized heroin,

resulted in a Parkinsonian syndrome indistinguishable from idiopathic PD in Californian drug addicts (Langston et al, 1983). This drug crosses the blood brain barrier, wherein it is metabolized to MPP+ and then enters dopaminergic neurons via the dopamine transporters leading to inhibition of mitochondrial complex I (NADH ubiquinone oxidoreductase) and profound dopaminergic loss and Parkinsonism (Nicklas et al, 1985). MPTP and other complex I inhibitors such as rotenone are now used widely to model PD in animals (Hirsch, 2007). A reduction in complex I activity has also been found in post mortem PD brains further suggesting a role for mitochondrial dysfunction in the pathogenesis of PD (Parker et al, 1989; Schapira et al, 1989).

1.5.4.1 PINK1-Parkin in mitochondrial dysfunction

There has been accumulating evidence of a function for PINK1 and another PD-associated gene, Parkin, in mitochondrial quality control. The first link was established in *Drosophila melanogaster* where PINK1 Knockout (KO) flies were found to have a similar phenotype to Parkin KO flies including muscle degeneration and abnormalities in mitochondrial morphology (Clark et al, 2006; Park et al, 2006). Moreover, the phenotype of PINK1 KO flies could be rescued by transgenic expression of Parkin but not vice versa, suggesting that Parkin is downstream of PINK1 (Clark et al, 2006; Park et al, 2006).

Recently there has been a flurry of reports confirming a link between PINK1 and Parkin in mammalian cells. The consensus of these reports is that Parkin, which normally resides in the cytoplasm translocates to the mitochondria when the

membrane potential is depolarized by mitochondrial uncoupling agents (e.g. CCCP) and this is dependent on the expression of wild-type but not kinase-inactive PINK1 (Fig. 1.7). Recruitment of Parkin to mitochondria appears to be a pre-requisite for mitophagy, a selective autophagic mechanism to dispose of dysfunctional mitochondria (Narendra et al, 2008; Narendra et al, 2010).

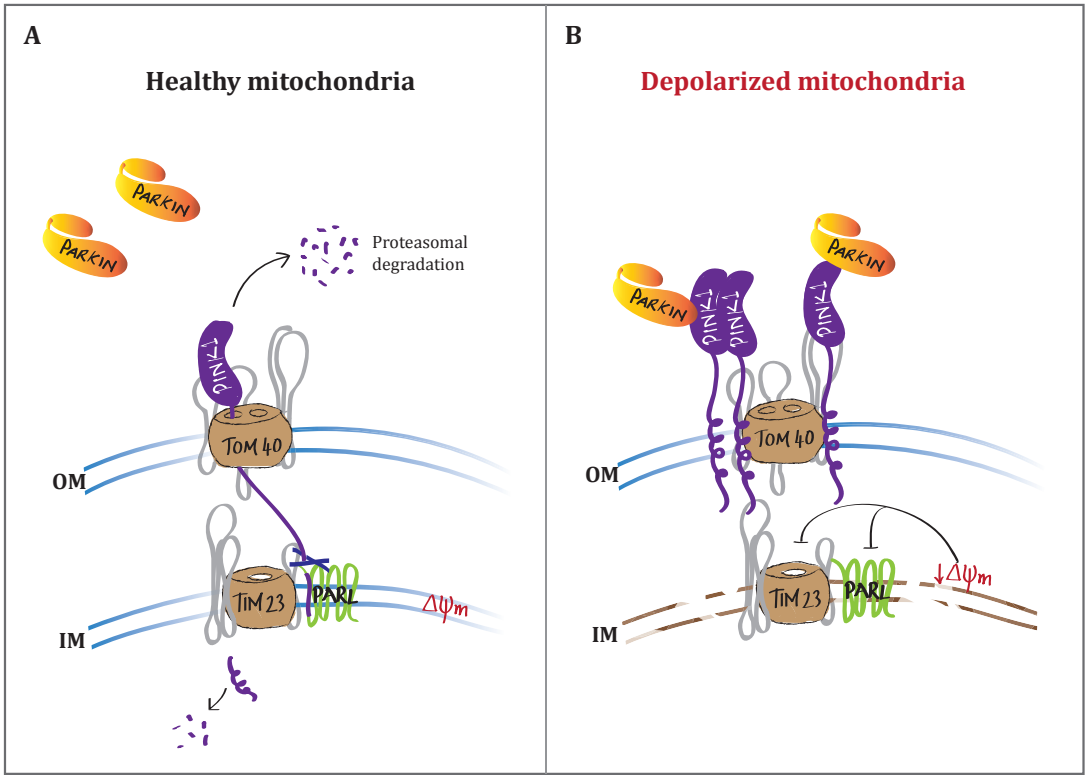

Figure 1.7 PINK1-Parkin pathway in mitochondrial dysfunction

Illustration depicts that **A)** in healthy mitochondria PINK1 undergoes a constant turnover in a membrane potential dependent manner and Parkin remains in the cytosol, whereas **B)** in depolarized mitochondria, rapid accumulation of PINK1 in the mitochondrial membrane helps in recruiting Parkin from the cytosol to the mitochondrial membrane to induce mitophagy. OM – Outer mitochondrial Membrane, IM - Inner mitochondrial Membrane, ΔΨ – mitochondrial membrane potential.

Dissipation of mitochondrial membrane potential also leads to rapid accumulation of PINK1, which is essential for translocation of Parkin (Narendra et al, 2010; Seibler et al, 2011; Vives-Bauza et al, 2010).

A quantitative proteomic approach in CCCP-treated Hela cells over-expressing Parkin showed an accumulation of Lys-48 and Lys-63 poly ubiquitylation in outer mitochondrial membrane proteins (Chan et al, 2011). The prevailing hypothesis is that, a modification of outer mitochondrial membrane proteins by Parkin-mediated ubiquitylation in response to CCCP treatment serves in recruiting autophagic machinery to dysfunctional mitochondria (Geisler et al, 2010). However, the mechanism by which PINK1 mediates translocation of Parkin to mitochondria and activates mitophagy is unclear.

1.5.4.2 Role of PINK1 in mitochondrial dynamics

Mitochondrial dynamics

Electron micrograph studies depict mitochondria as static, bean-shaped organelles. With advances in live-cell imaging, it is now recognised that mitochondria are highly dynamic organelles capable of changing their shape, size and sub-cellular distribution (Chan, 2006; Okamoto & Shaw, 2005). Such dynamic behavior is imparted by mitochondrial fission and fusion machinery and their transport along cytoskeletal tracks. Mitochondria exist in the form of fragmented spherical species or interconnected rod-like structures depending on whether fusion or fission predominates. Several dynamin-like GTPases have been identified which tightly regulate mitochondrial dynamics. Mitofusin1 and 2 (Mfn 1 and 2) are required for outer mitochondrial fusion and OPA1 induces inner membrane fusion. Drp1 (Dynamin related protein 1) is a cytosolic protein which when activated is recruited to mitochondrial membrane and promotes fission (Detmer & Chan, 2007).

Mitochondrial transport along cytoskeleton is essential to distribute it to various sub-cellular locations based on intracellular energy demand. In mammals, mitochondria travel along actin and microtubule tracks (Hollenbeck & Saxton, 2005; Ligon & Steward, 2000). Varying sub-cellular distribution of mitochondria is particularly evident in neuronal cells. Measurement of rates of mitochondrial transport in neurons indicates a speed ranging from 0.4μm/min (Li et al, 2004) to 0.1-1μm/sec (Morris & Hollenbeck, 1995). The direction of mitochondrial movement is classified as anterograde (away from nucleus) and retrograde (towards the nucleus).

In neurons, mitochondria with high membrane potential undergo anterograde transport in order to recruit them to sites of high-energy demands such as pre-synaptic and post-synaptic sites and active growth cones, while mitochondria with low-membrane potential undergo retrograde transport (Miller & Sheetz, 2004). Also, the motor proteins kinesin and dynein play a critical role in anterograde and retrograde transport, respectively (Hollenbeck & Saxton, 2005). Genetic screening in *Drosophila* identified two proteins, Miro and Milton, which play a crucial role in anterograde transport of mitochondria (Guo et al, 2005; Stowers et al, 2002). Milton is a kinesin binding protein, while Miro is a mitochondrial membrane bound atypical Rho GTPase with Ca^{2+} binding EF domains (Fransson et al, 2003). In yeast model system, disruption of Miro orthologue (Gem1) results in abnormal mitochondrial morphology and defects in cellular respiration. Fig. 1.8 depicts the dynamic features of mitochondria.

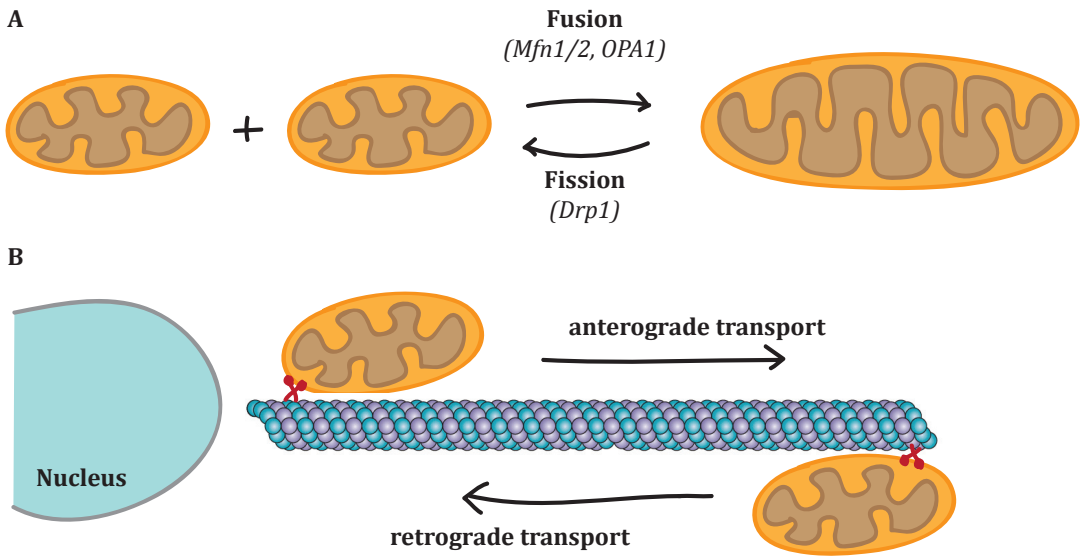

Figure 1.8 Mitochondrial dynamics

A) Mitochondrial fission and fusion regulate size and mitochondrial number, wherein two small mitochondria fuse together to form a larger one and conversely, a single mitochondrion can divide into two smaller ones by fission. **B)** Mitochondria can move along cytoskeletal tracks either in the anterograde direction (away from nucleus) or in the retrograde direction (towards the nucleus) and this ensures their availability in cellular regions that demand energy.

PINK1-Parkin in mitochondrial dynamics

Loss of function of PINK1 or Parkin in cultured cells or primary neurons from mouse models leads to a decrease in mitochondrial membrane potential and ATP production along with pronounced Drp-1 dependent mitochondrial fragmentation (Exner et al, 2007; Lutz et al, 2009). This phenotype can be rescued by either promoting fusion (expression of Mfn2 or OPA1) or by inhibiting fission (expression of dominant negative Drp-1) or by increased expression of either PINK1 or Parkin (Lutz et al, 2009). However, the opposite

is observed in PINK1 or Parkin deficient *Drosophila*, which exhibit an increase in mitochondrial fusion (Deng et al, 2008; Poole et al, 2008; Yang et al, 2008). Although the exact role of the PINK1-Parkin pathway in mitochondrial fisson/fusion is yet to be deduced, one possible hypothesis is that under conditions of cellular stress causing irreversible damage, this pathway could trigger fission in order to sequester and degrade damaged mitochondria.

Miro2 and Milton have been previously identified as potential interacting partners of PINK1 (Weihofen et al, 2009). Following up this interaction, studies were carried out in rat hippocampal neurons as well as *Drosophila* larval neurons, where overexpression of either PINK1 or Parkin was found to halt mitochondrial movement (Liu et al, 2012; Wang et al, 2011). Moreover, this study reported that Miro1 is a putative substrate of PINK1 and upon phosphorylation is degraded in a Parkin dependent manner. The working model for these findings is that Miro1 is required for mitochondrial transport across microtubules, but under conditions of mitochondrial damage, the PINK1-Parkin pathway leads to degradation of Miro1 to prevent damaged mitochondria from being transported prior to elimination by mitophagy (Fig. 1.9).

1.5.5 *Phenotype of PINK1 loss-of-function models*

As stated above, PINK1 null flies undergo adult muscle degeneration and also exhibit degeneration of a subset of dopaminergic neurons and the KO male flies are sterile (Yang et al, 2006). In addition, mutant PINK1 flies also show

reduced ATP levels and mitochondrial DNA (mtDNA) content (Clark et al, 2006; Park et al, 2006; Yang et al, 2006).

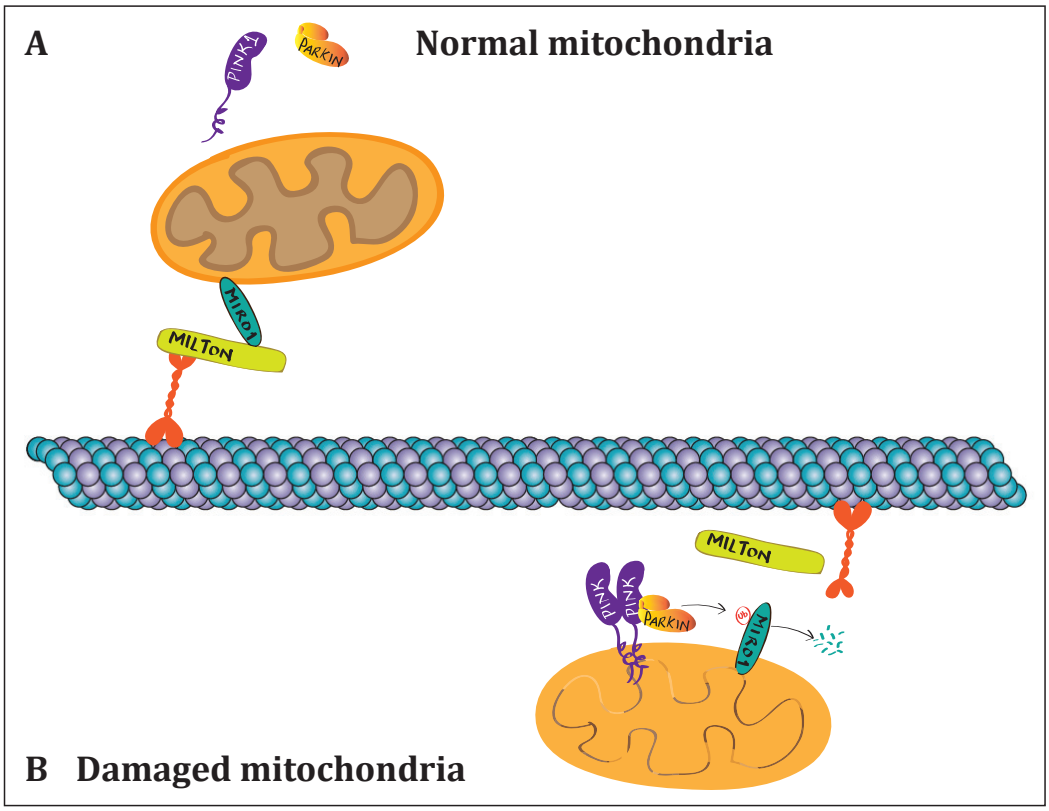

Figure 1.9 PINK1 in mitochondrial trafficking along microtubules

Illustration depicts the role played by PINK1 in regulating mitochondrial trafficking. **A)** A normal healthy mitochondria moves along microtubule by binding of mitochondrial trafficking proteins, Miro1 and Milton to Kinesin (in red), **B)** In a damaged mitochondrion, the stabilization of PINK1 and recruitment of Parkin lead to degradation of Miro1 and thus a disassembly of mitochondrial trafficking proteins occurs which halts mitochondrial movement.

The PINK1 null phenotype cannot be rescued when either PD-associated mutant forms of PINK1 are over-expressed (Yang et al, 2006) or expressed under the control of endogenous PINK1 promoter (Yun et al, 2008), consistent with PD-linked mutations being a result of loss of function. One report also

shows that in *Drosophila* neurons, PINK1 deficiency leads to defects in synaptic function due to immobilization of synaptic vesicles (Morais et al, 2009).

This can however, be rescued by addition of ATP to the synapse thus indicating that defects in synaptic vesicle transmission are secondary to a

decrease in ATP production (Morais et al, 2009). In mouse models, PINK1 deficiency itself does not lead to neuronal loss (Kitada et al, 1998; Zhou et al, 2007), however, systemic exposure to toxic insults such as MPTP, make them more vulnerable to dopaminergic neuronal loss (Haque et al, 2012). Both PINK1 KO flies as well as mouse models show a decrease in complex I activity which can be rescued by expressing wild-type PINK1 and not disease associated pathogenic mutants. However, it must be noted that unlike the scenario in fly models, KO mouse model does not show any gross change in mitochondrial morphology. Apart from studies in context of neuronal function, one study shows that PINK1 is indispensible for heart function, which requires highly developed cardiac muscle mitochondria (Billia et al, 2011). This study describes that PINK1 KO mice develop left ventricular dysfunction and cardiac hypertrophy as early as 2 months of age and this may be due to defects in mitochondrial function and an increase in oxidative stress (Billia et al, 2011).

Primary fibroblasts and neurons isolated from PINK1 KO mouse models show a significant reduction in mitochondrial membrane potential (Gautier et al, 2012; Yao et al, 2011). Whilst the enzyme activity of electron transport chain complex remained normal in PINK1 deficient cells, it was found that mPTP pore opening

was a contributing factor to the decrease in membrane potential (Gautier et al, 2012). Also, this reduction in membrane potential is specific to neuronal cells as PINK1-deficient myocytes display a high basal membrane potential perhaps due to enhanced glycolysis in these cells capable of rescuing metabolic defects of PINK1 deficiency (Yao et al, 2011).

1.6 Aims and scope of this thesis

In 2004, disease-segregating mutations in a little studied gene called PTEN-induced kinase 1 (PINK1) were identified in families with early-onset autosomal recessive Parkinson's disease (Valente et al, 2004). Whilst the function of the protein kinase remained unknown, elegant analysis in *Drosophila melanogaster* revealed that loss-of-function of PINK1 in flies led to mitochondrial deficits and this phenotype could be rescued by over-expressing another Parkinson's associated gene called parkin; thus establishing the first link between these two genes (Clark et al, 2006; Park et al, 2006). PINK1 is a unique kinase, since it localizes to the mitochondrial membrane and many cellular studies had found that under basal conditions it is rapidly degraded but its total protein levels becomes selectively stabilized in mitochondria upon mitochondrial depolarization (Narendra et al, 2010). Nevertheless when I embarked on my PhD, many fundamental questions regarding the biochemical function of PINK1 remained unknown including how it was regulated; what was its physiological substrate and how did disease mutations impact on PINK1 activity and downstream function.

Our laboratory made a crucial breakthrough when it discovered catalytically active insect orthologues of PINK1 (Woodroof et al, 2011). In the first part of my thesis (**Chapter 3**), I describe how I have exploited this knowledge to discover that Parkin is a direct substrate of PINK1. Phosphopeptide mapping revealed that PINK1 phosphorylated Parkin at a highly conserved Serine 65 residue within the Ubl domain of Parkin, which led to activation of its E3-ubiquitin ligase

activity *in vitro*. I also discovered that human PINK1 is activated upon mitochondrial depolarization, enabling it to phosphorylate Parkin at Ser65 *in vivo,* providing the first evidence of kinase activity of human PINK1. Once activated, I found that PINK1 also undergoes autophosphorylation at various residues including Thr 257 and that this can be used to monitor PINK1 activity *in vitro*.

I have also investigated whether PINK1 exists in a complex in cells and sought to determine novel binding partners of PINK1 in the hope that these might also be crucial regulators of PINK1 activity. To this end I undertook a SILAC based interactor screen aimed at identifying novel interacting partners of PINK1. A number of proteins were found to interact with PINK1 when it is stabilized in the mitochondria upon mitochondrial depolarization (**Chapter 4**). Further validation was performed by knockdown analysis of these interacting proteins in order to understand their role in regulating PINK1 activity.

A final aim of my thesis was to identify novel substrates of PINK1 by a SILAC based phosphoproteomic analysis of cells expressing either wild type or kinase inactive PINK1, subjected to mitochondrial depolarization (**Chapter 5**). From this screen I identified nine new putative PINK1 substrates. I was able to establish that a highly conserved phosphorylation site Ser111, common to three members of a Rab GTPase sub-family is regulated by PINK1. This discovery paves the way for future work to to establish the physiological relevance of these phosphorylation sites mediated by PINK1 on GTPase activity.

In addition to fundamental discoveries of the PINK1 kinase, this work establishes novel biomarkers to assess PINK1-Parkin signaling *in vivo* and also provides evidence for new signaling pathways regulated by PINK1. This opens up several avenues to explore the fundamental role of PINK1 and further understand how dysregulation of its function leads to the molecular pathogenesis of PD.

Chapter 2

Materials and Methods

2 Materials and Methods

2.1 Materials

2.1.1 *Commercial reagents*

Common salts and buffers were from BDH (Lutterworth, UK) or Sigma-Aldrich (Poole, UK). Cellophane films and All Blue Precision Plus pre-stained protein markers were from BioRad (Herts, UK). siRNA buffer was from Dharmacon. 40% (w/v) 29:1 Acrylamide: Bis-Acrylamide solution was from Flowgen Bioscience. Protein A-agarose, Protein G-Sepharose, Glutathione-Sepharose, Enhanced chemiluminescence (ECL) kit, Hyperfilm MP was purchased from GE Healthcare (Piscataway, USA). [γ^{32}P]-labeled ATP was from Perkin Elmer. Pre-cast NuPAGE Novex SDS polyacrylamide 4-12% Bis-Tris gels, NuPAGE MES and MOPS running buffer (20X), 10X NuPAGE sample reducing agent, 4X NuPAGE LDS sample buffer, NuPAGE transfer buffer, Colloidal blue staining kit, ProLong Gold, SYBR DNA gel stain were from Invitrogen (Paisley, UK). Instant Blue staining solution was purchased from Expedion (Cambridgeshire, UK). Coomassie protein assay reagent (Bradford reagent) was from Pierce (Chester, UK). Photographic developer (LX24) and liquid fixer (FX40) were from Kodak (Liverpool, UK). X-ray films were from Konica Corporation (Japan). Agarose was from Melford Laboratories (Chelsworth, UK). Restriction enzymes, DNA ligase and DNA ladder were from New England Biolabs (Hertfordshire, UK). Taq DNA polymerase in storage buffer A, sequencing grade trypsin and nucleotide mix (dNTP) were from Promega (UK). Site-directed mutagenesis was carried out using the QuikChange® site-directed- mutagenesis method

(Stratagene) with KOD polymerase (Novagen). Plasmid Maxi kits were from Qiagen Ltd (Crawley, UK). Acetonitrile (HPLC grade) and trifluoroacetic acid (TFA) were from Rathburn Chemicals (Walkerburn, UK). Protease inhibitor cocktail tablets and proteinase K were purchased from Roche (Lewes, UK). Protran BA nitrocellulose membrane (pore size - 0.45µm) was purchased from Schleicher and Schuell (Anderman and Co. Ltd., Surrey, UK). Immobilon PVDF membrane (pore size - 0.45µm) was purchased from Sigma. Adenosine 5'-triphosphate sodium salt (ATP), anti-HA-agarose, anti-FLAG-agarose, ammonium persulphate (APS), ampicillin, benzamidine, benzonase, bovine serum albumin (BSA), bromophenol blue (BPB), brilliant blue, doxorubicin, dimethyl pimelimidate (DMP), dimethyl sulphoxide (DMSO), ethidium bromide, glutathione, iodoacetamide, phenylmethanesulphonylfluoride (PMSF), Ponceau S, sodium dodecyl sulphate (SDS), sodium tetraborate, N,N,N',N'-Tetramethylethylenediamine (TEMED), triethylammonium bicarbonate, Triton-X-100 and Tween-20 were from Sigma-Aldrich (Poole, UK). Skimmed milk (Marvel) was from Premier Beverages (Stafford, UK). Maleimide-PEG 5000Da was from Iris Biotech GmBH (Germany). FLAG-Ubiquitin was purchased from Boston Biochem. HRP-conjugated secondary antibodies and SuperSignal West Dura extended duration substrate were from Thermo-scientific (Essex, UK). 3mm chromatography paper was from Whatman International Ltd (Maidstone, UK). Spin-X columns were from Corning Incorporated (NY, USA). Bio-Spin 6 size exclusion columns were purchased from BioRad (Herts, UK).

2.1.2 *Tissue culture reagents*

6 well plates, cell culture dishes and cryovials were from Corning Incorporated (NY, USA). Cell scrapers were from Costar (Cambridge, USA). Dulbecco's modified eagle medium (DMEM), Opti-MEM reduced serum media, Foetal bovine serum (FBS), tissue culture grade Dulbecco's phosphate buffered serum (PBS), Trypsin/EDTA solution, L-glutamine, non-essential amino acids, vitamins, sodium pyruvate and antibiotic/antimycotic were from GIBCO (Paisley, UK). Polyethylenimine (PEI) was from Polysciences (Warrington, PA). Penicillin/streptomycin solution, hygromycin, tetracycline, blasticidin, Zeocin, Lipfectamine 2000 were from Invitrogen. Dialysed Foetal Calf Serum (FCS) and DMEM w/o Arg, Lys and Met were from Biowest. Following unlabeled and isotopically labeled amino acids were purchased for SILAC experiments; L-arginine and L-lysine (Sigma–Aldrich) for R0K0 (light); L-arginine-HCl (U-13C6) and L-lysine-2HCl (4,4,5,5,D4) for R6K4 (medium); and L-arginine-HCl (U-13C6, 15N4) and ^{13}C-Llysine-2HCl (U-^{13}C6, ^{15}N2) for R10K8 (heavy) (Cambridge Isotope Laboratory). Polybrene, puromycin, and the MISSION™shRNA and siRNA constructs were from Sigma-Aldrich. The following chemicals used to induce mitochondrial depolarization were purchased from SIGMA: Oligomycin, Antimycin, Valinomycin, FCCP, CCCP, Dopamine, 6-OHDA, MPP+Iodide, Rotenone, Ionomycin, 3-N- Propionic acid, L-BSO (L-Buthionine Sulfoxime), H202, Diamide, Doxorubicin. Phenformin (SIGMA) and Deferiprone (SIGMA).

2.1.3 *Instruments*

The Procise 494C Sequenator was from Applied Biosystems (Foster City, USA). Centrifuge tubes, rotors and centrifuges were from Beckmann (Palo Alto, USA). Trans-Blot Cells, automatic western blot processors and gel dryer apparatus were from BioRad (Herts, UK). SpeedVacs were from CHRIST (Osterode, Germany). HPLC system components were obtained from Dionex (Camberley, UK). Thermomixer IP shakers were purchased from Eppendorf (Cambridge, UK). The Biofuge microcentrifuge was from Haraeus Instruments GmBH (Osterode, Germany). pH meters and electrodes were from Horiba (Kyoto, Japan). X-Cell SureLock Mini-cell electrophoresis systems and X-Cell II Blot modules were from Invitrogen (Paisley, UK). X-omat autoradiography cassettes, with intensifying screens, were from Kodak (Liverpool, UK). The Konica automatic film processor was from Konica Corporation (Japan). The LiCOR odyssey infrared imaging system was from LiCOR biosciences (Cambridge, UK). CO_2 incubators were from Mackay and Lynn (Dundee, UK). Tissue culture class II safety cabinets were from Medical Air Technology (Oldham, UK). The PCR thermocycler (PTC-200) was from MJ Research. The 96-well Versamax plate reader was from Molecular Devices (Wokingham, UK). The Vydac 218TP54 C18 reverse phase HPLC column was from Separations group. The LTQ-Orbitrap mass spectrometer and Nanodrop were from Thermo Scientific. Scintillation counter (Tri-Carb 2800 TR) was from Perkin-Elmer. Vibrax-VR platform shaker was from IKA. Vydac 218TP54 C18 reverse phase HPLC column was from Separations Group. Dionex HPLC system components were from Dionex GINA50 autosampler, Dionex P580 pump, DionexUVD1705 detector, EG&G Berthold Radioflow Detector LB509 and Gilson FC204 fraction collector.

2.1.4 *In-house reagents*

Primers were synthesised by the University of Dundee oligonucleotide synthesis service. Bacterial culture medium Luria Bertani (LB) broth and LB agar plates were provided by the University of Dundee media kitchen facility. The Protein Production Team at Division of Signal Transduction and Therapy (DSTT) expressed and purified all proteins used in kinase activity assays. His-SUMO-Protein purification of recombinant Parkin was carried out by the Protein Production and Assay Development (PPAD) team. His-UCHL1 was purchased from Ubiquigent (UK).

2.1.5 *Antibodies*

In-house sheep polyclonal antibodies (Table 2.1) were produced by the Division of Signal Transduction Therapy (DSTT, University of Dundee). Antisera were raised in sheep by Diagnostics Scotland (Carluke - Lanarkshire, UK). All in-house antibodies were affinity purified on CH-Sepharose covalently coupled to the corresponding antigen.

In-house phospho-specific antibodies were generated by conjugating the phopho-peptide immunogen to BSA and also separately to keyhole limpet haemocyanin (KLH). These BSA and KLH conjugates were then injected into sheep along with Freund's Adjuvant. Three weeks later, sheep were injected with a booster and the first bleed was collected a week later. This was repeated to produce a total of 3-4 bleeds. Each bleed was allowed to clot overnight at 4°C, centrifuged at 1500xg for 60min at 4°C and filtered through glass wool

prior to storage at -20°C. To purify the antibodies, serum was heated for 20min at 56°C and filtered through a 0.4 micron filter. The anti-serum was diluted with an equal volume of 50mM Tris-HCL pH 7.5 containing 2% Triton-X 100 and passed through a column of phospho-peptide immunogen couple to Sepharose. Antibodies were eluted with 50mM Glycine (pH 2.5) and dialyzed overnight against PBS. Solubility of respective non-phospho peptide was determined and dissolved in a buffer of appropriate pH range.

Antibodies were used at a concentration of 1µg/ml in 5% skimmed milk in TBST (0.1% Tween20). Phospho-specific antibodies were used at a concentration of 1µg/ml in 5% BSA in TBST supplemented with non-phospho peptide (10µg/ml) to increase specificity.

Antibody	Immunogen	Sheep Number	Bleed Number
PINK1 (175-250 human)	GST-human PINK1 (175-250)	S085D	3rd
PINK1 phospho Thr 257	CAGEYGAVT*YRKSKR (residues 250-262 of human PINK1)	S114D	3rd
PARKIN human	GST-full length PARKIN human	S966C	3rd
PARKIN phospho Ser 65	RDLDQQS*IVHIVQR [residues 60 - 72 of human PARKIN]	S210D	2nd
Rab8a phospho Ser 111	RNIEEHAS*ADVEKMR [residues 104 - 117 of human]	S503D	2nd
Rab8b phospho Ser 111	RNIEEHAS*SDVERMR [residues 104 - 117 of human]	S504D	3rd

Table 2.3 In house antibodies

Commercial antibodies used in this thesis are listed in Table 2.2. Antibodies were diluted using 5% BSA in TBST (0.1% Tween20) in appropriate dilutions.

Antibody	Catalogue Number	Company	Host	Antibody dilution
PINK1 human polyclonal	BC-100-494	Novus	Rabbit	1:1000
PARKIN human monoclonal	PRK8	SantaCruz	Mouse	1:2000
GAPDH	2118	Cell Signaling	Rabbit	1:5000
Hsp60	4870S	Cell Signaling	Rabbit	1:2000
HtrA2/OMI	2176	Cell Signaling	Rabbit	1:1000
FLAG-HRP	A8592	SIGMA		1:7000
HA-HRP	12013819001	Roche		1:2000
VDAC2	sab2501095	SIGMA	Goat	1:1000
Miro1	HPA010687	SIGMA	Rabbit	1:1000
Miro2	H00089941-A01	Abnova	Mouse	1:1000
TOMM40	18409-1-AP	Protein Tech Group Inc.	Rabbit	1:2000
TIMM50	AB23938	Abcam	Goat	1:1000
TOM22	T6319	SIGMA	Mouse	1:2000
ANT2	H00000292-B01P	Abnova	Mouse	1:1000
ANT3	14841-1-AP	Protein Tech Group Inc.	Rabbit	1:1000
C1QBP	ab24733	Abcam	Mouse	1:25,000
IMMT/Mitofilin	10179-1-AP	Protein Tech Group Inc.	Rabbit	1:1000
Total AMPK	2532	Cell Signaling	Rabbit	1:1000
Phospho T172 AMPK	2535	Cell Signaling	Rabbit	1:1000
Total ACC	3662	Cell Signaling	Rabbit	1:1000
Phospho S79 ACC	3661	Cell Signaling	Rabbit	1:1000
Total ERK1/2	9102	Cell Signaling	Rabbit	1:1000
Phospho T202, Y204 Erk1/2	4736S	Cell Signaling	Rabbit	1:1000
Total JNK 1/2	9252	Cell Signaling	Rabbit	1:1000
Phospho T183, Y185 JNK1/2	4668S	Cell Signaling	Rabbit	1:1000

Table 2.4 List of Commercial antibodies

2.1.6 *DNA constructs*

Table 2.3 and Table 2.4 list all mammalian and bacterial expression clones respectively, used in this thesis. PINK1 constructs were cloned by Dr.Maria M.

Deak, Parkin constructs by Dr. Mark Peggie and Ms. Nikki Wood. RabGTPase constructs were cloned by Dr. Mark Peggie and srGAP1 by Ms. Rachel Toth.

Protein expressed	Vector	Clone number
PINK1 – FLAG Wild-type (WT)	pcDNA5-FRT/TO	DU17461
PINK1-FLAG Kinase Dead – D384A	pcDNA5-FRT/TO	DU17462
FLAG-empty	pcDNA5 FRT/TO	DU 41457
Parkin	pCMV5	DU23306
Parkin S65A	pCMV5	DU39808
Parkin	pcDNA5-FRT/TO	DU23307
Parkin S65A	pcDNA5-FRT/TO	DU39797
HA-Parkin	pCMV5	DU23310
HA-Rab8a	pCMV-HA-1	DU35414
HA-Rab8a S111A	pCMVHA-1	DU43528
HA-Rab8b	pCMVHA-1	DU39856
HA-Rab8b S111A	pCMVHA-1	DU43564
HA-RAB13	pCMVHA-1	DU 43140

Table 2.5 List of constructs in mammalian expression vector

Recombinant Protein expressed	Vector	Clone number
GST- α – synuclein	pGEX-6	DU 30005
GST-DJ1	pGEX6P-1	DU 3391
GST-LRRK2 Kinase inactive D2017/A (1326-end)	pGEX-6	DU10594
GST-OMI	pGEX-6	DU17745
GST-GAK Kinase inactive D191/A	pGEX-6	DU38360
GST-FBXO7	pGEX-6P2	DU42160
GST-VPS35	pGEX-6	DU38573
GST-TRAP1	pGEX-6	DU17444
GST-PARL	pGEX-6	DU17743
GST-NCS1	pGEX-6	DU30410
GST-MIRO1	pGEX-6	DU38256
GST-Parkin (1-108)	pGEX6P-1	DU37370
GST-Parkin (1-108) S65A	pGEX6P-1	DU37374
MBP-PARK14 (PLA2G6)	pMAL4c	DU38361
MBP-ATP13A2	pMAL4C	DU 38296
His-SUMO-Miro2 (1-592)	pET6 His-SUMO	DU43242
His-SUMO-Miro1 (1-592)	pET6 His-SUMO	DU40832
GST-VDAC1	pGEX-6	DU30855
GST-VDAC2	pGEX-6	DU38503
GST-TOMM40	pGEX-6	Du38299

Table 2.6 List of constructs in bacterial expression vector

2.1.7 *Buffers*

All lysis buffers contain chelating agents such as EDTA and EGTA to chelate divalent cations, which are co-factors for proteolytic activity. Sodium fluoride, sodium pyrophosphate, sodium β-glycerophosphate inhibit serine/threonine protein phosphatases; and sodium orthovanadate (Na3VO4) inhibits protein tyrosine phosphatases. Benzamidine and PMSF are added to inhibit serine proteases and metallo, aspartyl, cysteinyl, and seryl proteinases. Sodium orthovanadate was prepared by several rounds of boiling, cooling to room temperature on ice and then adjusted to pH 10. This was repeated until the pH was stable at pH 10 and the solution remained colourless. This ensures that the majority of sodium orthovanadate is in the monomeric state enabling inhibition of tyrosine phosphatases. Buffers used in this thesis are listed in Table 2.5.

Buffer	Composition
Mammalian cell Lysis Buffer	25 mM Tris (pH 7.5), 1 mM EDTA, 1 mM EGTA, 1% Triton X-100, 50 mM NaF, 5 mM sodiumpyrophosphate, 1 mM sodium orthovanadate, 10 mM sodium **b**-glycerophosphate, 1 mM benzamidine, 0.2 mM PMSF, 0.1% 2-mercaptoethanol, 0.27 M sucrose and one mini Complete™protease inhibitor cocktail tablet per 10ml of lysis buffer.
Mitochondrial fractionation buffer	20 mM HEPES, 3 mM EDTA, 1% (w/v) 1 mM sodium orthovanadate,10 mM sodium β-glycerophosphate, 250 mM sucrose, 50 mM NaF, 5 mM sodium pyrophosphate, pH 7.5 and one mini Complete™protease inhibitor cocktail tablet per 10ml of lysis buffer.
Recombinant protein purification E.coli lysis buffer	50 mM Tris-HCl (pH 7.5), 150 mM NaCl, 1 mM EDTA, 1 mM EGTA, 5% (v/v) glycerol, 1% (v/v) Triton X-100, 0.1% (v/v) 2-mercaptoethanol, 1 mM benzamidine and 0.1 mM PMSF.
Recombinant protein purification wash buffer	50 mM Tris-HCl (pH 7.5), 500 mM NaCl, 0.1 mM EGTA, 5% (v/v) glycerol, 0.03% (v/v) Brij-35, 0.1% (v/v) 2-mercaptoethanol, 1 mM

	benzamidine and 0.1 mM PMSF. Equilibration buffer contained 50 mM Tris-HCl (pH 7.5), 150 mM NaCl, 0.1 mM EGTA, 5% (v/v) glycerol, 0.03% (v/v) Brij-35, 0.1% (v/v) 2-mercaptoethanol, 1 mM benzamidine and 0.1 mM PMSF.
Recombinant protein purification equilibration buffer	50 mM Tris-HCl (pH 7.5), 150 mM NaCl, 0.1 mM EGTA, 5% (v/v) glycerol, 0.03% (v/v) Brij-35, 0.1% (v/v) 2-mercaptoethanol, 1 mM benzamidine and 0.1 mM PMSF.
Recombinant protein purification elution buffer	Equilibration buffer containing 12mM Maltose/20mM L-Glutathione
Recombinant protein storage buffer	Equilibration buffer with the addition of 0.27 M sucrose and glycerol-PMSF and benzamidine were omitted.
TBS-Tween buffer	50 mM Tris-HCl (pH 7.5), 0.15 M NaCl and 0.1% (v/v) Tween-20.
5X sodium dodecyl sulphate (SDS) sample buffer	250 mM Tris-HCl (pH 6.8), 5% SDS, 5% (v/v) 2 - mercaptoethanol, 32.5% (v/v) glycerol, 0.05% bromophenol blue.
Tris-Glycine SDS running buffer	25 mM Tris-HCl (pH 8.3), 192 mM glycine, 0.1% (w/v) SDS.
Tris-Glycine transfer buffer	48 mM Tris-HCl (pH 8.3), 39 mM glycine, 20% (v/v) methanol.
Kinase assay reaction buffer	50mM Tris-HCl (pH 7.5), 0.1 mM EGTA, 10 mM MgCl2, 2 mM DTT and 0.1 mM [**γ**-32P] ATP (approx. 500 cpm/pmol).
Enhanced chemiluminescence Reagent (ECL)	**ECL1:** 100 mM Tris-HCl pH 8, 2.5 mM Luminol, 0.4 mM p-Coumaric Acid. **ECL2:** 100 mM Tris-HCl pH 8, 5.6 mM H2O2. Stored in the dark at 4ºC. Equal volumes ECL1 and ECL2 are mixed immediately before the use.

Table 2.7 List of common buffers

2.2 Methods

2.2.1 Molecular biology methods

2.2.1.1 Transformation of competent E.coli

Calcium competent E.coli DH5α cells were provided by Dr Maria Deak and Dr Mark Peggie using a previously described method (Inoue et al, 1990). For each transformation, approximately 10ng DNA was added to 35µl of competent cells and incubated on ice for 5min. Cells were then subjected to heat shock at 42°C for 90 s in a water bath to induce the uptake of DNA and briefly placed back

on ice. Bacteria were streaked onto LB agar plates containing 100µg/ml ampicillin and plates incubated at 37°C overnight. DNA for mammalian cell transfection was amplified in *E.coli* DH5α strain and for bacterial protein expression was transformed in *E.coli* BL21 DE3 RIL (codon plus) cells (Stratagene).

2.2.1.2 Purification of plasmid DNA from E.coli

Transformed DH5α E.coli were cultured in 150ml LB containing 200mg/L ampicillin at 37°C overnight and cells were pelleted by centrifugation at 3000rpm for 15min. Plasmid DNA was purified using a Qiagen plasmid Maxi kit according to the manufacturer's instructions. This yields an approximate of 0.3-1mg plasmid DNA.

2.2.1.3 Measurement of DNA and RNA concentration

DNA or RNA was diluted in sterile MilliQ water in a disposable cuvette and the absorbance at 260nm was measured. MilliQ water alone was used as a blank control. A 50µg/ml solution of double-stranded DNA, a 30µg/ml solution of single stranded DNA oligonucleotide or a 40µg/ml solution of single-stranded DNA has an absorbance of 1.0. The absorbance at 280nm was also measured to allow the calculation of the 260nm:280nm ratio, an indicator of DNA purity. A 260:280 ratio greater than 1.6 is indicative of a highly pure sample.

2.2.1.4 Restriction enzyme digests of plasmid DNA

Restriction digests were carried out using 1µg DNA in the presence of 2µl 10X stock of the appropriate digestion buffer and 1U of restriction enzyme in a final volume of 20µl. Reactions were incubated at 37°C for 3hrs and analyzed via

agarose gel electrophoresis.

2.2.1.5 Agarose gel electrophoresis

The appropriate amount of agarose (in order to generate 0.8-1.5% agarose gels) was boiled in 1X TAE buffer. SYBR stain was added and the solution cooled before being poured into a plastic mould. Electrophoresis was carried out at 120V for 40- 60min.

2.2.1.6 DNA mutagenesis

All mutagenesis was performed using the QuikChange site directed mutagenesis method (Stratagene) with KOD polymerase (Novagen). DNA constructs were verified by DNA sequencing.

2.2.1.7 DNA sequencing

The sequencing of plasmid or PCR product DNA was carried out by the DNA sequencing service (School of Life Sciences, University of Dundee) using DYEnamic ET terminator chemistry (Amersham Biosciences) on Applied Biosystems automated DNA sequencers.

2.2.2 Mammalian Cell culture

2.2.2.1 Cell culture

Cells were maintained at 37°C in 5% CO_2 water saturated incubator and allowed to reach 80-90% confluency prior to passaging. Human Embryonic Kidney 293 (HEK293) and HEK293T were grown in Dulbecco's modified eagle medium (DMEM) supplemented with 10% (v/v) foetal bovine serum (FBS), 2mM L-glutamine, 100U/ml penicillin and 0.1mg/ml streptomycin. Mouse embryonic

fibroblasts (MEFs) were grown in DMEM containing 10% (v/v) FBS, 2mM L-glutamine, 100U/ml penicillin and 0.1mg/ml streptomycin, 1X non-essential amino acids and 1mM sodium pyruvate. HEK293 Flp In TRex stable cell lines were maintained in the same media supplemented with 15µg/ml of Blasticidin and 100µg/ml of Hygromycin and filtered through a 0.2µm vacuum filtration unit.

2.2.2.2 Freezing/thawing of cell lines

Confluent cells grown in T-75 flasks were trypsinized and collected in culture media by centrifuging at 1200 rpm for 3 min. Culture media were aspirated and cells resuspended in 3 ml of freezing media (50% DMEM/ 40%FBS/ 10% DMSO). Aliquots of cells (1 ml) in cryovials were stored in a Nalgene Mr Frosty Freezing Container at -80°C for 2 days, and transferred to liquid nitrogen. To thaw the cells, each vial was placed in 37°C water bath for 3 min and cells were added to a T-25 flask containing 10 ml of culture media. Cells were allowed to attach and given a media change a day later to remove trace amounts of DMSO.

2.2.2.3 Transfection of mammalian cells

HEK293/HEK293T cells grown to 30-40% confluency in 10-cm-diameter dishes were transiently transfected using Polyethylenimine (PEI) from Polysciences. PEI stock (1 mg/ml) was prepared by dissolving it in 20 mM HEPES (pH 7). Aliquots were filter sterilized (0.22 µm) and stored at -80°C. For transfection of one 10 cm dish, 5 µg of DNA and 20 µg of PEI (1:4 ratio) were added to 1 ml of DMEM media (antibiotic-and serum-free). The mixture was vortexed for 20 sec and further incubated at room temperature for 15 min before being added to cells. Cells were harvested 36-48 h post transfection.

2.2.2.4 Generation of stable cell lines

To ensure low-level uniform expression of recombinant proteins, manufacturer's instructions (Invitrogen) were followed to generate stable cell lines that express FLAG-tagged forms of proteins (cDNA subcloned into pcDNA5-FRT-TO plasmid) in a tetracycline inducible manner. Flp-In T-REx-293 host cells containing integrated FRT recombination site sequences and Tet repressor, were co-transfected with 9 µg of pOG44 plasmid (which constitutively expresses the Flp recombinase), and 1 µg of pcDNA5/FRT/TO vector containing a hygromycin resistance gene for selection of the gene of interest with FLAG tag under the control of a tetracycline-regulated promoter. Cells were selected for hygromycin and blasticidin resistance three days after transfection by adding new medium containing hygromycin (100 µg/ml) and blasticidin (7.5 µg/ml). After 3 weeks of selection, colonies were trypsinized and expanded. Expression of the recombinant protein was induced with 0.1 µg/ml of tetracycline for 24 hours.

2.2.2.5 siRNA knockdown of PINK1 expression

To knock down PINK1 gene expression, HEK293 cells were transfected separately with two sets of Mission siRNA oligos (Sigma) designated as siRNA #1 (5'-CCAUCAAGAUGAUGUGGAATT-3') or siRNA #2 (5'-CAGAGAAGUGUUGUGUGGATT-3') and scrambled control siRNA (Sigma). Cells were transfected using TransFectin Lipid Reagent (Bio-Rad) and incubated for 48 h before CCCP treatment. The final concentration of siRNA was 30 nM. Over-expression of additional genes in a knockdown background was achieved via co-transfection with the siRNA.

2.2.2.6 shRNA knockdown

The MISSION pLKO.1-puro lentivirus plasmid vector (3 µg) containing the shRNA sequence (refer to Table 2.6) was transfected together with packaging (3 µg) and envelope (3 µg) plasmids in a 10 cm dish containing HEK293T cells of 70% confluency using 36 µl of PEI. The lentiviral particles were collected 72 h after transfection, filtered (0.45 µm pore size) and used to infect HEK293Flp In TRex cells stably expressing PINK1 in the presence of 5µg/ml polybrene. Lentiviral particles (5 ml/10 cm-dish) were used to infect cells at 60-70% confluency. The cells were selected with 3 µg/ml puromycin and experiments carried out within a week after infection.

2.2.2.7 Treatment of cells with mitochondrial stimulations

To uncouple mitochondria, cells were treated with 10 µM CCCP (Sigma) dissolved in DMSO. An equivalent volume of DMSO was used as a control. In addition, cells were incubated with the following agonists for 3 h including: 1 µM Oligomycin (Sigma), 10 µM Antimycin A (Sigma), 2 µM Valinomycin (Sigma), 10 µM FCCP (Sigma), 10 µM Dopamine (Sigma), 100 µM 6-Hydroxy-dopamine (Sigma), 100 µM MPP+ (Sigma), 1 µM rotenone (Sigma), 5 µM ionomycin (Sigma), 10 µM 3-nitropropionic acid (Sigma), 50 µM L-BSO (Sigma), 50 µM (Sigma), 0.5 µM Phenformin (Sigma). Cells were treated with 1 mM Deferiprone (3-Hydroxy-1,2-dimethyl-4 (1H)-pyridone; Sigma) for 24 h.

Target Gene	shRNA no.	TRC Number	Sequence	Region
TOMM40	#1	TRCN0000219098	GTACCGGCAAAGGGTTGAGTAACCATTTCTCGAGAAATGGTTACTCAACCCTTTGTTTTTTG	**CDS**
	#2	TRCN0000231155	CCGGTGAATGGCGCTTCGGGATTCTCTCGAGAGAATCCCGAAGCGCCATTCATTTTTG	**3'UTR**
TOM22	**#1**	TRCN0000060883	CCGGGCAGATACTTCTAGGACCTAACTCGAGTTAGGTCCTAGAAGTATCTGCTTTTTG	**CDS**
	#2	TRCN0000230173	CCGGGCAGCCATGCAGATGGTTATTCTCGAGAATAACCATCTGCATGGCTGCTTTTTG	**3'UTR**
IMMT	**#1**	TRCN0000135616	CCGGGTCTAGAAATGAGCAGGTTTACTCGAGTAAACCTGCTCATTTCTAGACTTTTTTG	**3'UTR**
	#2	TRCN0000136189	CCGGGCTAAGGTTGTATCTCAGTATCTCGAGATACTGAGATACAACCTTAGCTTTTTTG	**CDS**
TIMM50	**#1**	TRCN0000072464	CCGGGACACCATGTAAAGGATATTTCTCGAGAAATATCCTTTACATGGTGTCTTTTTG	CDS
	#2	TRCN0000072463	CCGGGCTACCATACCCAGCTAATTTCTCGAGAAATTAGCTGGGTATGGTAGCTTTTTG	**3'UTR**
C1QBP	**#1**	TRCN0000057103	CCGGCCCAATTTCGTGGTTGAAGTTCTCGAGAACTTCAACCACGAAATTGGGTTTTTG	CDS
	#2	TRCN0000057104	CCGGGCGAAATTAGTGCGGAAAGTTCTCGAGAACTTTCCGCACTAATTTCGCTTTTTG	CDS
MIRO2	**#1**	TRCN0000072918	CCGGCCCAGAATTCTCAGGGCTCTACTCGAGTAGAGCCCTGAGAATTCTGGGTTTTTG	**3'UTR**
	#2	TRCN0000072919	CCGGCGTCTACAAGCACCATTACATCTCGAGATGTAATGGTGCTTGTAGACGTTTTTG	CDS
VDAC2	**#1**	TRCN0000150602	CCGGGATCTCAACAAGAGCTGTATTCTCGAGAATACAGCTCTTGTTGAGATCTTTTTTG	**3'UTR**
	#2	TRCN0000151179	CCGGGCAGCTAAATATCAGTTGGATCTCGAGATCCAACTGATATTTAGCTGCTTTTTTG	CDS
Scramble			CCGGCCTAAGGTTAAGTCGCCCTCGCTCTAGCGAGGGCGACTTAACCTTAGGTTTTT	

Table 2.8 List of shRNA sequences used in this thesis

2.2.2.8 Cell lysis and mitochondrial fractionation

Cells were lysed using mammalian cell lysis buffer as listed in Table 2.5. Lysates were clarified by centrifugation at 13,000 rpm for 10 min at 4 °C and the supernatant was collected. For mitochondrial fractionation, cells were lysed in mitochondrial fractionation buffer (refer to Table 2.5) at 4 °C. Cells were disrupted using a glass hand held homogeniser (20 passes) and lysates clarified by centrifugation for 10 min at 800g at 4°C. The supernatant was removed and further centrifuged at 16,600g for 10min. The resultant supernatant was retained as the cytosolic fraction. The pellet containing the mitochondrial fraction was resuspended in buffer containing 1% Triton X-100 and centrifuged at 13,000 rpm for 10 min. This final supernatant contained solubilized mitochondrial proteins. All lysates were snap-frozen at -80°C until use.

2.2.2.9 Gel filtration of mitochondrial fraction

The AKTA explorer chromatography system was operated according to manufacturer's instructions using Unicorn 4.1 software. All buffers, lysates and markers were sterile filtered before loading onto the column. A HiLoad^{TM} 26/60 Superdex^{TM} 200 preparative grade column was attached and equilibrated overnight with three column volumes of gel filtration buffer (50 mM Tris/HCl pH 7.4, 1 mM EDTA pH 8.0, 150mM NaCl, 0.1% (v/v) 2-mercaptoethanol). Flp In TRex HEK 293 cells stably expressing wild-type PINK1 were induced for protein expression and treated with either DMSO or 10 µM CCCP for 3 h. Cells were subjected to mitochondrial fractionation as described in 2.2.3.9. Lysates were

snap frozen before centrifugation and stored at -80°C until required. Lysates were thawed on ice and cleared by centrifugation at 15,000 g for 30 min. The supernatant was sterile filtered on 0.22 µm Steriflip columns and the protein concentration of each lysate was estimated. Equal amounts (5 mg, 1 ml) of each protein lysate were loaded onto the Superdex column. Between runs the column was washed through with two column volumes of buffer. Fractions of 1 ml (200) were collected at a flow rate of 1.5 ml/min. Molecular weight markers from BioRad with added Dextran blue were resuspended in water and run after the lysates. The void volume of the column is 100 ml (Dextran Blue 2000 kDa is the marker for the void volume). The 670 kDa marker (thyroglobulin) eluted in fractions 117-129. The 158 kDa marker (bovine γ-globulin) eluted in fractions 165-180. The 44 kDa marker (chicken ovalbumin) eluted in fractions 207-225. Fractions from 98 to 228 were transferred to eppendorfs and snap-frozen. 100 µl of every third sample from 99 to 207 was denatured in LDS sample buffer, boiled for 5 min at 95 °C and 5 µl of each denatured fraction was subjected to western blot analysis.

2.2.3 Protein Biochemistry

2.2.3.1 Purification of recombinant proteins

Maltose binding protein (MBP) fusion proteins were purified by the following protocol: briefly, BL21 Codon plus transformed cells were grown at 37 °C to an OD^{600} of 0.3, then shifted to 16 °C and induced with 250 µM IPTG (isopropyl β-D-thiogalactoside) at OD^{600} of 0.5 and were further grown at 16°C for 16 h.

Cells were pelleted at 4000 rpm., and then lysed by sonication in lysis buffer. Lysates were clarified by centrifugation at 30 000g for 30 min at 4°C followed by incubation with 1 ml per litre of culture of amylose resin for 1.5 h at 4°C. The resin was washed thoroughly in wash buffer, then equilibration buffer, and proteins were then eluted. Proteins were dialysed overnight at 4 °C into storage buffer, snap-frozen and stored at -80°C until use. GST-fusion proteins were purified by similar methods except that recombinant GST-fusion proteins were affinity purified on glutathione-Sepharose and eluted with buffer containing 20 mM glutathione. GST-VPS35 was cleaved with GST-PreScission protease at **4°**C overnight. His-UCHL1 was purchased from Ubiquigent (UK). His-SENP1 catalytic domain (residues 415–643) was purified as follows: transformed BL21 cells were grown in LB (Luria Broth), 50 µg/ml carbenicillin until OD^{600} of 0.6, then induced with 300 mM IPTG (isopropyl β-D-1-thiogalactopyranoside) and expressed overnight at 15 °C. Cells were collected, lysed and protein purified using Ni^{2+} -nitriloacetic acid- Sepharose chromatography, followed by dialysis into 50 mM HEPES pH 7.5, 10% glycerol, 150 mM NaCl, 1 mM DTT).

His-SENP1 catalytic domain (residues 415–643) was purified as follows: transformed BL21 cells were grown in LB (Luria Broth), 50 mg/ml carbenicillin until OD600. 0.6, then induced with 300 mM IPTG (isopropyl b-D-1-thiogalactopyranoside) and expressed overnight at 15°C. The cells were collected, lysed and the protein was purified using Ni^{2+}-nitriloacetic acid-Sepharose chromatography, followed by dialysis into 50mM HEPES pH 7.5, 10% glycerol, 150 mM NaCl, 1 mM DTT).

Untagged Parkin (His-SUMO cleaved) was expressed and purified using a modified protocol from Helen Walden's laboratory (Chaugule et al, 2011). BL21 cells were transformed with His-SUMO tagged Parkin constructs, overnight cultures were prepared and used to inoculate 12x1L LB medium, 50 mg/ml carbenicillin, 0.25 mM $ZnCl_2$. The cells were grown at 37°C until the OD^{600} was 0.4 and the temperature was reduced to 16 °C. At OD^{600} of 0.8, expression was induced with 25 mM IPTG. After overnight incubation the cells were collected and lysed in 75 mM Tris pH 7.5, 500 mM NaCl, 0.2 % Triton X-100, 25 mM imidazole, 0.5 mM Tris(2- carboxyethyl)phosphine (TCEP), 1 mM Pefablok, 10 mg/ml Leupeptin. After sonication and removal of insoluble material, His-SUMO-Parkin was purified via Ni^{2+}-NTA-Sepharose chromatography. The protein was collected by elution with 400 mM imidazole in 50 mM Tris, pH 8.2, 200 mM NaCl, 10 % glycerol, 0.03 % Brij 35, 0.5 mM TCEP. This was dialysed twice against 50 mM Tris pH 8.2, 200 mM NaCl, 10 % glycerol, 0.5 mM TCEP in the presence of His-SENP1 (415–643) at a ratio of 1 mg His-SENP1 per 5 mg His-SUMO-Parkin. The protease, the His-SUMO tag and any uncleaved protein was removed by two subsequent incubations with Ni^{2+}NTA–Sepharose. The cleaved Parkin was further purified in 50 mM Tris, pH 8.2, 200 mM NaCl, 20 % glycerol, 0.03 per cent Brij-35, 0.5 mM TCEP over a Superdex 200 column.

2.2.3.2 Estimation of protein concentration

Protein concentration of purified proteins and cleared cell lysates was evaluated using the Bradford method in a 96 well plate format (Bradford, 1976). 0.25 ml of Bradford reagent (Pierce) was added to 5µl of diluted sample (cell lysates were usually diluted 20-fold in water). 5ul of water was used as a blank. For a

standard curve 5ul of serial dilutions of BSA were used (1, 0.5, 0.25 and 0.125 mg/ml). Absorbance at 595 nm was measured using a 96 well plate reader. All samples were measured in triplicate and a standard curve was generated for each analysis. Bradford method is a colorimetric protein assay, based on an absorbance shift from 465 nm (red) to 595 nm (blue) upon binding to proteins. The Coomassie dye binds to arginines, aromatic amino acids, and histidines. For purified proteins, Coomassie staining of polyacrylamide gel verified sample purity additionally.

2.2.3.3 Covalent coupling of antibodies to Protein G-Sepharose

Antibodies were covalently coupled to protein G-Sepharose with a dimethyl pimelimidate (DMP) cross-linking procedure. DMP has two functional imine groups, which interact with free amine groups at pH range 7.0-10.0 to form amidine bonds. Antibody-coupled beads (1 µg antibody per 1 ul beads) were prepared by incubating antibody with Protein – G Sepharose beads at 4°C for 1hr. The beads were washed 5 times with 10 volumes of 0.1 M sodium borate pH 9 and then resuspended in 10 volumes of 0.1 M sodium borate pH 9 containing freshly added dimethyl pimelimidate (a fresh batch used every time) to a concentration of 20 mM and incubated for 30 min at room temperature with gentle mixing. The beads were pelleted and then reincubated with dimethyl pimelimidate. The beads were washed 4 times with 10 volumes of 50 mM glycine pH 2.5 to remove all the antibodies that were not covalently coupled to the beads. The beads were then washed twice with 0.2 M Tris-HCl pH 8 and

incubated in this buffer for a further 2 h at room temp with gentle mixing to ensure that any residual DMP was quenched by reaction with the amine group of Tris. The antibody-coupled beads were stored in PBS containing 0.02% (w/v) sodium azide at 4ºC for up to one month.

2.2.3.4 Immunoprecipitation

For immunoprecipitation, unless otherwise indicated, 1 mg of cell lysate was incubated with 5 µg of coupled antibody for 2 h at 4°C or O/N for protein pull-down. The mixture was centrifuged for 1 min at 800 g and supernatant was removed. For kinase assays, the immunoprecipitates were washed twice with 1 ml of lysis buffer containing 0.5 M NaCl and twice with 1 ml of Buffer A (50 mM Tris pH 7.5, 0.1 mM EGTA) and assayed as described in section 2.2.4.1. For co-immunoprecipitation, the immunoprecipitates were washed twice with 1 ml of lysis buffer containing 0.15 M NaCl and once with 1 ml of Buffer A, resuspended in 1x SDS Sample Buffer and subjected to Sodium dodecyl sulphate polyacrylamide gel electrophoresis (SDS-PAGE). All procedures were carried out at 4 °C.

2.2.3.5 Resolution of protein samples via SDS-PAGE

SDS-PAGE is used to separate proteins on the basis of their apparent molecular weight. The anionic detergents, sodium dodecyl sulphate (SDS) and lithium dodecyl sulphate (LDS), bind to proteins giving them a resulting negative charge that is proportional to their mass. As a result, the speed of migration of a protein through a constant gradient polyacrylamide gel matrix is a linear function of the logarithm of its molecular weight, with small proteins migrating faster than large proteins. Separation gels were prepared containing 375 mM

Tris HCl pH 8.6, 0.1 % SDS, 8-15 % acrylamide (depending on the size of the protein) with final addition of N,N,N',N'- tetramethylethylenediamine (TEMED) and ammonium persulphate (APS) to initiate polymerisation. Gels were allowed to polymerise for 30min. Stacking gels contained 125 mM Tris HCl pH 6.8, 0.1 % SDS, 4 % acrylamide, TEMED and APS.

Cell lysates, immunoprecipitates and purified proteins were prepared in 1X LDS sample buffer containing 1X sample reducing agent (for use with pre-cast NuPAGE 4-12% Bis-Tris gels) or 1X SDS sample buffer (for use with homemade acrylamide gels) and heated to 92 °C for 2 min. Samples were loaded onto gels along with Precision plus protein standards which have apparent molecular weight markers of 250, 150, 100, 75, 50, 37, 25, 20, 15 and 10 kDa. Electrophoresis was carried out at 90 V for 30 min prior to an increase of the voltage to 180V for a further 1 hr and gels were either stained or transferred for immunoblotting.

2.2.3.6 Coomassie staining of polyacrylamide gels

Gels were incubated in Instant Blue solution for 1 hr followed by de-staining in water. Gels were scanned on a Li-Cor Odyssey infrared system for imaging and quantification. For mass spectrometry, gels were stained with Colloidal coomassie (Invitrogen) according to the manufacturer's instructions.

2.2.3.7 Desiccation of polyacrylamide gels

Gels containing ^{32}P-labeled proteins were dried to enhance autoradiographic signal. Gels were incubated in 5 % glycerol prior to encasement between two sheets of cellophane. The gel was then dried in a GelAir Dryer.

2.2.3.8 Autoradiography of polyacrylamide gels

Coomassie stained gels were placed in an X-Omat autoradiography cassette and exposed to Hyperfilm MP for different lengths of time. Typically exposures were carried out for between 30 min to 48 hr in order to detect radioactively labeled proteins. For long exposures, the cassette was placed in -80 °C freezer to improve autoradiographic signal. Films were developed using a Konica automatic developer. For identification of phosphorylation sites by mass spectrometry, wet gels were autoradiographed before excision of the bands.

2.2.3.9 Transfer of proteins to nitrocellulose membranes

Gels after being subjected to electrophoresis were assembled into a gel membrane ‘sandwich’ and loaded into a BioRad Mini Trans-blot electrophoretic transfer cell. Prior to assembly, nylon sponge pads, Whatman 3mm filter papers and nitrocellulose membranes were soaked in transfer buffer containing 20 % (v/v) methanol. The transfer cell was submerged in transfer buffer and electrotransfer carried out at 100 V for 1.5 hr.

2.2.3.10 Immunoblotting

Membranes were blocked for 30 min in TBS-Tween buffer containing 5 % (w/v) skimmed milk or BSA and incubated with the appropriate antibody at 4°C

overnight. Membranes were washed 3 times with TBS-T, incubated with horseradish peroxidase (HRP)-conjugated secondary antibodies for 1 hr and washed another 3 times with TBS-T. Finally, membranes were incubated with the enhanced chemiluminescence reagent (either in-house or commercial reagents) and exposed to X-ray films for different lengths of time. As before, films were developed using a Konica automatic developer.

2.2.4 In vitro assays

2.2.4.1 Kinase assays

In assays utilising *E.coli*-expressed wild-type or kinase dead (D359A) MBP-TcPINK1, reactions were set up in a volume of 40 µl, with substrates at 2 µM and kinase at 0.5 µg in 50 mM Tris-HCl (pH 7.5), 0.1 mM EGTA, 10 mM $MgCl_2$, 2 mM dithiothreitol (DTT) and 0.1 mM [γ-^{32}P] ATP (approximately 50 cpm/pmol). Assays were incubated at 30°C with shaking at 1200 rpm and terminated after the indicated time by addition of SDS sample buffer. In mammalian HEK293 immunoprecipitation kinase assays, C-terminal-FLAG tagged wild-type or kinase dead (D384A) PINK1 was immunoprecipitated from 5 mg of mitochondrial enriched extracts using anti-FLAG agarose beads and activity measured in a reaction volume of 40 µl consisting of 50 mM Tris-HCl (pH 7.5), 0.1 mM EGTA, 10 mM MgCl2, 2 mM DTT, 0.1 mM [γ-^{32}P] ATP (2000 cpm/pmol) and 5 µM of indicated substrate. Assays were incubated at 30°C with shaking at 1200 rpm and terminated after 30 min by addition of SDS sample buffer. For all assays, reaction mixtures were resolved by SDS-PAGE. Proteins were detected by Coomassie staining and gels were imaged using an Epson scanner and

dried completely using a gel dryer (Bio-Rad). Incorporation of [γ-^{32}P] ATP into substrates was analysed by autoradiography using Amersham Hyper-Film ECL.

Calculation of specific activity of γ-^{32}P ATP for *in vitro* kinase assay

The bench limit for usage of ATP is 8 MBq for *^{32}P*. The activity of neat γ-^{32}P ATP ordered is 3000 mCi/mmol at a concentration of 10mCi/ml. For a working stock, a custom-made order pre-diluted to a concentration of 350 µCi/ml (diluted with 1 mM cold ATP) is purchased. Usually a volume of 2.5 ml is purchased and made into 25 aliquots of 100µl each and stored in the communal freezer in the radioactive room. Note that under normal circumstances, our lab manager Allison Bridges takes care of making aliquots. Going by the bench limit, not more than 6 aliquots (100 µl each) can be used at any given time on your bench. Experiments that exceed bench limit must be performed in the enclosed radioactive room.

For a kinase assay we require a final concentration of 100 µM ATP. 1 mCi ideally corresponds to 2.22 x 10^9 cpm and hence this would approximately correspond to a count of 500,000 cpm per µl measured from an aliquot of γ-^{32}P ATP, using a scintillation counter (this value depends on the amount of decay that the radioactive material has undergone). The final concentration of ATP in a kinase assay is 100 µM. The calculation for specific activity of γ-^{32}P ATP used in our assay is as follows:

Reaction volume: 40 µl

Amount of γ-^{32}P ATP from aliquot to achieve a concentration 100 µM = 4 µl

(A) 4 µl contains 4 x 500,000cpm = 20,00,000 cpm of hot radioactive tracer

Molar concentration of 100 µM cold ATP = 100 pmol

(B) A 40 µl reaction will have, 40 x 100 = 4000 pmols of cold ATP

Specific activity of γ-^{32}P ATP used in a kinase assay = **(A)/(B)**

= 20,00,000/4000

= 500 cpm/pmol

For reactions that require a higher specific activity, the neat ATP can de diluted less to achieve more than >500,000 cpm/µl.

For calculation of stoichiometry of incorporation, the kinase assay reaction is resolved by SDS-PAGE and substrate bands are excised and counted in a scintillation counter. Based on the number of counts obtained we can calculate the number of moles of ATP incorporated per mole of protein used in the assay (Hastie et al, 2006). Stoichiometry is represented as mol of ATP/mol of protein.

2.2.4.1 Ubiquitylation assay

Wild-type or Ser65Ala Parkin (2 mg) were initially incubated with the indicated amounts of E. coli-expressed wild-type or kinase-inactive (D359A) MBP-TcPINK1 in a reaction volume of 25 ml (50 mM Tris-HCl (pH 7.5), 0.1 mM EGTA, 10 mM MgCl2, 1 % β-mercaptoethanol and 0.1 mM [γ-32P] ATP (approx. 500 cpm/pmol); in parallel to confirm the phosphorylation). Kinase assays were incubated at 30°C with shaking at 1000 rpm for 60 min followed by addition of ubiquitylation assay components and Mastermix to a final volume of 50 ml (50 mM Tris-HCl (pH 7.5), 0.05 mM EGTA, 10 mM MgCl2, 0.5%

2-mercaptoethanol, 0.12 mM human recombinant E1 purified from Sf21 insect cell line, 1 mM human recombinant UbcH7 purified from E. coli, 0.05 mM FLAG-Ubiquitin (Boston Biochem) and 2 mM ATP. Ubiquitylation reactions were incubated at 30°C with shaking at 1000 rpm for 60 min and terminated by addition of SDS sample buffer. For all assays, reaction mixtures were resolved by SDS-PAGE. Ubiquitylation reactions were subjected to immunoblotting with anti-FLAG antibody (Sigma, 1:7500), anti-Parkin or anti-MBP antibodies. Incorporation of [γ-^{32}P] ATP into substrates was analysed by autoradiography.

2.2.4.2 Lambda phosphatase assay

C-terminal-FLAG-tagged wild-type or kinase-inactive (D384A) PINK1 were immunoprecipitated from 5mg of mitochondrial enriched extracts using anti-FLAG agarose beads. Wild-type PINK1 was incubated with or without 1000 U of Lambda phosphatase (NEB) in a reaction volume of 40 µl consisting of 50 mM Tris pH 7.5, 1 mM $MnCl_2$ and 2 mM DTT. In addition wild-type PINK1 was treated with 1000 U of lambda phosphatase in the presence of 50 mM EDTA. Assays were incubated at 30 °C for 30 min with shaking at 1200 rpm. The beads were washed three times in 50 mM Tris pH7.5, 0.1 mM EGTA and then utilized in an *in vitro* kinase assay with GST-parkin UBL (1-108) as the substrate. Samples were further analyzed as described in 2.2.6.1.

2.2.5 Mass spectrometry

2.2.5.1 Sample preparation

Proteins were reduced with 10 mM DTT at 92°C for 5min and alkylated with 50mM Iodoacetamide before resolving by SDS-PAGE and stained using Colloidal coomassie staining solution. Samples for mass spectrometry were prepared in a laminar flow hood. Protein bands were excised from the gel using a sterile scalpel and placed in a 1.5 ml Eppendorf tube. Gel pieces were washed sequentially with 0.5 ml of water, 50% acetonitrile/water, 0.1 M NH4HCO3 and 50% acetonotrile/50 mM NH4HCO3. All washes were performed for 10 min on a Vibrax shaking platform. Once colourless, gel pieces were shrunk with 0.3 ml acetonitrile for 15 min. Acetonitrile was aspirated and trace amounts removed by drying sample in a Speed-Vac. Gel pieces were then incubated for 16 h with 5 mg/ml trypsin in 25mM triethylammonium bicarbonate (TEA) at 30 °C on a shaker. An equal volume of acetonitrile (same as trypsin) was added to each sample and further incubated on a shaking platform for 15 min. The supernatants were transferred to clean tubes and dried by Speed-Vac. Another extraction was performed by adding 100 ml 50 % acetonitrile/2.5 % formic acid for 15 min. This supernatant was combined with the first extract and dried by Speed Vac.

2.2.5.2 Mass spectrometry analysis

All mass spectrometric (MS) analysis was performed by Dr. David Campbell, Robert Gourlay and Joby Varghese (College of Life Science, University of Dundee). Analysis of the tryptic peptides by LC-MS were performed on a

Thermo LTQ-Orbitrap system. The MS data was analysed through the Mascot search engine (www.matrixscience.com) against the human International Protein Index database. Tryptic phosphopeptides were identified by LC-MS on an ABI 4000 Q-TRAP system using precursor ion scanning in negative mode to search for release of the (PO3)- ion (-79 Da) allowing for +/-1 Da (Williamson et al, 2006), followed by MS/MS analysis in positive mode. The resulting data files were searched against the appropriate sequence, using Mascot run on an in-house server, with a peptide mass tolerance of 1.2 Da, a fragment mass tolerance of 0.8 Da, and with variable modifications allowing for phosphorylation of serine/threonine or tyrosine and for methionine oxidation or dioxidation. MassFingerPrinting results from Mascot were viewed using a software package from ProteinGURU (www.proteinguru.com).

2.2.5.3 *In vitro 32P-labelling of PARKIN and identification of phosphorylation sites*

GST-Parkin (1 μg) purified from *E. coli* was incubated with 2 μg of either wild type MBP-TcPINK1 (1-570) or kinase dead MBP-TcPINK1 (D359A) for 60 min at 30 °C in 50 mM Tris-HCl (pH 7.5), 0.1 mM EGTA, 10 mM MgCl2, 2 mM dithiothreitol (DTT) and 0.1mM [γ-^{32}P] ATP (approximately 20,000 cpm/pmol) in a total reaction volume of 25 μl. The reaction was terminated by addition of LDS sample buffer with 10 mM DTT, boiled, and alkylated with 50 mM iodoacetamide before samples were subjected to electrophoresis on a Bis-Tris 4-12% polyacrylamide gel, which was then stained with Colloidal Coomassie blue (Invitrogen). Phosphorylated parkin was digested with trypsin and >95% of

^{32}P radioactivity incorporated in the gel bands was recovered. Peptides were chromatographed on a reverse phase HPLC Vydac C_{18} column (Cat# 218TP5215, Separations Group, Hesperia, CA) equilibrated in 0.1 % (v/v) trifluoroacetic acid and the column developed with a linear acetonitrile gradient at a flow rate of 0.2 ml/min and fractions (0.1 ml each) were collected and analysed for ^{32}P radioactivity by Cerenkov counting. Isolated phosphopeptides were analysed by LC-MS-MS on a Dionex 3000 nano liquid chromatography system coupled to a Thermo LTQ-orbitrap mass spectrometer. The resultant data files were searched using Mascot (www.matrixscience.com) run on an in-house system against a database containing the parkin sequence, with a 10 p.p.m. mass accuracy for precursor ions, a 0.8 Da tolerance for fragment ions, and allowing for Phospho (ST), Phospho (Y), Oxidation (M) and Dioxidation (M) as variable modifications. Individual MS/MS spectra were inspected using Xcalibur 2.2 software. The site of phosphorylation of these ^{32}P-labeled peptides was determined by solid-phase Edman degradation on an Applied Biosystems 494C sequencer of the peptide coupled to Sequelon-AA membrane (Applied Biosystems) as described previously (Campbell & Morrice, 2002).

2.2.5.4 In vivo Phospho-site mapping of PINK1 substrate

Flp-In T-Rex HEK 293 cell lines stably expressing empty vector, wild-type or kinase-inactive PINK1–FLAG were sequentially co-transfected with the respective HA-tagged substrates, induced with 0.1μg/ml of Doxycycline and then incubated with 10 μM CCCP or DMSO control for 3 hr before whole cell lysis. Approximately 30mg of lysate was subjected to immunoprecipitation with anti-FLAG-agarose and then eluted in LDS sample buffer. Samples were boiled

with 10 mM DTT, and then alkylated with 50 mM iodoacetamide before being subjected to electrophoresis on a Bis-Tris 10 % polyacrylamide gel, which was then stained with Colloidal Coomassie blue. Coomassie-stained bands migrating with the expected molecular mass of parkin were excised from the gel and digested with trypsin and samples underwent phosphosite analysis with LTQ-Orbitrap Velos. Individual MS/MS spectra were inspected using Xcalibur 2.2 software.

2.2.5.5 In vivo phospho-site mapping of human PINK1

10 mg of mitochondrial extract from Flp-In T-Rex HEK 293 cell lines stably PINK1–FLAG were subjected to immunoprecipitation with anti-FLAG-agarose and then eluted in LDS sample buffer. Samples were boiled with 10 mM DTT, and then alkylated with 50 mM iodoacetamide before being subjected to electrophoresis on a Bis-Tris 4-12% gradient polyacrylamide gel, which was then stained with Colloidal Coomassie blue. Coomassie-stained bands migrating with the expected molecular mass of PINK1-FLAG were excised from the gel and digested with trypsin and samples were analysed either by an Applied Biosystems 4000 Q-TRAP system with precursor ion scanning as described previously (Williamson et al, 2006) or on the LTQ-Orbitrap Velos system with multistage activation.

2.2.5.6 N-terminal Edman Sequencing

HEK293 cells were transiently transfected with wild-type PINK1-FLAG and then underwent whole cell lysis. 100mg of lysate was subjected to immunoprecipitation with anti-FLAG agarose and then eluted in LDS sample buffer. Samples were boiled with 10 mM DTT, and then alkylated with 50mM

iodoacetamide before being subjected to electrophoresis on a Bis-Tris 10% polyacrylamide gel, which was then transferred to Immobilon PVDF (Polyvinylidene difluoride) membrane and stained briefly with Coomassie Blue. The band corresponding to the processed form of PINK1 was excised and subjected to Edman degradation in an Applied Biosystems ProCise 494 Sequencer. The resulting HPLC profiles were analysed with Model 610 software (Applied Biosystems).

2.2.6 Stable Isotope Labeling with Amino acids in Culture (SILAC)

2.2.6.1 Preparation of SILAC media

SILAC DMEM (high glucose without NaHCO3, L-glutamine, arginine, lysine and methionine; Biosera #A0347) was supplemented with methionine, glutamine, NaHCO3, 10 % dialysed FBS (Hyclone) and the following combinations of unlabeled and isotopically-labeled arginine (84 µg/ml) and lysine (146 µg/ml): L-arginine and L-lysine (Sigma–Aldrich) for R0K0 (light); L-arginine-HCl (U-13C6) and L-lysine-2HCl (4,4,5,5,D4) for R6K4 (medium); and L-arginine-HCl (U-13C6, 15N4) and 13C-Llysine-2HCl (U-13C6, 15N2) for R10K8 (heavy). The SILAC medium was filtered through a 0.22-µm filter and cells cultured for five passages in these media for maximum incorporation of labeled amino acids.

2.2.6.2 PINK1 triple SILAC-based interactor screen

Flp In TRex HEK293 cells stably expressing FLAG empty were grown in ‘light’ SILAC medium. Flp In HEK293 cells stably expressing PINK1-FLAG Wild-type was grown in ‘medium’ as well as ‘heavy’ SILAC medium. All cell lines were

grown for at least 5 passages in SILAC media to ensure maximal incorporation of labeled amino acids. Experimental set-up is listed in Table 2.7. Mitochondrial and cytosolic fractions were made from the different conditions listed in the Table 2.7. 0.7 mg of mitochondrial fraction and 3.3 mg of cytosolic fraction from each condition were immunoprecipitated individually with 10 µl of FLAG-agarose beads. Mitochondrial immunoprecipitates from all three SILAC conditions of replicate 1 and 2 were pooled together, respectively. Similarly, cytosolic fractions were also pooled together. Pooled immunoprecipitates were resolved by SDS-PAGE and the gel was stained using Colloidal Coomassie blue. The gel was further cut into 8 pieces per lane and subjected to mass spectrometry sample preparation as described in 2.2.6.1.

Experiment	'light'	'medium'	'heavy'
Replicate 1	***Cell line:*** FLAG empty	***Cell line:*** PINK1-FLAG wild type	***Cell line:*** PINK1 – FLAG wild type
	Stimulation: 10µM CCCP for 3 hours	***Stimulation:*** DMSO treated control	***Stimulation:*** 10µM CCCP for 3 hours
Reciprocal replicate 2	***Cell line:*** FLAG empty	***Cell line:*** PINK1-FLAG wild type	***Cell line:*** PINK1-FLAG wild type
	Stimulation: 10µM CCCP for 3 hours	***Stimulation:*** 10µM CCCP for 3 hours	***Stimulation:*** DMSO treated control

Table 2.9 PINK1 SILAC-based interactor screen experimental set-up

Tryptic peptides of proteins from SILAC-labeled cells were analysed by Orbitrap mass spectrometry and raw mass spectrometric data files for each experiment were collated into a single quantitated dataset using MaxQuant (version 1.0.13.13) (http://www.maxquant.org) and Mascot search engine (Matrix Science, version 2.2.2) software. Enzyme specificity was set to that of Trypsin, allowing for cleavage N-terminal to proline residues and between aspartic acid and proline residues. Other parameters were: (i) Variable modifications: methionine oxidation and protein N-acetylation; (ii) Fixed modifications: cysteine carbamidomethylation; (iii) Database: target-decoy human MaxQuant (ipi.HUMAN.v3.52.decoy) (containing 148,380 database entries); (iv) Labels: R6K4 or R10K8; (v) MS/MS tolerance: 0.5 Da; (vi) Minimum peptide length: 6; (vii) Top MS/MS peaks per 100 Da: 5; (viii) Maximum missed cleavages: 2; (ix) Maximum of labeled amino-acids: 3; (x) False Discovery Rate (FDR): 1 %; (xi) Posterior Error Probability: 1; (xii) Minimum ratio count: 2. The protein ratios were calculated using all peptides. As well as taking the FDR into account, proteins were considered identified if they had at least one unique peptide and considered quantified if they had at least one quantified SILAC pair. Data quality was also assessed manually, and only high confidence results reported. SILAC analysis was performed by Francois-Michel Boisvert (Angus Lamond's lab, GRE, Dundee) and Chandana Kondapalli.

2.2.6.3 PINK1 SILAC phosphoproteomics

PINK1 SILAC phosphoproteomics was performed in collaboration with Matthias Trost (MRC PPU, Dundee). Flp In TRex HEK293 cells stably expressing either

FLAG empty, PINK1-FLAG wild type or PINK1-FLAG Kinase dead were grown in 'light', 'heavy' and 'medium' SILAC media, respectively, for at least 5 passages. Experimental set-up is listed in Table 2.8. Experiments were set-up as two biological replicates with a technical replicate in each and hence is considered to have n=4, which is beneficial to achieve statistical significance.

Cells in each condition were stimulated with 10 µM CCCP for 3 hr and were scraped using a hand-made cell scraper (obtained from Michel Desjardin's lab, Montreal in appropriate amount of homogenization buffer (8.55 % w/v Sucrose in 3 mM Imidazole pH 7.4 supplemented with protease inhibitor and phosphatase inhibitor cocktail from Roche and Benzonase from Roche). The

'light'	'medium'	'heavy'
Cell line: FLAG empty	***Cell line:*** PINK1-FLAG Kinase dead	***Cell line:*** PINK1 – FLAG wild type
Stimulation: 10µM CCCP for 3 hours	***Stimulation:*** 10µM CCCP for 3 hours	***Stimulation:*** 10µM CCCP for 3 hours

Table 2.10 PINK1 SILAC phospho-proteomic experimental set-up

cells were lysed by mechanical disruption using a stainless steel Dounce Homogenizer by subjecting to 6 passes (Fisher, cat# 08-414-20A). The lysate was centrifuged at 3000 rpm for 10 min at 4 °C to spin down cell debris and the supernatant was collected in Ultra-clear centrifuge tubes 14x95 mm (Beckman, cat# 344060) and subjected to ultra-centrifugation at 100,000 g for 30 min.

Resultant pellet corresponds to a crude mitochondrial fraction. 1 % RapiGest (RAPIGEST^{TM} SF from Waters – Cat # 186002123), 50 mM Tris pH 8.0, 1 mM TCEP + phosphatase inhibitors (without EDTA) to were added to a cell pellet aiming for ~10 mg/ml protein concentration and the resultant solution vortexed briefly. Rapigest is an acid cleavable SDS-like detergent that is removed by addition of 1 % TFA and solid-phase extraction (SPE).

The following protocol was followed for Rapigest cell lysis (from Matthias Trost's lab).

- Add 0.5-1 ul of Benzonase to remove DNA. Incubate for 3 min on ice.
- Sample should be clear, if not, add more RapiGest buffer.
- Heat at 70-95° for 5 min. Allow cooling to room temperature.
- Add 5 mM iodoacetamide in Tris pH 8.0 for 20 min in dark (RT, shaker).
- Add 10 mM DTT in Tris for 20 min in dark (RT, shaker). At this stage it would be a good point to freeze.
- Accurate protein estimation was performed by EZQ protein estimation method (Molecular probes kit – R33200).*

**A small amount of heavy and medium labeled samples were taken to check labelling efficiency. Also, small amounts of heavy, medium and light labeled samples were mixed at 1:1:1 ratio, digested and checked by mass spectrometry if samples were indeed at a 1:1:1ratio. Only after performing this the samples were taken for enzymatic digestion.*

- Dilute 1:10 with 50 mM Tris 8.0 (to allow trypsin to work) and vortex.
- Perform a quick centrifugation to spin down foam.

- Mix lysates from the three different conditions from each experimental replicate in equal amounts, respectively (9mg total).
- Digest with 1:100 trypsin for 3 h, then another 1:100 overnight and leave on Thermoshaker 37°C. (for large amounts use Worthington trypsin at 1:75 twice) (Only low-bind tubes and low-bind tips were used with the start of Trypsin digestion).
- Acidify to final lysate with 1% Triflouroacetic acid (TFA) to cleave RapiGest.
- Shake for 1h at 37°C at 1000 rpm.
- Pellet by spinning at max speed for 30 min (set to room temp).
- SPE (Solid-phase extraction) clean up of supernatant was done.
- Lyophilise or elute with 800 ul of 80% Acetonitrile (ACN), 0.1% Formic acid and subject it to HILIC (Hydrophilic interaction chromatography – performed by Bob Gourlay from Mass spectrometry team, MRC PPU). HILIC enables phospho-peptide enrichment and for every sample separated by HILIC, we collect fractions 10-35, which are lyophilized and each of these will undergo a subsequent TiO_2 phosphopeptide enrichment.

TiO_2 Enrichment of Phosphopeptides

TiO_2 micro-columns were prepared in-house by the Trost laboratory. Sample loading, washing and elution were performed by centrifuging (5,000 rpm, 5 min) the micro-column. Each micro-column was used once to avoid contamination. The following materials were utilised: Titansphere (TiO_2), 150x4.6 mm, 5 µm (GL, Life science), pH indicator strips colorpHast (EMD), High Performance

extraction disk C-8 47 mm (3 M Empore), Trifluoroacetic acid (TFA), Lactic Acid (Ph Eur grade, Fluka) c=13.42 M, Acetonitrile (AcN)-Fisher Scientific, Ammonium hydroxide 28-30 % (NH_4OH)-Sigma-Aldrich, 20 µL pipette tip.

The following protocol was used to prepare the micro-columns:

Preparation of TiO_2 micro-columns (Illustrated in Fig. 2.1):

1- Insert C8 extraction disk in a 20 µL pipette tip.

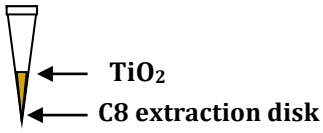

2-Load 25 µL (1.25 mg, 5 mm) of 50mg/mL "homogeneous" TiO_2 solution in each tip, making sure that the TiO_2 solution is always homogeneous by constantly stirring it with a magnetic bar. This ensures that the same amount of TiO_2 is reproducibly added into each pipette tip.

3- Elute the acetonitrile.

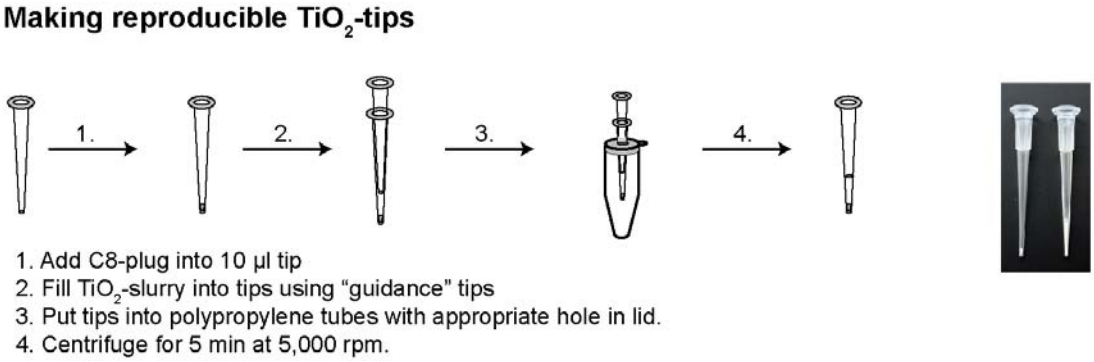

Figure 2.1 Preparation of TiO_2 tips for phospho-peptide enrichment

TiO_2 enrichment procedure (Illustrated in Fig.2.2):

Condition micro-columns with 10 µL of 3% TFA in 70% AcN solution. Reconstitute sample (250µg) in 50 µL of 250mM lactic acid/3% TFA/70% AcN. Verify if pH is acidic (~2) using a pH indicator strip. Load sample on a 1.25 mg TiO_2 micro- column. Wash micro-column with 10 µL of 250mM lactic acid/3% TFA/70% AcN. Wash micro-column with 30 µL of 3% TFA in 70% AcN. Wash with 10 µl 0.1% TFA. Put 1 µL of 50% TFA in a new eppendorf (LoBind) and elute phosphopeptides with 10-30 µL of 1% NH_4OH pH10.5 into this tube. At the loading step, adjust the gas pressure or centrifugation speed to obtain a very slow elution rate (3,000-5,000 rpm) to have a higher recovery of phosphopeptides and enrichment level. Inject 1/3rd of the eluate into mass spec straight away. Store in liquid N_2 or -80C.

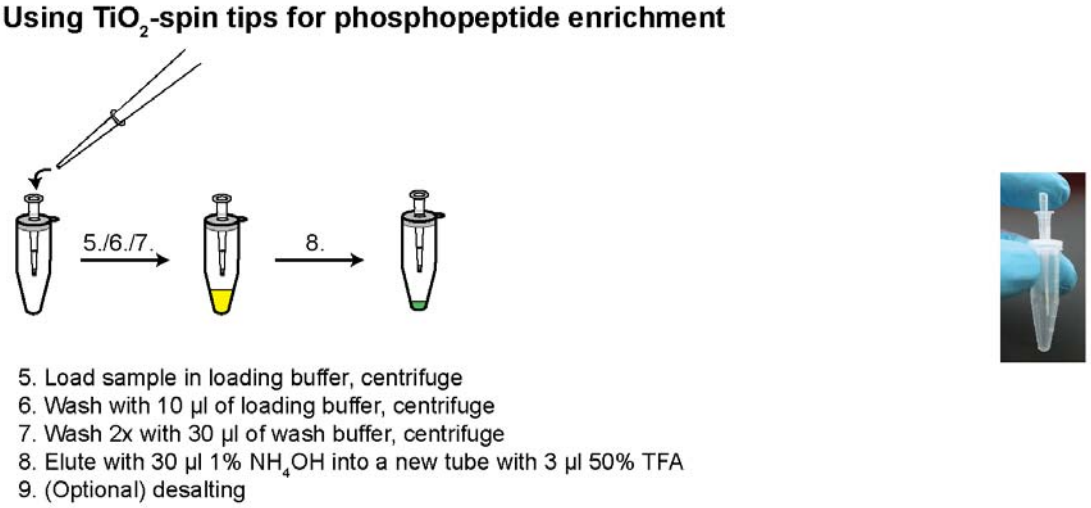

Figure 2.2 Phospho-peptide enrichment procedure using TiO_2 tips

Chandana Kondapalli performed the experiment. Matthias Trost and Brian Dill performed Max-quant analysis of phospho-peptides identified by mass

spectrometry. Data quality was also assessed manually, and only high confidence results reported.

2.2.6.4 Sequence alignment

Sequence alignments were prepared using ClustalW algorithm and visualised using Jalview 10.0.

2.2.6.5 Statistical analysis

All experiments presented in this thesis were performed at least two times with significant reproducibility across replicates.

Chapter 3

Elucidation of PINK1 signal transduction pathway

3 Elucidation of PINK1 signal transduction pathway

3.1 Introduction

Ever since the discovery of autosomal recessive mutations in PINK1 in 2004, causative of early-onset Parkinson's disease (Valente et al, 2004), there has been great excitement in probing the regulation and function of this enzyme. Despite considerable research, there was little understanding of the kinase activity of PINK1, its physiological substrates and how this links to pathogenesis of PD. In order to establish a functional pathway for PINK1, a crucial first step has been to determine its enzymatic properties. Human PINK1 in our hands was found to be inactive, however, a major advance made by our lab was the discovery that insect orthologues of PINK1, including an orthologue from the red flour beetle, *Tribolium castaneum* (TcPINK1), are catalytically active when expressed in *Escherichia coli* (Woodroof et al, 2011). I have exploited this discovery to employ TcPINK1 as a biochemical tool to uncover PINK1 substrates. I initially explored whether TcPINK1 could phosphorylate 11 PD-linked genes and/or 7 putative PINK1 interacting proteins. My analysis revealed that PINK1 robustly phosphorylates another PD-linked protein, namely the RING-IBR-RING E3 ubiquitin ligase, Parkin.

Further, I have mapped the phosphorylation site to a highly conserved residue, Serine 65 (Ser65) in Parkin, which regulates its E3-ubiquitin ligase activity. In parallel studies, I have discovered that human PINK1 is activated upon mitochondrial depolarization, enabling it to phosphorylate Parkin at Ser65 *in vivo,*

providing the first evidence of kinase activity for mammalian PINK1. Once activated, PINK1 also undergoes autophosphorylation at various residues including Threonine 257 (Thr257), which represents a novel marker for its activation state.

3.2 PART I – Phosphorylation of Parkin by catalytically active insect orthologue of PINK1

3.2.1 *Insect PINK1 phosphorylates Parkin in vitro*

In the human kinome tree, PINK1 exists in a lone branch being unrelated to any other known protein kinases (refer to Fig. 1.3). Multiple sequence alignment of the kinase domain of PINK1 with CaMKI, CaMKII and PKA reveals a high degree of conservation of sub-structural motifs that are required for catalytic activity (Fig. 3.1). In addition, PINK1 also contains three unique insert regions in the N-lobe of the kinase domain, which are as of yet unknown function (Fig. 3.1). Although human PINK1 contains a highly conserved kinase domain and all the motifs necessary for activity, in our laboratory and those of other groups, human PINK1 expressed in a variety of different systems was found to be inactive. A recent breakthrough in our lab was the identification of insect orthologues of PINK1, including that of Tribolium castaneum (TcPINK1), that are catalytically active when expressed in *E.coli* (Woodroof et al, 2011). The discovery of TcPINK1 served as a valuable tool to delineate evolutionarily conserved downstream signaling pathways of PINK1. Catalytically active recombinant TcPINK1 was used to directly phosphorylate 11 different proteins encoded by genes linked to Mendelian inherited-PD and 7 proteins reported in literature to be putative PINK1 interacting proteins by *in vitro* kinase assay using ^{32}P-adenosine triphosphate

[γ-^{32}P ATP] ATP (Fig. 3.2A). This strikingly revealed that wild-type but not kinase-inactive TcPINK1 phosphorylated full length Parkin, but not any of the other PD-linked proteins or interacting proteins tested (Fig. 3.2A and B).

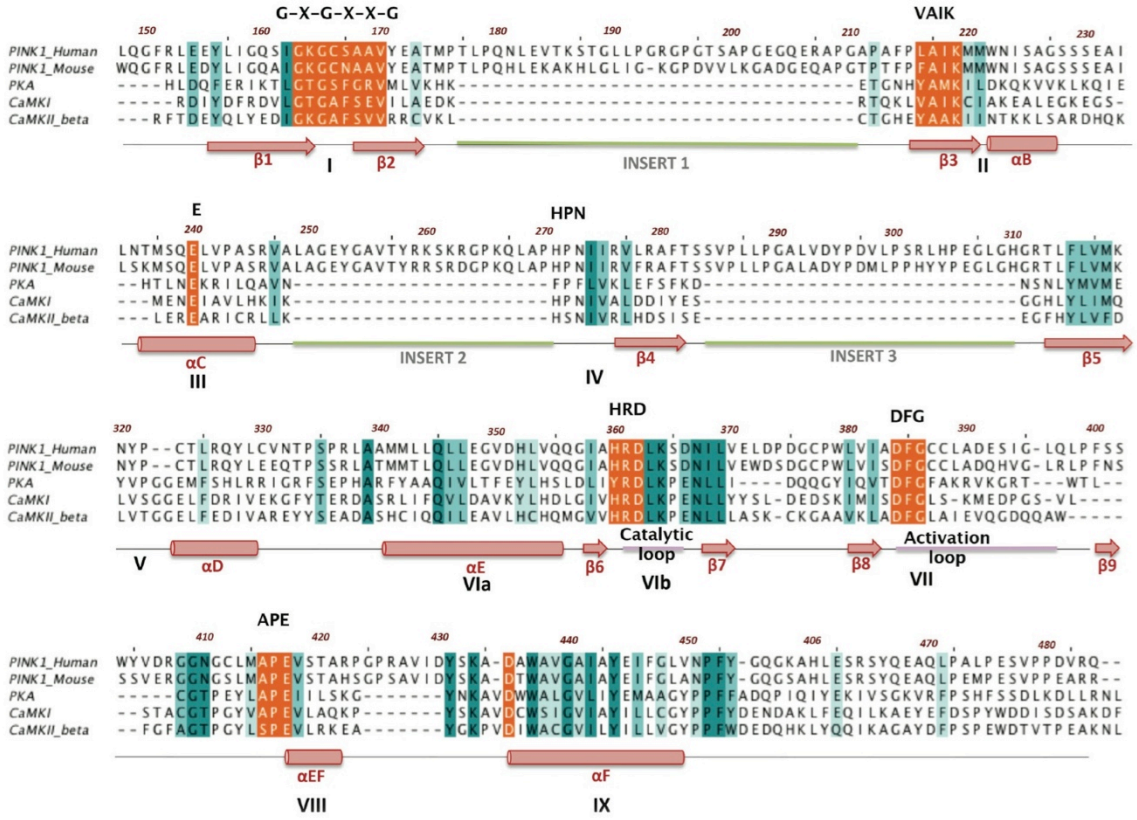

Figure 3.1 Conservation of hallmark motifs in PINK1 required by active kinases

Multiple sequence alignment (MSA) of human and mouse PINK1 along with Protein Kinase A (PKA) and calcium and calmodulin dependent kinase 1 (CamKI) and 2 (CamKII) shows the presence of conserved motifs (highlighted in orange) present in most active kinases. Green bars represent the three unique insertions in PINK1. The secondary structure of PINK1 determined by JPred (http://www.compbio.dundee.ac.uk/www-jpred/) is represented below the MSA, wherein arrows represent β-sheet and cylinders represent α-helix.

3.2.2 *Mapping of phosphorylation site on Parkin*

In order to identify the phosphorylation site on Parkin, Parkin was initially phosphorylated by TcPINK1 using γ-^{32}P ATP; digested with trypsin and tryptic peptides analysed by chromatography on a C18 column. Two major ^{32}P-labelled

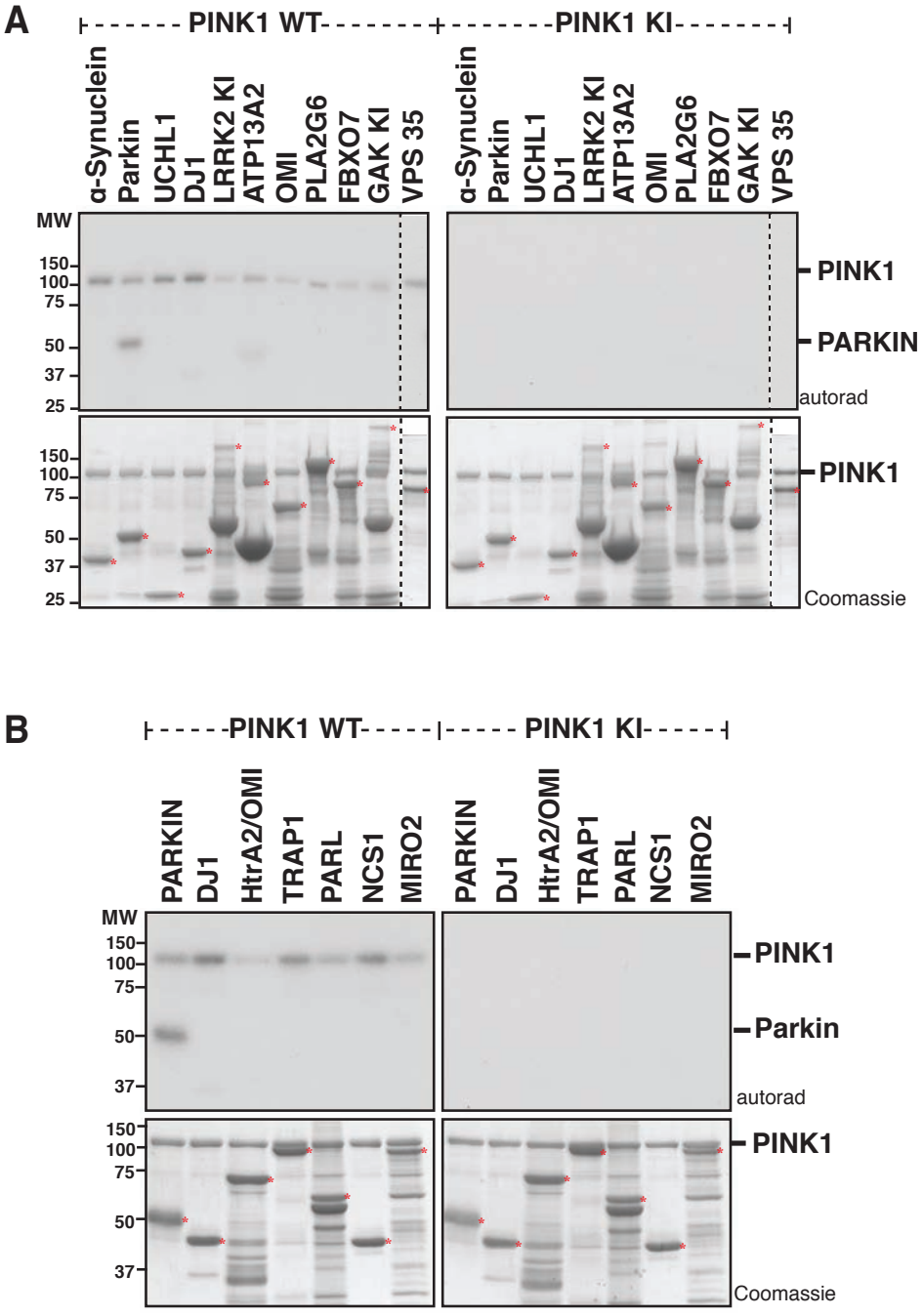

Figure 3.2. Insect PINK1 phosphorylates Parkin *in vitro*

(A) The indicated PD-linked proteins (1 mM) were incubated with either full-length MBP-fusion of wild-type TcPINK1 (1–570) or kinase-inactive (KI) TcPINK1 (D359A) (0.5 µg) and [γ-32P] ATP for 30 min. Assays were terminated by addition of SDS loading buffer and separated by SDS-PAGE. Proteins were detected by Colloidal Coomassie blue staining (lower panel) and incorporation of [γ-32P] ATP was detected by autoradiography (upper panel). Similar results were obtained in three independent experiments. Fine dividing lines indicate that reactions were resolved on separate gels. The substrate bands on the Coomassie gel are denoted with a small red asterisk. All substrates were of human sequence and expressed in E. coli unless otherwise indicated.

(B) As in (A) except that proteins reported to interact with PINK1 were tested as PINK1 substrates. Similar results were obtained in three independent experiments.

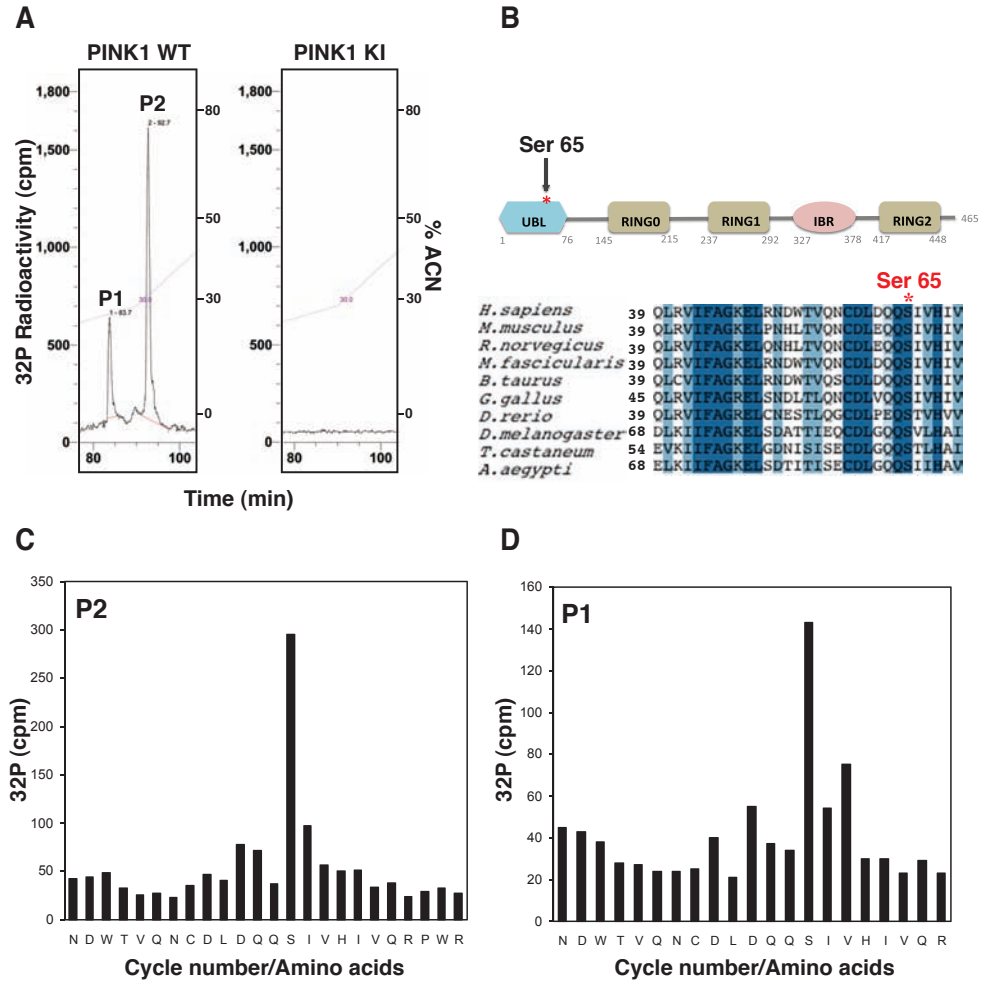

Figure 3.3 Insect PINK1 phosphorylates Parkin at Ser65, a highly conserved residue within its N-terminal Ubl domain

(A) Full-length GST-Parkin (1 µg) was incubated with 2 µg of either wild-type TcPINK1 (1–570) or KI TcPINK1 (D359A) in the presence of $Mg2^{+}$[γ-32P] ATP for 60 min. Assays were terminated by addition of LDS loading buffer, separated by SDS-PAGE and proteins were detected by Colloidal Coomassie blue staining. Phosphorylated Parkin was digested with trypsin. The resultant peptides were separated by reverse phase HPLC on a Vydac C18 column equilibrated in 0.1% (v/v) trifluoroacetic acid and the column developed with an acetonitrile gradient (diagonal line). The flow rate was 0.2 ml/min and fractions (0.1 ml each) were collected and analysed for 32P radioactivity by Cerenkov counting. Two major ^{32}P-labelled peaks (P1, P2) were identified following incubation with wild-type TcPINK1 (left). No peaks were identified following incubation with kinase-inactive TcPINK1 (right).

(B) Schematic of domain organization of Parkin and sequence alignment showing a high degree of conservation of Ser65 residue from mammals to invertebrates.

(C & D) Phosphopeptides P2 and P1 were sequenced by solid-phase Edman sequencing followed by mass spectrometry. The amino-acid sequence of LC-MS/MS analysis is shown using amino acid single-letter code. *Abbreviations:* Ubl, ubiquitin-like; IBR, in-between-RING; RING, really interesting new gene.

phosphopeptides were observed (Fig. 3.3A). A combination of solid-phase Edman sequencing and mass spectrometry described previously (Campbell & Morrice, 2002), revealed that both of these encompassed variants of a peptide phosphorylated at Serine 65 (Fig. 3.3 C and D). Ser65 is located within the N-terminal Ubl (Ubiquitin-like-domain) domain of Parkin, and is highly conserved from mammals to invertebrates (Fig. 3.3B).

3.2.3 *Stoichiometry and specificity of Parkin phosphorylation*

To determine the stoichiometry of Parkin phosphorylation, a time course of was undertaken, which revealed that TcPINK1 could indeed phosphorylate Parkin in a time-dependent manner reaching a maximal stoichiometry of phosphorylation of approximately 0.25 moles of ^{32}P-phosphate per mole of protein (Fig. 3.4A). Mutation of Ser65 to Alanine prevented phosphorylation of full-length Parkin as well as an N-terminal Parkin fragment consisting of the Ubl-domain; therefore confirming that Ser65 is the major site for PINK1-mediated phosphorylation (Fig. 3.4C). It was also interesting to observe that the isolated Ubl domain of Parkin was phosphorylated to a higher stoichiometry than full-length Parkin perhaps indicating that there is a structural constraint in accessing the Serine residue in full-length Parkin. In fact, a recent study in Parkin has shown that the N-terminal Ubl domain interacts with its C-terminal region to form a closed conformation (Chaugule et al, 2011). Based on this, a C-terminal truncation of Parkin (1-383) was made in order to test if this could relieve its closed conformation and make Serine 65 more accessible to PINK1. Phosphorylation of Parkin (1-383) was observed to be slightly more than full-length Parkin, however the interpretation is

confounded by the observation that this C-terminal Parkin truncation mutant is highly unstable and degraded (Fig. 3.4D)

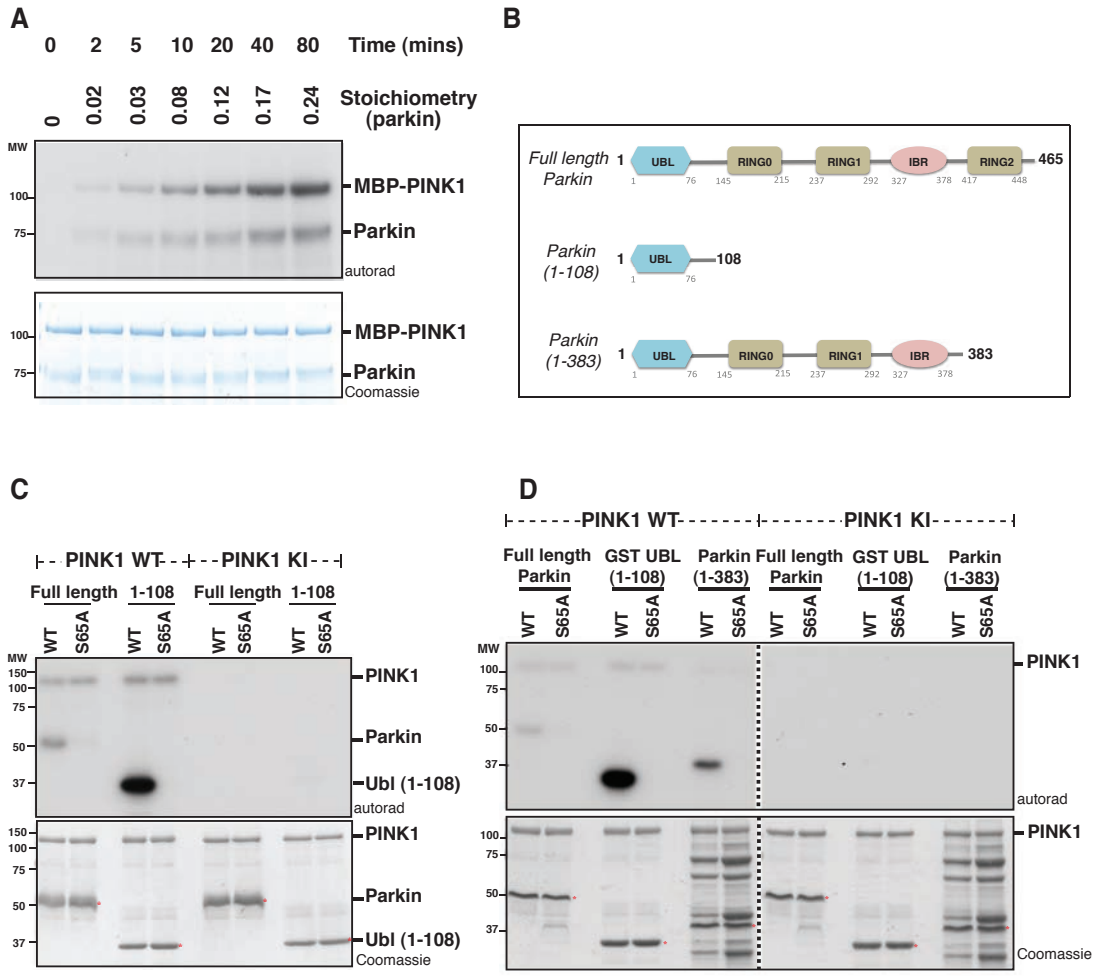

Figure 3.4 Specificity of PINK1 mediated phosphorylation of Parkin

(A) MBP-TcPINK1 (0.5 µg) was incubated in the presence of GST-Parkin (1 µg) and [γ-32P] ATP for the times indicated and assays terminated by addition of SDS loading buffer. Samples were subjected to SDS-PAGE and proteins detected by Colloidal Coomassie blue staining (lower panel) and incorporation of [γ-32P] ATP was detected by autoradiography (upper panel). Gel pieces corresponding to Parkin were quantified by Cerenkov counting to calculate stoichiometry. Similar results were obtained in two independent experiments.

(B) Schematic of different truncated versions of Parkin used for *in vitro* kinase assays.

(C and D) Full-length wild-type TcPINK1 (1–570) and kinase inactive TcPINK1 (D359A) against wild-type or S65A mutants of full-length Parkin, GST-fusion of isolated Ubl-domain-containing N-terminal fragment (residues 1–108) or C-terminal truncated Parkin (1-383). The indicated substrates (2mM) were incubated in the presence of the indicated enzyme (1 µg) and [γ-32P] ATP for 30 min. Assays were terminated by addition of SDS loading buffer and separated by SDS-PAGE. Proteins were detected by Colloidal Coomassie blue staining (lower panel) and incorporation of [γ-32P] ATP was detected by autoradiography (upper panel). The substrate bands are denoted by a small red asterisk.

3.2.4 *PINK1 phosphorylation of Parkin at Ser65 mediates activation of Parkin E3 ubiquitin ligase activity*

As discussed earlier, a recent study provided strong evidence that the Ubl domain of Parkin acts as an auto-inhibitory domain by binding to a region within the C-terminus thereby suppressing catalytic activity (Chaugule et al, 2011). Given that Ser65 lies within the core of the Ubl domain, we hypothesized that phosphorylation of Ser65 might relieve the autoinhibition thereby activating the E3 ligase activity of Parkin. To investigate this, an E3 ligase auto-ubiquitylation assay was performed to assess Parkin catalytic activity using highly purified full length recombinant Parkin expressed in E. coli with no epitope tags that can interfere with the autoinhibitory effect of the Ubl domain (Chaugule et al, 2011). Agne Kazlauskaite, a current PhD student in our lab, performed this part of the study. Prior to undertaking the E3 ligase activity assay, Parkin was phosphorylated with increasing levels of TcPINK1 in the presence of γ-^{32}P ATP so that we could verify PINK1 mediated phosphorylation of Parkin (middle panels in Fig. 3.5). To assess Parkin E3 ligase activity, aliquots of these reactions were added to a reaction containing E1 ubiquitin-activating ligase, UbcH7 conjugating E2 ligase, ubiquitin and Mg-ATP. After 60 min, reactions were terminated with SDS sample buffer in the presence of dithiothreitol (DTT) and reactions analysed by immunoblot analysis with antibodies that detect ubiquitin, Parkin and TcPINK1.

In the absence of PINK1 phosphorylation we confirmed previous findings and found that Parkin displayed no significant E3 ligase activity and no evidence of formation of polyubiquitin chains were observed (lane 1 in Fig. 3.5A).

Remarkably, when increasing levels of TcPINK1 were added to the reaction at concentrations in which phosphorylation of Parkin was detected (middle panel of Fig. 3.5A), we observed a marked dose-dependent appearance of non-DTT-reducible low molecular weight polyubiquitylated species migrating between approximately 30 and 50 kDa (top panel of Fig. 3.5A). Consistent with this being mediated by phosphorylation of Parkin at Ser65 by TcPINK1, the appearance of polyubiquitin chains was inhibited by introducing a point mutation in PINK1 that ablates catalytic activity (Fig. 3.5B) or by mutating Ser65 in Parkin to a non-phosphorylatable Ala residue (Fig. 3.5C). Thus, based on this *in vitro* analysis, it is clear that TcPINK1 mediated phosphorylation of Parkin at Ser65 is a crucial event that leads to activation of the E3 ubiquitin ligase activity of Parkin.

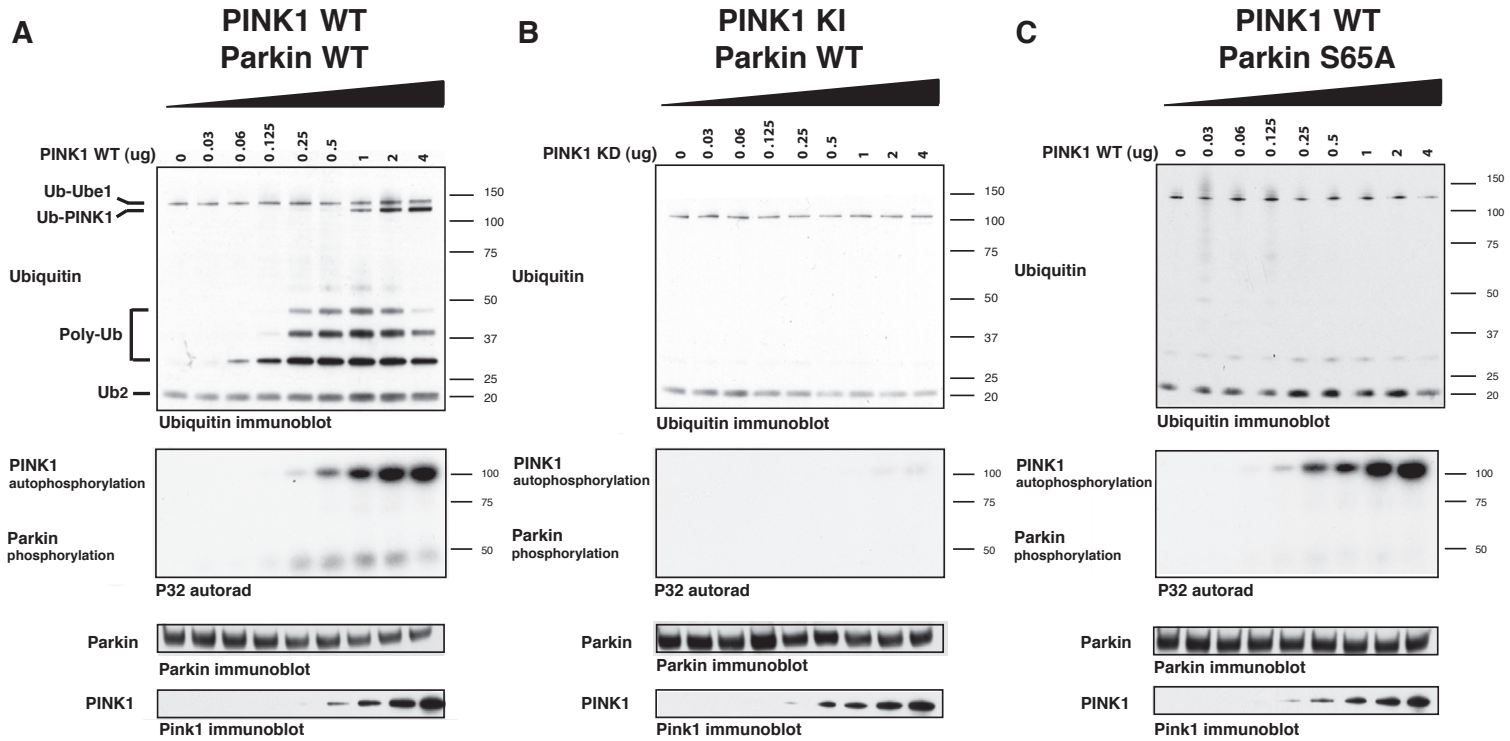

Figure 3.5 PINK1 phosphorylation of Ser65 mediates activation of Parkin E3 ligase activity (performed by Agne Z. Kazlauskaite)

Wild-type **(A)** but not kinase-inactive **(B)** PINK1 activates wildtype Parkin, but does not affect the activity of Ser65Ala (S65A) mutant Parkin **(C).** Wild-type or S65A Parkin were phosphorylated with indicated amounts of wild-type or kinase-inactive (D359A) MBP-TcPINK for 60 min. Phosphorylated Parkin was subjected to *in vitro* - ubiquitylation assay for 60min, reaction terminated in SDS loading buffer and resolved by SDS-PAGE. Ubiquitin, Parkin and PINK1 were detected using anti-FLAG, anti-Parkin and anti-MBP antibodies, respectively. Incorporation of [γ-32P] ATP was detected by autoradiography (lower panel). Ubiquitin attached to the E1 (Ub-Ube1) and ubiquitin dimer (Ub2) formation occurred in the assay in all conditions **(A-C).** Ubiquitylation of PINK1 (Ub-PINK1) is indicated in **(A).** Polyubiquitin chain formation (poly-Ub) upon Parkin activation **(A)** is indicated. Representative of n=3.

3.3 PART II – Evidence of Parkin Ser^{65} phosphorylation by human PINK1 in mammalian cells

3.3.1 *Human PINK1 is stabilized by mitochondrial depolarization*

In order to study human PINK1 in mammalian cells, Flp-In TRex HEK293 (Human Embryonic Kidney) inducible cell lines stably expressing C-terminal FLAG-tagged human PINK1 were generated as described in 2.2.3.4. This Flp-In cell line allows for integration and expression of PINK1 at a specific genomic location enabling doxycycline induced expression of PINK1 at levels nearer that of endogenous PINK1 expression and much less than transient over-expression cell systems. We chose a C-terminal tag since the N-terminal region of PINK1 contains a mitochondrial targeting sequence that undergoes cleavage upon mitochondrial localization. Stable cell lines expressing either FLAG-tag alone (negative control), human wild-type-C-terminal FLAG-tagged PINK1 or human Kinase inactive (D384A)–C-terminal FLAG tagged PINK1 were generated and induced for expression with 0.1µg/ml of doxycyline for 24 hours (Fig. 3.6A).

As described in 1.4.3, the sub-cellular localization and stabilization of PINK1 was tested in PINK1 stable cell lines. As seen in previous studies, it was observed that both full-length (63kDa) and cleaved forms (53kDa) of PINK1 exist under basal conditions (Fig. 3.6B). A previous study has established that PINK1 gets selectively stabilized in mitochondria upon treatment with mitochondrial uncoupling agents (such as valinomycin or CCCP - (m-chlorophenylhydrazone)) and in order to confirm this, a dose response and time

course of CCCP stimulation was performed (Appendix Fig. 6.1 A & B) (Matsuda et al, 2010; Narendra et al, 2010). This confirmed that optimal stabilization of full length PINK1 in mitochondria occurs with 10μM CCCP and the stabilization is maximal within 3 hours of stimulation (Appendix Fig. 6.1 A & B). A time course and dose response of proteasomal inhibition using the 20S proteasomal inhibitor, MG-132, shows an accumulation of the 53kDa cleaved form of PINK1 (Appendix 6.1 C & D).

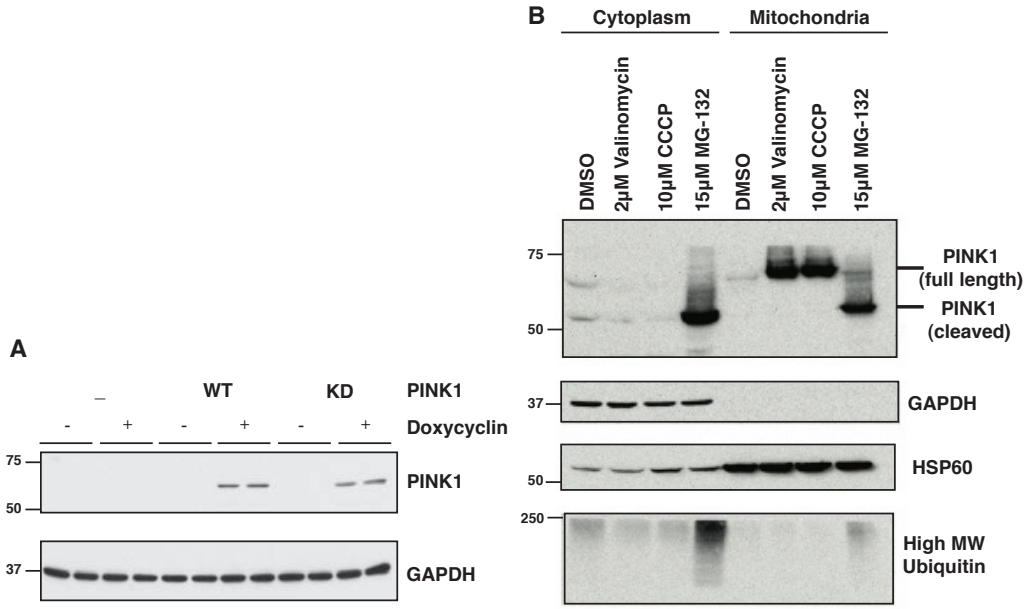

Figure 3.6 PINK1 is stabilized upon mitochondrial depolarization

(A) FlpIn TRex HEK293 cell lines stably expressing either FLAG-alone, human PINK1 wild-type-C-terminal FLAG or human PINK1 kinase inactive-C-terminal FLAG were stimulated for protein expression using 0.1μg/ml of doxycycline for 24 hours. Whole cell lysates were blotted for PINK1 using anti-PINK1 (Novus) and GAPDH as loading control.

(B) HEK293 cells stably expressing PINK1 wild-type-FLAG were induced for protein expression and stimulated with the indicated amounts of valinomycin, CCCP or MG-132 for 3 hours. Cells were fractioned into cytosolic and mitochondrial fractions and were blotted for PINK1 using anti-PINK1 (Novus) antibody. GAPDH and HSP60 serve as cytosolic and mitochondrial markers respectively and high molecular weight ubiquitin species served as a control for proteasomal inhibition.

Using these optimized conditions, Flp-In T-Rex cell HEK293 lines stably expressing PINK1-FLAG were treated with 10μM CCCP or 2μM valinomycin for 3 hours. Both act differentially to depolarize the mitochondrial membrane potential by uncoupling ATP synthesis from the electrochemical gradient.

A pronounced stabilization of full-length PINK1 migrating at 63kDa occurred with both conditions in the mitochondrial fraction compared to DMSO treatment (Fig. 3.6B). In contrast the expression of PINK1 in the cytosolic fraction appeared to reduce with uncouplers. The stabilization was also 20S proteasome independent as cells treated with MG-132 in parallel had a differential effect on PINK1 with stabilization of the processed form of PINK1 at 53kDa in cytoplasm and mitochondria (Fig. 3.6B). N-terminal Edman-sequencing of PINK1 confirmed that the cleaved protein begins at residue 104 (Appendix 6.2) consistent with previous work indicating that human PINK1 is proteolysed between residues Ala^{103}-Phe^{104} by the mitochondrial rhomboid protease, PARL (Deas et al, 2011; Jin et al, 2010; Meissner et al, 2011). In conclusion, this initial characterisation of PINK1 stable cells suggested that PINK1 undergoes constant turnover under basal conditions with sequential cleavage followed by removal of the cleaved form via proteosomal degradation. This turnover can be interupted and PINK1 selectively stabilized when cells are subjected to mitochondrial depolarization.

3.3.2 *CCCP induces a band-shift in wild-type but not kinase-inactive mitochondrial PINK1*

A 3 h CCCP treatment induced a marked increase in levels of full length wild-type PINK1 in the mitochondrial fraction with a concomitant decrease in protein levels in the cytoplasmic compartment (Fig. 3.7). The level of full length PINK1 was also considerably increased in whole cell lysates consistent with CCCP stabilizing full length PINK1. We then sought to examine the effects of CCCP on the stabilization of kinase-inactive PINK1. Kinase-inactive PINK1 also undergoes stabilization in the mitochondria upon CCCP treatment (Fig. 3.7). However, CCCP stimulation induced a significant reduction in the electrophoretic mobility ('band-shift') of wild-type PINK1 when compared to the kinase-inactive form (Fig. 3.7). In fact, this phenomenon was been best observed when proteins were resolved by an 8% isocratic Tris-glycine SDS-polyacrylamide gel (Appendix 6.3 shows a comparison of 8% vs. 10%) and was less pronounced in gradient gels (Appendix 6.4).

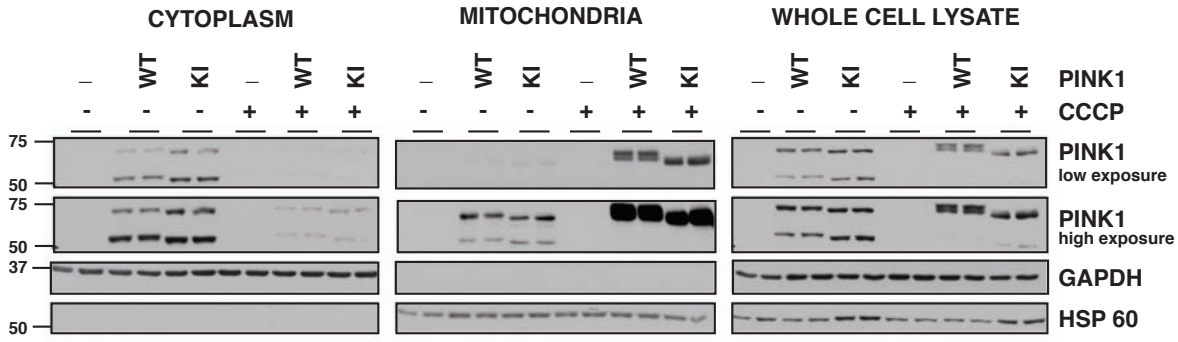

Figure 3.7 CCCP induces a bandshift in wild-type but not kinase inactive PINK1

Flp-In T-Rex HEK293 cell lines stably expressing FLAG alone, wild-type or kinase-inactive PINK1-FLAG were induced for with doxycycline for protein expression. Cells were treated with 10mM CCCP for 3h and lysates subjected to sub-cellular fractionation. 25µg of cytoplasmic or mitochondrial lysate were resolved by 8% SDS-PAGE. Relative purity of the fractions was confirmed using cytoplasmic and mitochondrial markers, namely GAPDH and HSP60, respectively. Whole cell lysates were also made from the same lysates and 25 µg was resolved by 8% SDS-PAGE.

3.3.3 *Autophosphorylation of CCCP-stabilized mitochondrial PINK1*

The presence of a CCCP-induced band-shift in wild-type PINK1 and not in the kinase-inactive form raised a possibility for an autophosphorylation event in the catalytically active form of the kinase. This, being a common feature of many protein kinases, prompted us to investigate whether mitochondrial depolarization could stimulate phosphorylation of any residues on PINK1. We undertook mass spectrometric phosphopeptide analysis of wild-type and kinase-inactive full-length PINK1 after immunoprecipitation from mitochondrial fractions of CCCP-treated cells and also of wild-type mitochondrial PINK1 from CCCP-untreated and treated cells in an independent experiment (Appendix 6.4 and Fig. 3.8A). We were able to unambiguously identify one phosphorylation site at Thr257 (Fig. 3.8A). Several other residues of PINK1 were phosphorylated in CCCP treated cells but at lower stoichiometry making their identification challenging. A phospho-specific antibody was raised against the Thr257 phosphorylation site and HEK293 FlpIn TRex stable cell lines were generated with a mutation of Thr257 to Alanine in order to characterize the phospho-specific antibody (Fig. 3.8B). Employment of the Phospho Thr257 antibody confirmed that CCCP treatment markedly stimulated phosphorylation of wild-type but not kinase-inactive PINK1 at Thr257, suggesting that this residue is an autophosphorylation site (Fig. 3.8C). Mutation of Thr257 to Ala abolished detection of phosphorylated PINK1 confirming the specificity of the Thr257 antibody (Fig. 3.8C). Thr257 is located within the second insert region (residues 247–270) (Fig. 3.8D) and this site is not highly conserved between species (Appendix 6.5). Nevertheless my analysis suggests that monitoring

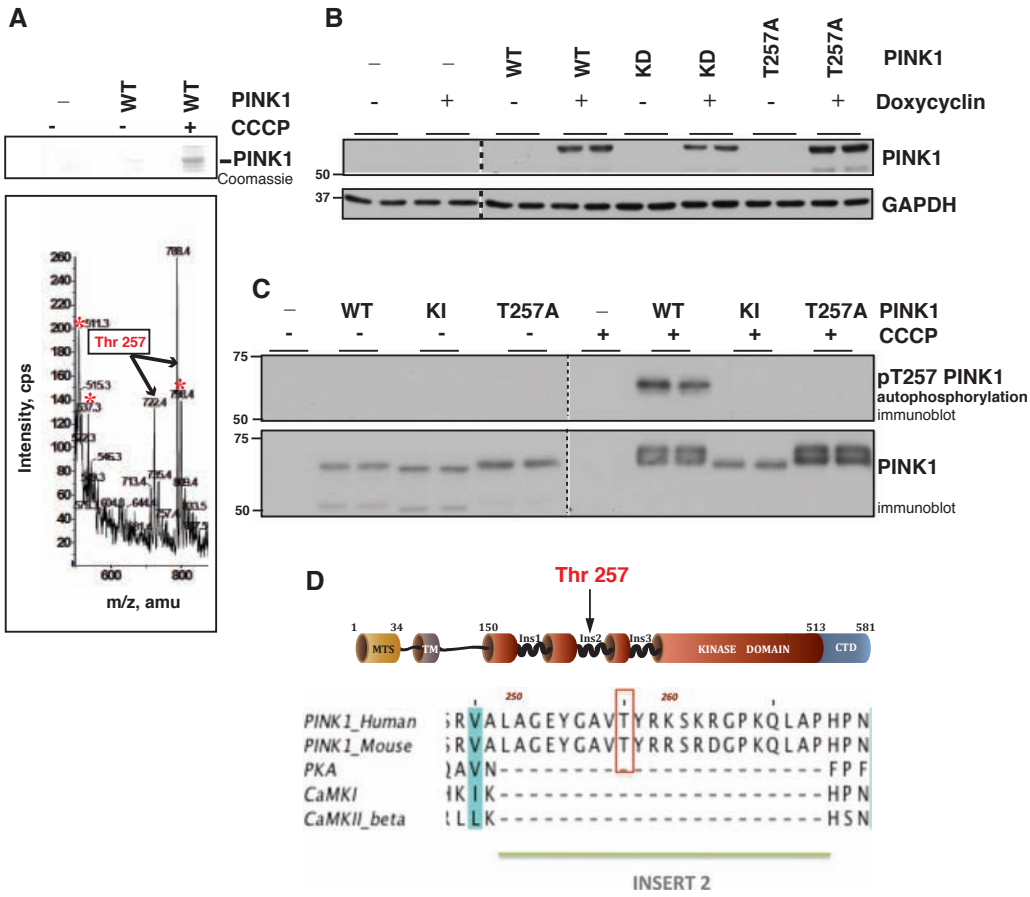

Figure 3.8. Autophosphorylation of PINK1 induced by mitochondrial uncoupling

(A) Flp-In T-Rex HEK293 cell lines stably expressing FLAG alone, or wild-type PINK1-FLAG were treated with DMSO or 10 mM of CCCP for 3 h. Recombinant PINK1 was immunoprecipitated from 10mg of mitochondrial extract, subjected to 4–12% gradient SDS-PAGE and stained with colloidal Coomassie blue. Bands corresponding to PINK1-FLAG were excised from the gel, digested with trypsin, and subjected to precursor-ion scanning mass spectroscopy. The major phosphopeptide that is indicated 'Thr257' was seen only in cells expressing wild-type PINK1-FLAG treated with CCCP and not in the other two conditions. The figure shows the signal intensity (cps, counts of ions per second) of the HPO_3^- ion (279 Da) seen in negative precursor ion scanning mode versus the ion distribution (m/z) for the Thr257 phosphopeptide. The observed values of 722.4 and 788.4 are for the VALAGEYGAVTYR and VALAGEYGAVTYRK variants, respectively, of the Thr257 peptide as $[M-2H]^{2-}$ ions. Other un-assignable phosphopeptides are marked with an asterisk.

(B) FlpIn TRex HEK293 cell lines stably expressing either FLAG-alone, wild-type PINK1-FLAG, kinase-inactive PINK1-FLAG or phospho-mutant PINK1 (T257A)-FLAG were stimulated for protein expression and whole cell lysates were blotted for PINK1 using anti-PINK1 (Novus) and GAPDH as loading control.

(C) 0.5 mg of mitochondrial extracts (treated with DMSO or 10 mM of CCCP for 3 h) of stable cell lines expressing FLAG empty, wild-type PINK1-FLAG, kinase-inactive PINK1-FLAG (D384A) and phospho-mutant PINK1 Thr257Ala (T257A) were immunoprecipitated with anti-FLAG agarose and probed with anti-phospho-Thr257 PINK1 antibody and anti-PINK1 antibody.

(D) Multiple sequence alignment of human and mouse PINK1 with kinases such as PKA, CamKI and CamKII confirms presence of Thr257 residue in the second insertion of PINK1 kinase domain.

phosphorylation of this residue could serve as a useful cell based marker for PINK1 activity *in vivo*.

3.3.4 *Human PINK1 phosphorylates Parkin at Ser^{65} in vivo*

Having established that PINK1 is activated in cell lines upon mitochondrial depolarisation, I next investigated whether human PINK1 is capable of phosphorylating Parkin *in vivo*. Full-length human HA-Parkin was over-expressed in Flp-In TRex HEK293 cells stably expressing wildtype human PINK1, or kinase-inactive human PINK1 (D384A) (Fig. 3.9A). Cells were treated with or without CCCP for 3 h—conditions that induce stabilization and activation of PINK1 at the mitochondria (Fig. 3.7). Parkin was immunoprecipitated and phosphorylation site analysis undertaken by mass spectrometry. This strikingly revealed that Parkin was phosphorylated at Ser65, but only in cells expressing wild-type human PINK1 that had been stimulated with CCCP (Fig. 3.9A). No detectable phosphorylation of Ser65 was observed in the absence of CCCP treatment or in cells expressing kinase-inactive PINK1 (Fig.3.8A). This result indicates that CCCP treatment activates PINK1 enabling it to phosphorylate Parkin. We also detected phosphorylation of a previously reported site on Parkin (Ser131) (Avraham et al, 2007). In contrast to Ser65, phosphorylation of Ser131 was constitutive and not modulated by CCCP or PINK1 (Fig. 3.9A). We failed to detect phosphorylation of Parkin at another previously reported PINK1 site (Thr175) (Kim et al, 2008).

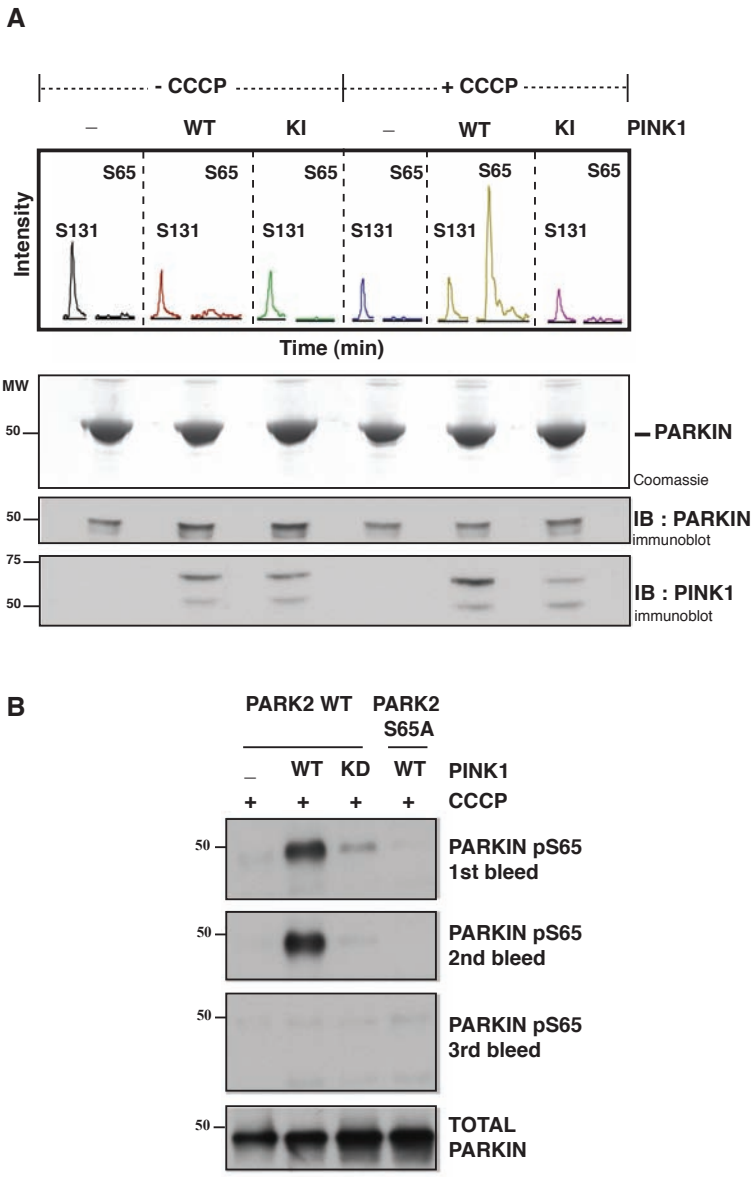

Figure 3.9 Human PINK1 phosphorylates Parkin at Ser65 *in vivo*

(A) Flp-In T-Rex HEK293 cells expressing FLAG-empty, wild-type PINK1-FLAG, and kinase-inactive PINK1-FLAG (D384A) were co-transfected with HA-Parkin, induced with doxycycline and stimulated with 10 mM of CCCP for 3 h. 30mg of whole-cell extract were immunoprecipitated with anti-HA-agarose, resolved by SDS-PAGE and stained with colloidal Coomassie blue. Bands corresponding to mass of HA-Parkin were excised, digested with trypsin, and subjected to high performance liquid chromatography with tandem mass spectrometry (LC-MS-MS) on an LTQ-Orbitrap mass spectrometer. Extracted ion chromatogram analysis of Ser131 and Ser65 phosphopeptide (3^+ R.NDWTVQNCDLDQQ**S**IVHIVQRPWR.K +P). Y-axis corresponds to phosphopeptide signal intensity and x-axis to retention time.

(B) Flp In TRex HEK293 cells stably expressing either FLAG alone, wild-type PINK1-FLAG or kinase-inactive PINK1-FLAG was over-expressed with untagged-Parkin. Cells were induced with doxycycline, stimulated with CCCP and 0.25mg of whole cell lysates were immunoprecipitated with S966C covalently coupled Parkin antibody and blotted with the indicated antibodies.

We next raised a phospho-specific antibody against the Parkin Ser65 phosphorylation site. For characterization of the phospho-specific antibody, stable cell lines expressing either FLAG alone, PINK1-FLAG wild-type or PINK1-FLAG kinase-dead were over-expressed with untagged-Parkin and stimulated with CCCP for 3 hours. All three bleeds of the phospho-antibody were tested and demonstrated that the 1st and 2nd bleeds was able to robustly detect phosphorylation in cells expressing wild-type PINK1 (Fig. 3.9B). The specificity of the antibody was confirmed by absence of any detectable phosphorylation in cells over-expressing Parkin containing a mutation of the phospho-site Ser65 to alanine (S65A). Further, the phospho-Ser65 antibody did not detect any Ser65 phosphorylation under basal conditions indicating that this event specifically occurs during mitochondrial depolarization (Fig. 3.10A). Interestingly, we could also detect phosphorylation of Ser65 in cells treated with CCCP that do not over-express wild-type PINK1 (Fig.3.10A). This suggested that endogenous PINK1 was present in HEK293 cells and could phosphorylate Parkin.

To test whether endogenous PINK1 was indeed expressed in, HEK 293 cells, Ning Zhang, a post-doc in the lab, undertook a timecourse of CCCP stimulation in native HEK293 cells at the times indicated (Fig.3.10B). Whole cell lysates were immunoprecipitated with a an in-house sheep polyclonal PINK1 antibody (raised against aa 175-250 of human PINK1) and immunoblotted with a commercial rabbit polyclonal PINK1 antibody (Novus Biologicals). This revealed the presence of a band that migrated at the predicted mass of endogenous

PINK1 and was being stabilized by CCCP in a time dependent manner (Fig. 3.10B). This band was significantly reduced when cells were transfected for 48h with two different PINK1 siRNA probes but not scrambled siRNA confirming its identity as endogenous PINK1 (Fig. 3.10C). Importantly, siRNA-mediated knockdown of PINK1 severely abrogated phosphorylation of Ser65, indicating that endogenous PINK1 can phosphorylate Parkin Ser65 *in vivo* (Fig. 3.10C).

3.3.5 Human mitochondrial PINK1 directly phosphorylates Parkin at Ser^{65} in vitro

To test whether Parkin was a direct substrate of human PINK1, wild-type or kinase-inactive PINK1 was immunoprecipitated from the mitochondrial fraction of cells treated with CCCP and tested to see whether it could phosphorylate the Ubl domain of Parkin *in vitro* (Fig. 3.11). This revealed that wild-type PINK1 isolated from CCCP-treated cells but not from non-treated cells could phosphorylate the Ubl domain of Parkin (Fig.3.11). Importantly, kinase-inactive PINK1 isolated from CCCP-stimulated cells failed to phosphorylate the Ubl domain of Parkin. Mutation of Ser65 to Ala also prevented wild-type PINK1isolated from CCCP-stimulated cells from phosphorylating the Ubl domain of Parkin (Fig.3.11). These observations confirm that Parkin at Ser65 is a direct substrate of human PINK1.

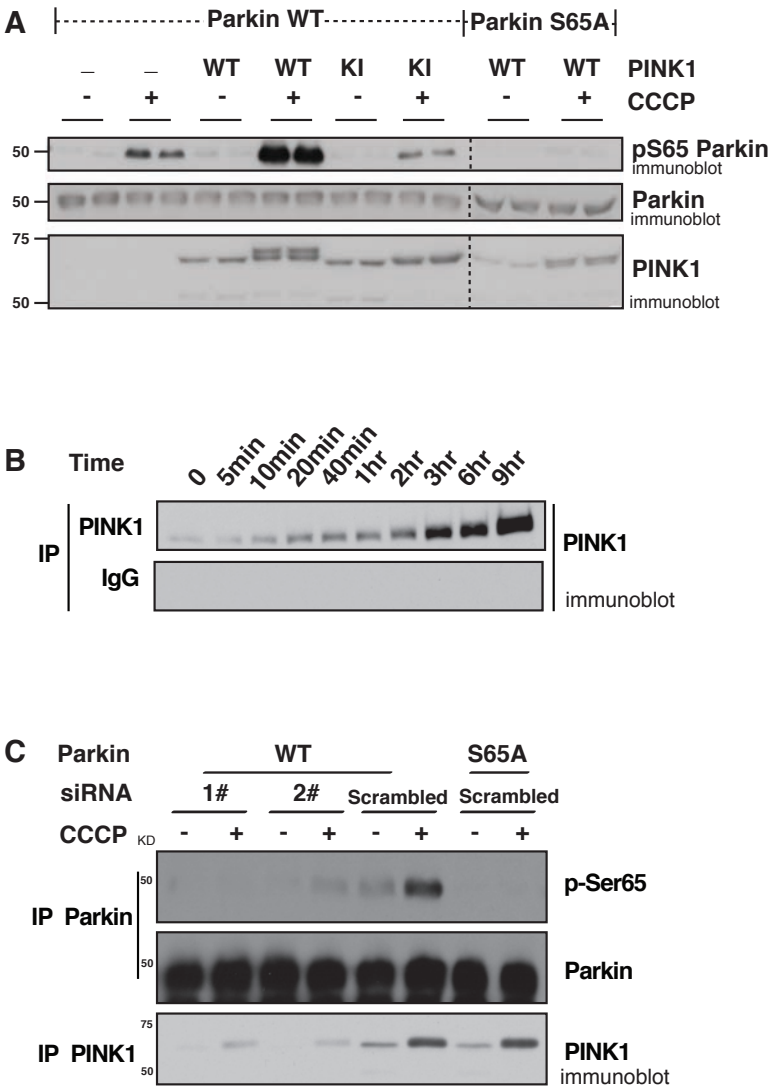

Figure 3.10 Endogenous PINK1 phosphorylates Parkin *in vivo*

(A) Flp In TRex HEK293 cells stably expressing either FLAG alone, wild-type PINK1-FLAG or kinase-inactive PINK1-FLAG were over-expressed with untagged-Parkin. Cells were induced with doxycycline, stimulated with CCCP or DMSO and 0.25mg of whole cell lysates were immunoprecipitated with S966C Parkin antibody and blotted with the indicated antibodies.

(B) HEK293 cells were stimulated at the indicated time points with 10 mM of CCCP. 1mg of whole-cell lysates were immunoprecipitated with anti-PINK1 antibody (S085D) or pre-immune IgG covalently coupled to protein G Sepharose and resolved by 8% SDS-PAGE. Immunoblotting was performed with anti-PINK1 antibody (Novus). Representative of three independent experiments performed by Ning Zhang.

(C) HEK293 cells were co-transfected with PINK1 siRNA (#1 or #2) or scrambled siRNA (scrambled) and untagged wild-type (WT) or Ser65Ala (S65A) mutant Parkin as indicated. Cells were treated with or without 10 mM CCCP for 3 h. 0.25 mg of 1% Triton whole-cell lysate were subjected to immunoprecipitation with S966C covalently coupled Parkin antibody covalently and immunoblotted with the indicated antibodies. 5% of IP was used to blot for total Parkin blots. 0.25 mg of whole-cell lysates was immunoprecipitated with anti-PINK1 antibody (S085D) and immunoblotted with anti-PINK1 antibody (Novus). Representative of three independent experiments performed by Ning Zhang.

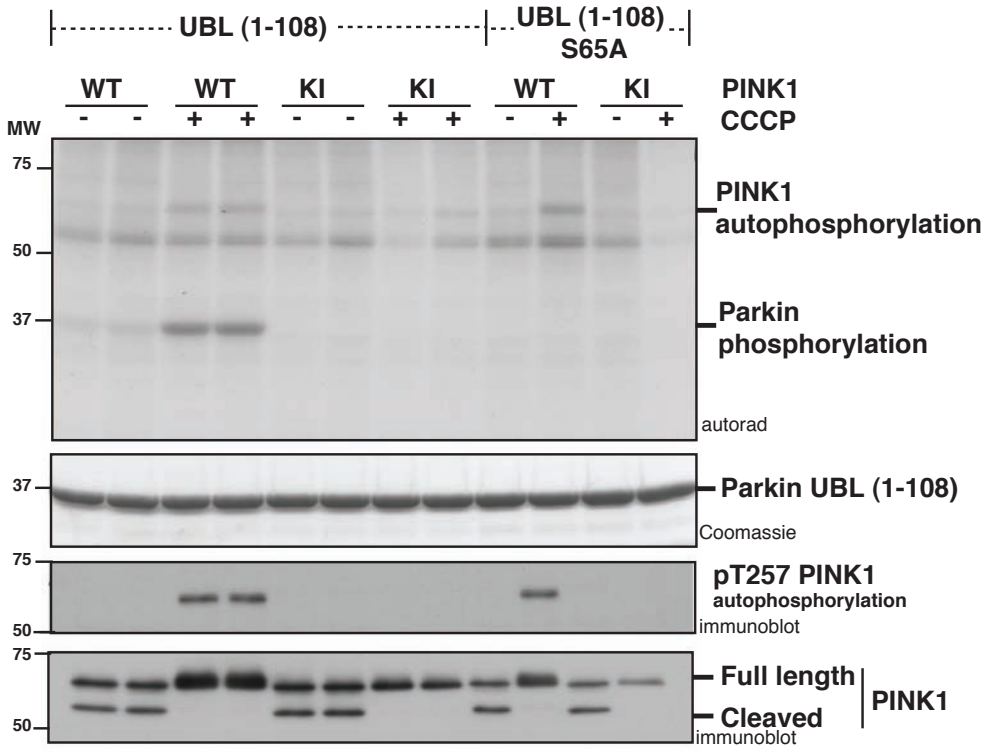

Figure 3.11 *In vitro* phosphorylation of Parkin by human PINK1

Flp-In T-Rex HEK293 cells expressing wild-type PINK1-FLAG, and kinase-inactive PINK1-FLAG was induced for protein expression for 24h. Cells were then treated with 10 mM of CCCP for 3 h and lysates subjected to sub-cellular fractionation. 5mgs of mitochondrial lysate was subjected to immunoprecipitation with anti-FLAG agarose and used in an *in vitro* radioactive kinase assay with [γ-32P]-Mg^{2+}ATP and E. coli expressed recombinant GST-Parkin Ubl domain (residues 1–108) (Ubl) and mutant GST-Parkin (residues 1–108) Ser65Ala (Ubl S65A), purified from E. coli. One half of the assay reaction was run on a 10% SDS-PAGE and was subjected to autoradiography. Colloidal Coomassie stained gel shows equal loading of recombinant substrate. The other half of the reaction was immunoblotted with anti-phospho-Thr257 PINK1 and total PINK1 antibodies following 8% SDS-PAGE.

3.3.6 *Time course of PINK1 activation and phosphorylation of Parkin*

I next investigated the timecourse of PINK1 activation. I performed a CCCP-induced timecourse of PINK1 stable cell lines transfected with untagged Parkin. This revealed that the stabilization of full-length PINK1 at mitochondria is rapid

with significant stabilization seen within 5 min of CCCP treatment and is maximal by 40 min and then sustained for up to 3 h (Fig. 3.12A). Loss of the cleaved form of PINK1 observed in the cytosol is particularly rapid and almost disappears within 5 min of CCCP treatment. However, the appearance of 'band-shift' and autophosphorylation of Thr257 occurred more slowly and was observed only after 40 min of CCCP treatment and was sustained for up to 3 h (Fig. 3.12A). There was no phosphorylation of Thr257 or band-shift of

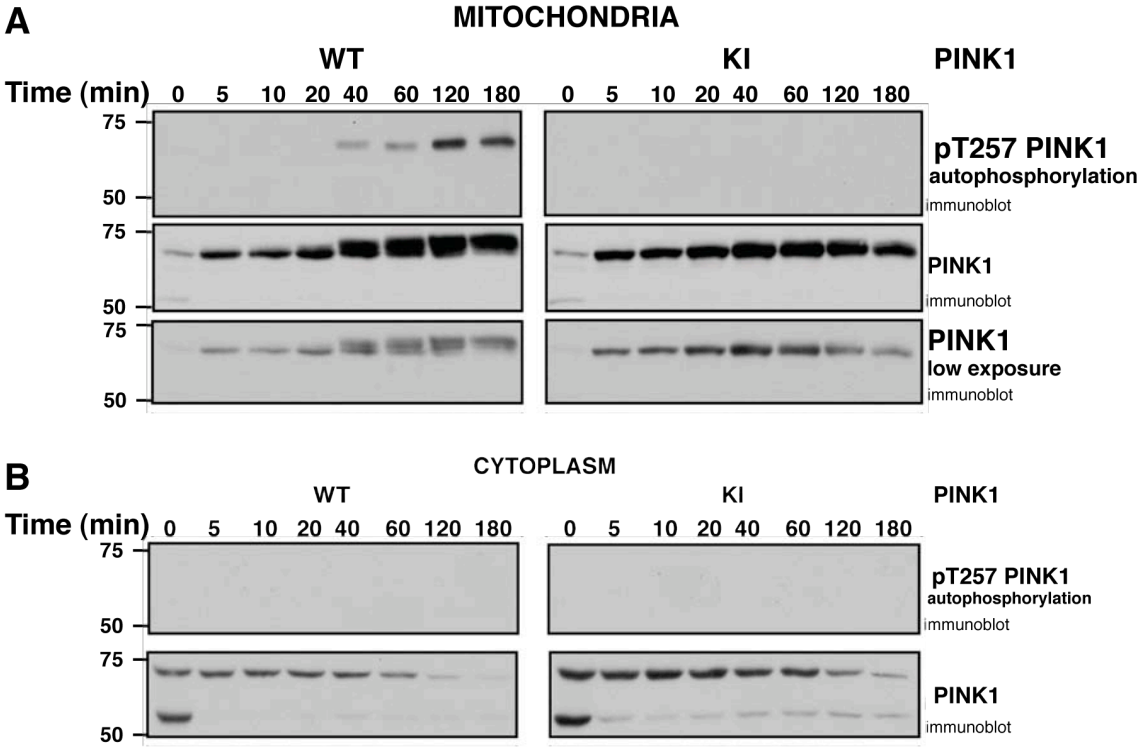

Figure 3.12 Timecourse of PINK1 activation *in vivo*

(A) Flp-In T-Rex HEK293 cells stably expressing PINK1-FLAG wild-type and kinase-inactive (D384A) were stimulated at the indicated time points with 10 mM of CCCP. 0.5 mg of mitochondrial extracts was immunoprecipitated with anti-FLAG agarose and immunoblotted with anti-phospho-Thr275 antibody or total PINK1 antibody.

(B) As in (A) cytoplasmic extracts were obtained at the indicated time-points and immunoprecipitated with anti-FLAG agarose and immunoblotted with PINK1 anti-phospho-Thr275 antibody or total PINK1antibody.

cytoplasmic PINK1 indicating that mitochondrial association is required for this event (Fig.3.12B). In contrast, monitoring Parkin Ser65 phosphorylation *in vivo* using the phospho-specific antibody against phospho-Ser65 indicated that Parkin Ser65 phosphorylation occurs at 5 min and becomes maximal and sustained from 40 min onwards (Fig. 3.13). This suggests that the kinetics of PINK1 activation against its substrate is significantly faster than the kinetics of PINK1 autophosphorylation, which is not surprising as most kinases undergo autophosphorylation as a consequence of enzymatic activation.

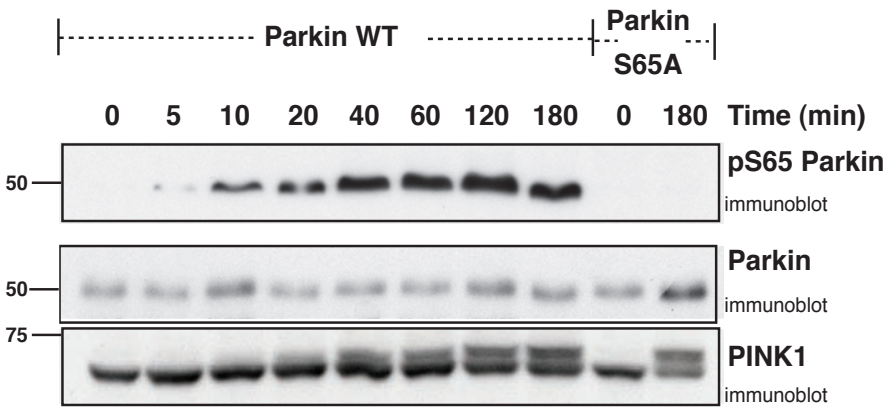

Figure 3.13 Timecourse of Parkin Ser65 phosphorylation *in vivo*

Flp-In T-Rex HEK293 cells stably expressing wild-type PINK1-FLAG were co-transfected with untagged wild-type (WT) or Ser65Ala (S65A) mutant Parkin; induced with doxycycline and stimulated with 10 mM of CCCP at the indicated time points. 0.25 mg of whole-cell lysate was immunoprecipitated with anti-Parkin covalently coupled antibody (S966C) and immunoblotted with anti-phospho-Ser65 antibody in the presence of dephosphorylated peptide. 1% of the IP was immunoblotted with total anti-Parkin antibody. 1.5 mg of whole-cell extract was immunoprecipitated with anti-FLAG agarose and immunoblotted with anti-PINK1 antibody (Novus). Representative of at least 3 independent experiments performed by Agne Kazlauskaite

3.3.7 *PINK1 Thr257 autophosphorylation is dispensable for Parkin phosphorylation in vivo*

I next investigated whether autophosphorylation of PINK1 at Thr257 was critical for downstream PINK1-Parkin signaling. I monitored Parkin phosphorylation in cells stably expressing PINK1-FLAG harbouring a phospho-mutant of Thr257 to Alanine. Parkin Ser65 phosphorylation was still observed in CCCP-treated cells expressing PINK1 T257A suggesting that phosphorylation of this residue is not crucial for activation of PINK1 *in vivo* (Fig. 3.14A). However, as described above, mass spectrometry analysis indicated that PINK1 is likely to be autophosphorylated at additional sites although it was not possible to identify these (Fig. 3.8A). I therefore investigated whether PINK1 autophosphorylation perhaps at these other sites was important for its activity. Lambda phosphatase treatment of mitochondrial PINK1 isolated from CCCP-treated cells induced complete dephosphorylation of Thr257 and led to a significant inhibition in kinase activity as judged by its phosphorylation of Parkin *in vitro* (Fig.3.14B). Addition of lambda phosphatase inhibitor EDTA prevented dephosphorylation of Thr257 and loss of the ability of PINK1 to phosphorylate Parkin. I also observed that phosphatase treatment did not collapse the CCCP-induced band-shift (Fig. 3.14B) indicating the presence of either phosphatase resistant sites or an additional protein modification on PINK1. Therefore, Thr257 is dispensable for Parkin phosphorylation *in vivo* (Fig. 3.14A). However, phosphorylation of PINK1 at additional sites other than Thr257 could contribute to CCCP-induced PINK1 activation. In future work it would be critical to define these sites.

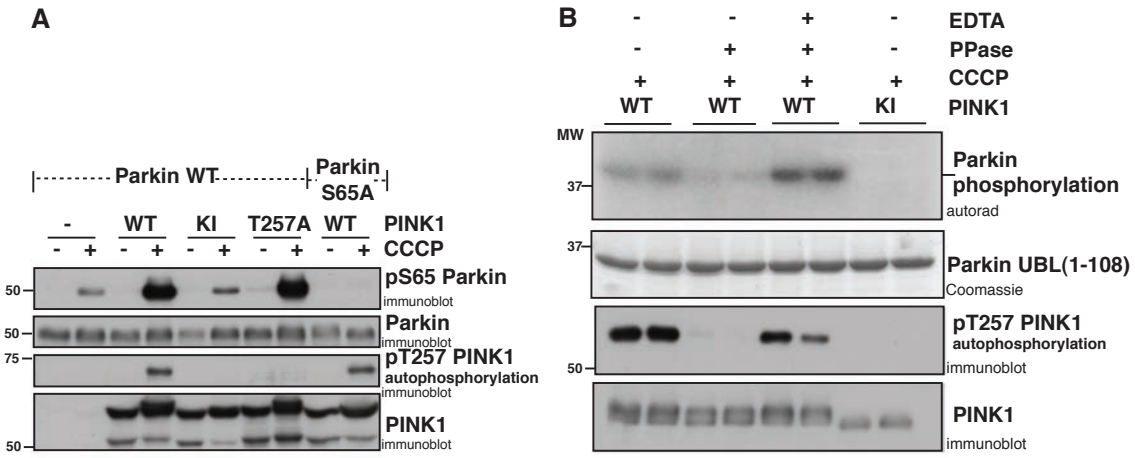

Figure 3.14 PINK1 Thr257 autophosphorylation is dispensable for Parkin phosphorylation

(A) Flp-In T-Rex HEK293 cells expressing FLAG-empty, wild-type PINK1-FLAG, kinase-inactive PINK1-FLAG and T257A PINK1-FLAG were co-transfected with untagged wild-type (WT) or Ser65Ala (S65A) mutant Parkin, induced with doxycycline and stimulated with 10 mM of CCCP for 3 h. Parkin and PINK1 immunoprecipitation and immunoblotting was performed as described in legend of Fig. 3.12.

(B) C-terminal-FLAG tagged wild-type or kinase-inactive (D384A) PINK1 were immunoprecipitated from 5 mg of mitochondrial enriched extracts using anti-FLAG agarose beads. Wild-type PINK1 was incubated with or without 1000 U of lambda phosphatase or treated with lambda phosphatase along with 50 mM EDTA. Kinase-inactive PINK1 was incubated in buffer alone without lambda phosphatase. Phosphatase treated PINK1 was taken for an *in vitro* kinase assay with GST-Parkin Ubl (1–108) as the substrate. Samples were analysed as described in legend to Fig. 3.11.

3.4 PART III – Investigation of the mechanism of PINK1 activation

3.4.1 PINK1 is specifically activated by depolarization of inner mitochondrial membrane potential

Within the inner mitochondrial membrane (IMM), the electron transport chain transfers electrons through a series of oxidation–reduction reactions coupled to the transfer of protons across the IMM and this efflux creates a proton electrochemical gradient known as the protomotive force. The protomotive force drives the re-entry of protons through the proton channel of the F1F0-ATP synthase crucial for ATP production and comprises mainly of an electrical component - the mitochondrial membrane potential (ΔΨm) - and a transmembrane pH gradient (ΔpH) (Abou-Sleiman et al, 2006) (Fig. 3.15).

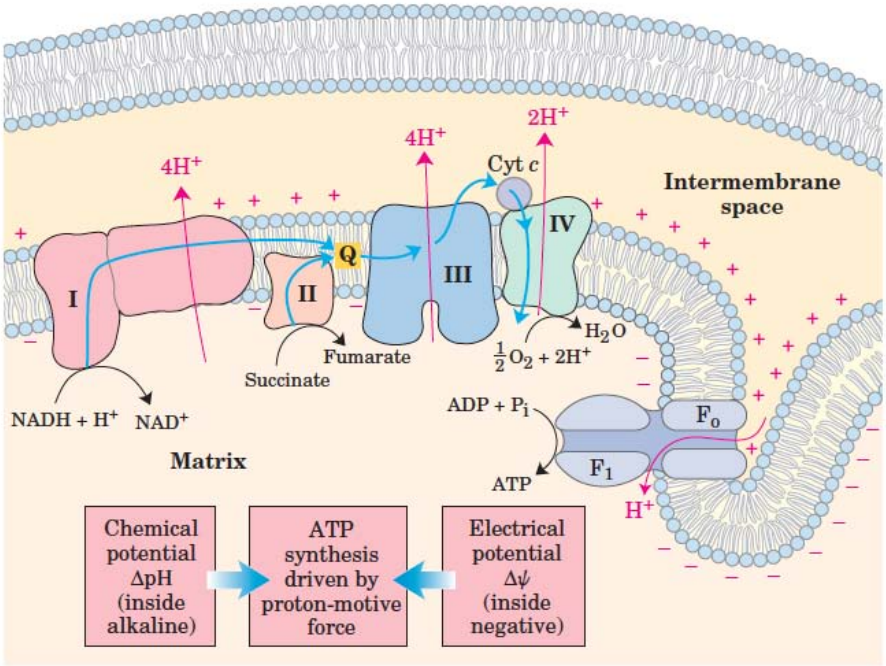

Figure 3.15 Illustration depicting mitochondrial electron transport chain Adapted from (Lehninger et al, 2005)

CCCP dissipates both ΔΨm and the pH gradient leading to impaired mitochondrial ATP synthesis. To determine the mechanism of activation of PINK1, a panel of agonists that have previously been reported to disrupt mitochondria by diverse modes of action were tested (Fig. 3.16A). Under the conditions tested only the proton ionophores CCCP, FCCP and the potassium-uniporter valinomycin were able to induce activation of PINK1 leading to Parkin Ser65 phosphorylation (Fig. 3.16B). In contrast to CCCP and FCCP, valinomycin depolarizes the ΔΨm but does not affect the pH gradient suggesting that PINK1 is specifically activated by loss of the ΔΨm. We did not observe any effect of an inhibitor of ATP synthase (oligomycin) or various inhibitors of the electron transport chain complexes that have previously been implicated in neurodegeneration models (MPP+, rotenone, 3-nitropropionic acid) when used alone (Fig. 3.16B).

3.4.2 *Further analysis of the effects of mitochondrial respiratory chain inhibition on PINK1 activation*

The mitochondrial membrane potential is critically dependent on ATP synthesis yet from Fig. 3.16 it is clear that inhibition of individual components of electron transport chain in HEK293 cells does not lead to PINK1 activation. However, I reasoned that since HEK293 being a cancer cell relies less on oxidative phosphorylation and more on glycolysis; depolarisation of the mitochondrial membrane potential may be less easily disrupted upon inhibition of individual components of the electron transport chain. I therefore investigated whether inhibition of complex I, II or III in combination with ATP synthase inhibition may

A

AGONIST	MODE OF ACTION	CONC.
Oligomycin	ATP synthase inhibitor	1μM
Antimycin A	Complex III inhibitor	10μM
Valinomycin	K+ uniporter	2μM
CCCP	H+ ionophore	10μM
FCCP	H+ ionophore	10μM
Dopamine	Neurotransmitter	10μM
6-OHDA	Neurotoxin	100μM
MPP+ iodide	Complex I inhibitor	100μM
Rotenone	Complex I inhibitor	1μM
Ionomycin	Ca2+ ionophore	5μM
3-NPA	Complex II inhibitor	10μM
L-BSO	Decreases GSH synthesis	50μM
H202	Oxidizing agent	50μM
Diamide	Thiol oxidizing agent	100μM
Doxorubicin	DNA interchelating agent	0.5μM
Deferiprone	Iron chelator	1mM
Phenformin	AMPK activator	0.5μM

B

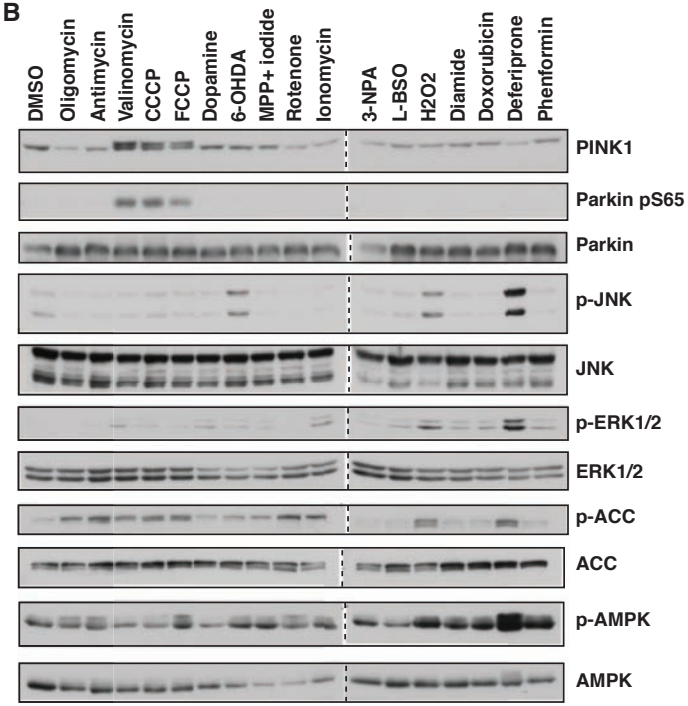

Figure 3.16 Inducers of mitochondrial depolarization specifically activate PINK1

(A) Table of agonists tested. **(B)** Flp-In T-Rex HEK293 cells expressing wild-type PINK1-FLAG were co-transfected with untagged wild-type Parkin, induced with doxycycline and stimulated with the indicated agonists for 3 h except for Deferiprone (24 h treatment). 0.25 mg of whole-cell lysate was subjected to immunoprecipitation with anti-Parkin covalently coupled antibody (S966C) and immunoblotted with anti-phospho-Ser65 antibody in the presence of dephosphorylated peptide. 10% of the IP was immunoblotted with total anti-Parkin antibody. 25μg of whole-cell lysate was immunoblotted with total PINK1 antibody (Novus), phospho-JNK (CST), total-JNK (CST), phospho-ERK1/2, total-ERK1/2 (CST), phospho-ACC (CST), total ACC (CST), phospho-AMPK (CST) and total AMPK (CST). Representative of two independent experiments

be sufficient to induce PINK1 activation. Consistent with this I observed that inhibition of Complex III (using antimycin) in combination with an ATP synthase inhibitor (Oligomycin) could indeed activate PINK1 as judged by Parkin Ser65 phosphorylation, which was comparable to that of CCCP stimulation (Fig. 3.17B).

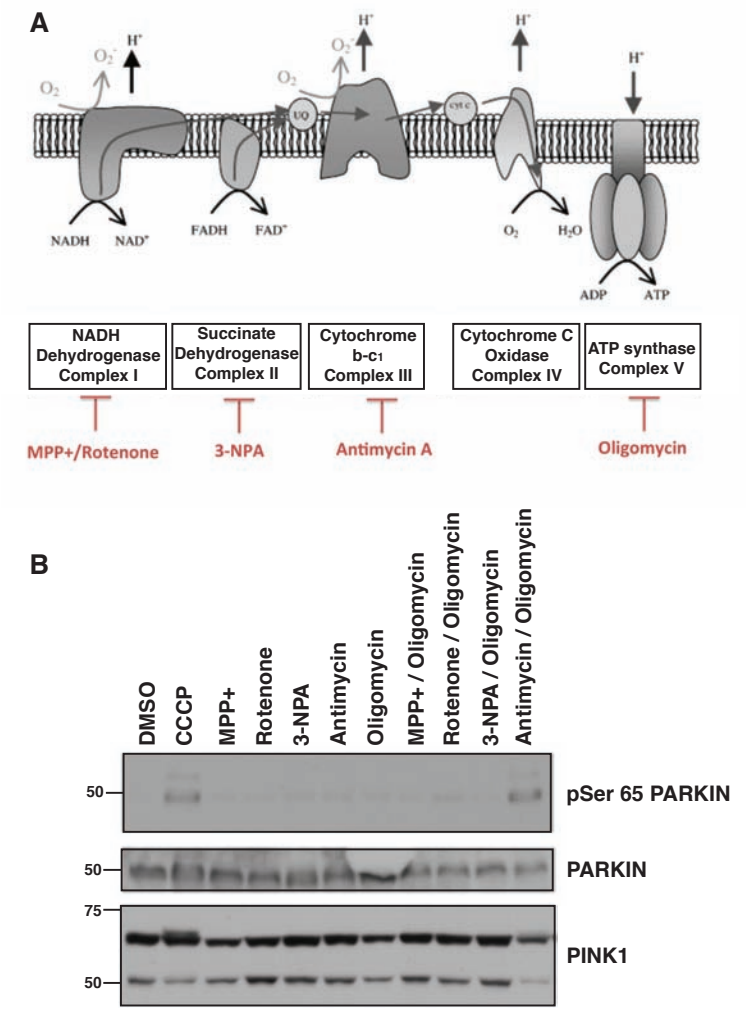

Figure 3.17 Activation of PINK1 by inhibition of Complex III and ATP synthase

(A) Illustration depicting the various inhibitors of mitochondrial electron transport chain used in this study.

(B) Flp In TRex HEK293 cells stably expressing wild-type PINK-FLAG were co-transfected with untagged wild-type Parkin and treated with the indicated electron transport chain inhibitors at concentrations listed in Fig. 3.16A for 3h. Samples were processed and immunoblotted as described in legend of Fig. 3.16B.

3.5 Discussion

Discovery of Parkin Ser65 phosphorylation as a substrate of PINK1

The first genetic link between PINK1 and Parkin was established by elegant studies using the *Drosophila* model system (Clark et al, 2006; Park et al, 2006). dPINK1 and dParkin null flies share similar degenerative phenotypes and over-expression of Parkin can rescue the phenotype of dPINK1 null flies and not vice versa, indicating that Parkin lies downstream of PINK1 (Clark et al, 2006; Park et al, 2006). Interestingly, patients with loss-of-function mutations of either PINK1 or Parkin display very similar clinical presentation of PD, which further argues towards a common signaling pathway between PINK1 and Parkin in human beings (Abeliovich & Flint Beal, 2006).

The phosphorylation site on Parkin was mapped to a highly conserved Ser65 residue in the N-terminal Ubl domain. Parkin belongs to the RING-in-between-RING (RBR) family of E3 ubiquitin ligases. RING family E3 ubiquitin ligases act as scaffolds by bringing together the E2 ubiquitin ligase and substrate to mediate catalytic transfer of ubiquitin (Fig.3.21B). Recent work suggest that Parkin and other RBR family members may function as a RING/HECT hybrid that directly catalyze ubiquitin transfer to a substrate via an intermediate thioester-linked ubiquitin adduct on a conserved cysteine (Cys 431) in the RING2 domain of Parkin (Fig.3.21A) (Wenzel et al, 2011). The figure below describes mechanisms of ubiquitin transfer mediated by RING and HECT family E3 ligases (Fig.3.21).

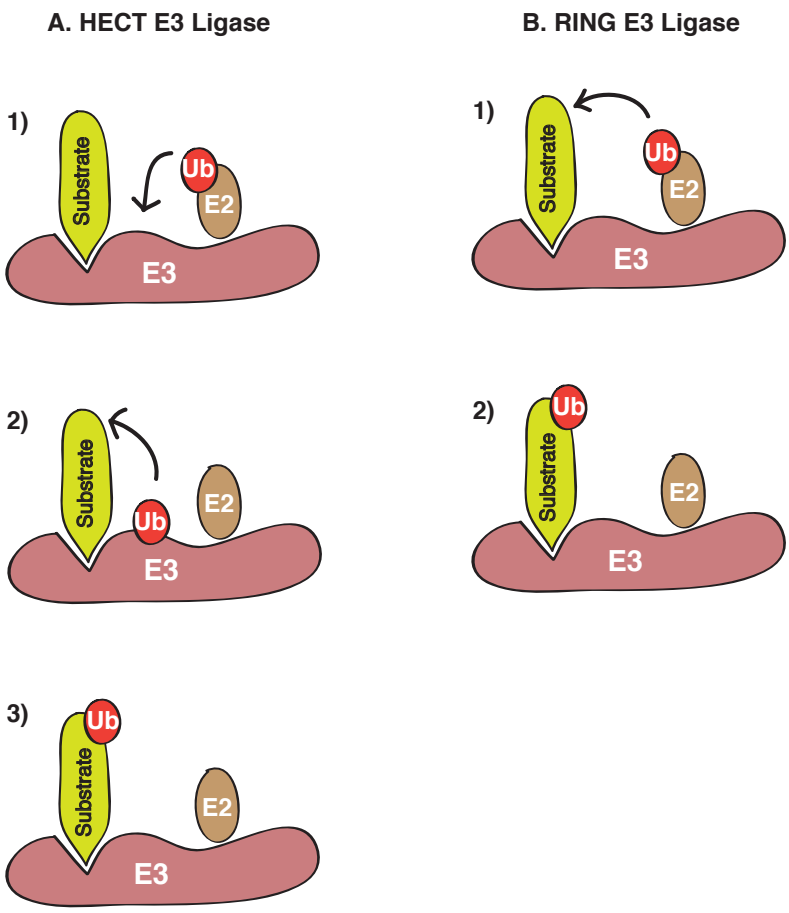

Figure 3.18 Mechanism of Ubiquitin transfer in HECT and RING family E3 ligases (Deshaies & Joazeiro, 2009)

(A) HECT E3 ubiquitin ligases contain a conserved cysteine that accepts ubiquitin from E2-Ub to form an E3-ubiquitin thioester linkage. Ubiquitin is then transferred from this covalent E3-intermediate to its substrate.

(B) RING E3 ligases mediate direct transfer of ubiquitin from E2-Ub to substrate

More recently, it has been proposed that the Ubl domain of Parkin acts as an auto-inhibitory domain, which prevents catalytic activity by binding to the C-terminal region that thereby abrogates ubiquitin binding to the C-terminus (Chaugule et al, 2011). However, the mechanism of activation of Parkin remained unknown in this study. Analysis of all available NMR and crystal

structures of Parkin revealed that the PINK1-mediated Parkin Ser65 phosphorylation site could lie in the fifth β-strand that makes up the ubiquitin-like fold that is partially exposed to the surface (PDB code: 2KNB (solution, mouse) (Trempe et al, 2009); PDB code: 1IYF (solution, human) (Sakata et al, 2003)) (depicted in Fig.3.22) or may sometimes lie within a loop adjacent to the strand suggesting some conformational flexibility around this region (PDB code: 1MG8 (solution, mouse) (Tashiro et al, 2003); PDB code: 2ZEQ (solution, mouse) (Tomoo et al, 2008)).

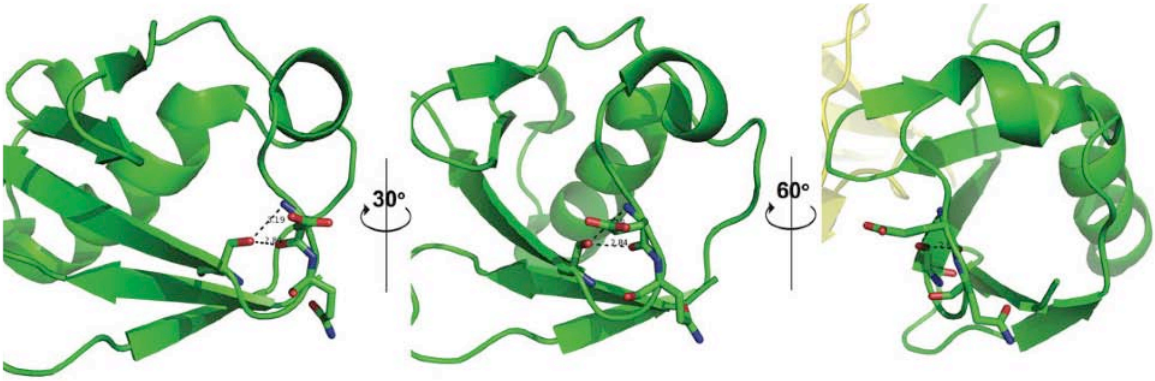

Figure 3.19 Structure of human Parkin Ubl domain

Three views representing a 90° rotation about the y-axis, depict the Ubl domain of Parkin with Ser65 highlighted and the contacts it make within 4 Angstroms (PDB code 1IYF). Provided by Helen Walden.

In our study, full length Parkin is phosphorylated to a lesser extent when compared to isolated Ubl domain, which suggests the presence of certain structural constraints in accessing Ser65 site by PINK1 in full length Parkin. It is therefore possible that upon interaction with PINK1, the Ubl domain can undergo a local conformational change enabling PINK1 to gain access to Ser65 for phosphorylation.

A low resolution crystal structure of full length rat Parkin has recently been published (Trempe et al, 2013). This study reveals an auto-inhibited structure of Parkin wherein the RING0 domain occludes the ubiquitin-binding catalytic Cys431 (present in RING2) by binding to RING2 domain. Another region of autoinhibition is mediated by an alpha helical REP (Repressor element of Parkin) domain, which lies in the linker region between IBR and RING2 domain. The REP helix binds to the RING1 domain and occludes the E2- binding site (Trempe et al, 2013) (Fig. 3.23B). Overall the structure does suggest that upon activation, Parkin would need to undergo a major conformational change to enable E2 binding as well as catalytic activity. The crystal structure of Parkin reveals that the Ubl domain lies close to the E2 binding site as well as the REP linker (Fig. 3.23B) However, the Ser65 residue lies away from the Ubl/RING1 interface and it is not possible to discern how phosphorylation of Ser65 might lead to activation (Trempe et al, 2013). It has already been found that a point mutant of the REP linker (W403A) aids relieving the auto-inhibition and enhancing E2 binding (Trempe et al, 2013) Hence in future, it would be important to test if Ser65 phosphorylation could also influence binding of Parkin to its cognate E2 (Fig. 3.23B).

In this work, Parkin activity has been assayed using an auto-ubiquitylation assay and monitoring the formation of short poly-ubiquitylated free chains. It would also be important to validate the findings using a physiological Parkin substrate/s to confirm that Ser65 phosphorylation does indeed enhance ubiquitylation of a physiological substrate of Parkin. My data also suggest that

small molecules that bind to and disrupt the Ubl domain-C-terminus auto-inhibitory interface may activate Parkin in a similar manner to Ser65 phosphorylation. Understanding how Ser65 phosphorylation confers activation will also be important in the development of small molecule activators in terms of understanding their mechanism.

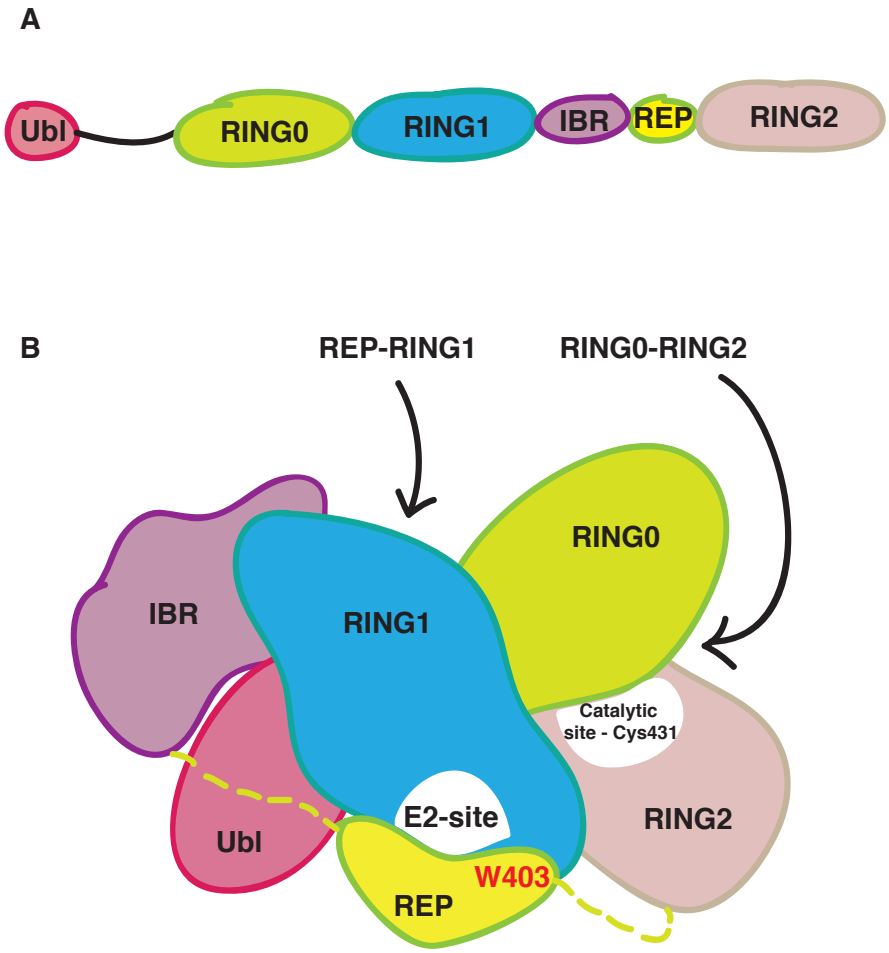

Figure 3.20 Schematic of auto-inhibition of Parkin

(A) Primary structure and domains of Parkin

(B) Schematic representation of auto-inhibition of Parkin showing the occluded catalytic site and E2 binding-site mediated by indicated interactions between RING0-RING2 and REP linker-RING1 respectively.

Phosphosite mapping of Parkin also identified Ser131 in addition to Ser65 phosphorylation site. Ser131 is constitutively phosphorylated and not influenced by PINK1 or CCCP. Ser131 lies within the linker region of Parkin between the Ubl and RING0 domain and unlike Ser65 is not fully conserved in lower organisms (e.g. leucine in Drosophila). A previous *in vitro* study has suggested that Ser131 may be phosphorylated by Cdk5 (Avraham et al, 2007) and further work would be required to define the importance of this phosphorylation site.

There has been one previous report that human PINK1 isolated from non-CCCP unstimulated cells can directly phosphorylate Parkin at a single threonine residue, Thr175 (Kim et al, 2008). In that study, a deletion fragment of PINK1 spanning residues 200–581 was used that would be predicted to be missing approximately the first 50 amino acids of the N-lobe of the PINK1 kinase domain including the conserved glycine-rich loop motif (residues 163–169), which in other kinases is essential for coordinating ATP. This construct of PINK1 would therefore be expected to be inactive. Moreover, in their study, the kinase-inactive mutant of the PINK1 [200–581] fragment still exhibited substantial kinase activity towards Parkin (Kim et al, 2008). Taken together these findings indicate that phosphorylation of Thr175 observed in that study was likely to be mediated by a contaminating kinase.

PINK1 activation concurs with its stabilization, since I begin to observe Parkin Ser65 phosphorylation from 5min of CCCP treatment reaching a maximal activation at 40min in cells. However, the time course of PINK1 auto-

phosphorylation takes longer, requiring around 40min with activation then being sustained for at least up to 3h. This observation is not surprising as most kinases display differential kinetics for autophosphorylation and substrate phosphorylation, where the latter occurs at a faster rate and is a better readout of kinase activity. Interestingly previous studies suggest that Parkin can translocate to mitochondria upon CCCP treatment to induce mitophagy and this is enhanced when PINK1 is co-expressed in cells (Geisler et al, 2010; Matsuda et al, 2010; Narendra et al, 2010; Vives-Bauza et al, 2010). The kinetics of Parkin translocation is 5min in cells co-expressing PINK1 compared with 30min when PINK1 is absent (Narendra et al, 2010). This strikingly matches the kinetics of Parkin Ser65 phosphorylation we observe and raises the possibility that phosphorylation can influence Parkin translocation to the mitochondria. In fact, a follow up study of our finding has shown that Ser65 phosphorylation is not only essential for efficient translocation of Parkin, but also important for Parkin-mediated degradation of mitochondrial outer membrane proteins in mitophagy (Shiba-Fukushima et al, 2012). A recent report has validated my findings that PINK1 phosphorylates Parkin at Ser65 in primary mouse neurons stably expressing PINK1 and Parkin by lentiviral transduction. (Koyano et al, 2013). In a separate study the same group provide further evidence that PINK1-mediated phosphorylation of Parkin at Ser65 drives formation of ubiquitin-thioester linkage on the catalytic Cys431 residue in RING2 domain of Parkin (Iguchi et al, 2013).

My data suggests that loss-of-function mutations in PINK1 would lead to suppression of Parkin E3 ligase activity and result in reduced ubiquitylation of Parkin's targets. This may explain why over-expression of Parkin in dPINK1 null flies restores ubiquitylation of targets and rescues the null phenotype (Clark et al, 2006; Park et al, 2006). It is possible that the key Parkin targets are located at the mitochondria and indeed several candidate mitochondrial substrates for Parkin have been proposed, including Mitofusin1 (Ziviani et al, 2010), VDAC1 (Geisler et al, 2010) and more recently PARIS (Shin et al, 2011) and Miro (Liu et al, 2012). In a recent report, a quantitative diGly proteomic approach was undertaken to define PARKIN-dependent ubiquitylome in response to mitochondrial depolarization (Sarraf et al, 2013).

Hence, to conclude this section, my studies have demonstrated that depolarization of ΔΨm induces stabilization and activation of PINK1 enabling it to directly phosphorylate Parkin at Ser65 within the N-terminal Ubl domain leading to activation of Parkin E3 ligase activity (Fig. 3.24C). Activation of Parkin is likely to involve major re-organisation from its basal auto-inhibited 'closed' conformation. Once Parkin is activated in depolarized mitochondria, it is likely to play a key role in ubiquitylation of mitochondrial proteins that may signal mitochondria for lysosomal degradation – this process termed as 'mitophagy' (Fig. 3.24B).

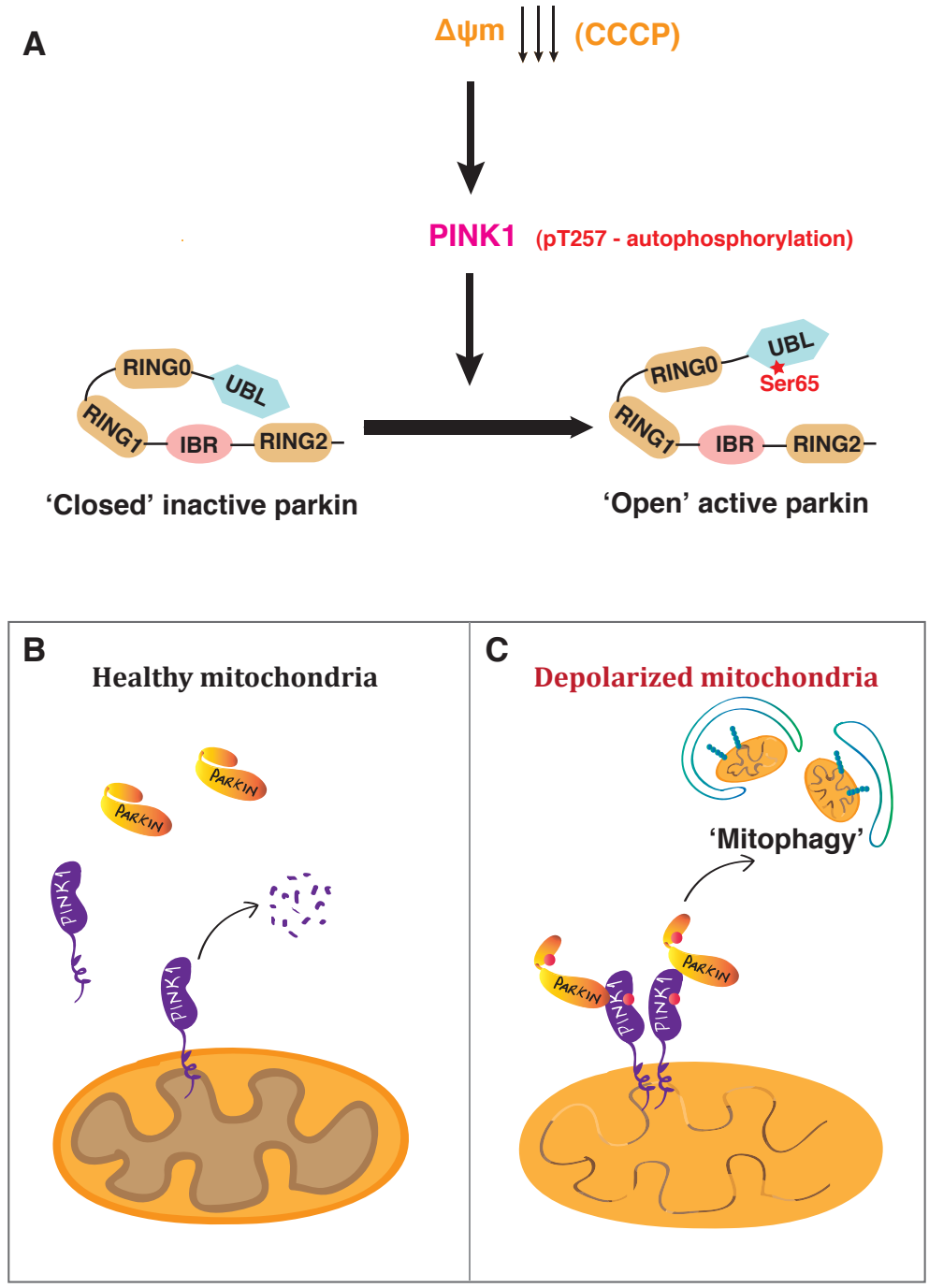

Figure 3.21 Model of Parkin activation by PINK1

(A) A linear pathway for PINK1-Parkin shows that under basal conditions, Parkin is kept in a closed inactive conformation by Ubl-mediated auto-inhibition. Following mitochondrial depolarization, PINK1 mediated phosphorylation of Parkin relieves its auto-inhibition and enables Parkin to become active to ubiquitylate target substrates.

(B) Illustration depicts that in normal healthy mitochondria, a constant turnover of PINK1 occurs and thus Parkin remains in its auto-inhibited state.

(C) In depolarized mitochondria, PINK1 stabilization occurs accompanied by autophosphorylation of PINK1 as well as phosphorylation of Parkin at Ser65. Parkin can then be activated and perhaps subsequently can sequester damaged mitochondria for lysosomal degradation.

Insights on PINK1 stabilization and autophosphorylation in mitochondria

Like many kinases, PINK1 was found to undergo autophosphorylation mainly at Thr257. Based on multiple sequence alignment, Thr257 lies in the middle of the second insertion loop and would likely be accessible for phosphorylation (Woodroof et al, 2011). However, my data suggests that autophosphorylation of Thr257 is not crucial for activation of PINK1. However, lambda phosphatase treatment of PINK1 substantially reduced its *in vitro* kinase activity suggesting that phosphorylation of PINK1 at other as yet unidentified sites are essential for its activation. Recently, another group has claimed that Ser228 and Ser402 are crucial auto-phosphorylation sites in PINK1, which when mutated to Ala can abrogate Parkin translocation to mitochondria (Okatsu et al, 2012). However, the authors of this study failed to provide direct evidence that Ser228 and Ser402 are phosphorylated either by mass spectrometry or by immunodetection with a phospho-specific antibody. Studies undertaken in our lab have also been unsuccessful at confirming phosphorylation of these sites. Nevertheless, whilst my data suggests that autophosphorylation at Thr257 is not critical for PINK1 activation, I believe this could potentially serve as a useful reporter for PINK1 activation.

In my hands, PINK1 also undergoes an electrophoretic mobility shift after CCCP treatment of wild-type but not kinase-inactive PINK1, which is incapable of autophosphorylation. There have been no previous reports of the occurrence of a band-shift in PINK1 and this was detected only when the protein was resolved by 8% isocratic Tris-Glycine SDS-PAGE. The bandshift was less pronounced in

gradient gels perhaps explaining why this observation was not made earlier. I was able to conclude that the band-shift is not a result of auto-phosphorylation, as lambda phosphatase of immunoprecipitated PINK1 could not abolish it. Thus, in future, it would be interesting to determine both the crucial auto-phosphorylation sites and/or covalent modifications induced by CCCP and investigate their role in PINK1 activation.

The specificity of PINK1 activation was explored by testing the effect of a wide range of mitochondrial toxins. This showed that PINK1 was efficiently activated only under conditions that depolarize ΔΨm (CCCP, FCCP or Valinomycin treatment), as judged by its ability to mediate Parkin Ser65 phosphorylation. Under these conditions PINK1 could be associated with a non-covalent activator at the mitochondrial membrane, such as another protein or a small molecular second messenger. In order to address which proteins could potentially interact with PINK1 and possibly play a role in its activation, a quantitative proteomic interactor screen was performed, which is discussed in Chapter 4.

Defects in electron transport chain have been implicated in PD and has been discussed in section 1.5.2. I observed that PINK1 activation is specific to mitochondrial depolarization and inhibition of individual components of the electron transport chain caused no effect in HEK293 cells. It has been reported in a previous study that a combination of complex III inhibition (using Antimycin A) and complex V inhibition (by Oligomycin) can cause translocation of Parkin

to mitochondria comparable to CCCP stimulation in HEK293T cells (Vives-Bauza et al, 2010). Using a fluorescent dye to detect mitochondrial membrane potential, they claim that this combination of electron transport chain inhibitors can lead to efficient reduction in mitochondrial membrane potential, PINK1 stabilization and downstream Parkin translocation. Using Parkin Ser65 phosphorylation as a read-out for PINK1 activation, I decided to test if this holds true in my study system. A combination of Complex I+V inhibition, Complex II+V inhibition and Complex III+V inhibition was performed. Complex IV inhibition leads to cell death and hence was omitted. Strikingly, I observed robust Parkin phosphorylation accompanied by PINK1 stabilization under conditions of complex III+V inhibition.

To conclude this chapter, I have reported important new information to support the notion that ΔΨm depolarization leads to stabilization and activation of PINK1 in the mitochondria and subsequent phosphorylation of Parkin at Ser65. Phosphorylation of Parkin occurs in its N-terminal Ubl domain, which leads to activation of its E3 ubiquitin ligase activity. In addition to this, I provide evidence that once activated PINK1 gets autophosphorylated at several residues, one of which we have identified as Thr257. Using Parkin Ser65 phosphorylation as a reporter for PINK1 activity, I confirm the specificity of PINK1 activation to occur only when mitochondrial membrane potential is perturbed.

Chapter 4

Identification of novel interacting partners of mitochondrial PINK1

4. Identification of novel interacting partners of mitochondrial PINK1

1.1 Introduction

PINK1 is unique amongst all known protein kinases by its primary localization in the mitochondria. Under basal conditions, PINK1 undergoes constant turnover in order to maintain a minimal level of expression in the mitochondria. Upon mitochondrial depolarization, PINK1 undergoes stabilization and subsequent activation in the mitochondria. Attempts to identify bona fide interacting partners of PINK1 have been hampered by the low expression of PINK1 under basal conditions (Weihofen et al, 2009). Since mitochondrial depolarization leads to dramatic stabilization of mitochondrial PINK1, I decided to identify binding partners of PINK1 under these conditions.

The last decade has seen a wide range of applications for mass spectrometry in studying protein-protein interactions. The standard approach involves affinity purification of protein complexes from a relevant tissue or cell type and analysis by mass spectrometry (Aebersold & Mann, 2003). Given that proteins are highly dynamic entities in terms of turnover and localisation, protein complexes can undergo a constant change in their composition. This called for the invention of more quantitative mass spectrometry methods to monitor dynamic complexes and can be achieved by either metabolic labeling of living cells, in which isotopically ‘heavy’ amino acids replace the naturally ‘light’ amino acids in growth medium or

by isotopic labeling of lysates (post-extraction) using enzymatic or chemical approaches (Gingras et al, 2007; Ong & Mann, 2005)).

I employed Stable Isotope Labeling with Aminoacids in Culture (SILAC) based quantitative affinity purification mass spectrometry for identifying PINK1 interactors. In SILAC-based approach, cells are cultured in media containing stable isotope-labeled amino acids for at least five generations to ensure near-complete metabolic labeling of the proteome (Ong et al, 2002). Two to three different conditions can be grown in a similar growth medium, which varies only by the presence of 'light' unlabeled, 'medium' or 'heavy' labeled amino acids (such as Lys or Arg) substituted with stable isotopic nuclei (such as ^{15}N, ^{13}C) (Fig. 4.1). Differentially labeled cell extracts are mixed in equal proportions and subjected to mass spectrometry (Fig.4.1).

Peptides that are derived from the labeled condition are identical to their corresponding ones from unlabeled condition in their amino acid sequence. However, the incorporation of stable isotopes in the labeled peptide imparts a mass difference compared to its unlabeled counterpart, which is detected by mass spectrometry. Therefore we can quantitatively measure the difference in relative amounts of the protein of interest between experimental conditions. SILAC can be used for various applications such as differential whole proteome analysis of cells, differential sub-cellular proteomics, studying protein turnover or analysis of affinity purified protein complexes.

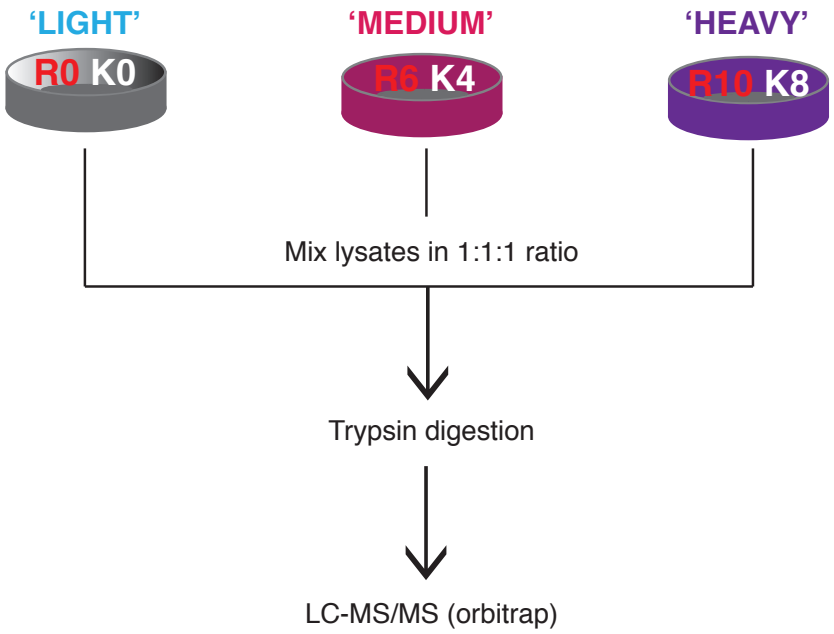

Figure 4.1. Stable Isotope Labeling of Amino acids in Culture (SILAC)

Illustration depicting a typical SILAC-based experiment in which cells from two to three experimental conditions are maintained in growth medium supplemented with 'light' amino acids and their stable isotopically labeled 'medium' or 'heavy' counterparts (labeled with ^{15}N, ^{13}C). Lysates from the three conditions are then combined in an equal ratio, proteolyzed and subjected to standard mass spectrometry to establish quantitative differences between conditions.

SILAC-based metabolic labeling has certain advantages over chemical labeling strategies. In chemical labeling, the two proteomes to be compared are required to be processed in precisely the same manner to enable relative quantitation. However, SILAC-based methods allows efficient metabolic labeling of cells (up to 98%) followed by mixing an equal population of unlabeled cells and subsequent biochemical fractionation, thus, minimizing errors in quantitation (Mann, 2006). Nonetheless SILAC also has disadvantages such its detection limit based on peptide abundance or size; and metabolic conversion of isotopic Arg to Pro, which generates artifacts in quantitation. The latter is avoided in most cases by reducing

the amount of Arg available in the SILAC medium, but, this may not suits cells with a high cellular metabolism (Scott et al, 2000).

4.2 SILAC-based immunoprecipitation mass spectrometry to identify novel binding partners of PINK1

4.2.1 Identification of PINK1 interacting proteins by SILAC method

The discovery that mitochondrial uncoupling agents such as CCCP can significantly enrich PINK1 in mitochondria makes it feasible to perform large-scale immunoprecipitation in order to identify potential interacting partners. Quality control of mitochondrial fractions was validated by immunoblotting mitochondrial and cytoplasmic fractions with various sub-mitochondrial markers (Appendix 6.6). I employed SILAC based immunoprecipitation mass spectrometry to address this question. A triple SILAC labeling experiment was performed: cells were grown in unlabeled media are termed as 'light' (R0KO), cells grown in media supplemented with $^{2}H_4$-Lysine and $^{13}C_6$-Arginine termed as 'medium' (R6K4) and cells grown in media supplemented with $^{15}N_2$ $^{13}C_6$-Lysine and $^{15}N_4$ $^{13}C_6$-Arginine termed as 'heavy' labeled (R10K8). FlpIn TRex HEK293 cells stably expressing wild-type PINK1-FLAG were cultured for at least five generations in 'medium' or 'heavy' SILAC media to ensure a high efficiency of metabolic labeling. As an experimental control, FlpIn TRex HEK293 cells expressing FLAG-vector were cultured in unlabeled 'light' medium.

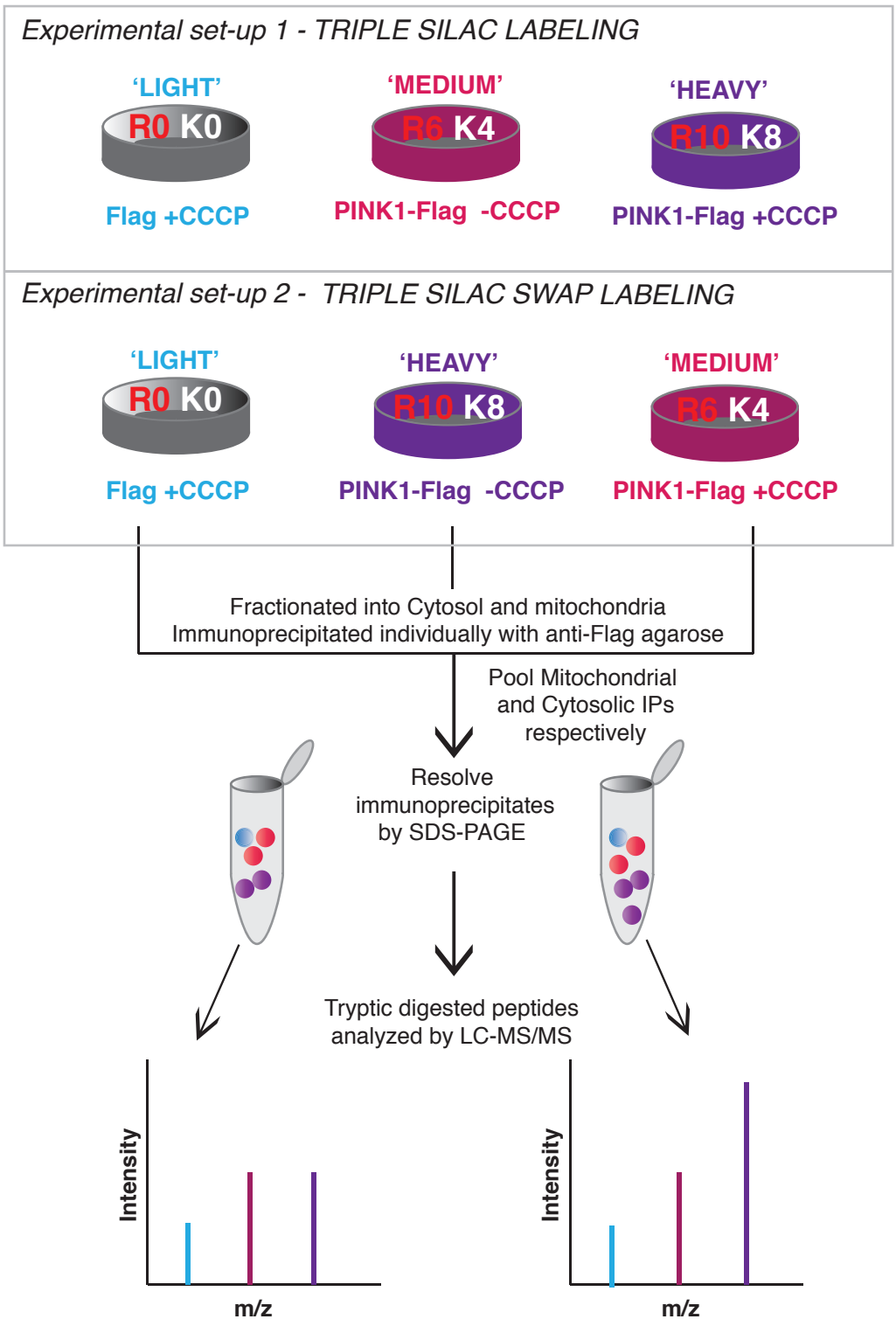

Figure 4.2. Triple SILAC based immunoprecipitation mass spectrometry

Flow chart depicting experimental set-up for the triple SILAC-based PINK1 immunoprecipitation mass spectrometry to identify potential binding partners of PINK1. The different conditions employed in the biological replicates are mentioned in the illustration.

As an additional control, I undertook a ‘swap’ experiment. In the first replicate, control ‘light’ labeled cells stimulated with CCCP, PINK1-FLAG expressing ‘medium’ labeled cells were unstimulated and PINK1-FLAG containing ‘heavy’ labeled cells were stimulated with CCCP. In the second biological replicate, control ‘light’ labeled cells were again stimulated with CCCP, but this time PINK1-FLAG ‘heavy’ labeled cells were unstimulated and PINK1-FLAG ‘medium’ labeled cells were stimulated with CCCP (Fig.4.2). All above conditions were induced for protein expression with doxycycline before treating with 10μM CCCP for 3h in the respective aforementioned conditions. Cells were fractionated into cytosolic and mitochondrial fractions in each condition.

Cytoplasmic immunoprecipitates from 33mg of ‘light’, ‘medium’ and ‘heavy’ labeled extract from each replicate were pooled respectively. Similarly, mitochondrial immunoprecipitates from 7mg of ‘light’, ‘medium’ and ‘heavy’ extract from each replicate were pooled respectively. Pooled immunoprecipitates were resolved by 4-12% Bis-Tris SDS-PAGE (Fig.4.4), and each lane was excised into 8 bands, proteolyzed with trypsin and identified by LC-MS/MS. Relative ratios of peptides between unstimulated and stimulated conditions were determined using MaxQuant (version 13.13.10) and were reproducible across experimental replicates with at least two peptides identified per protein (Table 4.1). Protein ratios in unstimulated and stimulated conditions that were below 2 fold were considered to be insignificant. PINK1 levels decreased in the cytoplasm upon CCCP stimulation (approximately 2 fold decrease) and increased approximately 20 fold

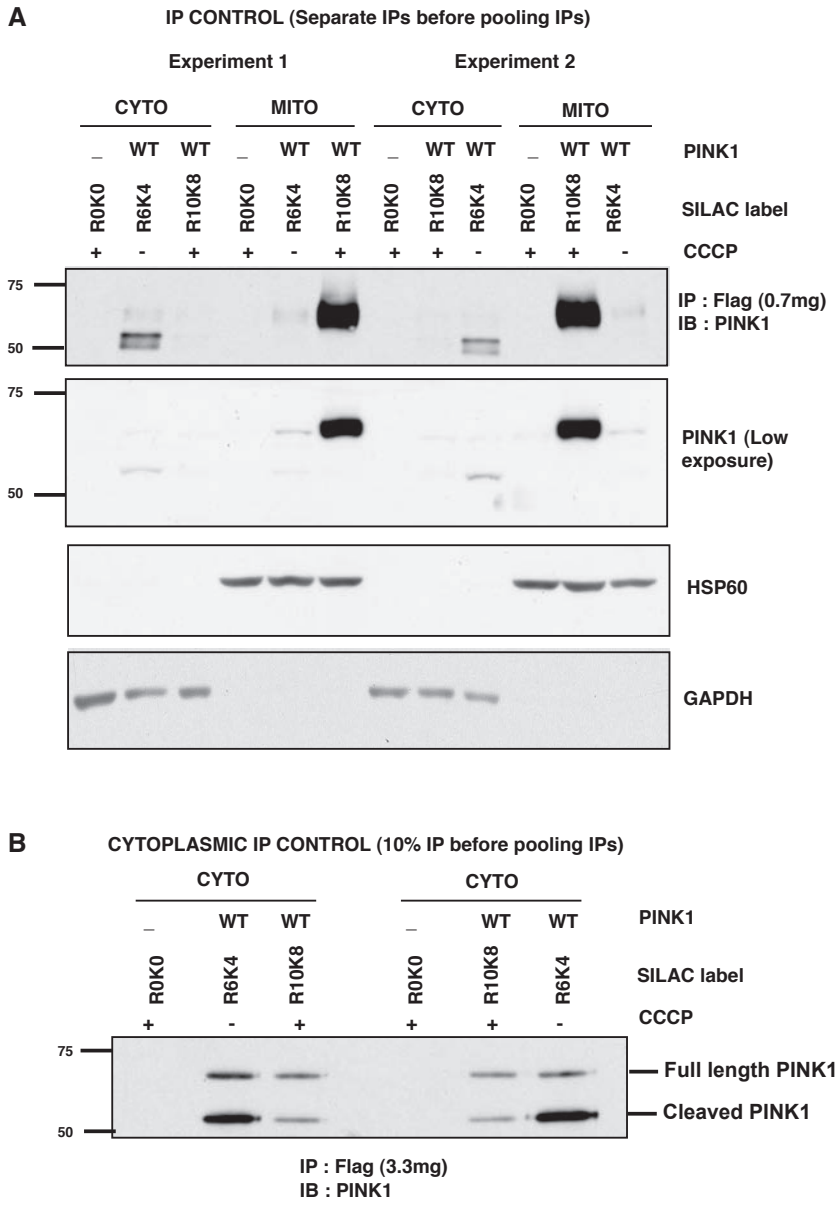

Figure 4.3. Immunoprecipitation control blots from individual SILAC labeled conditions

(A) FIpIn TRex HEK293 cells stably expressing FLAG-alone cultured in unlabeled medium was induced for protein expression and stimulated with 10μM CCCP for 3h. In experiment 1, 'medium' labeled Wild-type PINK1-FLAG cells were treated with DMSO and 'heavy' labeled cells were treated with 10μM CCCP for 3h. In experiment 2, the labeling is swapped, with 'heavy' being untreated and 'medium' being treated with CCCP. All of the above conditions were fractionated into cytosol and mitochondria and immunoprecipitated for 7mg PINK1 in each condition using anti- FLAG agarose. 10% of immunoprecipitates were blotted with anti-PINK1 antibody. The fractions were immunoblotted for GAPDH and HSP60 as cytoplasmic and mitochondrial markers.

(B) Five times more of cytoplasmic fractions were immunoprecipitated given that the levels of PINK1 in the cytoplasm were less compared to mitochondria. 33mg of cytoplasmic PINK1 from each condition in the two experimental replicates were immunoprecipitated using anti-FLAG agarose and 10% of immunoprecipitates were blotted with anti-PINK1 antibody.

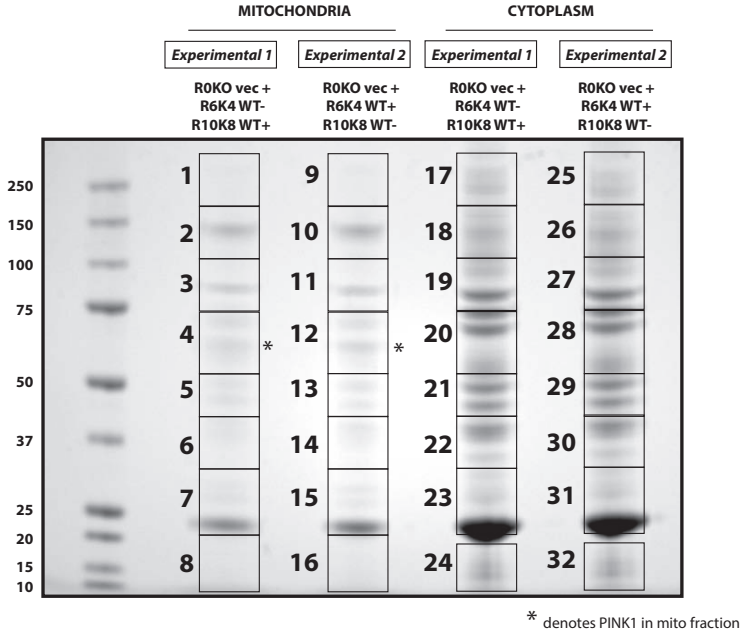

Figure 4.4. Pooled mitochondrial and cytosolic PINK1 immunoprecipitates for identification of interacting partners by SILAC method

Individual cytoplasmic and mitochondrial PINK1 immunoprecipitates from 'light', 'medium' and 'heavy' labeled conditions from each experimental replicate were pooled together respectively and resolved by 4-12% Bis-Tris SDS-PAGE. The gel was stained with Colloidal Coomassie blue and each lane was excised into 8 bands each of which undergoes in-gel tryptic digestion and identified by LC-MS/MS.

in the mitochondrial fraction as expected (Narendra et al, 2010). Approximately 600 cytoplasmic proteins were found to co-immunoprecipitate with cytoplasmic PINK1 but identified but none were significant interacting partners for cytoplasmic PINK1 (ratio < 2) except for HSP90 and Cdc37 chaperone proteins (Fig. 4.5). Upon CCCP stimulation I observed a 20-fold enrichment of mitochondrial PINK1 and significant enrichment of potential PINK1 binding partners (Table 4.1). Approximately 200 proteins co-immunoprecipitated with mitochondrial PINK1 but only 40 proteins were enriched at significant levels (ratio>2). Cytoskeletal proteins and ribosomal proteins were disregarded, as they are common contaminants in affinity purification mass spectrometry (Trinkle-Mulcahy et al, 2008). Heat shock proteins such as Cdc37 and HSP90

were found to interact with both cytoplasmic and mitochondrial PINK1 irrespective of CCCP simulation (Fig. 4.5). The following groups of proteins were of potential interest (Table 4.2):

1. Proteins that are a part of mitochondrial protein import machinery were enriched significantly upon CCCP stimulation.
2. Mitochondrial RhoGTPase Miro2, which has previously been reported as a PINK1 interactor and plays a role in mitochondrial dynamics (Weihofen et al, 2009). Mitofilin, previously reported as a PINK1 interactor and recently discovered to be crucial for maintaining mitochondrial cristae morphology (Weihofen et al, 2009; Zerbes et al, 2012).
3. Proteins that are involved in mitochondrial membrane permeability transition pore namely VDAC2, ANT2/3 and C1QBP.

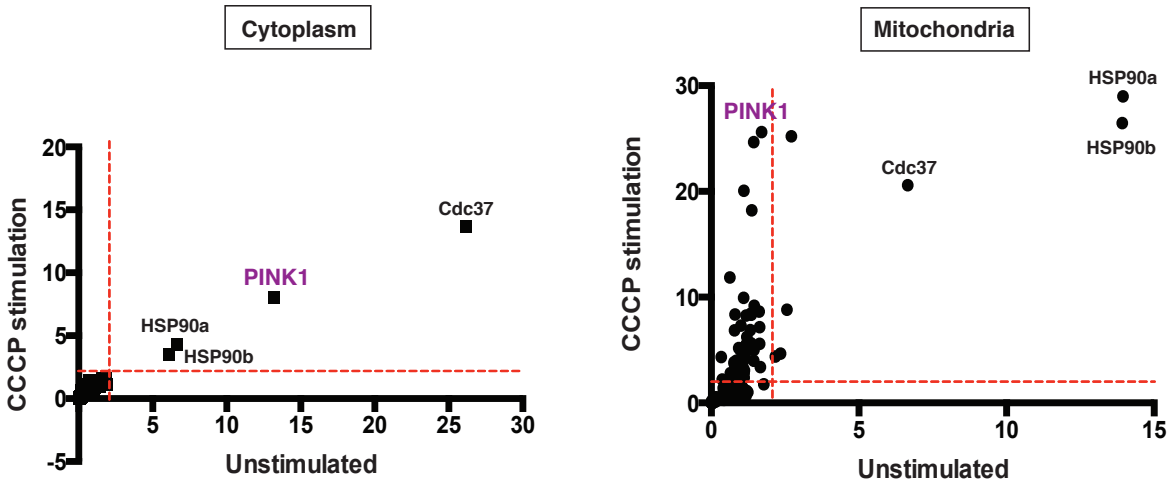

Figure 4.5. Unstimulated vs. stimulated SILAC-ratios of PINK1 interacting proteins from cytoplasm and mitochondrial fractions

SILAC peptide ratios from unstimulated condition are plotted along X-axis and CCCP stimulated conditions are plotted along Y-axis. Data point indicating enrichment of PINK1 is highlighted. Chaperone proteins that associate with PINK1 independent of CCCP stimulation in both cytoplasm and mitochondria are highlighted. Red-dotted line indicated a threshold of 2 fold and data-points that lie below this threshold are considered as insignificant interactors or common contaminants.

Interactors of cytoplasmic PINK1

Gene Names	Protein Names	M/L Cyto1 (UNSTIMULATED)	H/L Cyto2 (UNSTIMULATED)	H/L Cyto1 (CCCP STIMULATED)	M/L Cyto2 (CCCP STIMULATED)	PEP score
PINK1	***Serine/threonine-protein kinase PINK1***	***15.1***	***11.2***	***6.6***	***9.99***	***0***
Chaperones						
CDC37	Hsp90 co-chaperone Cdc37	30	22	13.1	14.2	3.47E-202
HSP90A	Heat shock protein HSP 90-alpha	6.4	6.9	3.8	4.7	0
HSP90B	Heat shock protein HSP 90-beta	5.8	6.3	3.1	3.9	0

Interactors of Mitochondrial PINK1

Gene Names	Protein Names	M/L Mito1 (UNSTIMULATED)	H/L Mito2 (UNSTIMULATED)	H/L Mito1 (CCCP STIMULATED)	M/L Mito2 (CCCP STIMULATED)	PEP score
PINK1	***Serine/threonine-protein kinase PINK1***	***1.5345***	***1.3343***	***19.618***	***29.701***	***0***
Chaperones						
CDC37	Hsp90 co-chaperone Cdc37	6.8643	6.4505	19.332	21.838	3.47E-202
HSP90A	Heat shock protein HSP 90-alpha	16.282	11.617	24.347	33.645	0
HSP90B	Heat shock protein HSP 90-beta	15.272	12.57	22.092	30.811	0
Mitochondrial outer membrane proteins						
TOMM40	Mitochondrial import receptor subunit TOM40	1.4646	1.9454	25.652	25.578	6.05E-105
TOMM22	Mitochondrial import receptor subunit TOM22	0.85433	4.5742	21.239	29.202	6.10E-84
MIRO2/RHOT2	Mitochondrial Rho GTPase 2	1.1805	1.0275	15.072	25.053	8.06E-72
FKBP-8	FK506-binding protein 8;Peptidyl-prolyl cis-trans isomerase	3.3671	1.7629	7.9825	9.6626	2.90E-73
VDAC-2	Voltage-dependent anion-selective channel protein 2	1.0424	1.1507	8.4782	11.404	1.98E-24
AIFM1;AIF	Apoptosis-inducing factor 1, mitochondrial	1.0835	0.83758	3.0281	3.0368	4.33E-11
Mitochondrial inner membrane proteins and matrix proteins						
TIMM50	Mitochondrial import inner membrane translocase subunit TIM50	1.1675	1.7344	7.7757	10.613	3.01E-148
C1QBP	Complement component 1 Q subcomponent-binding protein	1.1233	1.2804	4.6306	5.3191	1.86E-74
SLC25A5 / ANT 2	ADP/ATP translocase 2	0.9599	0.94088	3.5766	4.0143	1.23E-105
SLC25A6 / ANT 3	ADP/ATP translocase 3	0.96	1.1979	3.7877	4.1453	1.80E-121
IMMT / Mitofilin	Mitochondrial inner membrane protein;Mitofilin	1.0683	1.1816	2.9903	3.2031	2.22E-16
HSP60	Heat shock protein 60	1.2602	1.0599	5.2008	4.9212	1.35E-157
NDUFA4	NADH dehydrogenase [ubiquinone] 1 alpha subcomplex subunit 4 (complex IV SUBUNIT)	1.692	1.206	5.615	4.4229	0.0068081
AGK;MULK	Acylglycerol kinase, mitochondrial	1.0092	0.65553	2.2432	3.413	1.25E-07
Cytoskeletal and related proteins						
TUBB3	Tubulin beta-3 chain	1.7867	0.8835	7.7699	9.1026	0
TUBA1B	Tubulin alpha - 1b chain	1.5895	1.6491	7.5016	9.7819	0
TUBB5	Tubulin beta-5 chain	1.3467	1.3698	7.218	9.456	0
TUBB2C	Tubulin beta-2C chain	1.132	1.2291	6.6009	9.9121	0
FAM82A2	Regulator of Microtubule dynamics 3	0.66097	1.3413	6.3853	8.2235	7.20E-12

(Continued)

Ribosomal proteins						
RPL23	60S ribosomal protein L23	2.283	0.9923	7.6317	6.7087	1.64E-82
RPS23	40S ribosomal protein S23	0.94644	1.1039	5.2369	2.8069	1.18E-21
UBC;UBB;RPS27A;UBA80;UBCEP 1;UBA52;UBCEP2	UBC protein;Ubiquitin B;Ubiquitin B;40S ribosomal protein S27a,Ubiquitin C splice variant;60S ribosomal protein L40;CEP52;Ubiquitin;RPS27A protein;Ubiquitin C	1.1209	1.2858	6.7405	5.7497	3.51E-22
Proteins of unknown function and non-mitochondrial proteins						
TraBD	Tra-B domain containing protein	0.93861	1.8041	15.309	21.111	7.92E-190
MGST3	Microsomal glutathione S-transferase 3 variant	0.69696	0.87294	5.1275	8.6059	1.53E-15
TMEM160	Transmembrane protein 160	0.3711	0.88649	7.8495	15.894	2.50E-11
LBR	Lamin-B receptor	0.93386	0.922	5.5633	4.8277	3.92E-27
GNB4	Guanine nucleotide-binding protein subunit beta-4;	1.0976	0.8943	4.717	5.5497	0.00032442
CDIPT;PIS;PIS1	CDP-diacylglycerol--inositol 3-phosphatidyltransferase;Phosphatidylinositol synthase	1.1986	1.1544	4.6078	6.4307	1.90E-28
CAD	CAD protein	1.7482	1.5344	4.5967	6.5601	1.91E-108
FAF2	FAS-associated factor 2	1.0881	1.0543	4.489	4.7689	0.02339
SSR4;TRAPD	Translocon-associated protein subunit delta	0.99135	0.80342	3.7498	3.6406	1.37E-25
SEC61A1;SEC61A;SEC61A2	Protein transport protein Sec61 subunit alpha isoform 1	1.0144	0.92629	3.6438	3.9292	5.87E-07
SEC61B	Protein transport protein Sec61 subunit beta	1.0063	0.91129	3.3768	3.9037	0.017686
RCN2;ERC55	Reticulocalbin-2;Calcium-binding protein ERC-55;E6-binding protein	0.9154	0.85377	2.6226	3.3091	3.96E-53
PTPLAD1;BIND1	Protein tyrosine phosphatase-like protein PTPLAD1	0.95292	0.74701	2.5698	3.7506	9.96E-52
GPSN2;SC2	Synaptic glycoprotein SC2	0.86055	0.87583	2.3461	2.9176	0.00012203
DDOST	Dolichyl-diphosphooligosaccharide--protein glycosyltransferase 48 kDa subunit	1.1278	0.97423	2.518	2.6303	2.94E-10

Table 4.11. List of interacting partners of cytosolic and mitochondrial PINK1 identified by SILAC-based affinity purification mass spectrometry

List of proteins binding to cytoplasmic and mitochondrial PINK1 are classified based on function or cellular localization. Peptide ratios of both experimental replicates from unstimulated and CCCP stimulated condition are listed. PEP (Posterior Error Probability) score has been mentioned with a cut-off of <0.01 (99% confidence level).

Gene Name	Protein Name	Fold change over basal (average of H/M ratio)
PINK1	**Serine-Threonine protein kinase PINK1**	**18.8**
Proteins related to Mitochondrial dynamics		
MIRO2	Mitochondrial Rho-GTPase 2	13.3
Mitofilin/IMMT	Mitochondrial inner membrane protein	4.7
Proteins related to Mitochondrial protein import machinery		
TOMM40	Mitochondrial import receptor subunit TOMM40	14.5
TOMM22	Mitochondrial import receptor subunit TOMM422	24.8
TIMM50	Mitochondrial import inner membrane translocase subunit TIM50	10.7
Membrane permeability transition (MPT) pore complex proteins		
VDAC2	Voltage dependent anion channel 2	4.9
C1QBP	Complement 1q – sub-complement binding protein	3.8
ANT2/SLC25A5	ADP/ATP Translocase 2	3.3
ANT3/SLC25A6	ADP/ATP Translocase 2	3.5

Table 4.12. List of putative PINK1 interacting proteins in mitochondria

List of short-listed candidate proteins potentially interacting with mitochondrial PINK1. Fold change of peptide ratios of CCCP stimulation over unstimulated is being listed.

4.2.2 Validation of interacting proteins identified by SILAC with stably expressed exogenous PINK1

To verify PINK1 interacting proteins identified by SILAC, I undertook co-immunoprecipitation experiments using antibodies that detected endogenous protein of the various interactors. FlpIn TRex HEK293 cells stably expressing FLAG vector and PINK1-FLAG cells were induced for protein expression and treated with and without 10μM CCCP for 3h and mitochondrial fractions were prepared. PINK1 was immunoprecipitated using anti-FLAG agarose and was immunoblotted for the above interacting partners to confirm that they specifically co-immunoprecipitate with PINK1 when it gets stabilized in the mitochondria by CCCP. Most of the interacting proteins co-immunoprecipitate with mitochondrial PINK1 upon CCCP stimulation and the levels of the

interactors themselves did not change with CCCP treatment (Fig. 4.6). This suggests that the calculated enriched ratios from the SILAC analysis reflect binding to PINK1 and not simply greater protein abundance with CCCP. In contrast ANT2 and ANT3 show non-specific binding to FLAG and hence these proteins were excluded from further analysis (Fig. 4.6).

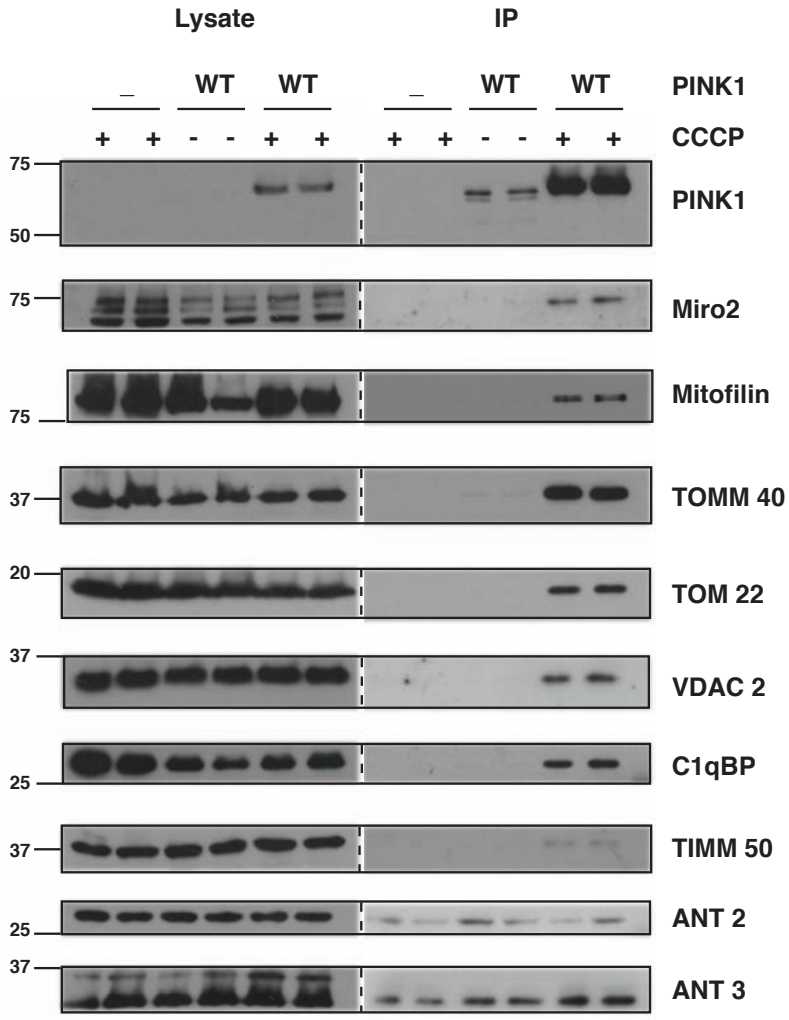

Figure 4.6. Validation of PINK1 interacting proteins by co-immunoprecipitation study with stably expressed PINK1

FlpIn TRex HEK293 cells stably expressing either FLAG-alone or wild-type PINK1-FLAG were induced for protein expression with doxycycline and treated with either DMSO control or 10μM CCCP for 3 h and cells were fractionated into mitochondria. 0.5mg of mitochondrial lysate was used for immunoprecipitation of PINK1 using anti-FLAG agarose and was immunoblotted using ant-PINK1 antibody. Co-immunoprecipitation of all endogenous interacting partners was performed using their respective antibodies. 25μg of lysate was used to immunoblot for the respective proteins to ensure that it serves as an input control for the immunoprecipitation study. Representative of two independent experiments.

4.2.3 Validation of interacting proteins identified by SILAC with endogenous PINK1

I next investigated whether the other confirmed interactors were capable of binding to endogenous PINK1. HEK293 cells were treated with or without 10μM CCCP for 6h and mitochondrial fractions were immunoprecipitated for endogenous PINK1 using an in-house anti-PINK1 (S085D) covalently coupled polyclonal antibody. All proteins co-immunoprecipitated specifically with endogenous PINK1 providing strong evidence that they may be physiological binding partners of PINK1 (Fig. 4.7).

4.2.4 Gel filtration analysis of mitochondrial PINK1 and its interacting proteins

Size exclusion chromatography has been widely used to study protein complexes and changes in their interaction between different experimental conditions (Munoz et al, 2009). Since most of the PINK1 interacting proteins are found in the mitochondrial fraction, I investigated whether PINK1 could be a part of a large protein complex and if so would these interacting proteins co-migrate in the same size. Size exclusion chromatography of mitochondrial fractions from untreated and CCCP stimulated FlpInTRex HEK293 cells stably expressing wild-type PINK1-FLAG were performed (Fig. 4.9). This indicated that PINK1 exists in a high-molecular weight complex (approximately 670kDa) in basal as well as CCCP stimulated conditions although the level of PINK1 differed between the two conditions (Fig. 4.9). Most of PINK1 interacting proteins co-migrated in the high- molecular weight complex while some of them such as

TIMM50 and C1QBP existed across a large range of sizes with a proportion still co-migrating with PINK1 (Fig. 4.8).

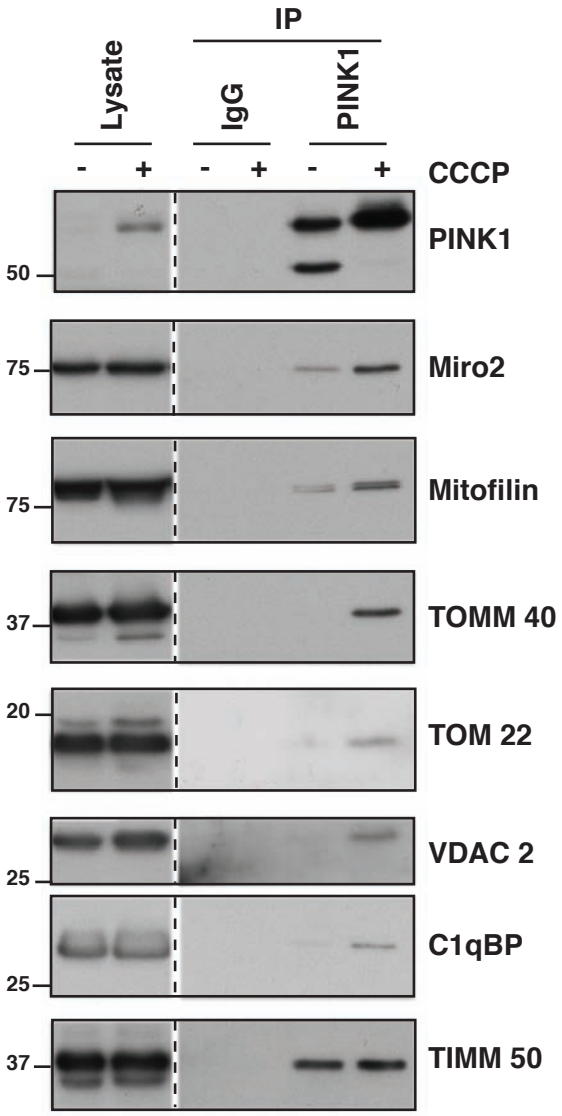

Figure 4.7 Validation of PINK1 interacting proteins by co-immunoprecipitation study with endogenous PINK1

HEK293 cells were treated with either DMSO control or 10μM CCCP for 6 h and cells were fractionated into mitochondria. 1mg of mitochondrial lysate was used for immunoprecipitation of using anti-PINK1 S085D or pre-immune IgG covalently coupled to protein-G sepharose. Immunoblotting was done using anti-PINK1 (Novus) antibody. Co-immunoprecipitation of all endogenous interacting partners was performed by immunoblotting with their respective antibodies. 25μg of lysate was used to immunoblot for the respective proteins to ensure that it serves as an input control for the immunoprecipitation study. Representative of two independent experiments.

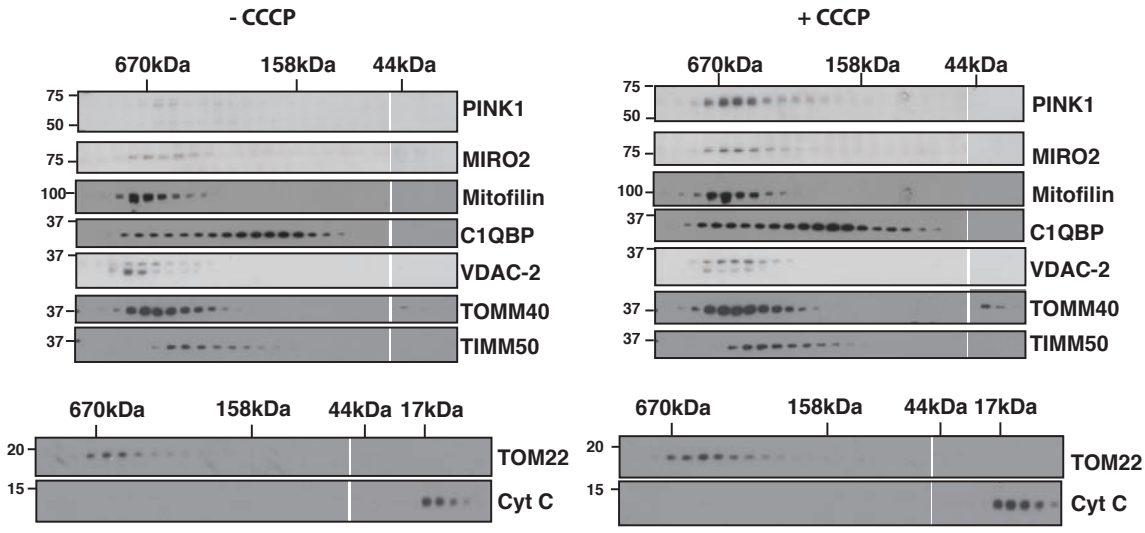

Figure 4.8. Gel filtration analysis of mitochondrial PINK1 and its interacting partners

FlpIn TRex HEK293 cells stably expressing wild-type PINK1 were induced for protein expression and treated with either DMSO control or 10μM CCCP for 3h and mitochondrial fractions were made. Extracts were analyzed by size-exclusion chromatography performed on a HiLoad 26/60 Superdex200 column in buffer containing 150mM NaCl and every third fraction was denatured for immunoblotting with indicated antibodies. Elution positions of Thyroglobulin (670kDa), γ-globulin (158kDa), Ovalalbumin (44 kDa) and Myoglobin (17kDa) are shown.

Cytochrome-C, which does not bind to PINK1 eluted as a monomer and served as a control for mitochondrial gel-filtration analysis (Fig. 4.8).

4.2.5 shRNA knockdown analysis of interactors to study their effect on activation of PINK1

Since none of the interacting proteins tested so far were substrates, I next investigated whether any of them could regulate PINK1 activity. I performed shRNA (short hair-pin RNA) mediated knockdown analysis of PINK1 interacting proteins and studied their effect on activation of endogenous PINK1. HEK293 cell lines that stably express shRNA against each interacting partner were

generated using lentiviral gene delivery. Two different shRNA oligonucleotides per gene were used for generation of two independent stable cells lines in order to ensure reproducibility across biological replicates. Untagged-Parkin was transiently expressed in the stable cell lines and cells were treated with either DMSO or 10μM CCCP for 5h. Immunoblotting confirmed robust knockdown for all interacting proteins (Fig. 4.9) however none led to a significant effect on PINK1 activation as judged by Parkin Ser65 phosphorylation.

4.2.6 Analysis of PINK1 interactors as potential substrates

I next investigated whether any of the identified interacting partners of PINK1 could be potential PINK1 substrates. Proteins listed in Table 4.2 were expressed in *E.coli*. Full length Miro2 and its orthologue, Miro1, were unstable probably due to possession of a short transmembrane region in their C-terminus (Fig. 4.10). In contrast, C-terminal domain truncation mutants (truncation from aa593-618) were highly stable when expressed with a His-SUMO fusion epitope tag (Fig. 4.10). GST-fusions of TOMM40 and VDAC2 were made and the protein quality was appreciable (Fig. 4.10). VDAC1, an orthologue of VDAC2 was also expressed as a GST-fusion protein and was used as a substrate in my panel. However, efforts to purify Mitofilin, TIMM50, TOM22 and C1QBP are currently ongoing and will be tested in future. I undertook *in vitro* kinase assays using a catalytically active insect orthologue of PINK1 (TcPINK1). Kinase inactive TcPINK1 served as a negative control and Parkin as a positive substrate control. TcPINK1 did not significantly

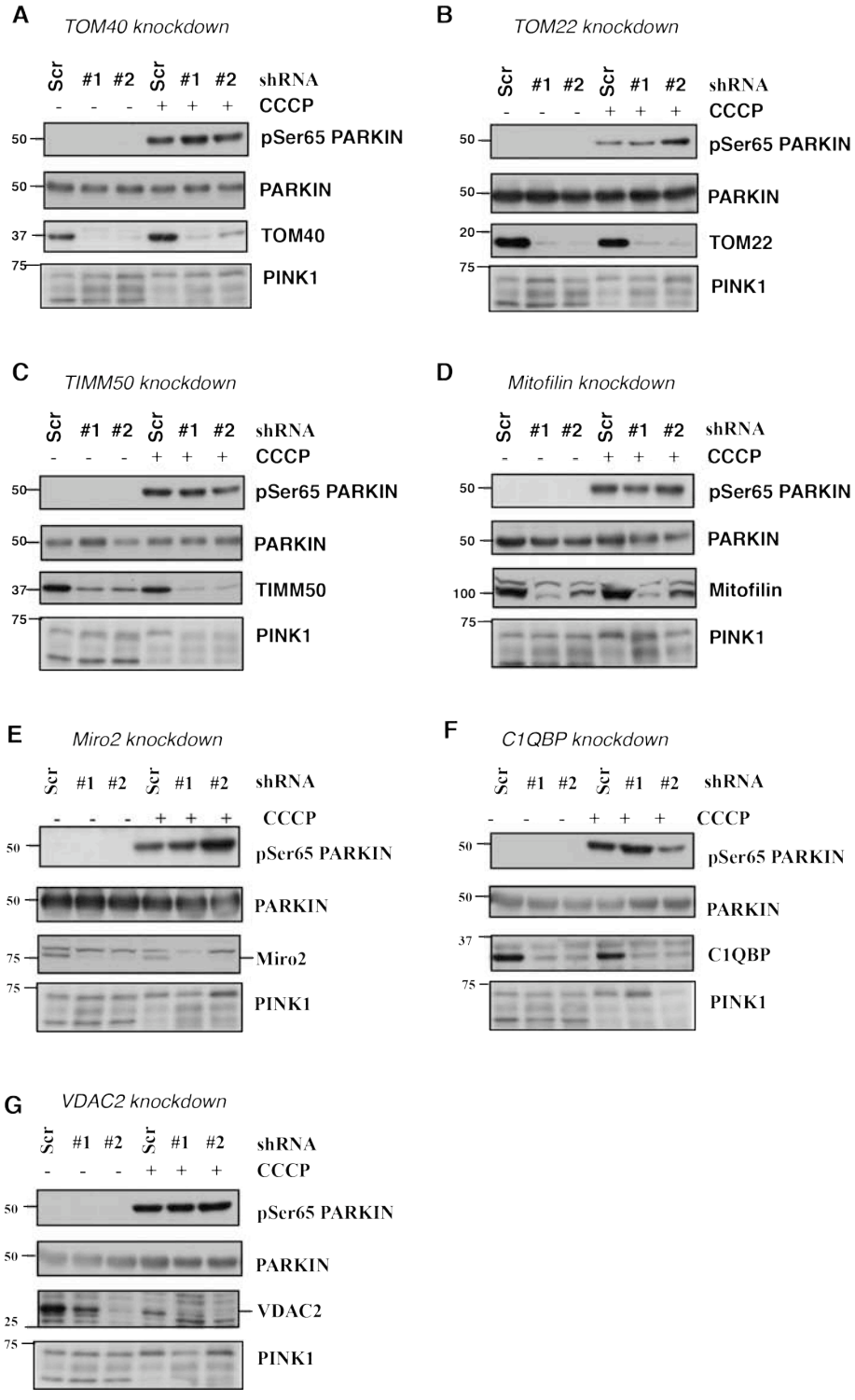

Figure 4.9. Effect of shRNA-mediated knockdown of interacting proteins on activation of PINK1

HEK293 cells stably expressing the shRNA against respective gene indicated above each panel, was transfected with untagged-Parkin and treated with either DMSO or 10μM CCCP for 5h. 0.5mg of whole cell lysate was immunoprecipitated with anti-PINK1 S085D covalently coupled antibody and immunoblotted with anti-PINK1 (Novus) antibody. 10μg of lysate was used to detect Parkin Ser65 phosphorylation using MJF-17 Parkin Ser65 monoclonal antibody. 25μg lysate was used to immunoblot the respective genes that are knocked down in this study.

phosphorylate any of the proteins compared to Parkin with only trace phosphorylation against TOM40 and VDAC1 (Fig. 4.10).

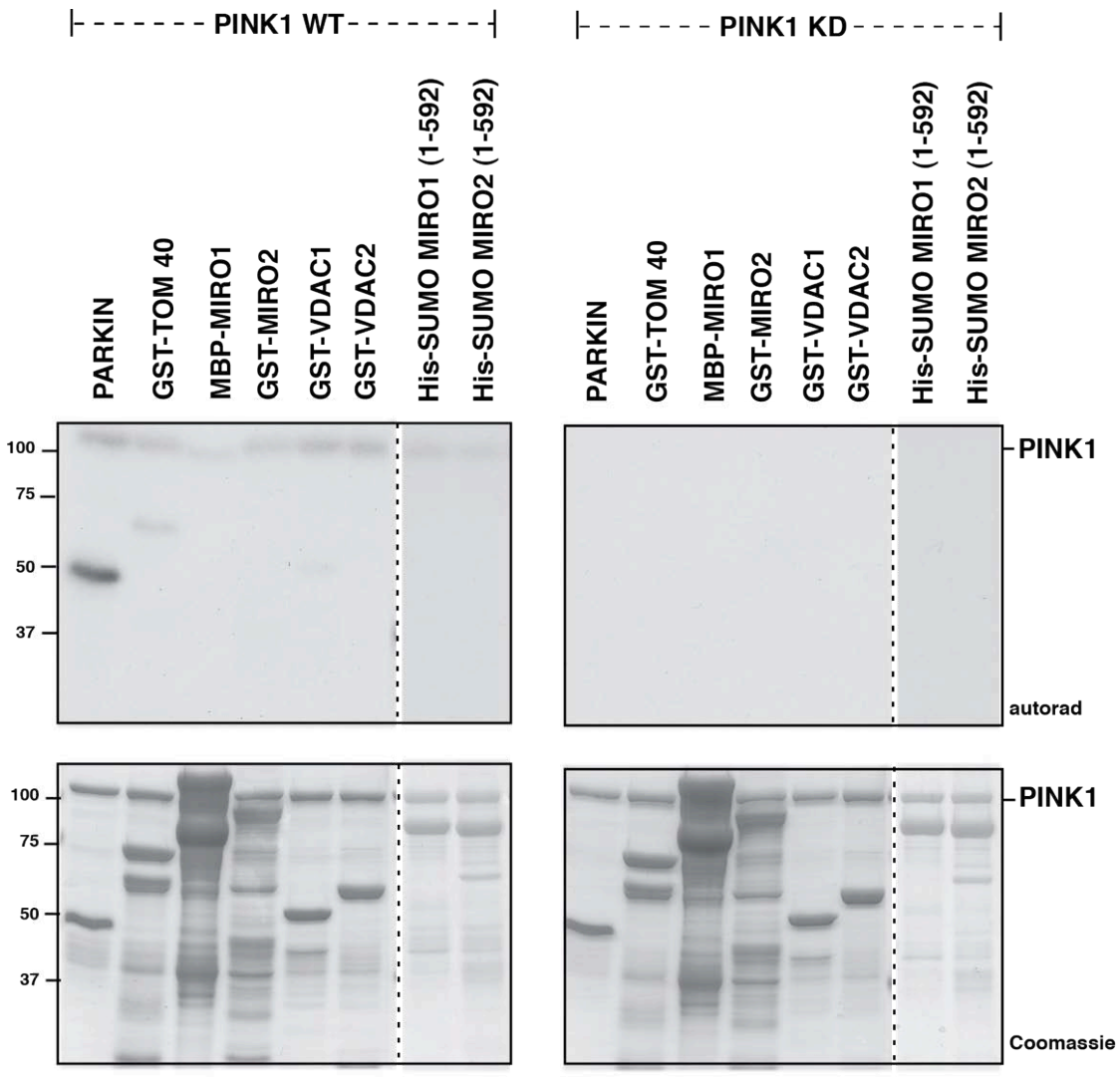

Figure 4.10. *In vitro* kinase assay of PINK1 interactors using TcPINK1

The indicated proteins (1 µM) were incubated with either full-length MBP-fusion of wild-type TcPINK1 (1–570) or kinase-inactive (KI) TcPINK1 (D359A) (0.5 mg) and [γ-32P] ATP for 30 min. Assays were terminated by addition of SDS loading buffer and separated by SDS-PAGE. Proteins were detected by Colloidal Coomassie blue staining (lower panel) and incorporation of [γ-32P] ATP was detected by autoradiography (upper panel). Similar results were obtained in two independent experiments. Fine dividing lines indicate that reactions were resolved on separate gels. All substrates were of human sequence and expressed in E. coli unless otherwise indicated

4.3 Discussion

Identification of novel interacting partners of PINK1 by affinity-purification based quantitative mass spectrometry

There has been no previous attempt to identify interacting partners of PINK1 comparing basal and depolarized conditions. Under basal conditions the constant turnover of PINK1 ensures a low level of expression in the mitochondria. When cells are treated with mitochondrial uncoupling agents such as CCCP, PINK1 levels decrease dramatically in the cytoplasm with a concomitant increase in levels of full length PINK1 in the mitochondria (refer to 3.7). Owing to such variability in expression levels of PINK1 I decided to undertake affinity purification coupled with quantitative mass spectrometry based method to fish out for potential PINK1 interacting proteins. Since PINK1 exists in two cellular compartments at any given time, I decided to perform the experiment with pull downs from cytoplasmic and mitochondrial fractions in order to identify a distinct set of interactors for each. This was accomplished by a triple labeling SILAC experiment.

My analysis revealed that cytoplasmic localized PINK1 does not have any significant interacting proteins except for chaperones such as Cdc37 and HSP90, which are also found to interact with mitochondrial PINK1 independent of CCCP stimulation. A previous mass spectrometry based study from basal conditions identified HSP90 and Cdc37 to be enriched with PINK1 (Weihofen et al, 2008). Given that PINK1 is a mitochondrial protein imported via the

presequence containing precursor pathway (refer to Fig.3.25), it is noteworthy that HSP90 also plays a role in delivering precursor proteins to outer mitochondrial import receptors (Young et al, 2003). Cdc37 is a co-chaperone that recruits intrinsically unfolded proteins (mostly kinases) to the chaperone HSP90 to prevent proteasomal degradation. A report on the autophagy related kinase Ulk1 suggests that its association with HSP90-Cdc37 complex is crucial for its stability as well as activation (Joo et al, 2011). In a recent analysis of protein kinases regulated by HSP90-Cdc37 chaperone system, PINK1 was found to be a strong interactor of HSP90 (Taipale et al, 2012). Hence, it is possible that these chaperones are involved in maintaining PINK1 stability although I cannot rule out that this association of chaperones is due to over-expression artifact (Fig. 4.5).

My SILAC-based affinity purification mass spectrometry approach demonstrates a 17-fold enrichment of PINK1 in the mitochondria upon depolarization. This is consistent previous analysis showing that uncoupling agents stabilize PINK1 in the mitochondria (Narendra et al, 2010). In addition to enrichment of PINK1, I found several interacting partners in the mitochondria. Although a total of 40 interactors, were identified some proteins were omitted, as they are common contaminants in mass spectrometry experiments (such as cytoskeletal proteins and ribosomal proteins). Chaperones and chaperone related proteins were also not considered for further analysis. Another group of interacting proteins listed in Table 4.1 were of unknown function of which some were non-mitochondrial proteins. Since antibodies were not available for this group of proteins, they

were not considered for further validation experiments. However, a group of 9 proteins were found to be significantly enriched with PINK1 which all localize to the mitochondria (Fig. 4.11) and for which reagents were available and I was able to validate all but 2 of these.

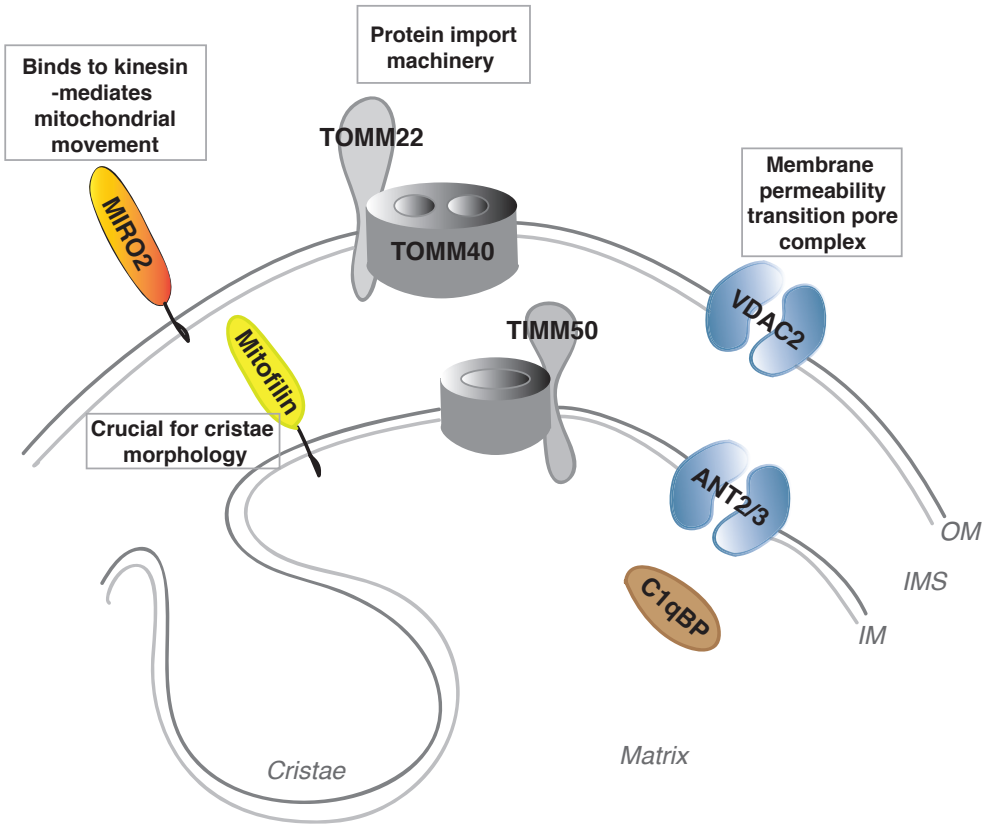

Figure 4.11. Illustration depicting sub-mitochondrial localization of putative PINK1 interactors

Putative PINK1 interactors are illustrated based on their sub-mitochondrial localization. Dialog box next to each protein or a group of proteins indicates their function in the mitochondria.

Insights into association of PINK1 with mitochondrial protein import machinery

Interaction of PINK1 with TOM40 and TOM22 mitochondrial import receptors is not unsurprising as all nuclear encoded mitochondrial proteins are imported via TOM40, which along with TOM22 and three small TOM subunits forms the

general protein import pore of the outer mitochondrial membrane (Dekker et al, 1998) (refer to Fig.3.25). Although I have determined that PINK1 exists in a large multi-protein complex with TOM40 and TOM22 by size-exclusion chromatography, shRNA-mediated knockdown of either TOM40 or TOM22 had no effect on import or activation of endogenous PINK1 as judged by Parkin phosphorylation. Recently, work by another group confirmed a stable interaction between PINK1 and TOM40/TOM22 complex in depolarized mitochondria and proposed that perhaps it is necessary for PINK1 to be in constant contact with the TOM complex, as this would allow rapid re-import of PINK1 to rescue repolarized mitochondria (Lazarou et al, 2012). However, my analysis reveals that PINK1 does not solely rely on the TOM40/TOM22 complex for import and it would be interesting to undertake shRNA knockdown of all the known TOM proteins to determine which are critical for PINK1 import.

I also found another mitochondrial import component, TIM50 to interact with PINK1. TIM50 plays a crucial role in transfer of precursor proteins from the TOM complex to the TIM23 complex in the inner mitochondrial membrane for import of proteins destined to mitochondrial matrix or inner membrane (Mokranjac et al, 2003; Mokranjac et al, 2009). Recently it was established that the C-terminal region of TIM50 binds to positively charged mitochondrial presequence present in the N-terminus of incoming precursor proteins imported into the mitochondria (Schulz et al, 2011). This is a crucial event to impart directionality to the import process, as recognition of presequences by TIM50

directs them into TIM23 import receptor (Schulz et al, 2011). My analysis suggest that the role of TIM50 in mitochondrial import does not appear to be essential since knockdown did not impair PINK1 import even under mitochondrial depolarization when it would be predicted that Tim23 would be inactivated. However, knockdown was not complete and it is possible that import was conferred by the residual TIM50 protein.

Insights into association of PINK1 with Miro2

Miro2 was the highest enriched PINK1-binding partner identified in our interaction screen. The Miro proteins (Miro1 and Miro2 in humans) are a family of atypical Rho GTPases tethered to the mitochondrial outer membrane (Fig. 4.12), which play a role in anterograde transport of mitochondria (Glater et al, 2006; Guo et al, 2005). The domain architecture of Miro proteins consists of tandem GTP binding domains separated by a linker region and calcium binding EF-hand motifs (Fransson et al, 2003). Calcium is known to halt mitochondrial movement and it has been speculated that Miro may play a role in this via its calcium-binding motif (Glater et al, 2006). Previously a mass spectrometry based analysis to identify potential interacting partners of immunoprecipitated mitochondrial PINK1 from basal conditions, identified Miro2 as an interactor (Weihofen et al, 2009).

Further studies by two independent groups reported that PINK1 plays a role in mitochondrial trafficking by regulating the level of Miro1, an orthologue of Miro2 (Liu et al, 2012; Wang et al, 2011). However, Miro1 was not found to bind

PINK1 in my screen and perhaps it would be important to test in future if HEK293 cells express Miro1. Given that Miro2 knockdown had no effect on downstream phosphorylation of Parkin, additional work is required to establish the physiological relevance of interaction between PINK1 and Miro2.

Insights into association of PINK1 with Mitofilin

A previous study that identified Miro2 as an interactor of mitochondrial PINK1 also found Mitofilin in their mass spectrometry based screen (Weihofen et al, 2009). From our co-immunoprecipitation study we observe an increased association of PINK1 with Mitofilin upon mitochondrial depolarization. Mitofilin is an inner mitochondrial membrane protein (Fig. 4.12) discovered to play a vital role in maintaining mitochondrial cristae morphology (John et al, 2005) and more recently was found to mediate this in complex with five partner proteins collectively called the MINOS complex (von der Malsburg et al, 2011). Besides regulating cristae morphology, Mitofilin was also found to associate with the outer membrane import receptors (TOM40 and SAM) to play a role in the biogenesis of outer mitochondrial membrane proteins with a β-barrel topology (Bohnert et al, 2012). Interestingly, defects in cristae morphology have been observed previously in PINK1 loss-of-function models (Clark et al, 2006; Exner et al, 2007).

Although I saw a stable interaction by co-immunoprecipitation studies, I found that knockdown of Mitofilin did not have any effect on PINK1 stabilization or activation upon CCCP stimulation. However, it is unknown whether Mitofilin

knockdown in HEK293 cells can alter cristae morphology and it would be important to perform electron micrograph studies to test this in future. Also, Mitofilin is enriched only around 2.8 fold upon CCCP stimulation and the interaction could perhaps happen only occur due to close proximity with PINK1 within the sub-mitochondrial milieu. Further work is required to confirm if this interaction is functionally relevant.

Insights into association of PINK1 with VDAC2 and C1QBP

VDAC2 and C1QBP are implicated in mitochondrial Membrane Permeability Transition (MPT) (Fig. 4.11). Mitochondrial MPT pore is a large non-specific channel in the inner mitochondrial membrane, which induces cell death by causing lethal changes in mitochondrial permeability (Halestrap, 2009). MPT pore opening can lead to loss of membrane potential, mitochondrial swelling and rupture and ultimately cell death and has implications in pathogenesis of neurodegenerative diseases. The proteins believed to be a part of this process are VDAC (Voltage dependent anion channel) in the outer membrane, ANT (Adenine nucleotide transporter) in the inner membrane and cyclophilin D in the mitochondrial matrix. However, it has now been established that VDAC and ANT are dispensable for membrane permeability transition (Baines et al, 2007; Kokoszka et al, 2004) leaving cyclophilin D as the only known regulator of MPT, with the core components of the pore yet to be identified. CIQBP, a mitochondrial matrix protein, was recently identified as an inhibitor of MPT pore opening by direct binding and inhibition of cyclophilin D (McGee et al, 2011). Interestingly, studies in PINK1 -/- mouse embryonic fibroblasts show a decrease

in mitochondrial membrane potential and an increase in MPT pore opening (Gautier et al, 2012). VDAC2 and C1QBP were confirmed as PINK1 interactors from co-immunoprecipitation studies. Similar to the shRNA analysis done for all PINK1 interactors, VDAC2 and C1QBP also were found to have no effect in regulating PINK1 activity *in vivo*. Perhaps this could be tackled in future to see if C1QBP can rescue defects of MPT pore opening in PINK1 -/- MEFs or shRNA silenced cells. VDACs (VDAC1, 2 and 3) have been reported to specifically interact with Parkin upon mitochondrial depolarization (Sun et al, 2012). Although we do not observe a regulatory role for VDAC2 in PINK1 activation, we did notice that the levels of VDAC2 decrease upon CCCP stimulation in cells stably expressing scrambled shRNA. This perhaps suggests that PINK1 mediated activation of Parkin upon CCCP stimulation can lead to degradation of VDAC2. Given the significant fold change (9 fold) in VDAC2 association with PINK1 upon CCCP stimulation, it is possible that the association of PINK1 with VDAC2 can mediate efficient ubiquitylation of VDAC2 simply because of proximity of Parkin, once it is activated by PINK1-mediated phosphorylation.

In conclusion, my SILAC analysis has identified a number of interactors for mitochondrial PINK1. Although I have validated these interactions biochemically, their functional relevance remains unknown. In future work it will be vital to study the other interacting proteins of unknown function since these may hold key roles in the regulation of PINK1 localization, stability and activity.

Chapter 5

Identification of novel substrates of PINK1

5. Identification of novel substrates of PINK1

5.1 Introduction

As stated in Chapter 3, I have determined that Parkin is a robust substrate of PINK1 and have established a biochemical link between these two PD-linked genes. However, I hypothesized that PINK1 may have additional substrates that are critical for mediating PINK1 downstream signaling in response to mitochondrial depolarization. To address this I undertook a SILAC-based quantitative phospho-proteomic approach in collaboration with Matthias Trost.

Phosphorylation is one of the most abundant post-translational modifications in a cell and the identification of substrates for all the known protein kinases has been a major goal of signal transduction research over the last three decades. Traditionally, most screens have employed *in vitro* approaches using radioactive [γ-^{32}P] ATP and recombinant protein kinase (Cohen & Knebel, 2006; Roskoski, 1983; Witt & Roskoski, 1975). However, kinases can often exhibit differential effects *in vitro* than *in vivo* and many robust *in vitro* substrates from such screens cannot be validated as physiological *in vivo* substrates. As described in 4.1, mass spectrometry has been a valuable tool to identify protein-protein interactions and with the invention of highly sensitive mass spectrometers and improved methodologies to isolate phosphopeptides, it has also become a powerful technology for analysis of *in vivo* phosphorylation (Chen & White, 2004; Mumby & Brekken, 2005). Typically most modern

protocols involve initial enrichment of phosphorylated peptides from the sample of interest followed by their identification by mass spectrometry. Recently, this has been made more quantitative by employing SILAC methodologies, which permits comparison of phosphorylation status of protein substrates across up to three different conditions/stimuli (Olsen et al, 2006).

Identification of protein phosphorylation sites on global scale has posed a significant analytical challenge due to a combination of relatively low abundance of many phosphopeptides and diverse physico-chemical properties of some phosphopeptides. However, several affinity-based methods have been developed for the isolation and identification of phosphorylated peptides (Trost et al, 2010).

1. Immobilized Metal Affinity Chromatography (IMAC): This method is based on selective binding of metal-ligand complexes with phosphate groups thereby selective enriching for phosphopeptides. The metal-ligand complex most commonly used is Fe(III) immobilized on nitrilotriacetate support (NTA). In order to reduce non-specific binding of peptides containing acidic residues such as glutamate and aspartate, their carboxylic group can be converted into methyl esters using methanolic HCl. IMAC can yield a higher distribution of multiply phosphorylated peptides.

2. Metal Oxide Affinity Chromatography (MOAC): This method is based on enriching phosphorylated amino acids using titanium-di-oxide (TiO_2) by a

similar mechanism as IMAC. Titanium di-oxide exhibits a high level of chemical, mechanical and thermal stability and selectively captures phosphopeptides in an acidic solution without the requirement for methyl esterification of peptides. Also, this affinity media can preferentially enrich singly and doubly phosphorylated peptides. Over the last few years, numerous studies have employed TiO_2 in large-scale phosphoproteomics for enrichment of numerous phosphopeptides from complex biological extracts. Other uncommon metal oxides used in MOAC are Aluminium hydroxide ($Al(OH)_3$), Zirconium oxide (ZrO_2) and Niobium oxide (Nb_2O_5).

3. Chromatographic enrichment methods: The negative charge of the phosphate moiety of a phosphopeptide enables them to be enriched by ion-exchange chromatography methods. Some methods employed are Strong Anion Exchange (SAX), which enriches negatively charged phosphopeptides or Hydrophilic Interaction Liquid Chromatography (HILIC), which can retain phosphopeptides owing to their high hydrophilicity. However, when compared to affinity-based methods, chromatography gives a low yield of phosphopeptides and hence it is often performed in combination with IMAC or TiO_2 enrichment.

To identify novel PINK1 substrates I have employed a SILAC based quantitative phosphoproteomic approach. Since PINK1 resides in the mitochondria, I focused on identifying phosphopeptides in the mitochondria using membrane enriched cell extracts that would contain mitochondria and other membrane-

bound organelles but largely excluding nuclear and cytosolic proteins. HEK293 FlpIn TRex cells stably expressing either FLAG alone, Kinase inactive PINK1 or wild-type PINK1 were stimulated with the uncoupling agent, CCCP and membrane enriched fractions were subjected to phosphopeptide analysis and compared across conditions to identify phosphopeptides that were potentially regulated by PINK1.

5.2 SILAC-based phosphoproteomics to identify novel substrates of PINK1

5.2.1 Workflow for SILAC-based phosphoproteomic approach

Flp In TRex HEK293 cells stably expressing either FLAG empty, wild-type PINK1-FLAG or Kinase-inactive PINK1-FLAG were grown in 'light', 'heavy' and 'medium' SILAC media, respectively, for at least 5 passages. Experiments were set-up as two biological replicates with a technical replicate in each (equivalent to n=4), to achieve statistical significance (Fig. 5.1). Cells in each condition were stimulated with 10μM CCCP for 3 hours and membrane-enriched fractions were made and solubilized in 1% RAPIGEST. Protein estimation was determined by the EZQ method of protein quantitation, which is compatible with RAPIGEST solubilized lysates and is a highly sensitive method to determine accurate protein concentration. RAPIGEST being an acid cleavable detergent can be extracted from the lysates prior to trypsin digestion of a mixture of equal amounts of lysate from the three experimental conditions (9mg per condition).

The experimental procedure is described in more detail in the Materials and Methods 2.2.7.3 (Fig. 5.2).

Digested peptides from each replicate were subjected to phospho-peptide enrichment by HILIC chromatography and around 15 eluates were collected per experiment (Appendix 6.7). Each eluate was further subjected to a second round of phospho-peptide enrichment using a TiO_2 column and analysed by mass spectrometry. Data analysis was done using MaxQuant.

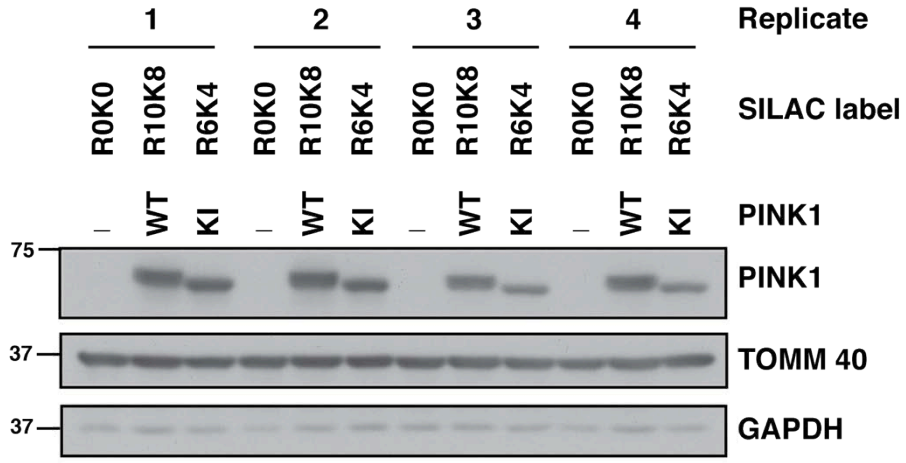

Figure 5.1 Control blots from individual SILAC labeled condition in the phosphoproteomics experiment

FlpIn TRex HEK293 cells stably expressing FLAG-alone were cultured in unlabeled medium, Wild-type (WT) PINK1-FLAG cells were 'heavy' labeled and Kinase inactive (KI) PINK1-FLAG were 'medium' labeled. All conditions were treated with 10µM CCCP for 3h and subjected to membrane enriched fractionation. 25µg of lysate was immunoblotted with anti-PINK1 antibody. Immunoblotting for TOMM40 and GAPDH serve as markers for mitochondria and cytoplasm and confirm mitochondrial enrichment.

As illustrated in Fig. 5.2 after trypsin digestion of the lysate mixture, a small amount is taken for mass spectrometry to determine labeling efficiency. Labeling efficiency of at least 95% is desirable for comparative and quantitative proteomics. Individual labeling efficiency for peptides with ‘heavy’ Arg and ‘heavy’ Lys (Fig. 5.3) and ‘medium’ Arg and ‘medium’ Lys (Fig. 5.4) were determined and compared to their respective unlabeled peptide. Density plots for incorporation of Arg and Lys-containing peptides show a labeling efficiency of approximately 96% in both ‘heavy’ and ‘medium’ labeled conditions (Fig. 5.3 and 5.4).

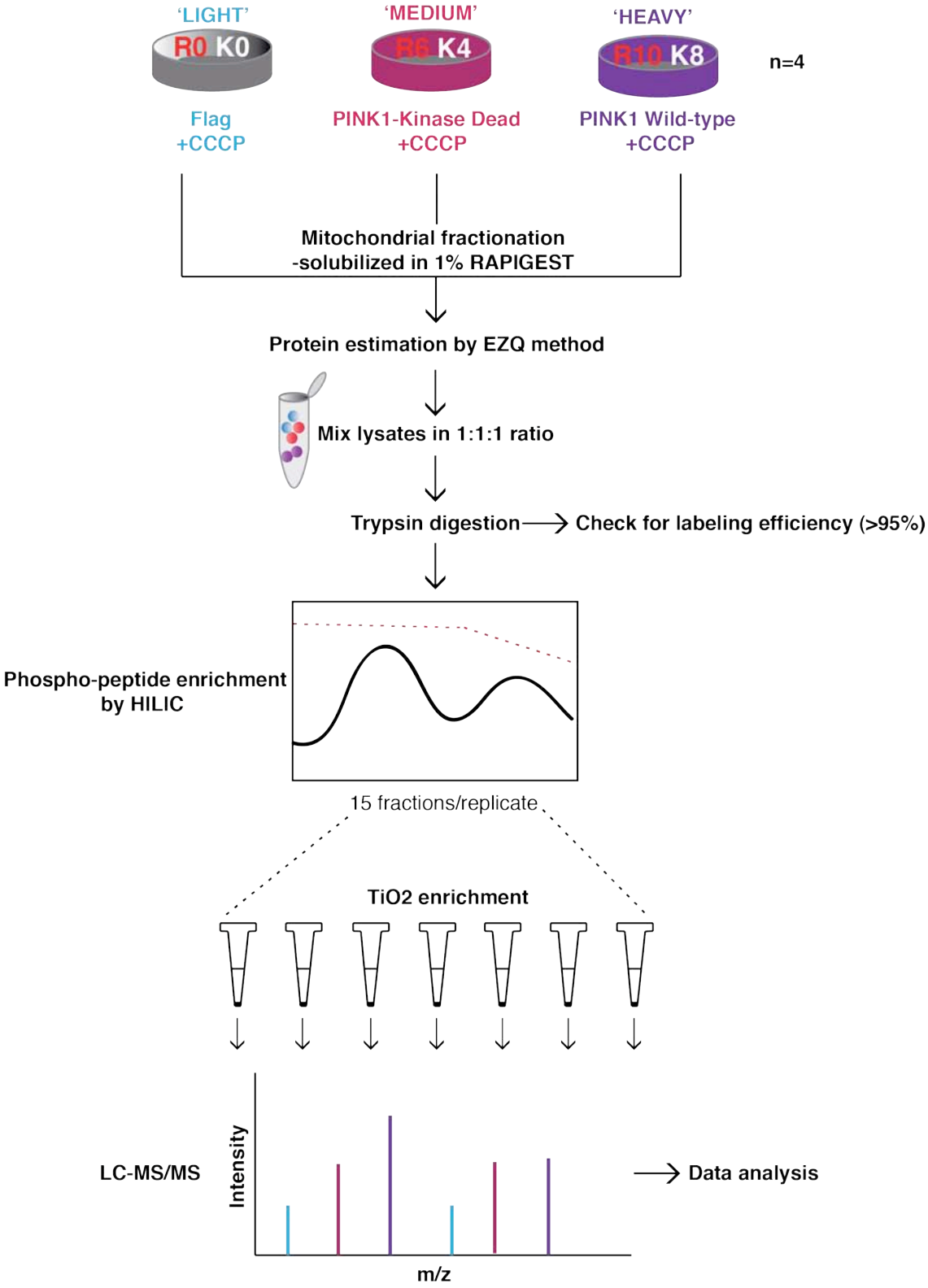

Figure 5.2 SILAC phospho-proteomic workflow for identification of PINK1 substrates .

Refer to 2.2.7.3 in Material and Methods for description of experimental procedure.

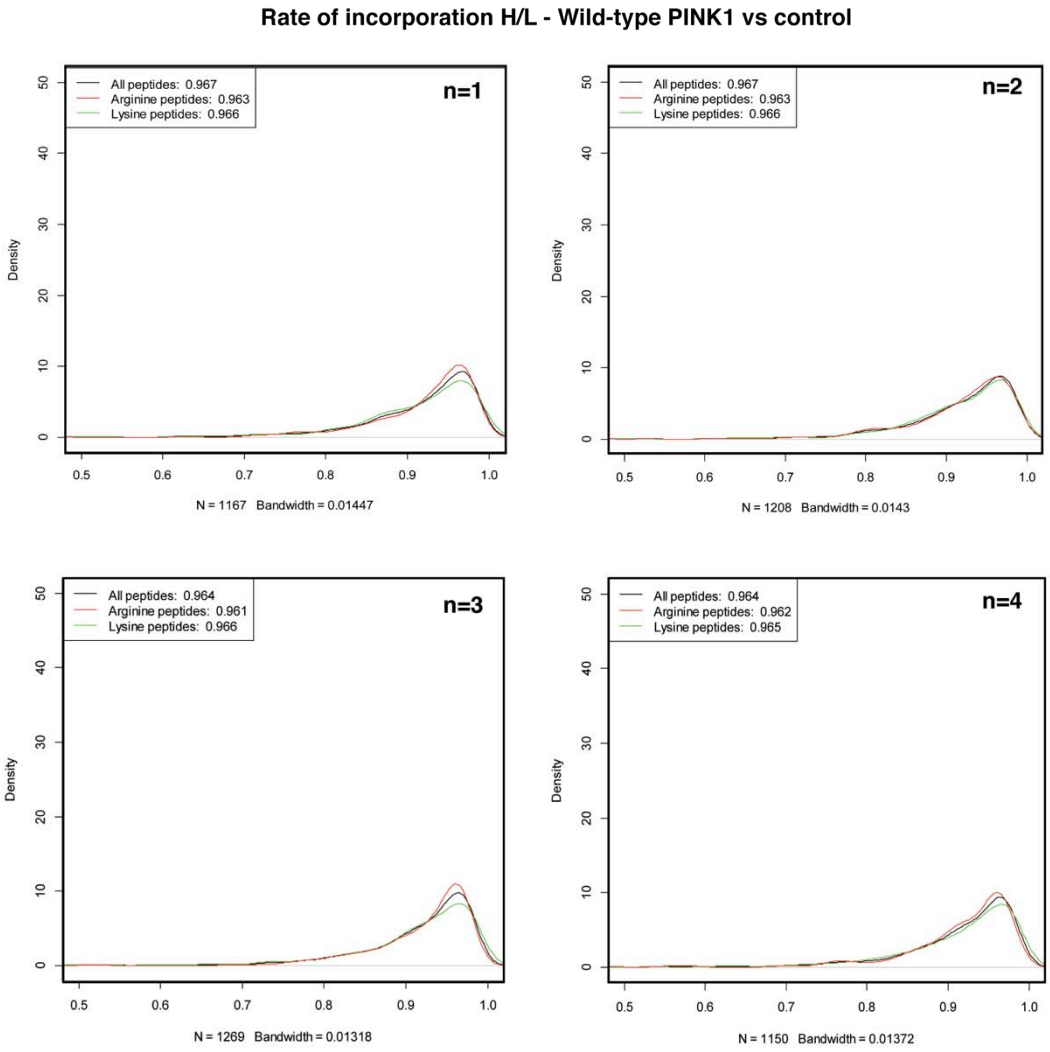

Figure 5.3 Density plot for incorporation of 'heavy' labeled Arg and Lys containing peptides

Density plot depicting labeling efficiency of 'heavy' labeled Arg and Lys amino acids used for metabolic labeling of HEK293 FlpIn TRex Wild-type PINK1-FLAG stable cell line. The inset shows median incorporation level for all peptides, Arg-containing peptides and Lys-containing peptides.

Scatter plots corresponding to peptide intensity from each experimental replicate versus average peptide intensity were plotted for labeled and unlabeled conditions and a good correlation was found between experimental replicates (R^2 = 0.83) (Fig. 5.5). A total of 14,213 phosphosites were identified among which 12,374 were quantified. Frequency plots were generated in order

to deduce phosphosites that were up regulated between the different experimental conditions.

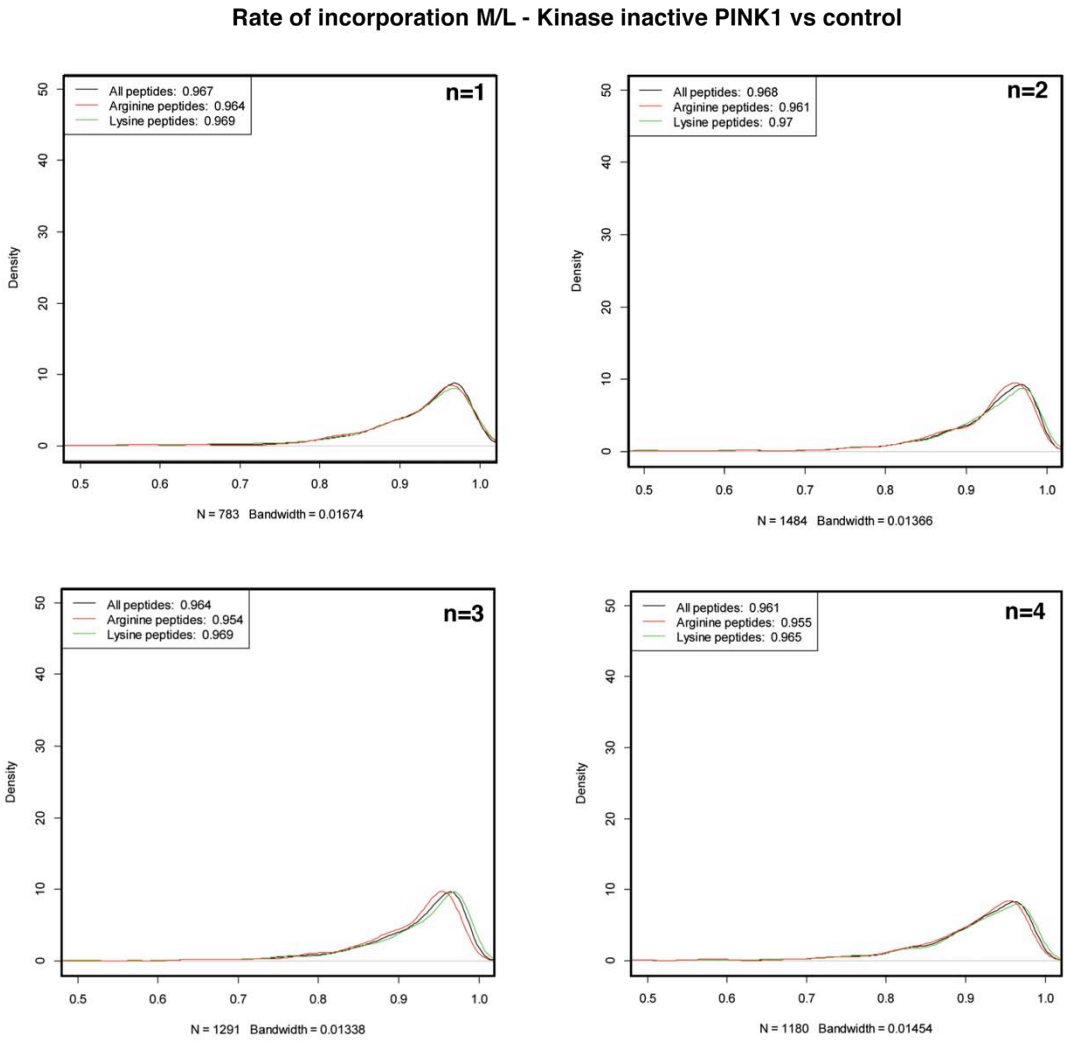

Figure 5.4 Density plot for incorporation of 'medium' labeled Arg and Lys containing peptides

Density plot depicting labeling efficiency of 'medium' labeled Arg and Lys amino acids used for metabolic labeling of HEK293 FlpIn TRex Kinase inactive PINK1-FLAG stable cell line. The inset shows median incorporation level for all peptides, Arg-containing peptides and Lys-containing peptides.

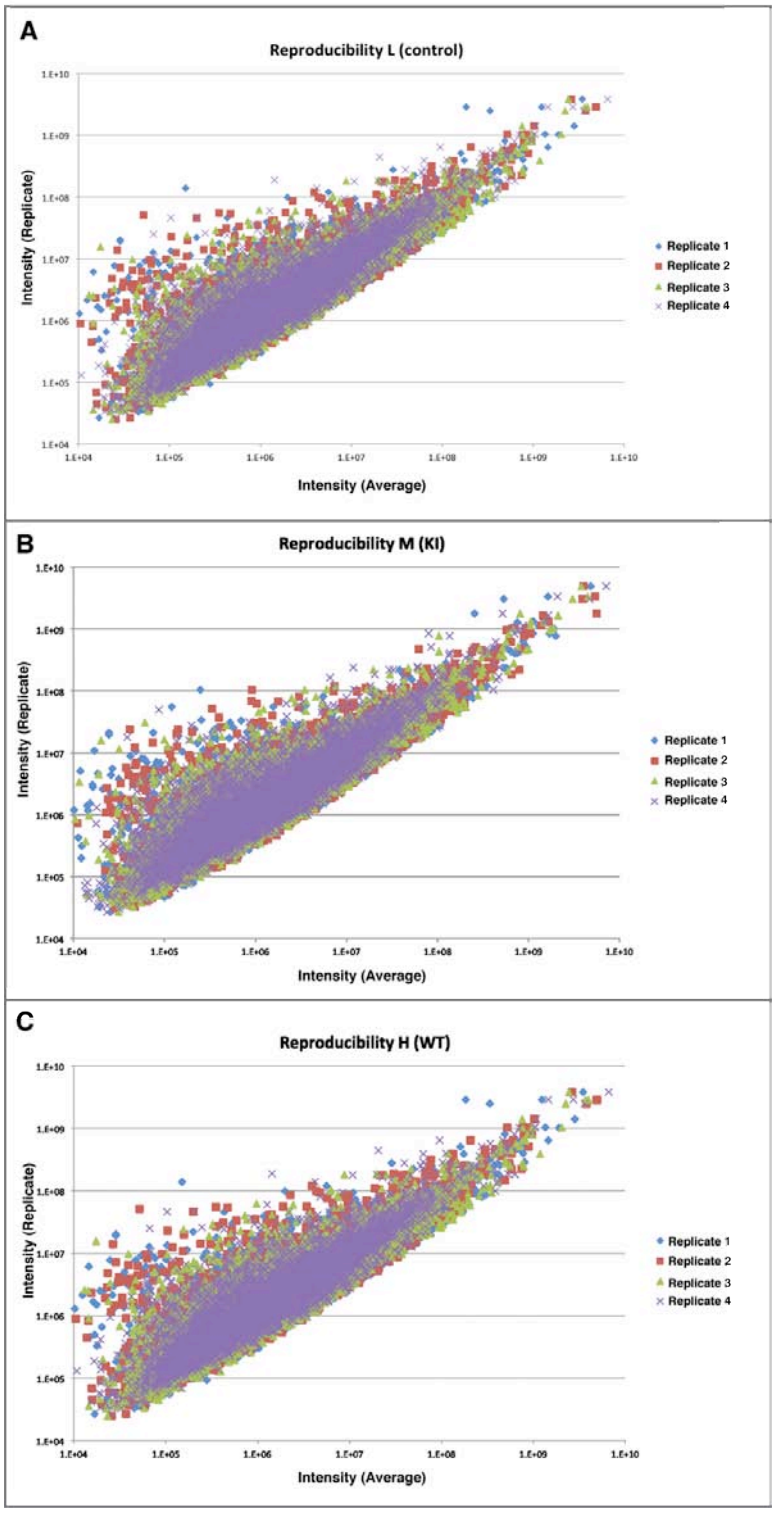

Figure 5.5 Reproducibility of proteomic data

Scatter plots showing a comparison of peptide intensity from each independent experimental replicate in **(A)** unlabeled condition, **(B)** 'medium' labeled condition and **(C)** 'heavy' labeled condition, with a strong correlation with the average peptide intensity.

The measured ratios for each condition were grouped into 'bins' and plotted along the x-axis (in logarithmic scale): H/M for wild-type PINK1 vs. kinase-inactive PINK1, H/L for wild-type PINK1 vs. control and M/L for kinase-inactive PINK1 vs. control. The frequency of occurrence of peptides in each binned ratio was plotted along the y-axis (Fig. 5.6). This plot showed a normal distribution curve with majority of peptides remaining unchanged between experimental conditions (Fig. 5.6).

Frequency plot of Wild-type PINK1 versus Kinase inactive PINK1 shows that 129 phosphosites are up regulated (> 3fold) (Fig. 5.6A). Frequency plots of Wild-type PINK1 versus control showed 73 up regulated sites (Fig. 5.6B) whereas Kinase-inactive versus control (Fig. 5.6B) had around 42 up regulated sites (Fig. 5.6C). Among the 73 phosphosites that were up regulated in wild-type PINK1 vs control, only 42 phosphosites overlapped with the ones that were up regulated (> 3 fold) in wild-type PINK1 vs kinase-inactive PINK1. Among these, 20 of them were found in at least two out of four experimental replicates (Table 5.1). Among the proteins listed in Table 5.1, only 8 proteins were consistently identified in all experimental replicates. 7 other proteins were identified in three out of four replicates and 5 of them were found only in two replicates. One of the up-regulated phosphosites identified corresponded to the Thr257 PINK1 autophosphorylation site, which in part validated the screen.

A

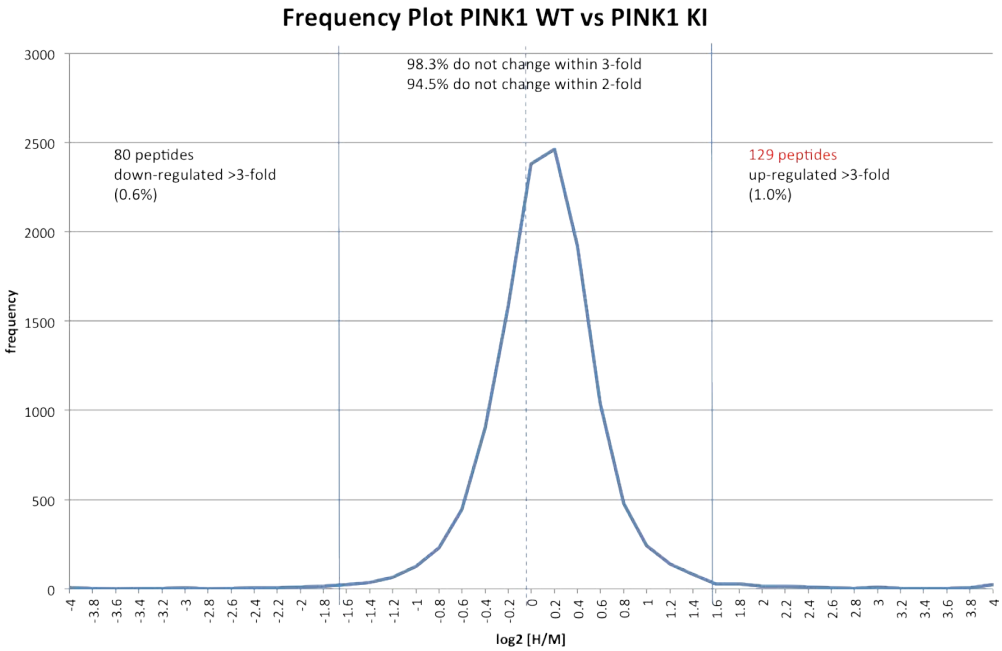
Frequency Plot PINK1 WT vs PINK1 KI
98.3% do not change within 3-fold
94.5% do not change within 2-fold
80 peptides
down-regulated >3-fold
(0.6%)
129 peptides
up-regulated >3-fold
(1.0%)
frequency
log2 [H/M]

B

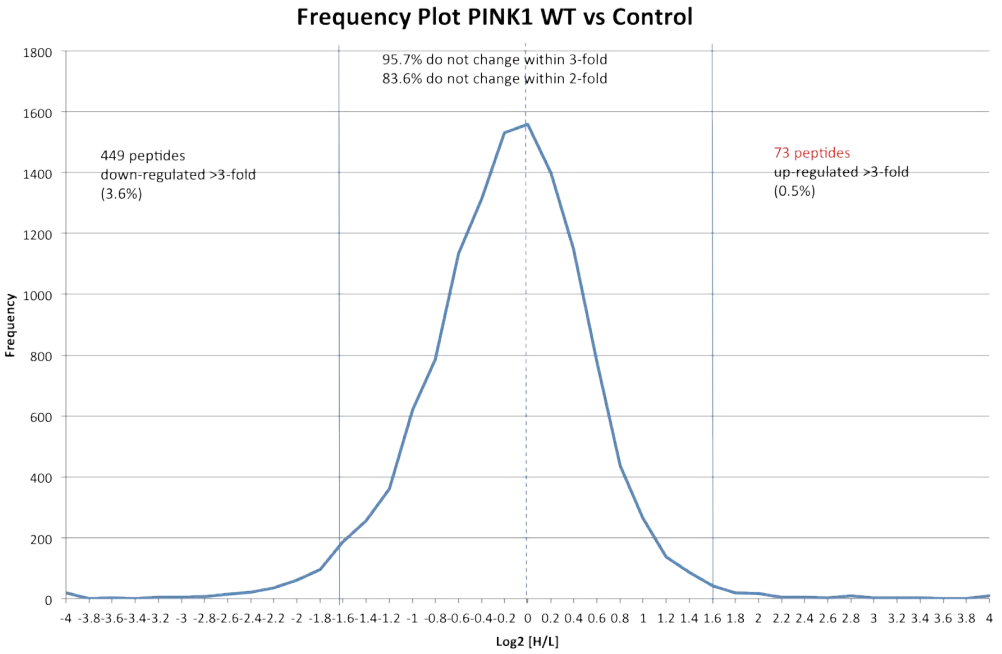
Frequency Plot PINK1 WT vs Control
95.7% do not change within 3-fold
83.6% do not change within 2-fold
449 peptides
down-regulated >3-fold
(3.6%)
73 peptides
up-regulated >3-fold
(0.5%)
Frequency
Log2 [H/L]

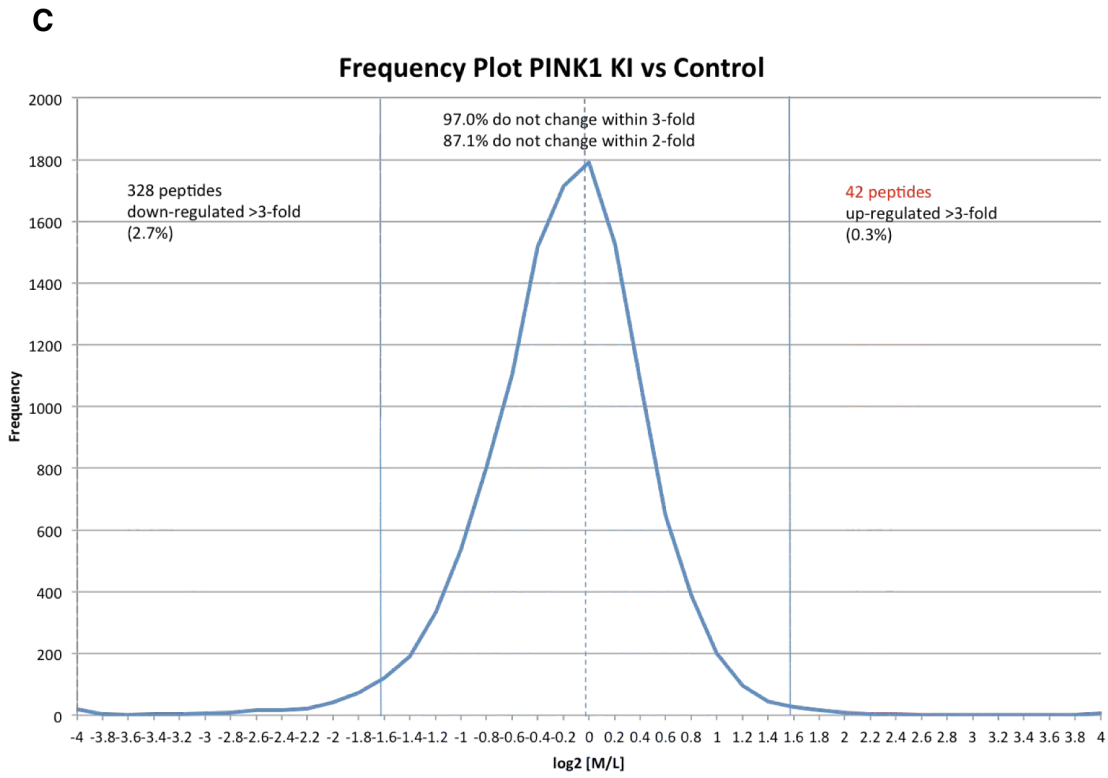

Figure 5.6 Frequency plot for phosphoproteomic data

Frequency plots of **(A)** Wild-type PINK1 vs Kinase inactive PINK1 (heavy/medium), **(B)** Wild-type PINK1 vs control (heavy/light) and **(C)** Kinase inactive PINK1 vs control (medium/light). The measured ratios for each case were grouped into ratio bins, and the y-axis shows the frequency of peptides detected per bin.

Although there were a reasonable number of putative substrates identified from my screen, some nuclear proteins (such as RHG35, GCFC1, ZNF36 and PRDM2) were excluded from further analysis since they are likely to represent nuclear membrane contamination during preparation of crude mitochondrial fractionation. Cytoskeletal protein (MAP1B), heat shock protein (DNAJB2) and translation initiation factor (EIF4E2) were not considered for further analysis.

PINK1 substrate screen by SILAC phosphoproteomics

Gene Names	Protein Names	M/L Exp.1	M/L Exp.2	M/L Exp.3	M/L Exp.4	H/L Exp.1	H/L Exp.2	H/L Exp.3	H/L Exp.4	H/M Exp.1	H/M Exp.2	H/MExp.3	H/M Exp.4	Sub-cellular location
		Kinase inactive PINK1				Wild-type PINK1				Wild-type/Kinase inactive PINK1				
PINK1	PTEN-induced kinase 1	1.4935	0.32995	0.19628	0.83112	18.555	6.307	18.508	13.579	12.436	20.611	89.097	15.178	Mitochondrial outer membrane
	Proteins found in all replicates													
Rab8A	Ras related protein Rab8A	1.6461	0.71596	0.65525	0.55304	17.002	15.284	16.623	29.373	10.117	23.702	15.015	54.213	Cell membrane;lipid anchor
Rab8B	Ras related protein Rab8b	0.26623	0.21329	0.38189	0.34449	9.1195	6.8317	6.1492	12.304	37.203	35.97	15.439	38.602	Cell membrane;lipid anchor
Rab13	RAB13 proten	0.12436	0.71352	0.30711	0.51769	17.068	22.269	9.6019	22.016	153.41	34.828	32.158	43.353	Tight junctions
RL40	Ubiquitin- C splice variant;Ribosomal protein S27A	0.62	0.33171	0.51932	0.49093	9.6547	7.4554	7.4266	7.681	15.378	19.041	14.426	18.98	Cytoplasm;nucleus
NF1	Neurofibromatosis factor 1	0.9229	0.95481	0.75839	0.82844	4.3382	2.5151	3.8388	2.408	*4.9167*	*2.6916*	*5.114*	*3.1368*	Cytoplasm;nucleus
RHG35/ARHGAP35	Glucocorticoid receptor DNA-binding factor	0.71101	0.68342	0.66863	1.3304	3.2085	3.1991	4.6426	2.7109	4.9438	4.8252	7.0218	2.2254	Cytoplasm;nucleus
EIF4E2	eIF4E-like protein 4E-LP	1.0163	0.92389	0.76638	0.76296	2.8376	1.7884	3.3783	3.9573	3.8738	1.2008	1.9809	4.3876	N/A
	Proteins found in 3 out of 4 replicates													
RHOT2	Mitochondrial Rho GTPase 2 Miro2	0.61656	0.43675	-	0.44564	5.2817	6.4096	-	7.975	8.7164	10.226	-	8.4064	Mitochondrial outer membrane
DLST	2-oxoglutarate dehydrogenase complex component E2;DLST	0.92004	0.78413	1.2818		28.191	21.566	39.386	-	30.665	27.454	28.83	-	Mitochondrion
GCFC1	GC-rich sequence DNA-binding factor homolog	0.89772	0.53051	-	1.7151	9.5433	5.7802	-	1.2354	11.922	12.519	-	0.69362	Nucleus
ZNF736	similar to Zinc finger protein 92	1.9795	2.5516	-	8.9844	31.425	30.193	-	84.571	16.837	12.208	-	9.5977	Nucleus
TMEM51	Transmembrane protein 51	0.59793	0.62588	-	0.80026	4.01	4.3437	-	7.1054	*6.8195*	*7.3124*	-	*8.6259*	Membrane; multi-pass membrane protein
BID	BH3-interacting domain death agonist BID	-	0.50725	0.52998	3.4994	-	5.9684	6.3241	8.0597	-	14.429	14.041	2.4002	Mitochondria;Cytoplasm
DNAJB2	(DNAJB2), mRNA;DnaJ homolog subfamily B member 2	-	0.57358	1.1494	0.90809	-	6.955	4.9539	1.2237	-	*12.058*	*4.6805*	*1.0571*	N/A
	Proteins found in 2 out of 4 replicates													
FAM21A	FAM21A protein;WASH complex subunit FAM21B	-	1.1358	-	0.9891	-	2.0076	-	6.4348	-	1.842	-	7.014	Early endosome membrane
KMT8;PRDM2	GATA-3-binding protein G3B	0.63834	-	0.9244	-	4.9702	-	4.6981	-	*8.2446*	-	*5.1782*	-	Nucleus
srGAP1	SLIT-ROBO Rho GTPase-activating protein 1	-	-	0.55655	0.5971	-	-	10.574	4.4148	-	-	21.461	7.7851	N/A
GPRIN3	GPRIN family member 3	0.46329	0.34485	-	-	2.064	13.525	-	-	*4.8818*	*43.152*	-	-	N/A
MAP1B	MAP1 light chain LC1;Microtubule-associated protein 1B	-	2.4468	-	1.577	-	7.1657	-	2.0433	-	3.0605	-	1.2838	Cytoskeleton

Table 5.1 Complete list of putative PINK1 substrates identified by SILAC phospho-proteomic screen

Gene Names	Protein Names	Fold change (H/M normalized)	Phospho (STY) Probabilities
PINK1	PTEN-induced putative kinase protein 1	14	VALAGEYGAVT(0.182)Y(0.818)R
	Proteins found in all replicates		
RAB8A	Ras-related protein Rab-8A	15	NIEEHAS(1)ADVEK
RAB8B	Ras-related protein Rab-8B	35	NIEEHAS(0.878)S(0.122)DVER
RAB13	RAB13 protein	43	SIKENAS(1)AGVER
RL40	Ubiquitin C splice variant;Ribosomal protein S27A	16	TLSDYNIQKES(0.995)T(0.005)LHLVLR
	Proteins found in 3 out of 4 replicates		
DLST	2-oxoglutarate dehydrogenase complex component E2	28	TPAFAES(0.985)VT(0.015)EGDVR
BID	BH3-interacting domain death agonist BID	14	HLAQVGDS(1)MDR
RHOT2	Mitochondrial Rho GTPase 2	8	ADLPEGVAVS(0.835)GPS(0.165)PAEFCR
TMEM51	Transmembrane protein 51	7.3	ADVEAS(1)PGNPPDR
	Proteins found in 2 out of 4 replicates		
SRGAP1	SLIT-ROBO Rho GTPase-activating protein 1	13	ADSEAS(0.139)S(0.861)GPVTEDK

Table 5.2 Short-list of putative substrates of PINK1

	-6	-5	-4	-3	-2	-1	0	1	2	3	4	5
Parkin	C	D	L	D	Q	Q	S	I	V	H	I	V
RAB8A	N	I	E	E	H	A	S	A	D	V	E	K
RAB8B	N	I	E	E	H	A	S	S	D	V	E	R
RAB13	S	I	K	E	N	A	S	A	G	V	E	R
RL40	Y	N	I	Q	K	E	S	T	L	H	L	V
DLST	T	P	A	F	A	E	S	V	T	E	G	D
RHOT2/MIRO2	V	A	V	S	G	P	S	P	A	E	F	C
BID	L	A	Q	V	G	D	S	M	D	R	S	I
TMEM51	R	A	D	V	E	A	S	P	G	N	P	P
srGAP1	A	D	S	E	A	S	S	G	P	V	T	E

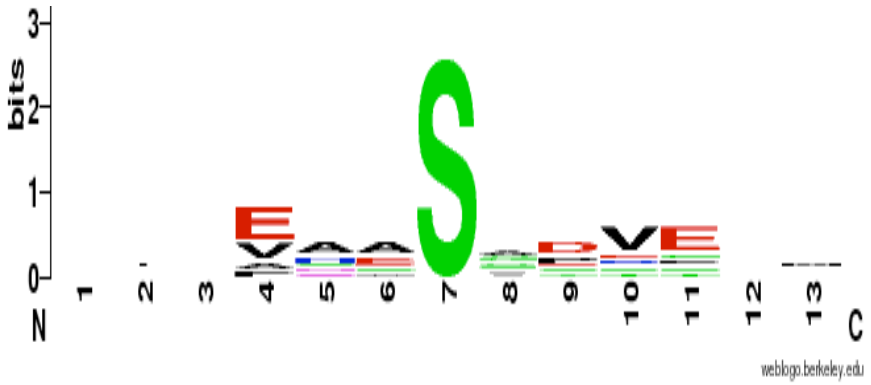

Figure 5.7 Phosphosite motif analysis of putative PINK1 substrates

The upper panel shows sequences encompassing the phosphosite identified in each putative PINK1 substrate listed in Table 5.2 along with Parkin Ser65 phosphosite sequence. The position of phosphosite is kept at zero and upstream and downstream sequences are marked with negative or positive numbering respectively. The lower panel shows a sequence logo generated from these peptide sequences using Weblogo (Version 2.8.2) http://weblogo.berkeley.edu/.

Among substrates that were detected in two replicates, FAM21A and GPRIN3 were excluded from the list, as one of the replicates did not show a significant fold change. NF1 (also known as neurofibromin) was found in all four replicates but owing to the size of the protein (319kDa) it was difficult to clone. Furthermore, this candidate was given less priority for further analysis since it is predominantly nuclear. I therefore decided to focus on nine putative PINK1 substrates in view of the significance of the fold change of their respective phosphosites upon PINK1 activation. Interestingly, three Rab GTPases namely RAB8A, RAB8B and RAB13 were identified in all experiments with a significant fold change when comparing wild-type versus kinase-inactive PINK1 (Table 5.2). The screen also identified the atypical mitochondrial Rho-GTPase Miro2, which I had previously found to be a significant interactor of PINK1 (Table 4.2). All of the putative PINK1 substrates identified were phosphorylated at serine residues, similar to the Parkin (Ser65) site described in Chapter 3. An alignment comparison of the surrounding residues of the phosphosite sequence of the putative substrates identified, along with the Parkin Ser65 phosphosite sequence suggested a possible preference of PINK1 for acidic residues at the -3 position and +2/+4 position.

5.2.2 Validation of Rab8A, Rab8B and Rab13 as PINK1 substrates

Three Rab GTPases namely RAB8A, RAB8B and RAB13 were identified as putative PINK1 substrates in my SILAC phospho-proteomic experiment. The

phosphosite identified in these Rab GTPases was significantly up regulated in cells containing wild-type PINK1 activated by mitochondrial depolarization in all experimental replicates. The phosphorylation site corresponded to Serine 111 residue, and multiple sequence alignment of individual Rab GTPases from higher mammals as well as Drosophila revealed a high degree of conservation of this site (Fig. 5.8 A, B and C).

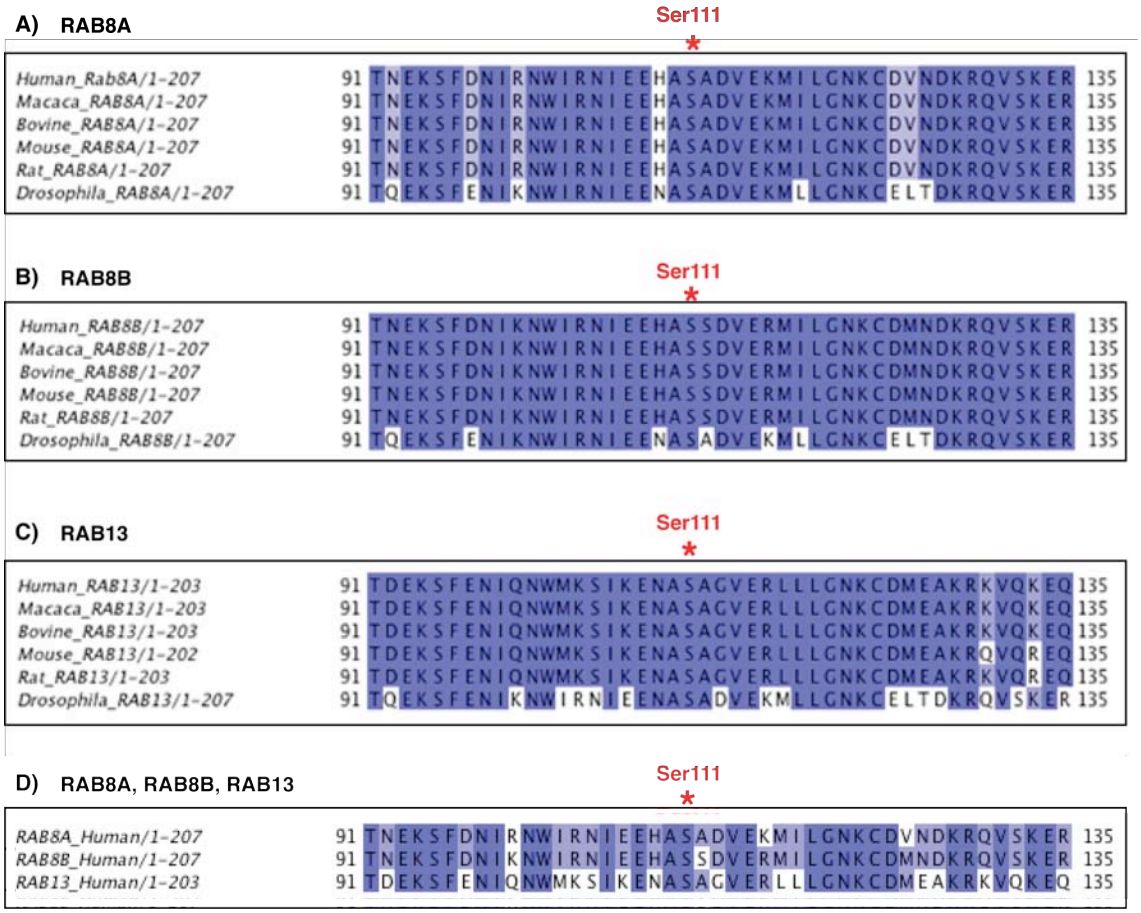

Figure 5.8 Multiple sequence alignment of Ser111 phosphorylation site in RAB8A, RAB8B and RAB13

Multiple sequence alignment (MSA) of orthologs from higher mammals and Drosophila performed for **(A)** RAB8A, **(B)** RAB8B and **(C)** RAB13. **(D)** MSA for human RAB8A, RAB8B and RAB13. Red asterisk shows the position of the Serine 111 phosphorylation site.

Full-length human HA tagged versions of the respective Rab GTPases (RAB8A, RAB8B and RAB13) were transiently over-expressed in Flp-In TRex HEK293 cells stably expressing FLAG alone, wild-type human PINK1, or kinase-inactive human PINK1 (D384A). Cells were treated with or without CCCP for 3 h-conditions that induce stabilization and activation of PINK1 at the mitochondria. The respective Rab GTPase was immunoprecipitated with HA-agarose and phosphorylation site analysis undertaken by mass spectrometry. This confirmed that RAB8A and RAB8B were phosphorylated at Ser111 in cells expressing wild-type human PINK1 that had been stimulated with CCCP (Fig. 5.9 and Fig. 5.10). No detectable phosphorylation of Ser111 in RAB8A or RAB8B was observed in the absence of CCCP treatment or in cells expressing kinase-inactive PINK1 (Fig. 5.9 and Fig. 5.10). Similarly for RAB13, I observed significant phosphorylation of Ser111 only in cells expressing wild-type PINK1 stimulated with CCCP and no detectable phosphorylation was observed in control cells or kinase inactive cells treated with CCCP (Fig. 5.11).

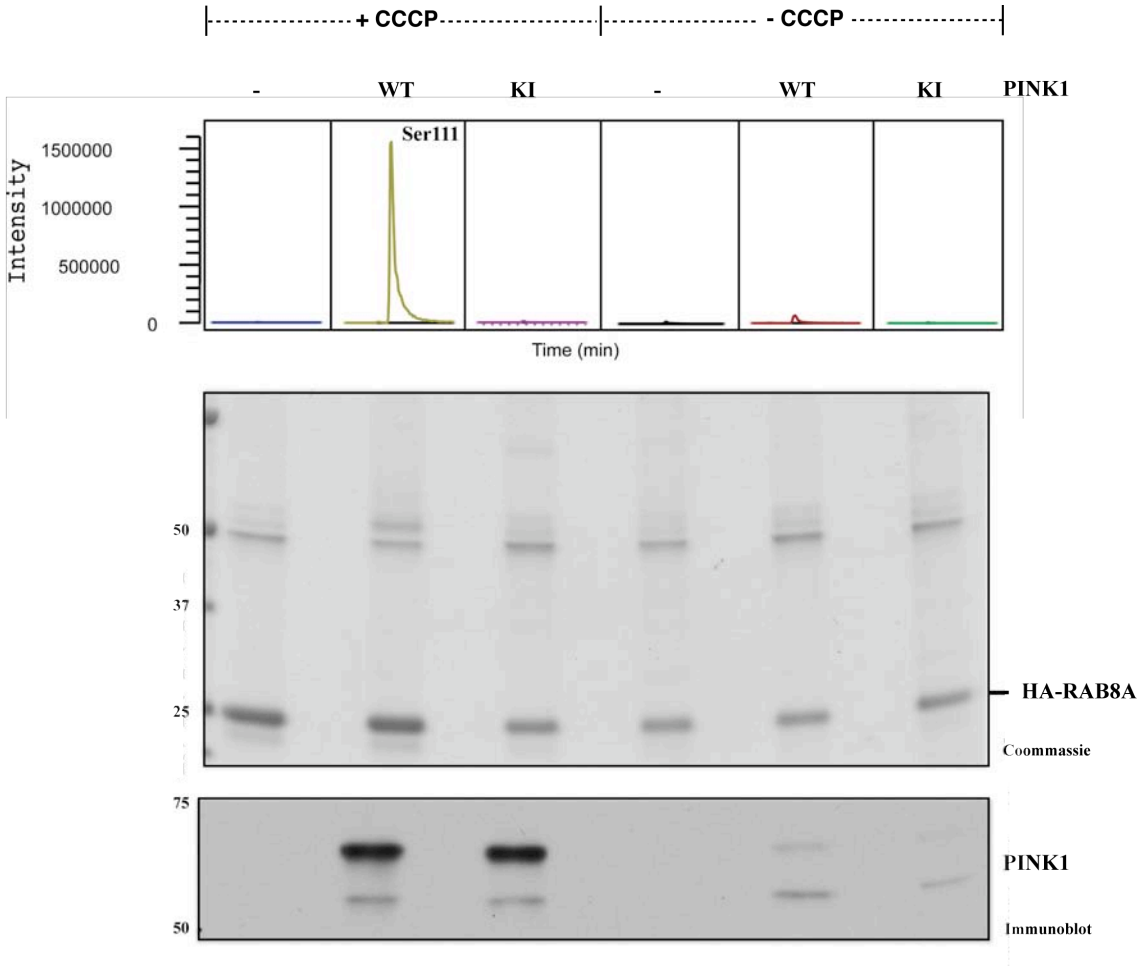

Figure 5.9 PINK1 phosphorylates RAB8A at Ser111 *in vivo*

Flp-In T-Rex HEK293 cells expressing FLAG-empty, wild-type PINK1-FLAG, and kinase-inactive PINK1-FLAG (D384A) were co-transfected with HA-RAB8A, induced with doxycycline and stimulated with 10 mM of CCCP for 3 h. 10mg of whole-cell extract were immunoprecipitated with anti-HA-agarose, resolved by SDS-PAGE and stained with colloidal Coomassie blue. Bands corresponding to mass of HA-RAB8A were excised, digested with trypsin, and subjected to high performance liquid chromatography with tandem mass spectrometry (LC-MS-MS) on an LTQ-Orbitrap mass spectrometer. Upper panel shows Extracted ion chromatogram analysis of Ser111 phosphosite with Y-axis corresponding to phosphopeptide signal intensity and x-axis to retention time.

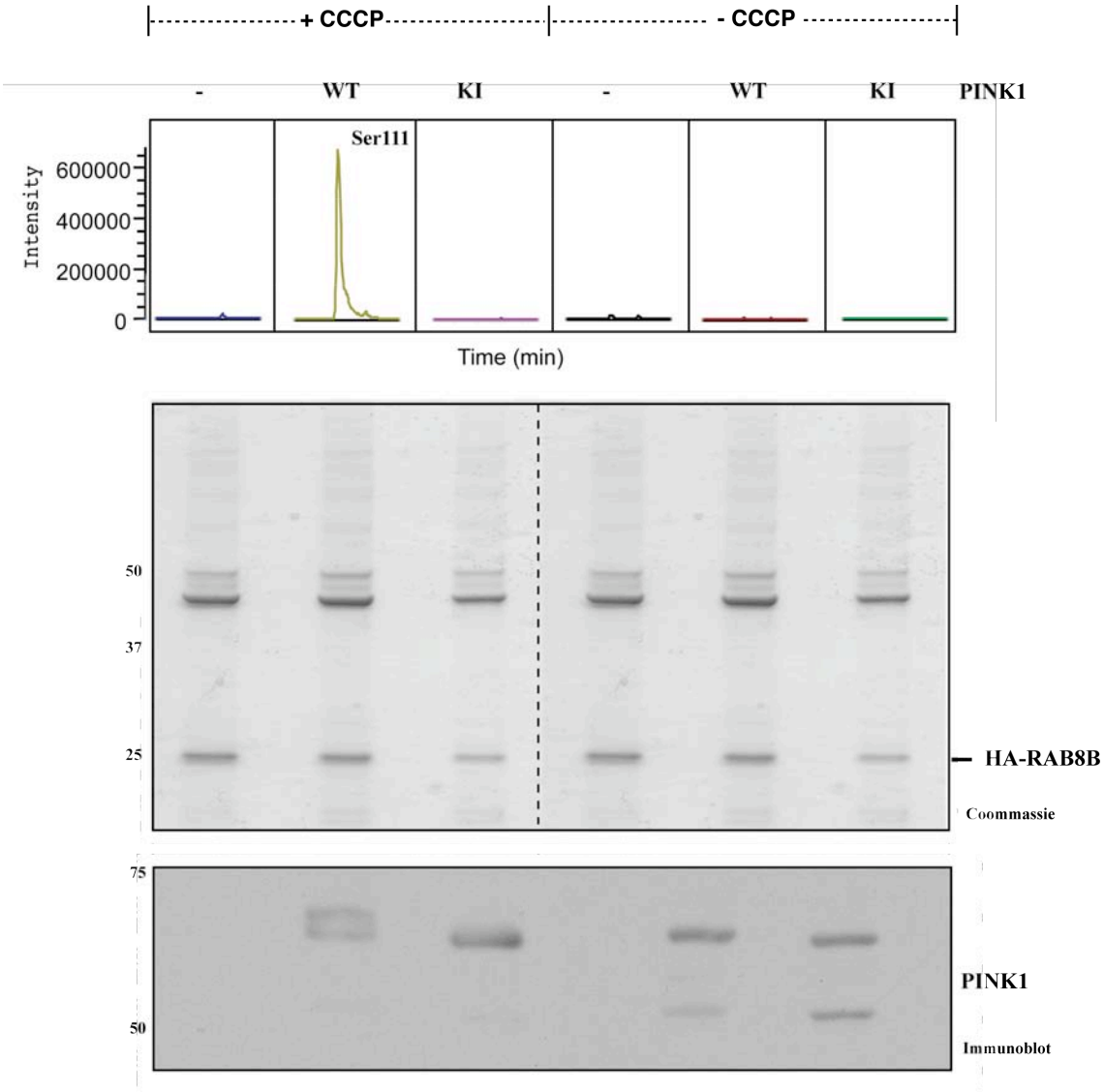

Figure 5.10 PINK1 phosphorylates Rab8B at Ser111 *in vivo*

Flp-In T-Rex HEK293 cells expressing FLAG-empty, wild-type PINK1-FLAG, and kinase-inactive PINK1-FLAG (D384A) were co-transfected with HA-RAB8B, induced with doxycycline and stimulated with 10 mM of CCCP for 3 h. 10mg of whole-cell extract were immunoprecipitated with anti-HA-agarose, resolved by SDS-PAGE and stained with colloidal Coomassie blue. Bands corresponding to mass of HA-RAB8B were excised, digested with trypsin, and subjected to high performance liquid chromatography with tandem mass spectrometry (LC-MS-MS) on an LTQ-Orbitrap mass spectrometer. Upper panel shows Extracted ion chromatogram analysis of Ser111 phosphosite with Y-axis corresponding to phosphopeptide signal intensity and x-axis to retention time.

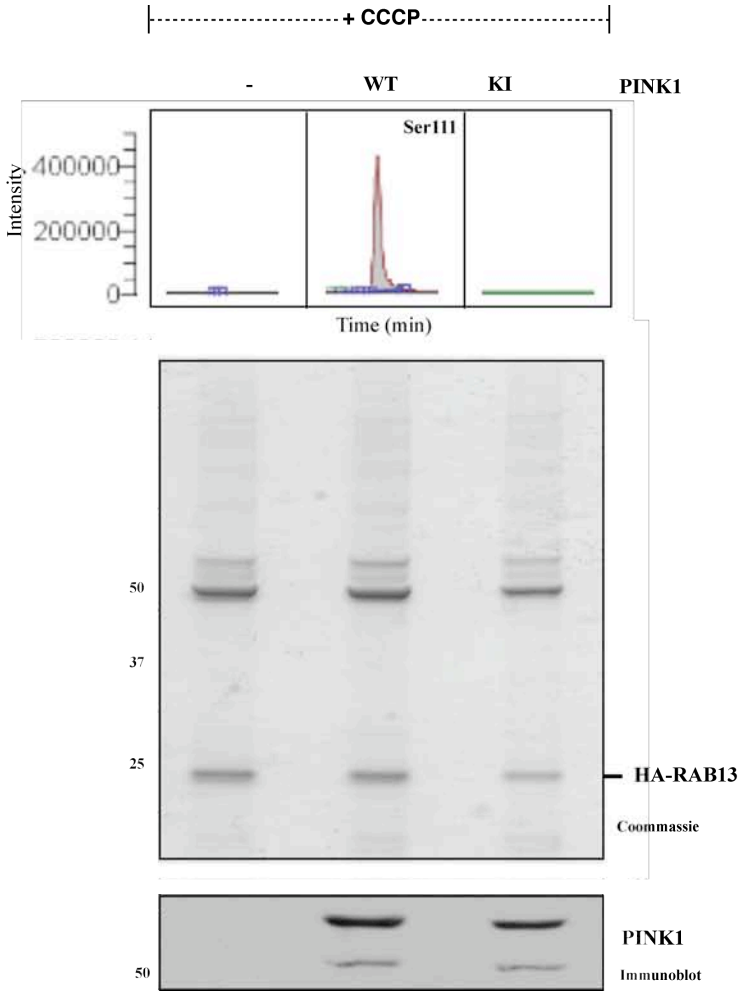

Figure 5.11 PINK1 phosphorylates RAB13 at Ser111 *in vivo*

Flp-In T-Rex HEK293 cells expressing FLAG-empty, wild-type PINK1-FLAG, and kinase-inactive PINK1-FLAG (D384A) were co-transfected with HA-RAB13 and stimulated with 10 mM of CCCP for 3 h. 10mg of whole-cell extract were immunoprecipitated with anti-HA-agarose, resolved by SDS-PAGE and stained with colloidal Coomassie blue. Bands corresponding to mass of HA-RAB13 were excised, digested with trypsin, and subjected to high performance liquid chromatography with tandem mass spectrometry (LC-MS-MS) on an LTQ-Orbitrap mass spectrometer. Upper panel shows Extracted ion chromatogram analysis of Ser111 phosphosite with Y-axis corresponding to phosphopeptide signal intensity and x-axis to retention time.

5.2.3 Characterization of Ser111 phosphosite specific antibody for RAB8A and RAB8B

I next raised phospho-specific antibodies against the Ser111 phosphorylation site for RAB8A, RAB8B and RAB13. For characterization of the antibodies, stable cell lines expressing either FLAG alone, PINK1-FLAG wild-type or PINK1-FLAG kinase-dead were over-expressed with either HA-RAB8A or HA-RAB8B and stimulated with either doxycycline alone or with CCCP for 3 hours. All three bleeds of each phospho-antibody were tested on the respective Rab GTPase that had been immunoprecipitated from cells under the various conditions stated above. For the RAB8A Ser111 phospho-specific antibody, the 2nd bleed was able to robustly detect phosphorylation in cells expressing

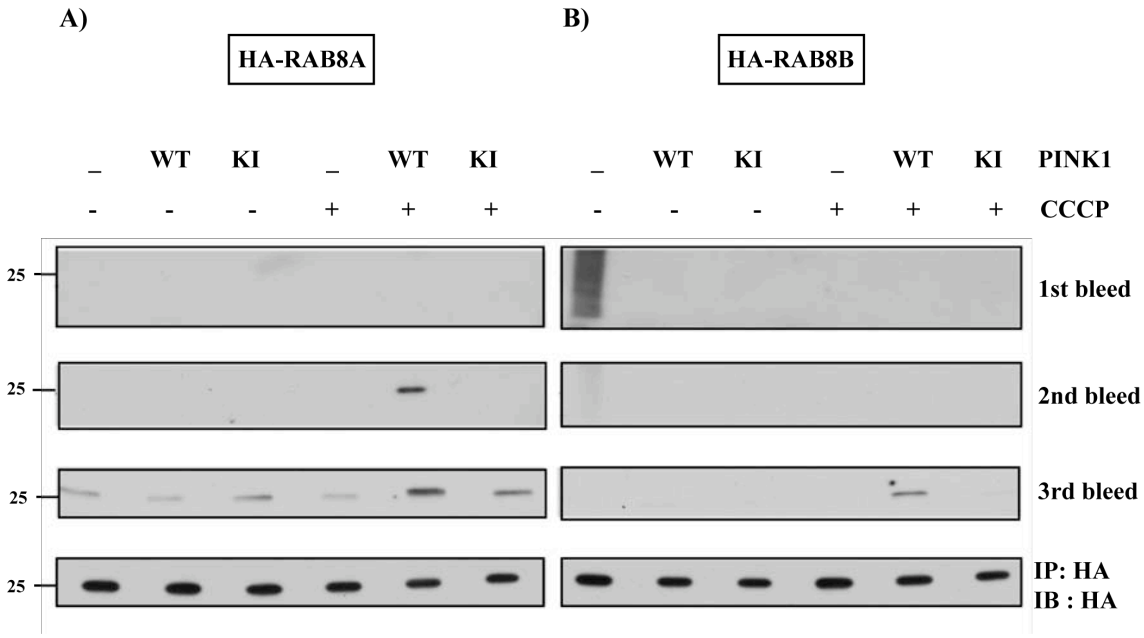

Figure 5.12 Characterization of RAB8A and RAB8B Ser111 phospho-specific antibody

Flp In TRex HEK293 cells stably expressing either FLAG alone, wild-type PINK1-FLAG or kinase-inactive PINK1-FLAG was over-expressed with **(A)** HA-RAB8A or **(B)** HA-RAB8B. Cells were induced with doxycycline, stimulated with either doxycline or CCCP and 0.25mg of whole cell lysates were immunoprecipitated with anti-HA agarose beads and blotted with the indicated antibodies.

wild-type but not kinase-inactive PINK1 (Fig. 5.12 A). For the RAB8B Ser111 phospho-specific antibody the 3rd bleed was able to detect phosphorylation in cells expressing wild-type PINK1 (Fig. 5.12 B). Further, the phospho-antibody for both RAB8A and RAB8B did not detect any Ser111 phosphorylation under basal conditions indicating that this only occurs during mitochondrial depolarization when PINK1 would be predicted to be active (Fig. 5.12). In contrast none of the bleeds for the RAB13 Ser111 phospho-specific antibody could detect phosphorylated RAB13 (data not shown).

5.2.4 Preliminary analysis of further putative PINK1 substrates

I undertook a multiple sequence alignment (MSA) of the other phosphosites identified as putative PINK1 substrates (from the SILAC screen) with their respective orthologues. The phosphosites identified in Ribosomal protein S27A (RL40), 2-oxoglutarate dehydrogenase (DLST), TMEM51 and SLIT-ROBO GAP1 (srGAP1) showed a high degree of conservation across all species. Furthermore, the srGAP1 phosphosite was highly conserved between its two paralogs srGAP2 and srGAP3. In contrast, for BH3-interacting death domain agonist (BID), the phosphorylation site was conserved in primates but not rodents (substitution for D) suggesting that it may not be critical for regulation of BID. For Miro2, mass spectrometry analysis could not distinguish between two potential sites in my screen: Ser535 with a probability 0.835 and Ser538 with a probability of 0.165 (Table 5.2). However, Ser535 is not conserved at all across species whereas Ser538 showed a relatively higher degree of conservation in higher organisms but not in Drosophila. In future work it will be crucial to

validate all these phosphosites *in vivo* using candidate-based mass spectrometry and raise phospho-specific antibodies against the most promising candidates.

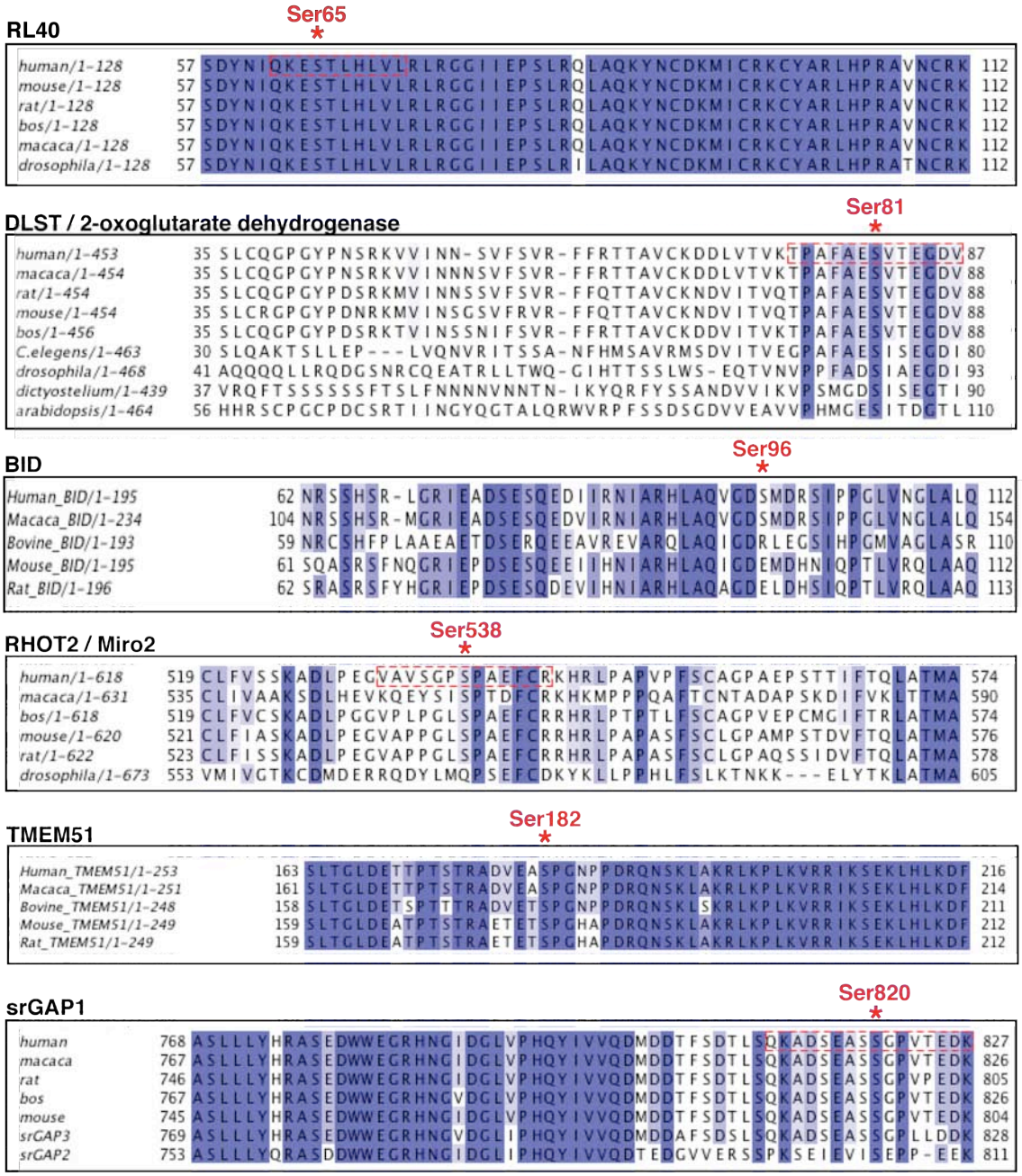

Figure 5.13 Multiple sequence alignment of PINK1 substrates identified from the SILAC phospho-proteomic screen

Multiple sequence alignment (MSA) of orthologs of RL40, DLST, BID, Miro2, TMEM51 and srGAP1 were performed. Red asterisk shows the position of the PINK1 mediated phosphorylation site with the amino acid residue number indicated above the asterisk.

5.3 Discussion

Identification of novel substrates of PINK1 by a SILAC phospho-proteomic approach

In Chapter 3, I have provided strong evidence that Parkin is a substrate of PINK. However, I wanted to explore alternate signaling pathways downstream of PINK1. Having established a cell line over-expressing either wild-type of kinase-inactive PINK1 wherein conditions of mitochondrial depolarization can specifically activate wild-type PINK1 (Fig. 3.7), I decided to employ this system to screen for novel PINK1 substrates by a quantitative SILAC phospho-proteomic approach.

Since PINK1 is stabilized and activated in the mitochondrial membrane, I hypothesised that PINK1 may have mitochondrial substrates. I therefore focused on a screen of membrane-enriched fractions that would include mitochondria rather than a whole phosphoproteome analysis. This would also be technically more tractable since fractionation would likely enhance the signal to noise ratio and make it more likely to capture less abundant phosphopeptides.

The SILAC phospho-proteomic screen employed three conditions in four experimental replicates; control cells stimulated with CCCP were unlabeled, wild-type PINK1 cells stimulated with CCCP (in order to activate PINK1) were

'heavy' labeled and kinase-inactive PINK1 cells stimulated with CCCP were 'medium' labeled. A total of 12,374 unique phosphosites were identified in my screen among which only 129 phosphosites (1% of the total identified) were significantly upregulated between wild-type vs. kinase-inactive PINK1.

Although 129 phosphosites were upregulated between wild-type and kinase-inactive PINK1, only 73 peptides were up regulated between wild-type PINK1 and control cells stimulated with CCCP. This could perhaps be due to the effect of endogenous PINK1 being activated by CCCP stimulation in control cells. The least number of up regulated phosphosites (42 phosphosites) was found in kinase-inactive PINK1 vs. control and these may represent non-specific phosphosites since endogenous PINK1 would be similarly activated in both cell lines. Among the 73 peptides up-regulated in wild-type vs. control, only 42 of them overlap with the peptides identified comparing wild-type vs. kinase-inactive. Furthermore, of these only 20 phosphosites were up regulated in two out of four experimental replicates and these were considered for further analysis. Among the 20 proteins identified I decided to focus on nine putative PINK1 substrates in view of the significance of the fold change of their respective phosphosites upon PINK1 activation.

Overview of members of a Rab GTPase sub-family comprising RAB8A, RAB8B and RAB13 and implications of potential regulation by PINK1.

In a eukaryotic cell, compartmentalization of various membrane-bound organelles was fundamental for the origin of special mechanisms to transport

proteins or lipids between distinct organelles. Such processes are tightly regulated to enable efficient utilization of the available space within a cell and are typically achieved by packaging contents that are required to be transported into vesicles, which bud from the membrane of a donor organelle and eventually fuse into an acceptor membrane. A large family of proteins called the Rab GTPases, which are part of the Ras superfamily of small GTPases, play a key role in regulating the intricate organization required for all membrane trafficking events in a cell (Schwartz et al, 2007; Stenmark & Olkkonen, 2001). Over 60 members of Rab GTPases have been identified in distinct intracellular membranes (Stenmark & Olkkonen, 2001) (Fig. 5.14).

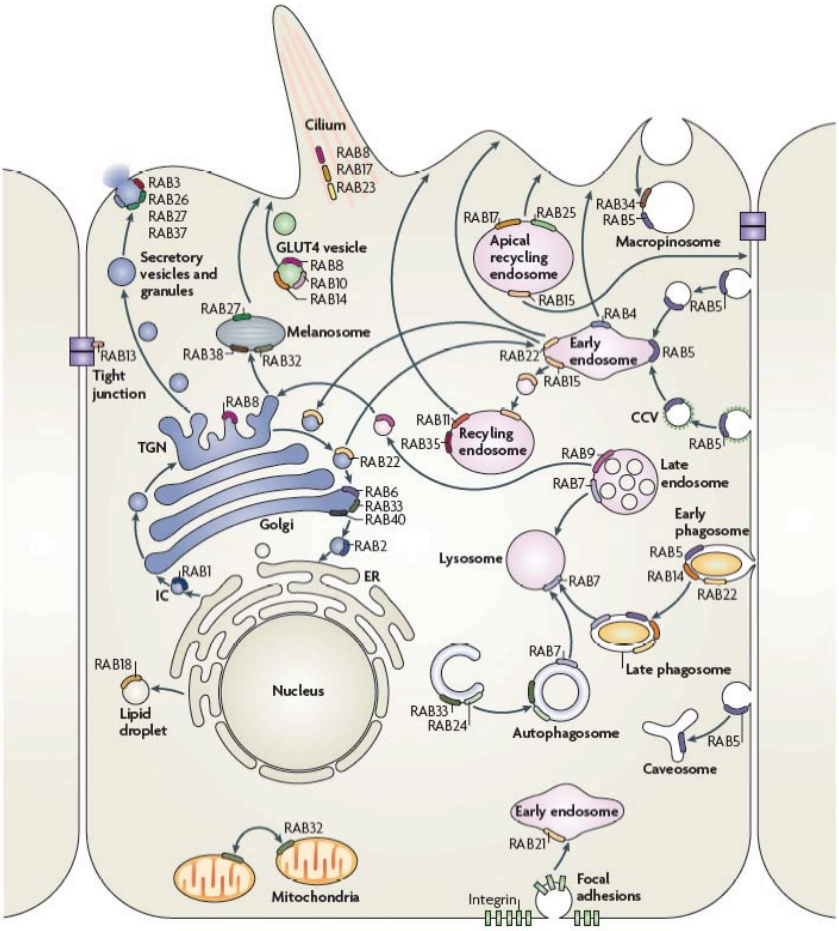

Figure 5.14 Sub-cellular localization of Rab GTPases

Adapted from (Stenmark, 2009)

Rab GTPases are themselves regulated by shuttling between two distinct conformational states: a GDP-bound 'off' state and a GTP-bound 'on' state (Stenmark, 2009) (Fig. 5.15). In the 'off' state, Rabs are usually bound to GDP-dissociation inhibitors (GDI). Once switched 'on' by exchange of GDP for GTP, catalyzed by Guanine nucleotide Exchange Factor (GEF), they can interact with several effector molecules based on which their downstream function is defined (Fig, 5.15). The switch from 'on' back to the 'off' state is achieved by hydrolysis of the bound GTP either by intrinsic GTPase activity or by GTPase Activating Protein (GAP) (Stenmark, 2009) (Fig. 5.15) .

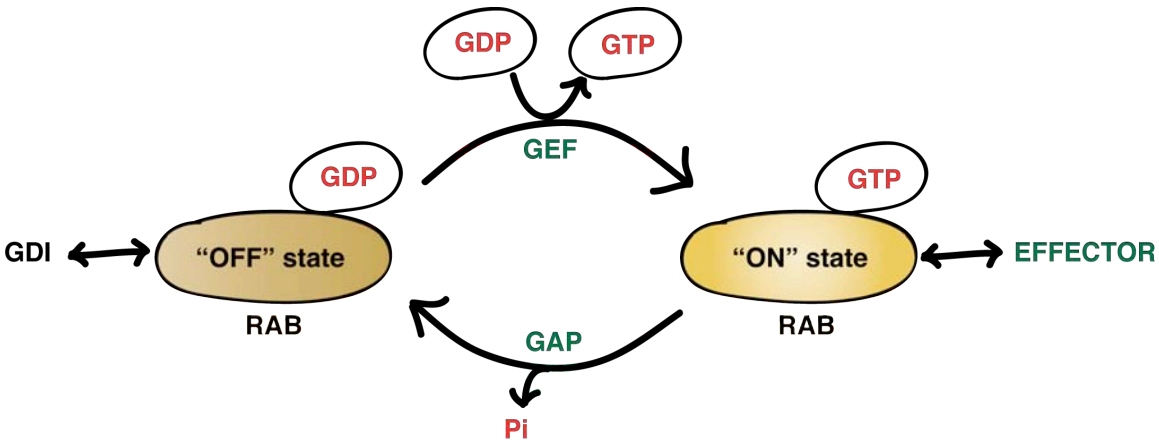

Figure 5.15 Rab GTPase cycle depicting a switch in conformational state

Illustration depicting the conformational switches between inactive "off" state and active "on" state in a Rab GTPase cycle. *Abbreviations: GDI – GTP dissociation inhibitor, GEF – Guanine exchange factor, GAP – GTPase activating protein.*

In my screen for putative PINK1 substrates, I have identified a highly conserved phosphosite to be significantly up regulated in three Rab GTPases namely RAB8A, RAB8B and RAB13. RAB8A and RAB8B are localized in the trans-golgi network and are implicated in trafficking between trans-golgi and plasma

membrane (Fig. 5.14) (Grigoriev et al, 2011). Rab13 is recruited to functional tight junctions from the cytosol (Fig. 5.14) (Marzesco et al, 2002). Interestingly, the phosphosite identified was highly conserved across the three Rab proteins and corresponds to a Serine 111 residue (Fig. 5.8). Interestingly this site is not conserved in any other Rab and all 3 Rabs that share Ser111 are found within the same phylogenetic branch in an evolutionary tree of all human Rab GTPases (Bock et al, 2001) (Fig. 5.16). Although Rab10 is also found within the same phylogenetic branch (Fig. 5.16), multiple sequence alignment revealed that Ser111 phosphorylation site is not conserved in Rab10 (data not shown). I further validated this site by candidate-based mass spectrometry in which I confirmed that these proteins were phosphorylated at Ser111 upon analysis of each respective Rab, isolated from wild-type PINK1 expressing cells stimulated by mitochondrial depolarization. In the case of RAB8A and RAB8B, I could also detect Ser111 phosphorylation using phospho-specific antibodies I generated against each site.

Most Rab proteins share a common structural fold comprising six β-sheets surrounded by five α-helices (Fig. 5.17A). Loop regions interspersed between the sheets and helices, are key structural elements for guanine nucleotide binding, magnesium ion co-ordination as well as GTP hydrolysis (Fig. 5.17A) (Stenmark & Olkkonen, 2001). Loop 2 and the region loop4-helix2-loop5 correspond to two important regions, which are crucial for conformational switches between active and inactive states and also for interaction with

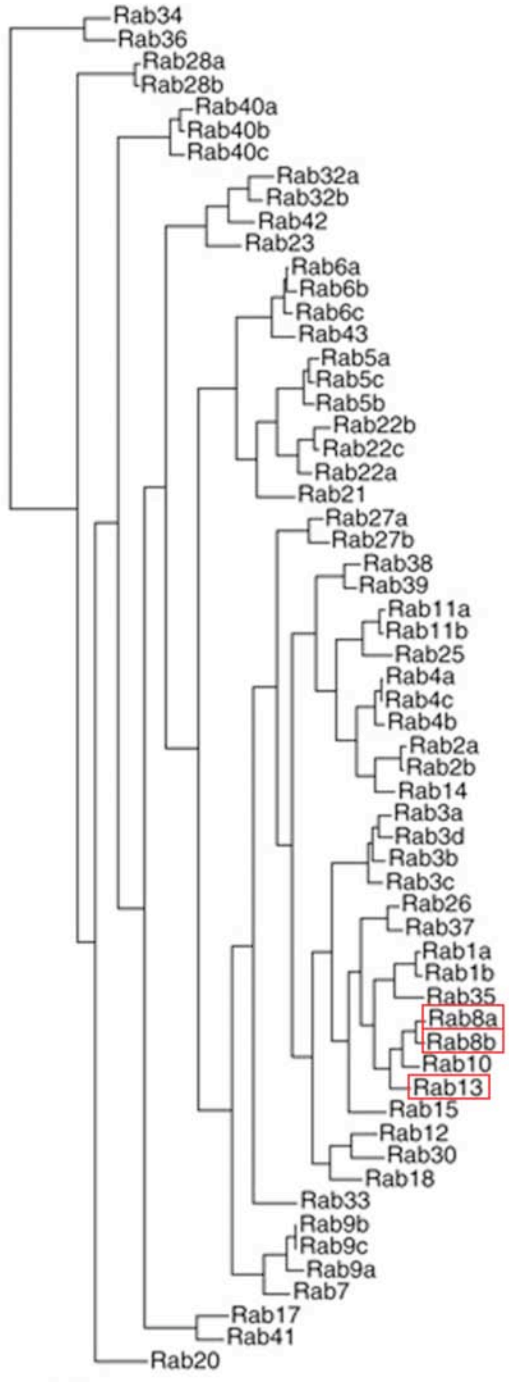

Figure 5.16 Phylogenetic tree of human Rab GTPases

Phylogenetic tree of all human Rab GTPases adapted from (Bock et al, 2001). A red box highlights the terminal branch containing RAB8A, RAB8B and RAB13 indicating that these proteins are evolutionarily conserved.

regulatory proteins such as GEFs and GAPs. Apart from these regions, Rab proteins also contain Rab-specific regions (RabF) required for unequivocal identification of Rab proteins (Fig. 5.17A). Also, they possess Rab sub-family specific sequences (RabSF), which are required to classify them into the ten Rab sub-families (Fig. 5.17A) (Moore et al, 1995). RabSF regions are believed to enable binding of effector proteins, which can specifically recognize a particular Rab sub-family apart from sensing the GTP-bound state. Multiple sequence alignment of human RAB8A, RAB8B and RAB13 revealed that they contain highly conserved sub-structural motifs that define Rab GTPases (Fig. 5.17B). Interestingly, I observed that the PINK1 mediated phosphorylation site, Ser111, is located in a loop region also corresponding to a RabSF region (Fig. 5.17B). Therefore this phosphorylation could possibly modify the interaction between the Rabs of interest and their effector proteins. However, an outstanding question is whether PINK1 directly phosphorylates Ser111 or whether the regulation of the phosphorylation site is indirect. I have recently optimized expression of each Rab protein in *E.coli*, and it would be crucial to test these as direct substrates of insect PINK1. If these were direct substrates then the next question would be to address the functional consequences of phosphorylation. Based on the location of the phosphorylation site in the GTPase domain, it would important to undertake binding studies to determine if phosphorylation influences the interaction of the Rab GTPase with its effector protein.

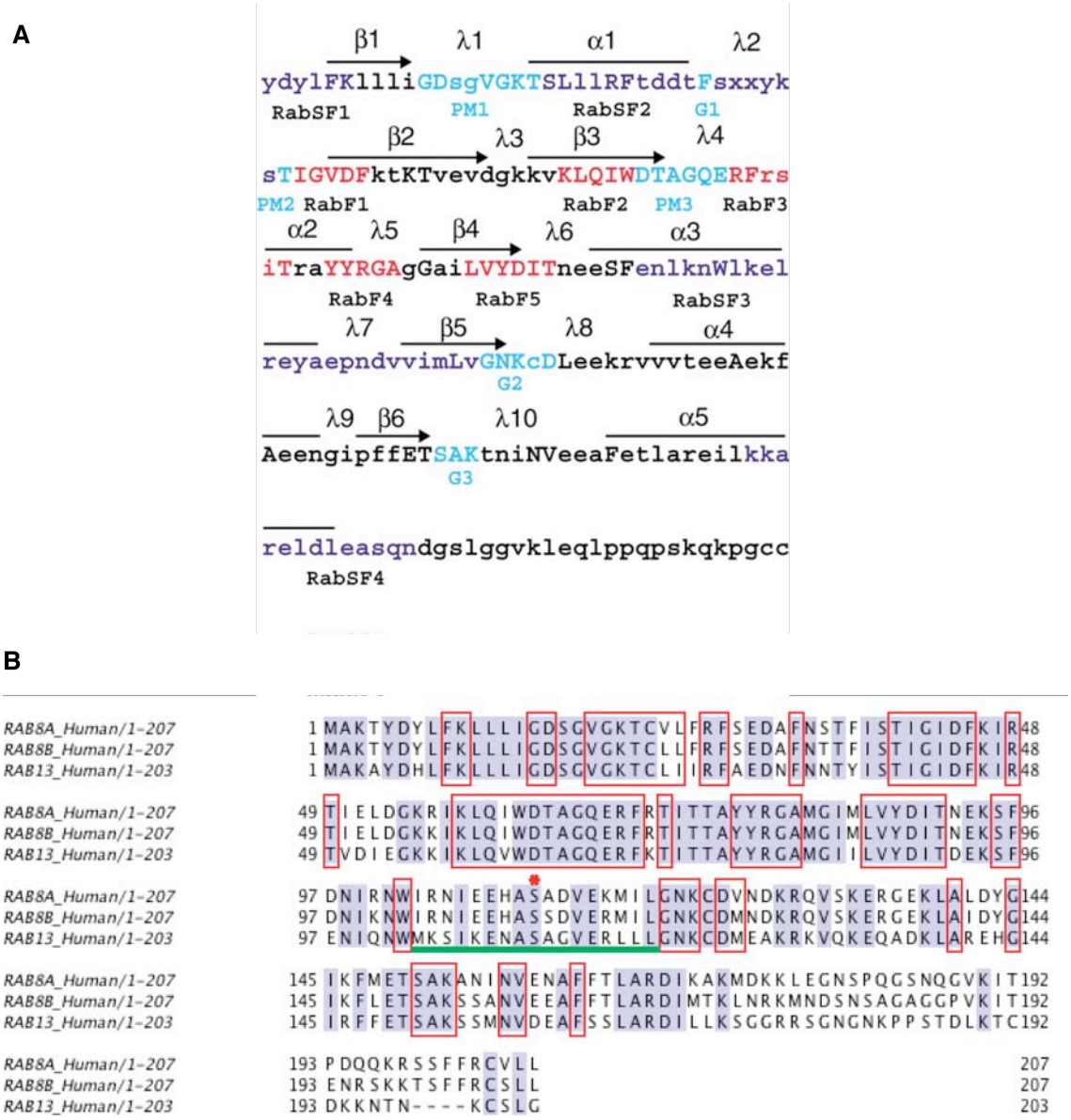

Figure 5.17 Sub-domain organization of Rab8A, 8B and 13

(A) HMM (Hidden Markov Model) based profile amino acid sequence of Rab GTPase superfamily adapted from (Stenmark & Olkkonen, 2001). Upper case letters correspond to highly conserved motifs found in HMM profile with probability > 0.5. Rab-specific residues RabF (1-4) highlighted in red, Sub-family specific motifs RabSF (1-4) highlighted in dark blue and highly conserved nucleotide binding motifs highlighted in cyan. G, Guanine-base binding motif, PM – phosphate/magnesium binding motif and secondary structure units (α-helices, β- sheets and λ – loops) are represented in this image.

(B) Multiple sequence alignment of RAB8A, RAB8B and RAB13 with red boxes highlighting all conserved motifs featured in (A). The green bar represents the loop region λ7 which is also a sub-family specific motif called RabSF3. Ser111 phosphorylation site is present in loop λ7 that lies in between RabF5 (Rab-specfic region) and G2 (Guanine-base binding motif). Lilac colour code indicates the degree of conservation, where darker colour represents higher conservation.

The discovery that PINK1 may regulate Rab GTPases and that this may be disrupted in patients harbouring PINK1 mutations suggests that the regulation and downstream function of Rabs may mediate a major mechanism in Parkinson's disease. Interestingly, work from Susan Lindquist's group has demonstrated that RAB8A as well as RAB1 and RAB3A could rescue neurotoxicity mediated by another PD-linked gene, α-synuclein (Gitler et al, 2008). Over-expression of α-synuclein is believed to disrupt vesicular trafficking between Endoplasmic reticulum (ER) to Golgi network, which is rescued by over-expression of these Rabs and this was observed in yeast, C. elegans and primary rat midbrain cultures over-expressing α-synuclein (Gitler et al, 2008). My discovery that PINK1 can phosphorylate RAB8A at Ser111 suggests that the Rab GTPase signaling pathway may lie at the nexus of PINK1 and α-synuclein mediated neurodegeneration in Parkinson's disease.

RAB8a has also been reported to have a critical role in synaptic function, where it is specifically involved in trafficking of AMPA-type glutamatergic receptors (AMPARs) to the surface of post-synaptic membrane during long-term potentiation (LTP) (Gerges et al, 2004). This study also reported that RAB8 is required only for synaptic delivery of AMPARs to the dendritic membrane, but not for trafficking of AMPAR from the shaft into the dendritic spine or for delivery into the synaptic membrane (Gerges et al, 2004). The effector proteins mediating these functions is unknown and it would be exciting to identify these and determine whether their interaction with Rab8a was dependent on PINK1

mediated Ser111 phosphorylation. This would be a very important study in light of a report that suggests specific impairment in corticostriatal long-term potentiation (LTP) and long-term depression (LTD) in PINK1 KO mice (Kitada et al, 2007).

Previous work in mammalian cells has found that RAB8a vesicles re-distribute to the cell periphery and this is linked to Protein Kinase C (PKC)-induced polarized transport of Rab8a vesicles (Hattula et al, 2002). Another group has investigated phosphorylation of Rab8a using recombinant *Bombyx mori* (silkmoth) RAB8A expressed in *E.coli* by PKC, and reported three sites namely Ser17, Ser111 and Ser132 to be phosphorylated by PKC (Uno et al, 2009; Uno et al, 2007). However, a major concern of this study was that the authors employed PKC isolated from rat brain and the *in vitro* kinase assay was performed without employing any negative control for enzyme activity. Therefore it remains unclear whether these Rab8a sites including Ser111 are regulated by PKC or a co-purifying contaminant kinase.

In my study I have provided strong evidence that Ser111 phosphorylation of members of a Rab GTPase sub-family is regulated by PINK1 activity and in future it would crucial to establish whether the phosphorylation is direct or indirect and determine the the functional relevance of this phosphorylation event in Rab signaling.

Additional putative substrates of PINK1: implications for understanding PINK1 signaling

Apart from the Rab GTPase sub-family members, six other proteins were identified as putative substrates of PINK1 in the phospho-proteomic screen. Much of this data is preliminary and needs to be validated as part of future work. A phosphosite on RL40 was found to be significantly up regulated in all four experimental replicates. RL40 encodes a ubiquitin fusion protein, with a ubiquitin moiety at the N-terminus and a ribosomal protein L-40 at the C-terminus (Wiborg et al, 1985). The human genome encodes for four genes that produce ubiquitin; UBB and UBC, which encode for poly-ubiquitin chains and RL40 (UBA52) and RPS27A, either of which consists of a single ubiquitin moiety fused to an unrelated ribosomal protein (Finley et al, 1989; Kimura & Tanaka, 2010; Redman & Rechsteiner, 1989).

Interestingly, the PINK1-mediated phosphorylation site on RL40 occurs at Serine 65 present in the Ubiquitin moiety, which is extremely exciting as I previously found that PINK1 phosphorylates Parkin at Serine 65 of its Ubl domain (see Chapter 3). A multiple sequence alignment of Polyubiquitin-B (UBB), Polyubiquitin-C (UBC), RL40, RPS27A and the Ubl domain (Ubiquitin-like domain) of Parkin revealed that the Serine 65 residue is highly conserved across all these proteins (Fig. 5.18). Although phospho-proteomic analysis predicts this to occur on RL40, the ubiquitin moiety is 100% identical in all four ubiquitin encoding genes and hence we cannot exclude the possibility that this phosphorylation may happen in either ubiquitin itself or in any of the ubiquitin

fusion proteins (RL40 or RPS27A). It would be interesting to express each of these 4 ubiquitin proteins and determine the stoichiometry of phosphorylation compared to the Ubl domain of Parkin. Furthermore, since the Serine 65 residue is in close proximity to Lysine 63 (K63), an important residue for formation of polyubiquitin chains, it would be crucial to investigate the effect of phosphorylation on chain formation.

Figure 5.18 Alignment of RL40 with Ubiquitin, RPS27A and Ubl domain of Parkin

Multiple sequence alignment was performed for Ubl domain of human Parkin, full length human RL40, full length human RPS27A, ubiquitin moiety of human UBB and UBC. The conserved PINK1-mediated Serine 65 phosphorylation site is indicated by a red asterisk. The blue colour code indicates the degree of conservation, where darker colour represents higher conservation.

Another putative PINK1 substrate identified in my screen is the atypical Rho GTPase Miro2, which I previously identified to be a strong PINK1 interactor (described in Chapter 4). Studies by two independent groups report that PINK1 plays a role in mitochondrial trafficking by regulating levels of a paralog of Miro2, Miro1 (Liu et al, 2012; Wang et al, 2011). One of these groups reported

that immunoprecipitated human PINK1 can phosphorylate recombinant Drosophila Miro at Ser156 and this event is crucial for proteasomal degradation of Miro in a PINK1-parkin dependent manner (Wang et al, 2011). However, this was not confirmed by another study (Liu et al, 2012) and also by my own findings in which I found that insect PINK1 could not directly phosphorylate Miro1 or Miro2 (Chapter 4). The phosphorylation site on Miro2 (Ser 538) found in my screen is highly conserved in Miro1. Whilst Miro2 may not be a direct substrate for PINK1, in future it would be important to validate whether phosphorylation of Miro2 at Ser538 is still regulated by PINK1 in human cells *in* vivo and if so to elucidate the kinase responsible for this since by default this kinase will be regulated by PINK1.

In conclusion, the major discovery I have made is that the phosphorylation status of members of a Rab GTPase sub-family (RAB8A, RAB8B and RAB13) is regulated by PINK1 under conditions of mitochondrial depolarization. The Ser111 residue phosphorylated by PINK1 is common to all three Rabs and occurs in a loop region that is crucial for binding of effector proteins. An important question to address in the future would be to explore the effect of this phosphorylation on Rab GTPase activity and effector binding.

Appendix

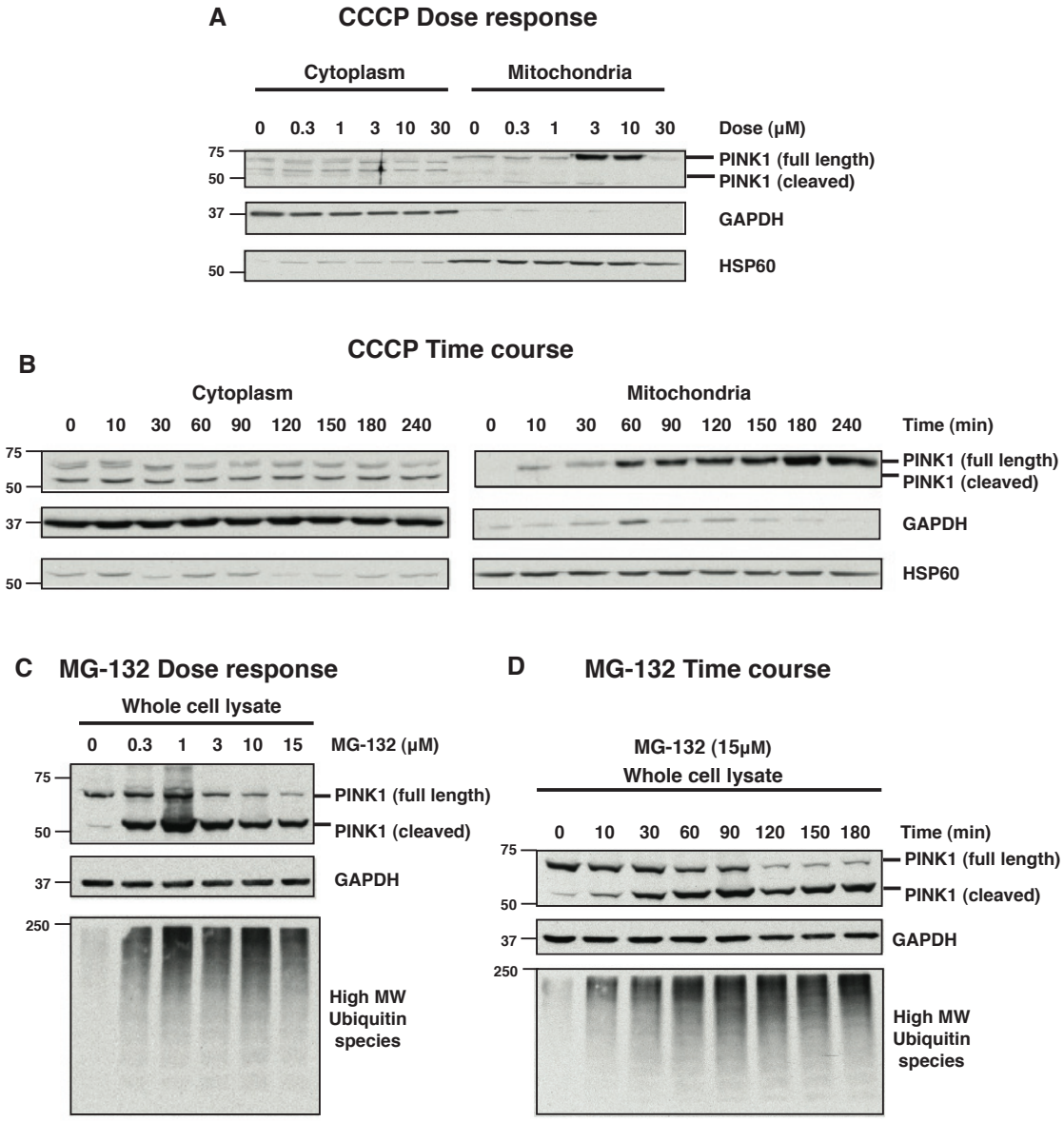

Figure 6.1 Dose response and time-course of CCCP and MG132 treatment

(A and C) Dose response : Flp In TRex HEK293 cells stably expressing PINK1 wild-type-Flag were induced for protein expression and stimulated with the indicated amounts of CCCP or MG-132 for 3 hours. Cells were fractioned into cytosolic and mitochondrial fractions for CCCP treated samples and into whole cell lysates for MG-132 treatment and blotted for PINK1 using anti-PINK1 (Novus) antibody. GAPDH and HSP60 serve as cytosolic and mitochondrial markers respectively and high molecular weight ubiquitin species served as a control for proteasomal inhibition.

(B and D) Time course : Flp In TRex HEK293 cells stably expressing PINK1 wild-type-Flag were induced for protein expression and stimulated with 10 μM CCCP or 15 μM MG-132 for the indicated time-points. Cells were fractioned into cytosolic and mitochondrial fractions for CCCP treated samples and into whole cell lysates for MG-132 treatment and blotted for PINK1 using anti-PINK1 (Novus) antibody. GAPDH and HSP60 serve as cytosolic and mitochondrial markers respectively and high molecular weight ubiquitin species served as a control for proteasomal inhibition.

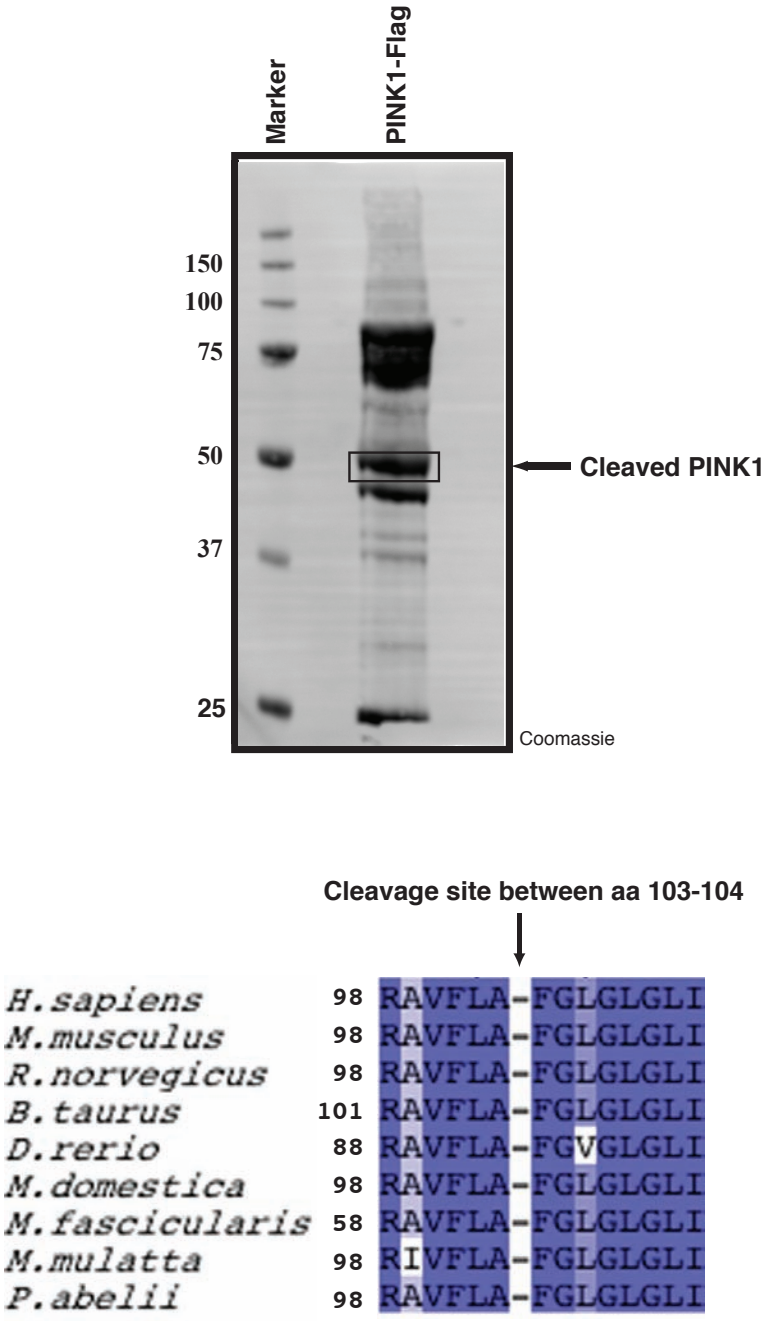

Figure 6.2 Mapping of PINK1 cleavage site by N-terminal Edman sequencing

HEK293 cells were transiently transfected with wild-type PINK1-FLAG and 100mg of whole cell lysate immunoprecipitated with anti-FLAG agarose. After electrophoresis, samples were transferred to Immobilon PVDF membrane and stained with Coomassie Blue. Coomassie stained PVDF membrane showing band corresponding to the cleaved form of PINK1 that was excised and subjected to Edman degradation and analysis. The amino acid sequence obtained in the gel band started with FGLGLG (residues 104 – 109) **(upper panel).** Representative of 3 independent experiments. Sequence alignment of residues around Phe^{104} in human PINK1 showing high degree of conservation amongst higher organisms **(lower panel)**. Cleavage site indicated by an arrow.

A

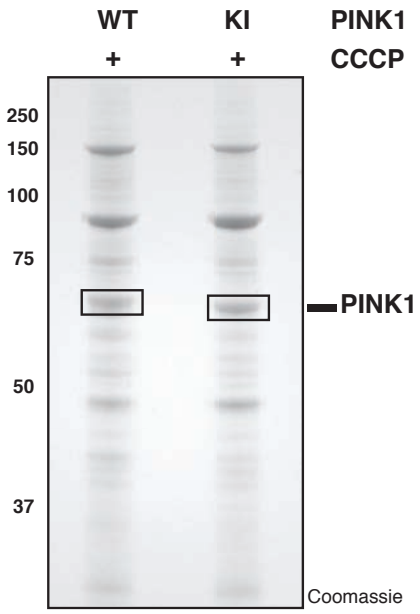

B

Observed Mass (m/z)	Theoretical Mass (m)	Sequence	Phosphorylated Residue	No. of experiments detected
789.38	1576.76	VALAGEYGAV**p**T**T**YRK	257	2

Figure 6.3 Mass spectrometry confirmation that phosphorylation of PINK1 Thr257 is an autophosphorylation site.

Flp-In T-Rex HEK 293 cell line stably expressing wild-type or kinase-inactive PINK1-FLAG were treated 10μM of CCCP for 3hrs.

(A) Recombinant PINK1 was immunoprecipitated from 10mg of mitochondrial extract for each condition using anti-FLAG-agarose, subjected to 4-12% gradient SDS-PAGE, and stained with colloidal Coomassie blue.

(B) The Coomassie-stained bands migrating with the expected molecular mass of PINK1-FLAG were excised from the gel, digested with trypsin, and subjected to LC-MS-MS on an LTQ-Orbitrap mass spectrometer.

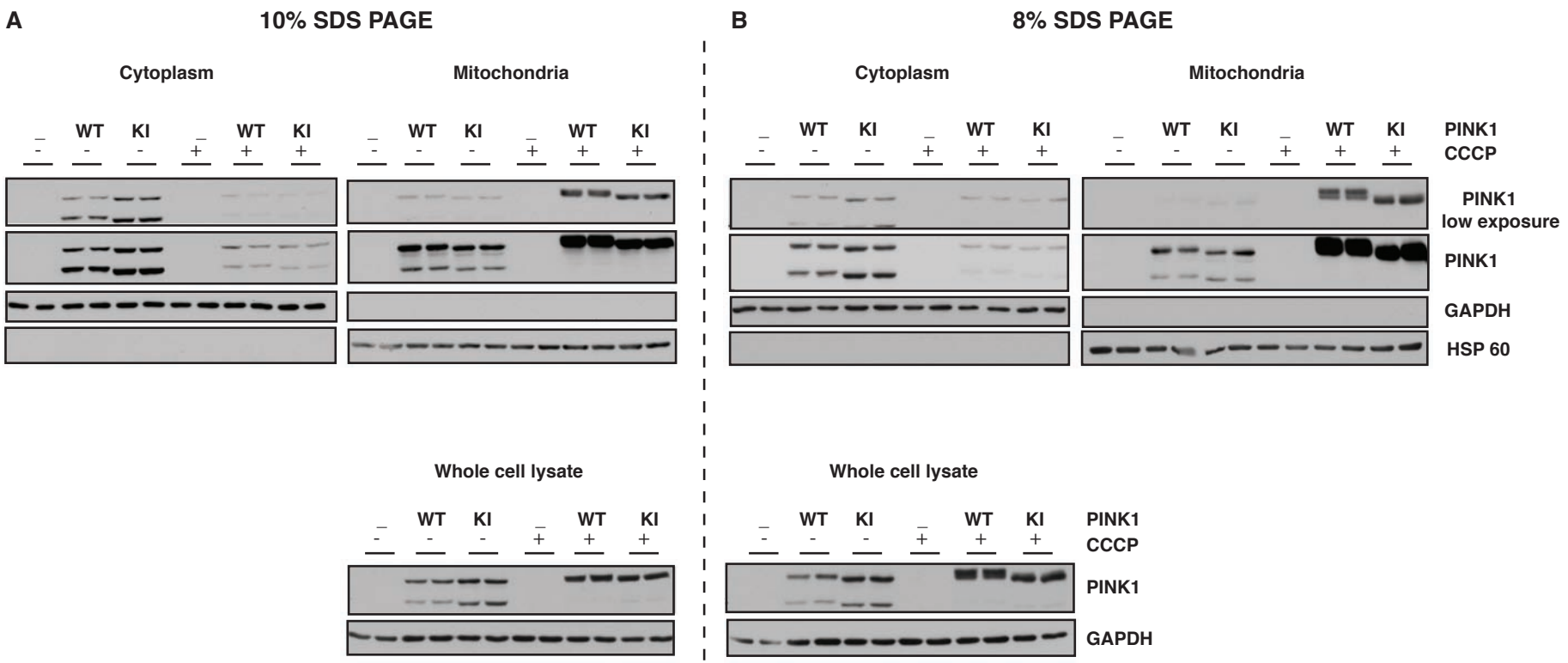

Figure 6.4 CCCP induced band-shift in wild-type PINK1 is resolved better by low percentage (8%) SDS-PAGE

Flp-In T-Rex HEK293 cell lines stably expressing FLAG alone, wild-type or kinase-inactive PINK1-FLAG were induced for with doxycycline for protein expression. Cells were treated with 10μM CCCP for 3h and lysates subjected to sub-cellular fractionation. 25μg of cytoplasmic or mitochondrial lysate were resolved by **(A)** 10 % SDS-PAGE or **(B)** 8% SDS-PAGE. Relative purity of the fractions was confirmed using cytoplasmic and mitochondrial markers, namely GAPDH and HSP60, respectively. Whole cell lysates were also made from the same lysates and 25 μg was resolved by 10% and 8% SDS-PAGE.

Figure 6.5 Multiple sequence alignment of all annotated orthologues of mammalian and insect PINK1

The blue colour code indicates the degree of conservation, where darker colour represents higher conservation. Green bars represent the three insertions in PINK1. Thr 257 auto-phosphorylation site is highlighted by a red box. A red asterisk marks the start and end of the kinase domain.

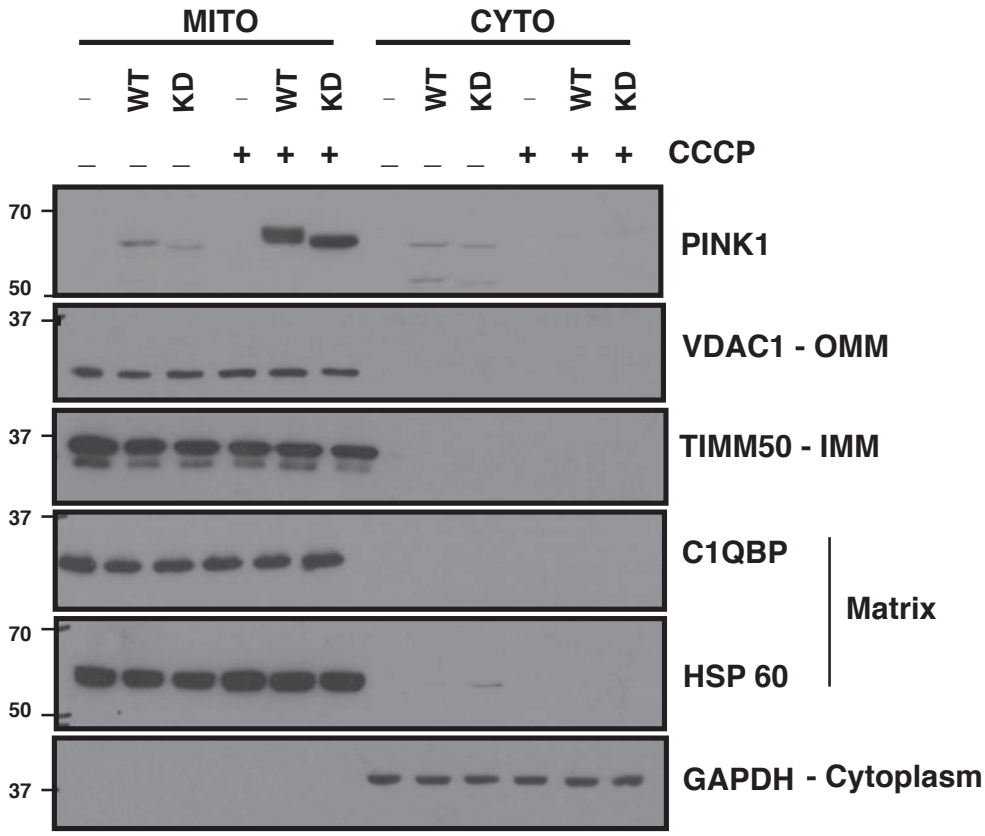

Figure 6.6 Quality control of mitochondrial fractionation

Flp-In T-Rex HEK293 cell lines stably expressing FLAG alone, wild-type or kinase-inactive PINK1-FLAG were induced for with doxycycline for protein expression. Cells were treated with 10μM CCCP for 3h and lysates subjected to sub-cellular fractionation. 25μg of cytoplasmic or mitochondrial lysate were resolved by SDS-PAGE and blotted for the different mitochondrial markers. GAPDH was used as a cytoplasmic marker. *Abbreviations: OMM- Outer Mitochondrial Membrane, IMM – Inner Mitochondrial Membrane.*

n=1

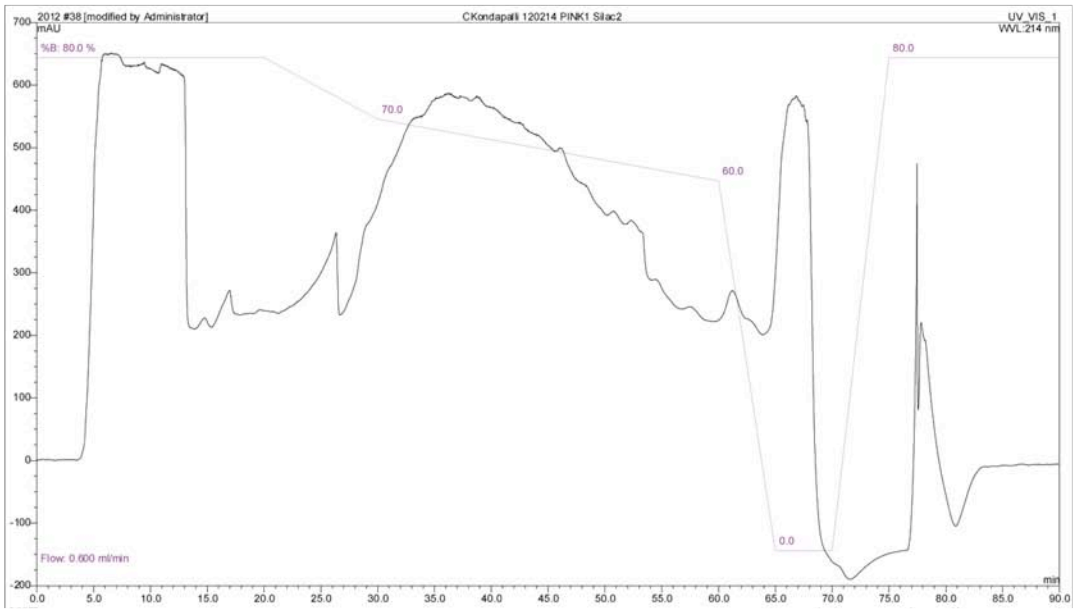

Fractions

1 ----------15

n=2

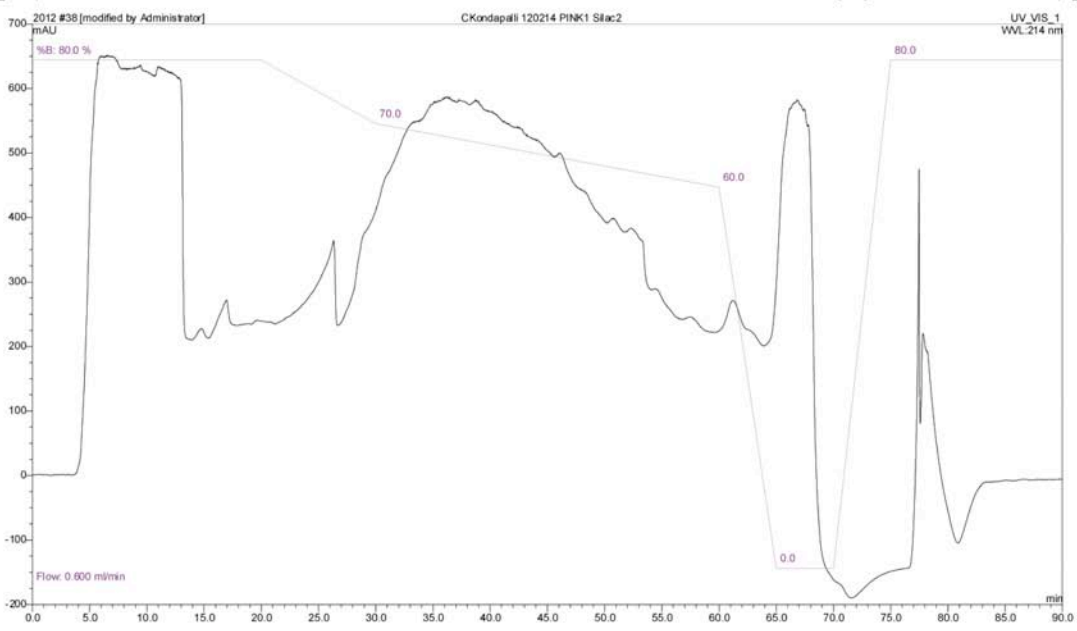

Fractions

1 ----------15

n=3

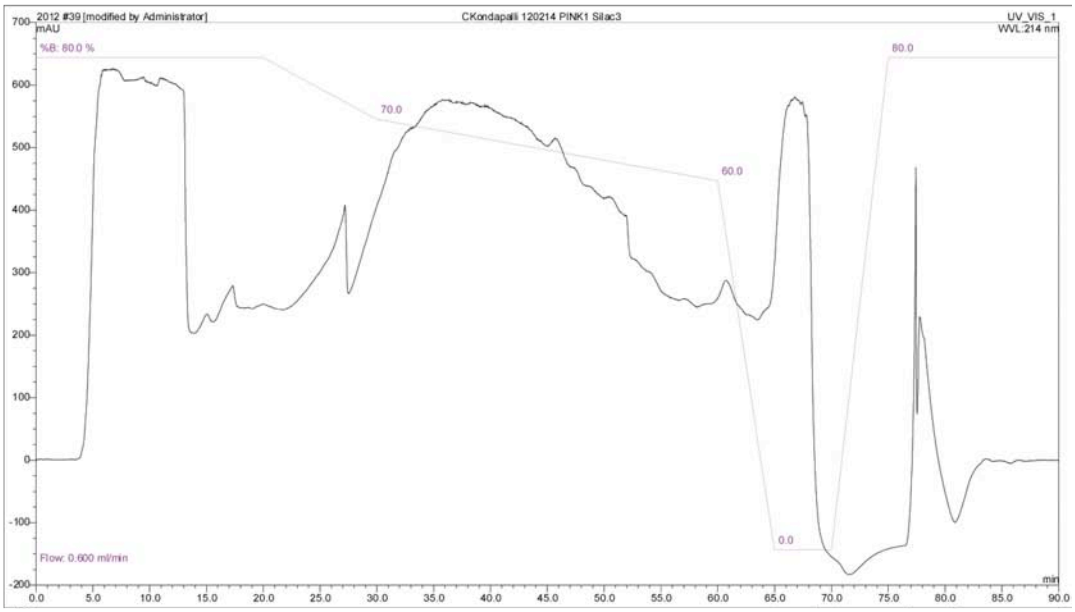

Fractions

1 ----------15

n=4

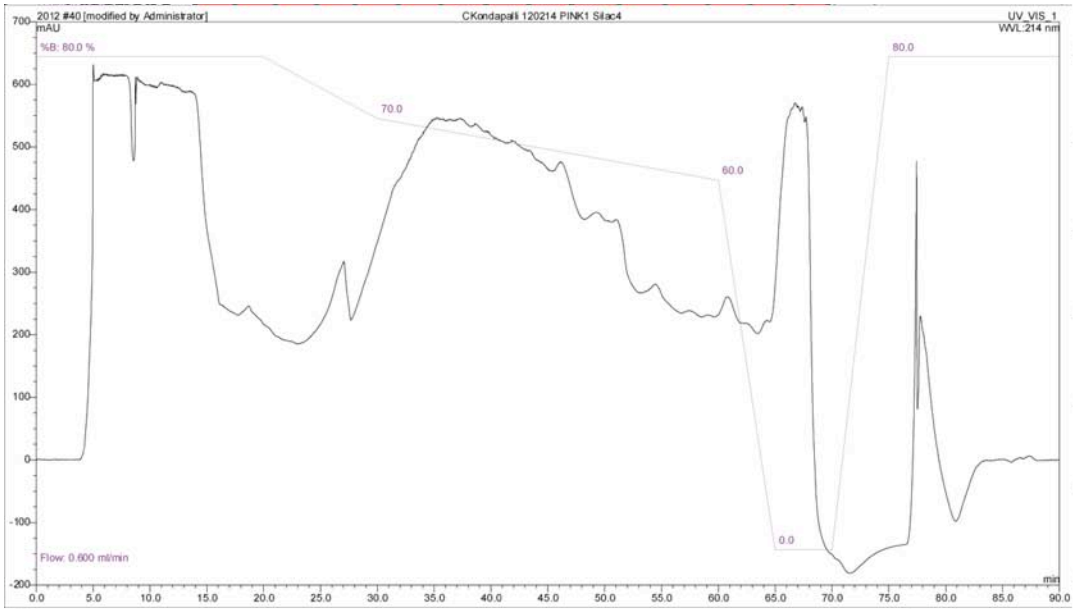

Fractions

1 ----------15

Figure 6.7 HILIC (Hydrophilic Interaction Liquid Chromatography) chromatogram

HILIC Chromatograms for all four experimental replicates employed. The chromatogram represents absorbance of the peptides eluted (in mAU) on the y-axis and retention time on the x-axis. Fractions enriched with phospho-peptides (1-15) were collected for TiO_2 enrichment.

Bibliography

Abeliovich A, Flint Beal M (2006) Parkinsonism genes: culprits and clues. *Journal of neurochemistry* **99:** 1062-1072

Abou-Sleiman PM, Muqit MM, Wood NW (2006) Expanding insights of mitochondrial dysfunction in Parkinson's disease. *Nature reviews Neuroscience* **7:** 207-219

Aebersold R, Mann M (2003) Mass spectrometry-based proteomics. *Nature* **422:** 198-207

Anderson PC, Daggett V (2008) Molecular basis for the structural instability of human DJ-1 induced by the L166P mutation associated with Parkinson's disease. *Biochemistry* **47:** 9380-9393

Appel-Cresswell S, Vilarino-Guell C, Encarnacion M, Sherman H, Yu I, Shah B, Weir D, Thompson C, Szu-Tu C, Trinh J, Aasly JO, Rajput A, Rajput AH, Jon Stoessl A, Farrer MJ (2013) Alpha-synuclein p.H50Q, a novel pathogenic mutation for Parkinson's disease. *Movement disorders : official journal of the Movement Disorder Society* **28:** 811-813

Avraham E, Rott R, Liani E, Szargel R, Engelender S (2007) Phosphorylation of Parkin by the cyclin-dependent kinase 5 at the linker region modulates its ubiquitin-ligase activity and aggregation. *The Journal of biological chemistry* **282:** 12842-12850

Baines CP, Kaiser RA, Sheiko T, Craigen WJ, Molkentin JD (2007) Voltage-dependent anion channels are dispensable for mitochondrial-dependent cell death. *Nature cell biology* **9:** 550-555

Bertoncini CW, Jung YS, Fernandez CO, Hoyer W, Griesinger C, Jovin TM, Zweckstetter M (2005) Release of long-range tertiary interactions potentiates aggregation of natively unstructured alpha-synuclein. *Proceedings of the National Academy of Sciences of the United States of America* **102:** 1430-1435

Billia F, Hauck L, Konecny F, Rao V, Shen J, Mak TW (2011) PTEN-inducible kinase 1 (PINK1)/Park6 is indispensable for normal heart function. *Proceedings of the National Academy of Sciences of the United States of America* **108:** 9572-9577

Blackinton JG, Anvret A, Beilina A, Olson L, Cookson MR, Galter D (2007) Expression of PINK1 mRNA in human and rodent brain and in Parkinson's disease. *Brain research* **1184:** 10-16

Bock JB, Matern HT, Peden AA, Scheller RH (2001) A genomic perspective on membrane compartment organization. *Nature* **409:** 839-841

Bohnert M, Wenz LS, Zerbes RM, Horvath SE, Stroud DA, von der Malsburg K, Muller JM, Oeljeklaus S, Perschil I, Warscheid B, Chacinska A, Veenhuis M, van der Klei IJ, Daum G, Wiedemann N, Becker T, Pfanner N, van der Laan M (2012) Role of

mitochondrial inner membrane organizing system in protein biogenesis of the mitochondrial outer membrane. *Molecular biology of the cell* **23:** 3948-3956

Bradford MM (1976) A rapid and sensitive method for the quantitation of microgram quantities of protein utilizing the principle of protein-dye binding. *Analytical biochemistry* **72:** 248-254

Burnett G, Kennedy EP (1954) The enzymatic phosphorylation of proteins. *The Journal of biological chemistry* **211:** 969-980

Campbell DG, Morrice NA (2002) Identification of protein phosphorylation sites by a combination of mass spectrometry and solid phase Edman sequencing. *Journal of biomolecular techniques : JBT* **13:** 119-130

Capdeville R, Buchdunger E, Zimmermann J, Matter A (2002) Glivec (STI571, imatinib), a rationally developed, targeted anticancer drug. *Nature reviews Drug discovery* **1:** 493-502

Chan DC (2006) Mitochondrial fusion and fission in mammals. *Annual review of cell and developmental biology* **22:** 79-99

Chan NC, Salazar AM, Pham AH, Sweredoski MJ, Kolawa NJ, Graham RL, Hess S, Chan DC (2011) Broad activation of the ubiquitin-proteasome system by Parkin is critical for mitophagy. *Human molecular genetics* **20:** 1726-1737

Chaugule VK, Burchell L, Barber KR, Sidhu A, Leslie SJ, Shaw GS, Walden H (2011) Autoregulation of Parkin activity through its ubiquitin-like domain. *The EMBO journal* **30:** 2853-2867

Chen WG, White FM (2004) Proteomic analysis of cellular signaling. *Expert review of proteomics* **1:** 343-354

Clark IE, Dodson MW, Jiang C, Cao JH, Huh JR, Seol JH, Yoo SJ, Hay BA, Guo M (2006) Drosophila pink1 is required for mitochondrial function and interacts genetically with parkin. *Nature* **441:** 1162-1166

Cohen P (2002a) The origins of protein phosphorylation. *Nature cell biology* **4:** E127-130

Cohen P (2002b) Protein kinases--the major drug targets of the twenty-first century? *Nature reviews Drug discovery* **1:** 309-315

Cohen P, Knebel A (2006) KESTREL: a powerful method for identifying the physiological substrates of protein kinases. *The Biochemical journal* **393:** 1-6

Conway KA, Lee SJ, Rochet JC, Ding TT, Williamson RE, Lansbury PT, Jr. (2000) Acceleration of oligomerization, not fibrillization, is a shared property of both alpha-synuclein mutations linked to early-onset Parkinson's disease: implications

for pathogenesis and therapy. *Proceedings of the National Academy of Sciences of the United States of America* **97:** 571-576

Corti O, Lesage S, Brice A (2011) What genetics tells us about the causes and mechanisms of Parkinson's disease. *Physiological reviews* **91:** 1161-1218

De Bondt HL, Rosenblatt J, Jancarik J, Jones HD, Morgan DO, Kim SH (1993) Crystal structure of cyclin-dependent kinase 2. *Nature* **363:** 595-602

Deas E, Plun-Favreau H, Gandhi S, Desmond H, Kjaer S, Loh SH, Renton AE, Harvey RJ, Whitworth AJ, Martins LM, Abramov AY, Wood NW (2011) PINK1 cleavage at position A103 by the mitochondrial protease PARL. *Human molecular genetics* **20:** 867-879

Deas E, Plun-Favreau H, Wood NW (2009) PINK1 function in health and disease. *EMBO molecular medicine* **1:** 152-165

Dekker PJ, Ryan MT, Brix J, Muller H, Honlinger A, Pfanner N (1998) Preprotein translocase of the outer mitochondrial membrane: molecular dissection and assembly of the general import pore complex. *Molecular and cellular biology* **18:** 6515-6524

Deng H, Dodson MW, Huang H, Guo M (2008) The Parkinson's disease genes pink1 and parkin promote mitochondrial fission and/or inhibit fusion in Drosophila. *Proceedings of the National Academy of Sciences of the United States of America* **105:** 14503-14508

Deshaies RJ, Joazeiro CA (2009) RING domain E3 ubiquitin ligases. *Annual review of biochemistry* **78:** 399-434

Detmer SA, Chan DC (2007) Functions and dysfunctions of mitochondrial dynamics. *Nature reviews Molecular cell biology* **8:** 870-879

Ehringer H, Hornykiewicz O (1960) [Distribution of noradrenaline and dopamine (3-hydroxytyramine) in the human brain and their behavior in diseases of the extrapyramidal system]. *Klinische Wochenschrift* **38:** 1236-1239

Exner N, Treske B, Paquet D, Holmstrom K, Schiesling C, Gispert S, Carballo-Carbajal I, Berg D, Hoepken HH, Gasser T, Kruger R, Winklhofer KF, Vogel F, Reichert AS, Auburger G, Kahle PJ, Schmid B, Haass C (2007) Loss-of-function of human PINK1 results in mitochondrial pathology and can be rescued by parkin. *The Journal of neuroscience : the official journal of the Society for Neuroscience* **27:** 12413-12418

Farrer MJ (2006) Genetics of Parkinson disease: paradigm shifts and future prospects. *Nature reviews Genetics* **7:** 306-318

Finley D, Bartel B, Varshavsky A (1989) The tails of ubiquitin precursors are ribosomal proteins whose fusion to ubiquitin facilitates ribosome biogenesis. *Nature* **338:** 394-401

Fischer EH, Krebs EG (1955) Conversion of phosphorylase b to phosphorylase a in muscle extracts. *The Journal of biological chemistry* **216:** 121-132

Fransson A, Ruusala A, Aspenstrom P (2003) Atypical Rho GTPases have roles in mitochondrial homeostasis and apoptosis. *The Journal of biological chemistry* **278:** 6495-6502

Fuchs J, Nilsson C, Kachergus J, Munz M, Larsson EM, Schule B, Langston JW, Middleton FA, Ross OA, Hulihan M, Gasser T, Farrer MJ (2007) Phenotypic variation in a large Swedish pedigree due to SNCA duplication and triplication. *Neurology* **68:** 916-922

Gautier CA, Giaime E, Caballero E, Nunez L, Song Z, Chan D, Villalobos C, Shen J (2012) Regulation of mitochondrial permeability transition pore by PINK1. *Molecular neurodegeneration* **7:** 22

Geisler S, Holmstrom KM, Skujat D, Fiesel FC, Rothfuss OC, Kahle PJ, Springer W (2010) PINK1/Parkin-mediated mitophagy is dependent on VDAC1 and p62/SQSTM1. *Nature cell biology* **12:** 119-131

Gerges NZ, Backos DS, Esteban JA (2004) Local control of AMPA receptor trafficking at the postsynaptic terminal by a small GTPase of the Rab family. *The Journal of biological chemistry* **279:** 43870-43878

Gingras AC, Gstaiger M, Raught B, Aebersold R (2007) Analysis of protein complexes using mass spectrometry. *Nature reviews Molecular cell biology* **8:** 645-654

Gitler AD, Bevis BJ, Shorter J, Strathearn KE, Hamamichi S, Su LJ, Caldwell KA, Caldwell GA, Rochet JC, McCaffery JM, Barlowe C, Lindquist S (2008) The Parkinson's disease protein alpha-synuclein disrupts cellular Rab homeostasis. *Proceedings of the National Academy of Sciences of the United States of America* **105:** 145-150

Glater EE, Megeath LJ, Stowers RS, Schwarz TL (2006) Axonal transport of mitochondria requires milton to recruit kinesin heavy chain and is light chain independent. *The Journal of cell biology* **173:** 545-557

Greene AW, Grenier K, Aguileta MA, Muise S, Farazifard R, Haque ME, McBride HM, Park DS, Fon EA (2012) Mitochondrial processing peptidase regulates PINK1 processing, import and Parkin recruitment. *EMBO reports* **13:** 378-385

Grigoriev I, Yu KL, Martinez-Sanchez E, Serra-Marques A, Smal I, Meijering E, Demmers J, Peranen J, Pasterkamp RJ, van der Sluijs P, Hoogenraad CC, Akhmanova

A (2011) Rab6, Rab8, and MICAL3 cooperate in controlling docking and fusion of exocytotic carriers. *Current biology : CB* **21:** 967-974

Guo X, Macleod GT, Wellington A, Hu F, Panchumarthi S, Schoenfield M, Marin L, Charlton MP, Atwood HL, Zinsmaier KE (2005) The GTPase dMiro is required for axonal transport of mitochondria to Drosophila synapses. *Neuron* **47:** 379-393

Halestrap AP (2009) What is the mitochondrial permeability transition pore? *Journal of molecular and cellular cardiology* **46:** 821-831

Hanks SK, Hunter T (1995) Protein kinases 6. The eukaryotic protein kinase superfamily: kinase (catalytic) domain structure and classification. *FASEB journal : official publication of the Federation of American Societies for Experimental Biology* **9:** 576-596

Haque ME, Mount MP, Safarpour F, Abdel-Messih E, Callaghan S, Mazerolle C, Kitada T, Slack RS, Wallace V, Shen J, Anisman H, Park DS (2012) Inactivation of Pink1 gene in vivo sensitizes dopamine-producing neurons to 1-methyl-4-phenyl-1,2,3,6-tetrahydropyridine (MPTP) and can be rescued by autosomal recessive Parkinson disease genes, Parkin or DJ-1. *The Journal of biological chemistry* **287:** 23162-23170

Hastie CJ, McLauchlan HJ, Cohen P (2006) Assay of protein kinases using radiolabeled ATP: a protocol. *Nature protocols* **1:** 968-971

Hattula K, Furuhjelm J, Arffman A, Peranen J (2002) A Rab8-specific GDP/GTP exchange factor is involved in actin remodeling and polarized membrane transport. *Molecular biology of the cell* **13:** 3268-3280

Hauschild A, Grob JJ, Demidov LV, Jouary T, Gutzmer R, Millward M, Rutkowski P, Blank CU, Miller WH, Jr., Kaempgen E, Martin-Algarra S, Karaszewska B, Mauch C, Chiarion-Sileni V, Martin AM, Swann S, Haney P, Mirakhur B, Guckert ME, Goodman V, Chapman PB (2012) Dabrafenib in BRAF-mutated metastatic melanoma: a multicentre, open-label, phase 3 randomised controlled trial. *Lancet* **380:** 358-365

Hirsch EC (2007) Animal models in neurodegenerative diseases. *Journal of neural transmission Supplementum***:** 87-90

Hollenbeck PJ, Saxton WM (2005) The axonal transport of mitochondria. *Journal of cell science* **118:** 5411-5419

Iguchi M, Kujuro Y, Okatsu K, Koyano F, Kosako H, Kimura M, Suzuki N, Uchiyama S, Tanaka K, Matsuda N (2013) Parkin-catalyzed ubiquitin-ester transfer is triggered by PINK1-dependent phosphorylation. *The Journal of biological chemistry* **288:** 22019-22032

Inoue H, Nojima H, Okayama H (1990) High efficiency transformation of Escherichia coli with plasmids. *Gene* **96:** 23-28

Jaleel M, Nichols RJ, Deak M, Campbell DG, Gillardon F, Knebel A, Alessi DR (2007) LRRK2 phosphorylates moesin at threonine-558: characterization of how Parkinson's disease mutants affect kinase activity. *The Biochemical journal* **405:** 307-317

Jin SM, Lazarou M, Wang C, Kane LA, Narendra DP, Youle RJ (2010) Mitochondrial membrane potential regulates PINK1 import and proteolytic destabilization by PARL. *The Journal of cell biology* **191:** 933-942

John GB, Shang Y, Li L, Renken C, Mannella CA, Selker JM, Rangell L, Bennett MJ, Zha J (2005) The mitochondrial inner membrane protein mitofilin controls cristae morphology. *Molecular biology of the cell* **16:** 1543-1554

Joo JH, Dorsey FC, Joshi A, Hennessy-Walters KM, Rose KL, McCastlain K, Zhang J, Iyengar R, Jung CH, Suen DF, Steeves MA, Yang CY, Prater SM, Kim DH, Thompson CB, Youle RJ, Ney PA, Cleveland JL, Kundu M (2011) Hsp90-Cdc37 chaperone complex regulates Ulk1- and Atg13-mediated mitophagy. *Molecular cell* **43:** 572-585

Kiely AP, Asi YT, Kara E, Limousin P, Ling H, Lewis P, Proukakis C, Quinn N, Lees AJ, Hardy J, Revesz T, Houlden H, Holton JL (2013) alpha-Synucleinopathy associated with G51D SNCA mutation: a link between Parkinson's disease and multiple system atrophy? *Acta neuropathologica* **125:** 753-769

Kim Y, Park J, Kim S, Song S, Kwon SK, Lee SH, Kitada T, Kim JM, Chung J (2008) PINK1 controls mitochondrial localization of Parkin through direct phosphorylation. *Biochemical and biophysical research communications* **377:** 975-980

Kimura Y, Tanaka K (2010) Regulatory mechanisms involved in the control of ubiquitin homeostasis. *Journal of biochemistry* **147:** 793-798

Kitada T, Asakawa S, Hattori N, Matsumine H, Yamamura Y, Minoshima S, Yokochi M, Mizuno Y, Shimizu N (1998) Mutations in the parkin gene cause autosomal recessive juvenile parkinsonism. *Nature* **392:** 605-608

Kitada T, Pisani A, Porter DR, Yamaguchi H, Tscherter A, Martella G, Bonsi P, Zhang C, Pothos EN, Shen J (2007) Impaired dopamine release and synaptic plasticity in the striatum of PINK1-deficient mice. *Proceedings of the National Academy of Sciences of the United States of America* **104:** 11441-11446

Klein C, Schlossmacher MG (2006) The genetics of Parkinson disease: Implications for neurological care. *Nature clinical practice Neurology* **2:** 136-146

Klein C, Westenberger A (2012) Genetics of Parkinson's disease. *Cold Spring Harbor perspectives in medicine* **2:** a008888

Knighton DR, Zheng JH, Ten Eyck LF, Ashford VA, Xuong NH, Taylor SS, Sowadski JM (1991) Crystal structure of the catalytic subunit of cyclic adenosine monophosphate-dependent protein kinase. *Science* **253:** 407-414

Kokoszka JE, Waymire KG, Levy SE, Sligh JE, Cai J, Jones DP, MacGregor GR, Wallace DC (2004) The ADP/ATP translocator is not essential for the mitochondrial permeability transition pore. *Nature* **427:** 461-465

Koyano F, Okatsu K, Ishigaki S, Fujioka Y, Kimura M, Sobue G, Tanaka K, Matsuda N (2013) The principal PINK1 and Parkin cellular events triggered in response to dissipation of mitochondrial membrane potential occur in primary neurons. *Genes to cells : devoted to molecular & cellular mechanisms* **18:** 672-681

Krebs EG, Fischer EH (1956) The phosphorylase b to a converting enzyme of rabbit skeletal muscle. *Biochimica et biophysica acta* **20:** 150-157

Lahiry P, Torkamani A, Schork NJ, Hegele RA (2010) Kinase mutations in human disease: interpreting genotype-phenotype relationships. *Nature reviews Genetics* **11:** 60-74

Langston JW, Ballard P, Tetrud JW, Irwin I (1983) Chronic Parkinsonism in humans due to a product of meperidine-analog synthesis. *Science* **219:** 979-980

Lazarou M, Jin SM, Kane LA, Youle RJ (2012) Role of PINK1 binding to the TOM complex and alternate intracellular membranes in recruitment and activation of the E3 ligase Parkin. *Developmental cell* **22:** 320-333

Lazarou M, Narendra DP, Jin SM, Tekle E, Banerjee S, Youle RJ (2013) PINK1 drives Parkin self-association and HECT-like E3 activity upstream of mitochondrial binding. *The Journal of cell biology* **200:** 163-172

Lehninger AL, Nelson DL, Cox MM (2005) *Lehninger principles of biochemistry*, 4th edn. New York: W.H. Freeman.

Lewy FH (1912) Paralysis agitans. *Pathologische Anatomie Handbuch der Neurologie Lewandowsky M (ed) Berlin, Germany, Springer-Verlag***:** 920-933

Li Z, Okamoto K, Hayashi Y, Sheng M (2004) The importance of dendritic mitochondria in the morphogenesis and plasticity of spines and synapses. *Cell* **119:** 873-887

Ligon LA, Steward O (2000) Role of microtubules and actin filaments in the movement of mitochondria in the axons and dendrites of cultured hippocampal neurons. *The Journal of comparative neurology* **427:** 351-361

Liu S, Sawada T, Lee S, Yu W, Silverio G, Alapatt P, Millan I, Shen A, Saxton W, Kanao T, Takahashi R, Hattori N, Imai Y, Lu B (2012) Parkinson's disease-associated

kinase PINK1 regulates Miro protein level and axonal transport of mitochondria. *PLoS genetics* **8:** e1002537

Lutz AK, Exner N, Fett ME, Schlehe JS, Kloos K, Lammermann K, Brunner B, Kurz-Drexler A, Vogel F, Reichert AS, Bouman L, Vogt-Weisenhorn D, Wurst W, Tatzelt J, Haass C, Winklhofer KF (2009) Loss of parkin or PINK1 function increases Drp1-dependent mitochondrial fragmentation. *The Journal of biological chemistry* **284:** 22938-22951

MacLeod D, Dowman J, Hammond R, Leete T, Inoue K, Abeliovich A (2006) The familial Parkinsonism gene LRRK2 regulates neurite process morphology. *Neuron* **52:** 587-593

Mann M (2006) Functional and quantitative proteomics using SILAC. *Nature reviews Molecular cell biology* **7:** 952-958

Manning G, Whyte DB, Martinez R, Hunter T, Sudarsanam S (2002) The protein kinase complement of the human genome. *Science* **298:** 1912-1934

Manyam BV (1990) Paralysis-Agitans and Levodopa in Ayurveda - Ancient Indian Medical Treatise. *Movement Disord* **5:** 47-48

Marzesco AM, Dunia I, Pandjaitan R, Recouvreur M, Dauzonne D, Benedetti EL, Louvard D, Zahraoui A (2002) The small GTPase Rab13 regulates assembly of functional tight junctions in epithelial cells. *Molecular biology of the cell* **13:** 1819-1831

Matsuda N, Sato S, Shiba K, Okatsu K, Saisho K, Gautier CA, Sou YS, Saiki S, Kawajiri S, Sato F, Kimura M, Komatsu M, Hattori N, Tanaka K (2010) PINK1 stabilized by mitochondrial depolarization recruits Parkin to damaged mitochondria and activates latent Parkin for mitophagy. *The Journal of cell biology* **189:** 211-221

McGee AM, Douglas DL, Liang Y, Hyder SM, Baines CP (2011) The mitochondrial protein C1qbp promotes cell proliferation, migration and resistance to cell death. *Cell cycle* **10:** 4119-4127

Meissner C, Lorenz H, Weihofen A, Selkoe DJ, Lemberg MK (2011) The mitochondrial intramembrane protease PARL cleaves human Pink1 to regulate Pink1 trafficking. *Journal of neurochemistry* **117:** 856-867

Miller KE, Sheetz MP (2004) Axonal mitochondrial transport and potential are correlated. *Journal of cell science* **117:** 2791-2804

Miller SG, Patton BL, Kennedy MB (1988) Sequences of autophosphorylation sites in neuronal type II CaM kinase that control Ca2(+)-independent activity. *Neuron* **1:** 593-604

Mokranjac D, Paschen SA, Kozany C, Prokisch H, Hoppins SC, Nargang FE, Neupert W, Hell K (2003) Tim50, a novel component of the TIM23 preprotein translocase of mitochondria. *The EMBO journal* **22:** 816-825

Mokranjac D, Sichting M, Popov-Celeketic D, Mapa K, Gevorkyan-Airapetov L, Zohary K, Hell K, Azem A, Neupert W (2009) Role of Tim50 in the transfer of precursor proteins from the outer to the inner membrane of mitochondria. *Molecular biology of the cell* **20:** 1400-1407

Moore I, Schell J, Palme K (1995) Subclass-specific sequence motifs identified in Rab GTPases. *Trends in biochemical sciences* **20:** 10-12

Morais VA, Verstreken P, Roethig A, Smet J, Snellinx A, Vanbrabant M, Haddad D, Frezza C, Mandemakers W, Vogt-Weisenhorn D, Van Coster R, Wurst W, Scorrano L, De Strooper B (2009) Parkinson's disease mutations in PINK1 result in decreased Complex I activity and deficient synaptic function. *EMBO molecular medicine* **1:** 99-111

Morris RL, Hollenbeck PJ (1995) Axonal transport of mitochondria along microtubules and F-actin in living vertebrate neurons. *The Journal of cell biology* **131:** 1315-1326

Mumby M, Brekken D (2005) Phosphoproteomics: new insights into cellular signaling. *Genome biology* **6:** 230

Munoz IM, Hain K, Declais AC, Gardiner M, Toh GW, Sanchez-Pulido L, Heuckmann JM, Toth R, Macartney T, Eppink B, Kanaar R, Ponting CP, Lilley DM, Rouse J (2009) Coordination of structure-specific nucleases by human SLX4/BTBD12 is required for DNA repair. *Molecular cell* **35:** 116-127

Muqit MM, Abou-Sleiman PM, Saurin AT, Harvey K, Gandhi S, Deas E, Eaton S, Payne Smith MD, Venner K, Matilla A, Healy DG, Gilks WP, Lees AJ, Holton J, Revesz T, Parker PJ, Harvey RJ, Wood NW, Latchman DS (2006) Altered cleavage and localization of PINK1 to aggresomes in the presence of proteasomal stress. *Journal of neurochemistry* **98:** 156-169

Narendra D, Tanaka A, Suen DF, Youle RJ (2008) Parkin is recruited selectively to impaired mitochondria and promotes their autophagy. *The Journal of cell biology* **183:** 795-803

Narendra DP, Jin SM, Tanaka A, Suen DF, Gautier CA, Shen J, Cookson MR, Youle RJ (2010) PINK1 is selectively stabilized on impaired mitochondria to activate Parkin. *PLoS biology* **8:** e1000298

Nicklas WJ, Vyas I, Heikkila RE (1985) Inhibition of NADH-linked oxidation in brain mitochondria by 1-methyl-4-phenyl-pyridine, a metabolite of the neurotoxin, 1-methyl-4-phenyl-1,2,5,6-tetrahydropyridine. *Life sciences* **36:** 2503-2508

Nyholm D (2006) Pharmacokinetic optimisation in the treatment of Parkinson's disease : an update. *Clinical pharmacokinetics* **45:** 109-136

Okamoto K, Shaw JM (2005) Mitochondrial morphology and dynamics in yeast and multicellular eukaryotes. *Annual review of genetics* **39:** 503-536

Okatsu K, Oka T, Iguchi M, Imamura K, Kosako H, Tani N, Kimura M, Go E, Koyano F, Funayama M, Shiba-Fukushima K, Sato S, Shimizu H, Fukunaga Y, Taniguchi H, Komatsu M, Hattori N, Mihara K, Tanaka K, Matsuda N (2012) PINK1 autophosphorylation upon membrane potential dissipation is essential for Parkin recruitment to damaged mitochondria. *Nature communications* **3:** 1016

Olsen JV, Blagoev B, Gnad F, Macek B, Kumar C, Mortensen P, Mann M (2006) Global, in vivo, and site-specific phosphorylation dynamics in signaling networks. *Cell* **127:** 635-648

Ong SE, Blagoev B, Kratchmarova I, Kristensen DB, Steen H, Pandey A, Mann M (2002) Stable isotope labeling by amino acids in cell culture, SILAC, as a simple and accurate approach to expression proteomics. *Mol Cell Proteomics* **1:** 376-386

Ong SE, Mann M (2005) Mass spectrometry-based proteomics turns quantitative. *Nature chemical biology* **1:** 252-262

Pankratz N, Pauciulo MW, Elsaesser VE, Marek DK, Halter CA, Wojcieszek J, Rudolph A, Shults CW, Foroud T, Nichols WC, Parkinson Study Group PI (2006) Mutations in DJ-1 are rare in familial Parkinson disease. *Neuroscience letters* **408:** 209-213

Park J, Lee SB, Lee S, Kim Y, Song S, Kim S, Bae E, Kim J, Shong M, Kim JM, Chung J (2006) Mitochondrial dysfunction in Drosophila PINK1 mutants is complemented by parkin. *Nature* **441:** 1157-1161

Parker WD, Jr., Boyson SJ, Parks JK (1989) Abnormalities of the electron transport chain in idiopathic Parkinson's disease. *Annals of neurology* **26:** 719-723

Parkinson J (1817) *An Essay on the Shaking palsy*, London: Whittingham and Rowland for
Sherwood, Neely and Jones.

Petit A, Kawarai T, Paitel E, Sanjo N, Maj M, Scheid M, Chen F, Gu Y, Hasegawa H, Salehi-Rad S, Wang L, Rogaeva E, Fraser P, Robinson B, St George-Hyslop P, Tandon A (2005) Wild-type PINK1 prevents basal and induced neuronal apoptosis, a protective effect abrogated by Parkinson disease-related mutations. *The Journal of biological chemistry* **280:** 34025-34032

Polymeropoulos MH, Lavedan C, Leroy E, Ide SE, Dehejia A, Dutra A, Pike B, Root H, Rubenstein J, Boyer R, Stenroos ES, Chandrasekharappa S, Athanassiadou A, Papapetropoulos T, Johnson WG, Lazzarini AM, Duvoisin RC, Di Iorio G, Golbe LI,

Nussbaum RL (1997) Mutation in the alpha-synuclein gene identified in families with Parkinson's disease. *Science* **276:** 2045-2047

Poole AC, Thomas RE, Andrews LA, McBride HM, Whitworth AJ, Pallanck LJ (2008) The PINK1/Parkin pathway regulates mitochondrial morphology. *Proceedings of the National Academy of Sciences of the United States of America* **105:** 1638-1643

Redman KL, Rechsteiner M (1989) Identification of the long ubiquitin extension as ribosomal protein S27a. *Nature* **338:** 438-440

Riederer P, Wuketich S (1976) Time Course of Nigrostriatal Degeneration in Parkinsons-Disease - Detailed Study of Influential Factors in Human-Brain Amine Analysis. *J Neural Transm* **38:** 277-301

Roskoski R, Jr. (1983) Assays of protein kinase. *Methods in enzymology* **99:** 3-6

Sakata E, Yamaguchi Y, Kurimoto E, Kikuchi J, Yokoyama S, Yamada S, Kawahara H, Yokosawa H, Hattori N, Mizuno Y, Tanaka K, Kato K (2003) Parkin binds the Rpn10 subunit of 26S proteasomes through its ubiquitin-like domain. *EMBO reports* **4:** 301-306

Sarraf SA, Raman M, Guarani-Pereira V, Sowa ME, Huttlin EL, Gygi SP, Harper JW (2013) Landscape of the PARKIN-dependent ubiquitylome in response to mitochondrial depolarization. *Nature* **496:** 372-376

Schapira AH, Cooper JM, Dexter D, Jenner P, Clark JB, Marsden CD (1989) Mitochondrial complex I deficiency in Parkinson's disease. *Lancet* **1:** 1269

Schulz C, Lytovchenko O, Melin J, Chacinska A, Guiard B, Neumann P, Ficner R, Jahn O, Schmidt B, Rehling P (2011) Tim50's presequence receptor domain is essential for signal driven transport across the TIM23 complex. *The Journal of cell biology* **195:** 643-656

Schwartz SL, Cao C, Pylypenko O, Rak A, Wandinger-Ness A (2007) Rab GTPases at a glance. *Journal of cell science* **120:** 3905-3910

Scott L, Lamb J, Smith S, Wheatley DN (2000) Single amino acid (arginine) deprivation: rapid and selective death of cultured transformed and malignant cells. *British journal of cancer* **83:** 800-810

Seibler P, Graziotto J, Jeong H, Simunovic F, Klein C, Krainc D (2011) Mitochondrial Parkin recruitment is impaired in neurons derived from mutant PINK1 induced pluripotent stem cells. *The Journal of neuroscience : the official journal of the Society for Neuroscience* **31:** 5970-5976

Shiba-Fukushima K, Imai Y, Yoshida S, Ishihama Y, Kanao T, Sato S, Hattori N (2012) PINK1-mediated phosphorylation of the Parkin ubiquitin-like domain

primes mitochondrial translocation of Parkin and regulates mitophagy. *Scientific reports* **2:** 1002

Shin JH, Ko HS, Kang H, Lee Y, Lee YI, Pletinkova O, Troconso JC, Dawson VL, Dawson TM (2011) PARIS (ZNF746) repression of PGC-1alpha contributes to neurodegeneration in Parkinson's disease. *Cell* **144:** 689-702

Silvestri L, Caputo V, Bellacchio E, Atorino L, Dallapiccola B, Valente EM, Casari G (2005) Mitochondrial import and enzymatic activity of PINK1 mutants associated to recessive parkinsonism. *Human molecular genetics* **14:** 3477-3492

Spillantini MG, Schmidt ML, Lee VM, Trojanowski JQ, Jakes R, Goedert M (1997) Alpha-synuclein in Lewy bodies. *Nature* **388:** 839-840

Steinberg RA, Cauthron RD, Symcox MM, Shuntoh H (1993) Autoactivation of catalytic (C alpha) subunit of cyclic AMP-dependent protein kinase by phosphorylation of threonine 197. *Molecular and cellular biology* **13:** 2332-2341

Stenmark H (2009) Rab GTPases as coordinators of vesicle traffic. *Nature reviews Molecular cell biology* **10:** 513-525

Stenmark H, Olkkonen VM (2001) The Rab GTPase family. *Genome biology* **2:** REVIEWS3007

Stowers RS, Megeath LJ, Gorska-Andrzejak J, Meinertzhagen IA, Schwarz TL (2002) Axonal transport of mitochondria to synapses depends on milton, a novel Drosophila protein. *Neuron* **36:** 1063-1077

Sun Y, Vashisht AA, Tchieu J, Wohlschlegel JA, Dreier L (2012) Voltage-dependent anion channels (VDACs) recruit Parkin to defective mitochondria to promote mitochondrial autophagy. *The Journal of biological chemistry* **287:** 40652-40660

Sutherland EW, Jr., Wosilait WD (1955) Inactivation and activation of liver phosphorylase. *Nature* **175:** 169-170

Taipale M, Krykbaeva I, Koeva M, Kayatekin C, Westover KD, Karras GI, Lindquist S (2012) Quantitative analysis of HSP90-client interactions reveals principles of substrate recognition. *Cell* **150:** 987-1001

Tashiro M, Okubo S, Shimotakahara S, Hatanaka H, Yasuda H, Kainosho M, Yokoyama S, Shindo H (2003) NMR structure of ubiquitin-like domain in PARKIN: gene product of familial Parkinson's disease. *Journal of biomolecular NMR* **25:** 153-156

Taymans JM, Van den Haute C, Baekelandt V (2006) Distribution of PINK1 and LRRK2 in rat and mouse brain. *Journal of neurochemistry* **98:** 951-961

Tomoo K, Mukai Y, In Y, Miyagawa H, Kitamura K, Yamano A, Shindo H, Ishida T (2008) Crystal structure and molecular dynamics simulation of ubiquitin-like domain of murine parkin. *Biochimica et biophysica acta* **1784:** 1059-1067

Trempe JF, Chen CX, Grenier K, Camacho EM, Kozlov G, McPherson PS, Gehring K, Fon EA (2009) SH3 domains from a subset of BAR proteins define a Ubl-binding domain and implicate parkin in synaptic ubiquitination. *Molecular cell* **36:** 1034-1047

Trempe JF, Sauve V, Grenier K, Seirafi M, Tang MY, Menade M, Al-Abdul-Wahid S, Krett J, Wong K, Kozlov G, Nagar B, Fon EA, Gehring K (2013) Structure of parkin reveals mechanisms for ubiquitin ligase activation. *Science* **340:** 1451-1455

Trinkle-Mulcahy L, Boulon S, Lam YW, Urcia R, Boisvert FM, Vandermoere F, Morrice NA, Swift S, Rothbauer U, Leonhardt H, Lamond A (2008) Identifying specific protein interaction partners using quantitative mass spectrometry and bead proteomes. *The Journal of cell biology* **183:** 223-239

Trost M, Bridon G, Desjardins M, Thibault P (2010) Subcellular phosphoproteomics. *Mass spectrometry reviews* **29:** 962-990

Uno T, Moriwaki T, Nakamura M, Matsubara M, Yamagata H, Kanamaru K, Takagi M (2009) Biochemical characterization of rab proteins from Bombyx mori. *Archives of insect biochemistry and physiology* **70:** 77-89

Uno T, Nakada T, Okamaoto S, Nakamura M, Matsubara M, Imaishi H, Yamagata H, Kanamaru K, Takagi M (2007) Determination of phosphorylated amino acid residues of Rab8 from Bombyx mori. *Archives of insect biochemistry and physiology* **66:** 89-97

Unoki M, Nakamura Y (2001) Growth-suppressive effects of BPOZ and EGR2, two genes involved in the PTEN signaling pathway. *Oncogene* **20:** 4457-4465

Valente EM, Abou-Sleiman PM, Caputo V, Muqit MM, Harvey K, Gispert S, Ali Z, Del Turco D, Bentivoglio AR, Healy DG, Albanese A, Nussbaum R, Gonzalez-Maldonado R, Deller T, Salvi S, Cortelli P, Gilks WP, Latchman DS, Harvey RJ, Dallapiccola B, Auburger G, Wood NW (2004) Hereditary early-onset Parkinson's disease caused by mutations in PINK1. *Science* **304:** 1158-1160

Valente EM, Bentivoglio AR, Dixon PH, Ferraris A, Ialongo T, Frontali M, Albanese A, Wood NW (2001) Localization of a novel locus for autosomal recessive early-onset parkinsonism, PARK6, on human chromosome 1p35-p36. *American journal of human genetics* **68:** 895-900

Van Laar VS, Berman SB (2009) Mitochondrial dynamics in Parkinson's disease. *Experimental neurology* **218:** 247-256

Vives-Bauza C, Zhou C, Huang Y, Cui M, de Vries RL, Kim J, May J, Tocilescu MA, Liu W, Ko HS, Magrane J, Moore DJ, Dawson VL, Grailhe R, Dawson TM, Li C, Tieu K, Przedborski S (2010) PINK1-dependent recruitment of Parkin to mitochondria in mitophagy. *Proceedings of the National Academy of Sciences of the United States of America* **107:** 378-383

von der Malsburg K, Muller JM, Bohnert M, Oeljeklaus S, Kwiatkowska P, Becker T, Loniewska-Lwowska A, Wiese S, Rao S, Milenkovic D, Hutu DP, Zerbes RM, Schulze-Specking A, Meyer HE, Martinou JC, Rospert S, Rehling P, Meisinger C, Veenhuis M, Warscheid B, van der Klei IJ, Pfanner N, Chacinska A, van der Laan M (2011) Dual role of mitofilin in mitochondrial membrane organization and protein biogenesis. *Developmental cell* **21:** 694-707

Walsh DA, Perkins JP, Krebs EG (1968) An adenosine 3',5'-monophosphate-dependant protein kinase from rabbit skeletal muscle. *The Journal of biological chemistry* **243:** 3763-3765

Wang X, Winter D, Ashrafi G, Schlehe J, Wong YL, Selkoe D, Rice S, Steen J, LaVoie MJ, Schwarz TL (2011) PINK1 and Parkin target Miro for phosphorylation and degradation to arrest mitochondrial motility. *Cell* **147:** 893-906

Weihofen A, Ostaszewski B, Minami Y, Selkoe DJ (2008) Pink1 Parkinson mutations, the Cdc37/Hsp90 chaperones and Parkin all influence the maturation or subcellular distribution of Pink1. *Human molecular genetics* **17:** 602-616

Weihofen A, Thomas KJ, Ostaszewski BL, Cookson MR, Selkoe DJ (2009) Pink1 forms a multiprotein complex with Miro and Milton, linking Pink1 function to mitochondrial trafficking. *Biochemistry* **48:** 2045-2052

Wenzel DM, Lissounov A, Brzovic PS, Klevit RE (2011) UBCH7 reactivity profile reveals parkin and HHARI to be RING/HECT hybrids. *Nature* **474:** 105-108

Whitworth AJ, Lee JR, Ho VM, Flick R, Chowdhury R, McQuibban GA (2008) Rhomboid-7 and HtrA2/Omi act in a common pathway with the Parkinson's disease factors Pink1 and Parkin. *Disease models & mechanisms* **1:** 168-174; discussion 173

Wiborg O, Pedersen MS, Wind A, Berglund LE, Marcker KA, Vuust J (1985) The human ubiquitin multigene family: some genes contain multiple directly repeated ubiquitin coding sequences. *The EMBO journal* **4:** 755-759

Williamson BL, Marchese J, Morrice NA (2006) Automated identification and quantification of protein phosphorylation sites by LC/MS on a hybrid triple quadrupole linear ion trap mass spectrometer. *Mol Cell Proteomics* **5:** 337-346

Winner B, Regensburger M, Schreglmann S, Boyer L, Prots I, Rockenstein E, Mante M, Zhao C, Winkler J, Masliah E, Gage FH (2012) Role of alpha-synuclein in adult

neurogenesis and neuronal maturation in the dentate gyrus. *The Journal of neuroscience : the official journal of the Society for Neuroscience* **32:** 16906-16916

Wise-Scira O, Dunn A, Aloglu AK, Sakallioglu IT, Coskuner O (2013) Structures of the E46K mutant-type alpha-synuclein protein and impact of E46K mutation on the structures of the wild-type alpha-synuclein protein. *ACS chemical neuroscience* **4:** 498-508

Witt JJ, Roskoski R, Jr. (1975) Rapid protein kinase assay using phosphocellulose-paper absorption. *Analytical biochemistry* **66:** 253-258

Woodroof HI, Pogson JH, Begley M, Cantley LC, Deak M, Campbell DG, van Aalten DM, Whitworth AJ, Alessi DR, Muqit MM (2011) Discovery of catalytically active orthologues of the Parkinson's disease kinase PINK1: analysis of substrate specificity and impact of mutations. *Open biology* **1:** 110012

Yaffe MB, Rittinger K, Volinia S, Caron PR, Aitken A, Leffers H, Gamblin SJ, Smerdon SJ, Cantley LC (1997) The structural basis for 14-3-3:phosphopeptide binding specificity. *Cell* **91:** 961-971

Yamano K YR (2013) PINK1 is degraded through the N-end rule pathway. *Autophagy* **9:** 0--1

Yang Y, Gehrke S, Imai Y, Huang Z, Ouyang Y, Wang JW, Yang L, Beal MF, Vogel H, Lu B (2006) Mitochondrial pathology and muscle and dopaminergic neuron degeneration caused by inactivation of Drosophila Pink1 is rescued by Parkin. *Proceedings of the National Academy of Sciences of the United States of America* **103:** 10793-10798

Yang Y, Ouyang Y, Yang L, Beal MF, McQuibban A, Vogel H, Lu B (2008) Pink1 regulates mitochondrial dynamics through interaction with the fission/fusion machinery. *Proceedings of the National Academy of Sciences of the United States of America* **105:** 7070-7075

Yao Z, Gandhi S, Burchell VS, Plun-Favreau H, Wood NW, Abramov AY (2011) Cell metabolism affects selective vulnerability in PINK1-associated Parkinson's disease. *Journal of cell science* **124:** 4194-4202

Young JC, Hoogenraad NJ, Hartl FU (2003) Molecular chaperones Hsp90 and Hsp70 deliver preproteins to the mitochondrial import receptor Tom70. *Cell* **112:** 41-50

Yun J, Cao JH, Dodson MW, Clark IE, Kapahi P, Chowdhury RB, Guo M (2008) Loss-of-function analysis suggests that Omi/HtrA2 is not an essential component of the PINK1/PARKIN pathway in vivo. *The Journal of neuroscience : the official journal of the Society for Neuroscience* **28:** 14500-14510

Zeqiraj E, Filippi BM, Deak M, Alessi DR, van Aalten DM (2009) Structure of the LKB1-STRAD-MO25 complex reveals an allosteric mechanism of kinase activation. *Science* **326:** 1707-1711

Zerbes RM, Bohnert M, Stroud DA, von der Malsburg K, Kram A, Oeljeklaus S, Warscheid B, Becker T, Wiedemann N, Veenhuis M, van der Klei IJ, Pfanner N, van der Laan M (2012) Role of MINOS in mitochondrial membrane architecture: cristae morphology and outer membrane interactions differentially depend on mitofilin domains. *Journal of molecular biology* **422:** 183-191

Zhang J, Zhang F, Ebert D, Cobb MH, Goldsmith EJ (1995) Activity of the MAP kinase ERK2 is controlled by a flexible surface loop. *Structure* **3:** 299-307

Zhou C, Huang Y, Shao Y, May J, Prou D, Perier C, Dauer W, Schon EA, Przedborski S (2008) The kinase domain of mitochondrial PINK1 faces the cytoplasm. *Proceedings of the National Academy of Sciences of the United States of America* **105:** 12022-12027

Zhou H, Falkenburger BH, Schulz JB, Tieu K, Xu Z, Xia XG (2007) Silencing of the Pink1 gene expression by conditional RNAi does not induce dopaminergic neuron death in mice. *International journal of biological sciences* **3:** 242-250

Ziviani E, Tao RN, Whitworth AJ (2010) Drosophila parkin requires PINK1 for mitochondrial translocation and ubiquitinates mitofusin. *Proceedings of the National Academy of Sciences of the United States of America* **107:** 5018-5023